

NIST Special Publication 1018-5

Fire Dynamics Simulator (Version 5)
Technical Reference Guide

Volume 3: Validation

Kevin McGrattan
Simo Hostikka
Jason Floyd
Bryan Klein



NIST Special Publication 1018-5

Fire Dynamics Simulator (Version 5) Technical Reference Guide

Volume 3: Validation

Kevin McGrattan
Bryan Klein
*Fire Research Division
Building and Fire Research Laboratory*

Simo Hostikka
*VTT Technical Research Centre of Finland
Espoo, Finland*

Jason Floyd
*Hughes Associates, Inc.
Baltimore, Maryland*

September 15, 2008
FDS Version 5.2
SVNRepository Revision : 2378



U.S. Department of Commerce
Carlos M. Gutierrez, Secretary

National Institute of Standards and Technology
William A. Jeffrey, Director

Preface

This is Volume 3 of the FDS Technical Reference Guide. Volume 1 describes the mathematical model and numerical method. Volume 2 documents past and present model verification work. Instructions for using FDS are contained in a separate User's Guide [1].

The three volumes of the FDS Technical Reference Guide are based in part on the “Standard Guide for Evaluating the Predictive Capability of Deterministic Fire Models,” ASTM E 1355 [2]. ASTM E 1355 defines *model evaluation* as “the process of quantifying the accuracy of chosen results from a model when applied for a specific use.” The model evaluation process consists of two main components: verification and validation. *Verification* is a process to check the correctness of the solution of the governing equations. Verification does not imply that the governing equations are appropriate; only that the equations are being solved correctly. *Validation* is a process to determine the appropriateness of the governing equations as a mathematical model of the physical phenomena of interest. Typically, validation involves comparing model results with experimental measurement. Differences that cannot be explained in terms of numerical errors in the model or uncertainty in the measurements are attributed to the assumptions and simplifications of the physical model.

Evaluation is critical to establishing both the acceptable uses and limitations of a model. Throughout its development, FDS has undergone various forms of evaluation, both at NIST and beyond. This volume provides a survey of validation work conducted to date to evaluate FDS.

About the Authors

Kevin McGrattan is a mathematician in the Building and Fire Research Laboratory of NIST. He received a bachelors of science degree from the School of Engineering and Applied Science of Columbia University in 1987 and a doctorate at the Courant Institute of New York University in 1991. He joined the NIST staff in 1992 and has since worked on the development of fire models, most notably the Fire Dynamics Simulator.

Simo Hostikka is a Senior Research Scientist at VTT Technical Research Centre of Finland. He received a master of science (technology) degree in 1997 and a doctorate in 2008 from the Department of Engineering Physics and Mathematics of the Helsinki University of Technology. He is the principal developer of the radiation and solid phase sub-models within FDS.

Jason Floyd is a Senior Engineer at Hughes Associates, Inc., in Baltimore, Maryland. He received a bachelors of science degree and a doctorate from the Nuclear Engineering Program of the University of Maryland. After graduating, he won a National Research Council Post-Doctoral Fellowship at the Building and Fire Research Laboratory of NIST, where he developed the combustion algorithm within FDS. He is currently funded by NIST under grant 60NANB5D1205 from the Fire Research Grants Program (15 USC 278f). He is the principal developer of the multi-parameter mixture fraction combustion model and control logic within FDS.

Bryan Klein is an Information Technology Specialist in the Building and Fire Research Laboratory of NIST. Before coming to NIST, Bryan worked for five years with Western Fire Center, Inc., performing a wide range of activities including fire modeling, data acquisition programming, and quantitative fire measurements. His current focus is on FDS development and user support, along with experimental model validation work.

Acknowledgments

Support for validation experiments and the preparation of the FDS manuals has been provided by the Office of Nuclear Regulatory Research of the US Nuclear Regulatory Commission (US NRC). Special thanks to Mark Salley and Jason Dreisbach for their efforts.

Anthony Hamins directed the NIST/NRC and WTC experiments, conducted smaller methane burner measurements, and quantified the experimental uncertainty of these and other experiments used in this study. Alex Maranghides was the Director of the Large Fire Laboratory at NIST at the time these tests were conducted, and he helped to design the experiments. Therese McAllister oversaw the instrumentation of the structural steel during the WTC experiments.

Rick Peacock of NIST assisted in the interpretation of results from the “NBS Multi-Room Test Series,” a set of three room fire experiments conducted at the National Bureau of Standards (now NIST) in the mid-1980’s.

Thanks to Bill Pitts, Nelson Bryner, and Erik Johnsson of NIST for their contribution of data for the “NIST Reduced Scale Enclosure Experiments.”

Thanks to VTT, Finland, for their contribution of experimental data, referred to in this document as the “VTT Large Hall Experiments.” Also, Jukka Hietaniemi, Jukka Vaari and Timo Korhonen have performed validation studies of various sub-models. The VTT Fire Research group continues to work on model development and validation of the model for various applications.

David Sheppard, currently of the Bureau of Alcohol, Tobacco and Firearms (ATF), conducted the experiments referred to as the “UL/NFPRF Test Series” on behalf of the Fire Protection Research Foundation (then known as the National Fire Protection Research Foundation) while working at Underwriters Labs in Northbrook, Illinois.

Thanks to Jerry Back, Craig Beyler and Phil DiNenno of Hughes Associates and Pat Tatem of the Naval Research Laboratory for their contribution of experimental data for the “HAI/NRL Wall Fire” series. Thanks also to Craig Beyler for assistance with the data for the “Beyler Hood Experiments.”

Thanks to Ken Steckler for providing details about the “Steckler Compartment Experiments” of 1979.

At the University of Maryland, Professor Fred Mowrer and Phil Friday were the first to apply FDS to the NRC-sponsored experiments referred to in this document as the “FM/SNL Test Series” (Factory Mutual and Sandia National Laboratories conducted these experiments). Thanks also to Steve Nowlen, the test director, for additional information.

Contents

Preface	i
About the Authors	iii
Acknowledgments	v
1 What is Model Validation?	1
1.1 Model Scenarios	1
1.2 Model Outputs	2
1.3 Model Accuracy	3
1.4 How to Use the Guide	3
2 Survey of Past Validation Work	5
2.1 Validation Work with Pre-Release Versions of FDS	5
2.2 Validation of FDS since 2000	6
2.2.1 Comparison with Full-Scale Tests Conducted Specifically for the Chosen Evaluation	6
2.2.2 Comparison with Engineering Correlations	7
2.2.3 Comparisons with Previously Published Full-Scale Test Data	7
2.2.4 Comparison with Standard Tests	13
2.2.5 Comparison with Documented Fire Experience	13
3 Description of Experiments	15
3.1 VTT Large Hall Tests	15
3.2 UL/NFPRF Sprinkler, Vent, and Draft Curtain Study	18
3.3 NIST/NRC Test Series	20
3.4 WTC Spray Burner Test Series	22
3.5 FM/SNL Test Series	22
3.6 NBS Multi-Room Test Series	25
3.7 Steckler Compartment Experiments	27
3.8 McCaffrey Plume Experiments	28
3.9 Smyth Slot Burner Experiment	28
3.10 Beyler Hood Experiments	28
3.11 NIST Reduced Scale Enclosure Experiments	28
3.12 Hamins Methane Burner Experiments	28
3.13 NRL/HAI Wall Heat Flux Measurements	28
3.14 Experimental Uncertainty	29

4 HGL Temperature and Depth	31
4.1 HGL Reduction Method	31
4.2 WTC Test Series	32
4.3 VTT Test Series	35
4.4 NIST/NRC Test Series	37
4.5 FM/SNL Test Series	42
4.6 NBS Multi-Room Test Series	44
4.7 Summary of Hot Gas Layer Temperature and Height	48
4.8 Steckler Compartment Experiments	50
5 Fire Plumes	59
5.1 McCaffrey's Plume Correlation	59
5.2 Heskestad's Flame Height Correlation	62
5.3 VTT Large Hall and FM/SNL Test Series	64
6 Ceiling Jets and Device Activation	67
6.1 WTC Test Series	67
6.2 NIST/NRC Test Series	67
6.3 FM/SNL Test Series	67
6.4 UL/NFPRF Sprinkler, Vent, and Draft Curtain Experiments	73
7 Gas Velocity	75
7.1 Steckler Compartment Doorway Velocity Profiles	75
8 Gas Species and Smoke	85
8.1 WTC and NIST/NRC Test Series, Oxygen and CO ₂	85
8.2 NIST/NRC Test Series, Smoke	93
8.3 Smyth Slot Burner Experiment	97
8.4 Beyler Hood Experiments	101
8.5 NIST Reduced Scale Enclosure (RSE) Test Series	103
9 Compartment Pressure	105
9.1 NIST/NRC Test Series	105
10 Surface Temperature	109
10.1 WTC Test Series, Steel Structural Members and "Slug" Calorimeters	109
10.2 NIST/NRC Test Series, Cables	126
10.3 WTC Ceiling and Wall Temperatures	136
10.4 NIST/NRC Test Series, Compartment Walls, Floor and Ceiling	146
11 Heat Flux	157
11.1 Hamins Methane Burner Heat Flux Measurements	157
11.2 NRL/HAI Wall Heat Flux Measurements	160
11.3 WTC Heat Flux Measurements	163
11.4 NIST/NRC Test Series, Heat Flux to Cables	172
Bibliography	183
References	191

List of Figures

3.1	Geometry of the VTT Large Fire Test Hall.	17
3.2	Plan view of the UL/NFPRF Experiments.	19
3.3	Geometry of the NIST/NRC Experiments.	21
3.4	Geometry of the FM/SNL Experiments.	24
3.5	Geometry of the NBS Multi-Room Experiments.	26
4.1	Summary of HGL temperature and height predictions, VTT, NIST/NRC, WTC, NBS and FM/SNL series	49
4.2	Summary of peak temperature predictions for the Steckler Compartment Experiments.	58
5.1	Summary of flame height predictions, Heskestad correlation.	63
5.2	Summary of plume temperature predictions, VTT and FM/SNL test series.	66
6.1	Summary of ceiling jet temperature predictions, WTC, NIST/NRC and FM/SNL test series.	72
6.2	Summary of sprinkler activation time predictions, UL/NFPRF test series.	74
7.1	Summary of velocity predictions, Steckler compartment experiments.	83
8.1	Summary of gas species predictions, NIST/NRC and WTC test series.	92
8.2	Summary of smoke concentration predictions, NIST/NRC test series	96
8.3	Temperature and gas species predictions 7 mm above burner, Smyth experiment.	98
8.4	Temperature and gas species predictions 9 mm above burner, Smyth experiment.	99
8.5	Temperature and gas species predictions 11 mm above burner, Smyth experiment.	100
8.6	Summary of gas species predictions, Beyler hood experiments.	102
8.7	Summary of CO and CO ₂ predictions, Pitts reduced-scale enclosure experiments.	104
9.1	Summary of pressure predictions, NIST/NRC test series.	108
10.1	Summary of steel temperature predictions, WTC test series.	125
10.2	Summary of cable surface temperature predictions, NIST/NRC test series.	135
10.3	Summary of wall and ceiling temperature predictions, WTC test series.	145
10.4	Summary of wall, floor and ceiling temperature predictions, NIST/NRC test series.	155
11.1	Radial heat flux predictions, Hamins methane burner experiments.	158
11.2	Vertical heat flux predictions, Hamins methane burner experiments.	159
11.3	Wall heat flux predictions, NRL/HAI experiments.	161
11.4	Wall heat flux predictions, NRL/HAI experiments.	162
11.5	Summary of heat flux predictions, WTC test series.	171
11.6	Summary of heat flux predictions to cables, NIST/NRC test series.	181

List of Tables

3.1	Summary of Steckler compartment experiments.	27
3.2	Summary of Hamins' uncertainty estimates.	29
5.1	Summary of parameters for the flame height predictions.	62
6.1	Results of the UL/NFPRF Experiments.	73
10.1	Locations of ceiling surface temperature measurements relative to the fire pan in the WTC series.	136
10.2	Wall thermocouple positions for the NIST/NRC series.	146
11.1	Summary of Hamins methane burner experiments.	157
11.2	Summary of the NRL/HAI Wall Heat Flux Measurements.	160
11.3	Heat flux gauge positions relative to the center of the fire pan in the WTC series.	163

Chapter 1

What is Model Validation?

Although there are various definitions of model validation, for example those contained in ASTM E 1355 [2], most define it as the process of determining how well the mathematical model predicts the actual physical phenomena of interest. Validation typically involves (1) comparing model predictions with experimental measurements, (2) quantifying the differences in light of uncertainties in both the measurements and the model inputs, and (3) deciding if the model is appropriate for the given application. This Guide only does (1) and (2). Number (3) is the responsibility of the model user.

A common question asked of any mathematical model is whether it is validated. To say that FDS is “validated” means that the model has been shown to be of a given level of accuracy for a given range of parameters for a given type of fire scenario. Although the FDS developers continuously perform validation studies, it is ultimately the end user of the model who decides if the model is adequate for the job at hand. Thus, this Guide provides the raw material for a validation study, but it does not and cannot be considered comprehensive.

The following sections discuss key issues that you must consider when deciding whether or not FDS has been validated. It depends on (a) the scenarios of interest, (b) the predicted quantities, and (c) the desired level of accuracy. Keep in mind that FDS can be used to model most any fire scenario and predict almost any quantity of interest, but the prediction may not be accurate because of limitations in the description of the fire physics, and also because of limited information about the fuels, geometry, and so on.

1.1 Model Scenarios

When doing a validation study, the first question to ask is, “What is the application?” There are countless fire scenarios to consider, but from the point of view of validation it is useful to divide them into two classes – those for which the fire is *specified* as an input to the model and those for which the fire is *predicted* by the model. The former is often the case for a design application, the latter for a forensic reconstruction. Consider each in turn.

Design applications typically involve an existing building or a building under design. A so-called “design fire” is specified either by a regulatory authority or by the engineers performing the analysis. Because the fire’s heat release rate is specified, the role of the model is to predict the transport of heat and combustion products throughout the room or rooms of interest. Ventilation equipment is often included in the simulation, like fans, blowers, exhaust hoods, HVAC ducts, smoke management systems, *etc.* Sprinkler and heat and smoke detector activation are also of interest. The effect of the sprinkler spray on the fire is usually less of interest since the heat release rate of the fire is specified rather than predicted. Detailed descriptions of the contents of the building are usually not necessary because these items are assumed to not contribute to the fire, and even if they are, the burning rate will be specified, not predicted. Sometimes, it is necessary to

predict the heat flux from the fire to a nearby “target,” and even though the target may heat up to some specified ignition temperature, the subsequent spread of the fire usually goes beyond the scope of the analysis because of the uncertainty inherent in object to object fire spread.

Forensic reconstructions require the model to simulate an actual fire based on information that is collected after the event, such as eye witness accounts, unburned materials, burn signatures, *etc.* The purpose of the simulation is to connect a sequence of discrete observations with a continuous description of the fire dynamics. Usually, reconstructions involve more gas/solid phase interaction because virtually all objects in a given room are potentially ignitable, especially when flashover occurs. Thus, there is much more emphasis on such phenomena as heat transfer to surfaces, pyrolysis, flame spread, and suppression. In general, forensic reconstructions are more challenging simulations to perform because they require more detailed information about the room contents, and there is much greater uncertainty in the total heat release rate as the fire spreads from object to object.

Validation studies of FDS to date have focussed more on design applications than reconstructions. The reason is that design applications usually involve specified fires and demand a minimum of thermophysical properties of real materials. Transport of smoke and heat is the primary focus, and measurements can be limited to well-placed thermocouples, a few heat flux gauges, gas samplers, *etc.* Phenomena of importance in forensic reconstructions, like second item ignition, flame spread, vitiation effects and extinction, are more difficult to model and more difficult to study with well-controlled experiments. Uncertainties in material properties and measurements, as well as simplifying assumptions in the model, often force the comparison between model and measurement to be qualitative at best. Nevertheless, current validation efforts are moving in the direction of these more difficult issues.

1.2 Model Outputs

For a given fire scenario, there are a number of different quantities that the model predicts, like gas temperature, heat flux, and so on. A typical fire experiment can produce hundreds of time histories of point measurements, each of which can be reproduced by the model to some level of accuracy. It is a challenge to sort out all the plots and graphs of all the different quantities and come to some general conclusion. For this reason, this Guide is organized by output quantity, not by individual experiment or fire scenario. In this way, it is possible to assess, over a range of different experiments and scenarios, the performance of the model in predicting a given quantity. Overall trends and biases become much more clear when the data is organized this way.

Keep in mind that for any fire experiment, FDS might predict a particular quantity accurately (within the experimental uncertainty bounds, for example), but another quantity less accurately. For example, in a series of 15 full-scale fire experiments conducted at NIST in 2003, sponsored by the U.S. Nuclear Regulatory Commission, the average hot gas layer (HGL) temperature predictions were within the accuracy of the experiments themselves, yet the smoke concentration predictions differed from the measurements by as much as a factor of 3. Why? Consider the following issues associated with various types of measurements:

- Is the measurement taken at a single point, or averaged over many points? In the example above, the HGL temperature is an average of many thermocouple measurements, whereas the smoke concentration is based on the extinction of laser light over a short length span. Model error tends to be reduced by the averaging process, plus most fire models, including FDS, are based on global mass and energy conservation laws that are expressed as spatial averages.
- Is the measured quantity time-averaged or instantaneous? For example, a surface temperature prediction is less prone to error in comparison to a heat flux prediction because the former is, in some sense, a time-integral of the latter.

- In the case of a point measurement, how close to the fire is it? The terms “near-field” and “far-field” are used throughout this Guide to describe the relative distance from the fire. In general, predictions of near-field phenomena are more prone to error than far-field. There are exceptions, however. For example, a prediction of the temperature directly within the flaming region may be more accurate than that made just a fire diameter away because of the fact that temperatures tend to stabilize at about 1000 °C within the fire itself, but then rapidly decrease away from the flames. Less accurate predictions typically occur in regions of steep gradients (rapid changes, both in space and time).

1.3 Model Accuracy

The desired accuracy for each predicted quantity depends on the technical issues associated with the analysis. You must ask the question: How accurate does the analysis have to be to answer the technical question posed? Returning to the earlier definitions of “design” and “reconstruction,” design applications typically are more accurate because the heat release rate is typically specified rather than predicted, and the initial and boundary conditions are better characterized – at least in the analysis. Mathematically, a design calculation is an example of a “well-posed” problem in which the solution of the governing equations is advanced in time starting from a known set of initial conditions and constrained by a known set of boundary conditions. The accuracy of the results is a function of the fidelity of the numerical solution, which is mainly dependent on the size of the computational grid.

A reconstruction is an example of an “ill-posed” problem because the outcome is known whereas the initial and boundary conditions are usually not. There is no single, unique solution to the problem, that is, it is possible to simulate numerous fires that produce the same general outcome. There is no right or wrong answer, but rather a small set of plausible fire scenarios that are consistent with the collected evidence. These simulations are then used to demonstrate to fire service personnel why the fire behaved as it did based on the current understanding of fire physics incorporated in the model. Most often, the result of the analysis is only qualitative. If there is any quantification at all, it could be in the time to reach critical events, like a roof collapse or room flashover.

1.4 How to Use the Guide

This Guide is merely a repository of calculation results. As FDS develops, it will expand to include new experimental measurements of newly modeled physical phenomena. With each minor release of FDS (version 5.2 to 5.3, for example), the plots and graphs will all be redone to ensure that changes to the model have not decreased the accuracy of a previous version. If you are embarking on a validation study, you might want to consider the following steps:

1. Survey Chapter 2 to learn about past efforts by others to validate the model for applications similar to yours
2. Identify in Chapter 3 experimental data sets appropriate for your application
3. Read the specific chapters for the quantities of interest

The experimental data sets and FDS input/output files are all managed via the on-line project archiving system. You might want to re-run examples of interest to better understand how the calculations were designed, and how changes in the various parameters might affect the results. This is known as a *sensitivity study*, and it is difficult to document all the parameter variations of the calculations described in this report. Thus, it is a good idea to determine which of the input parameters are particularly important.

Chapter 2

Survey of Past Validation Work

In this chapter, a survey of FDS validation work will be presented. Some of the work has been performed at NIST, some by its grantees and some by engineering firms using the model. Because each organization has its own reasons for validating the model, the referenced papers and reports do not follow any particular guidelines. Some of the works only provide a qualitative assessment of the model, concluding that the model agreement with a particular experiment is “good” or “reasonable.” Sometimes, the conclusion is that the model works well in certain cases, not as well in others. These studies are included in the survey because the references are useful to other model users who may have a similar application and are interested in even qualitative assessment. It is important to note that some of the papers point out flaws in early releases of FDS that have been corrected or improved in more recent releases. Some of the issues raised, however, are still subjects of active research. The research agenda for FDS is greatly influenced by the feedback provided by users, often through publication of validation efforts.

2.1 Validation Work with Pre-Release Versions of FDS

FDS was officially released in 2000. However, for two decades various CFD codes using the basic FDS hydrodynamic framework were developed at NIST for different applications and for research. In the mid 1990s, many of these different codes were consolidated into what eventually became FDS. Before FDS, the various models were referred to as LES, NIST-LES, LES3D, IFS (Industrial Fire Simulator), and ALOFT (A Large Outdoor Fire Plume Trajectory).

The NIST LES model describes the transport of smoke and hot gases during a fire in an enclosure using the Boussinesq approximation, where it is assumed that the density and temperature variations in the flow are relatively small [3, 4, 5, 6]. Such an approximation can be applied to a fire plume away from the fire itself. Much of the early work with this form of the model was devoted to the formulation of the low Mach number form of the Navier-Stokes equations and the development of the basic numerical algorithm. Early validation efforts compared the model with salt water experiments [7, 8, 9], and fire plumes [10, 11, 12, 13]. Clement validated the hydrodynamic model in FDS by measuring salt water flows using Laser Induced dye Fluorescence (LIF) [14]. An interesting finding of this work was that the transition from a laminar to a turbulent plume is very difficult to predict with any technique other than DNS.

Eventually, the Boussinesq approximation was dropped and simulations began to include more fire-specific phenomena. Simulations of enclosure fires were compared to experiments performed by Steckler [15]. Mell *et al.* [16] studied small helium plumes, with particular attention to the relative roles of baroclinic torque and buoyancy as sources of vorticity. Cleary *et al.* [17] used the LES model to simulate the environment seen by multi-sensor fire detectors and performed some simple validation work to check the model before using it. Large fire experiments were performed by NIST at the FRI test facility in Japan,

and at US Naval aircraft hangars in Hawaii and Iceland [18]. Room airflow applications were considered by Emmerich and McGrattan [19, 20].

These early validation efforts were encouraging, but still pointed out the need to improve the hydrodynamic model by introducing the Smagorinsky form of large eddy simulation. This addition improved the stability of the model because of the relatively simple relation between the local strain rate and the turbulent viscosity. There is both a physical and numerical benefit to the Smagorinsky model. Physically, the viscous term used in the model has the right functional form to describe sub-grid mixing processes. Numerically, local oscillations in the computed flow quantities are damped if they become large enough to threaten the stability of the entire calculation.

During the 1980s and 1990s, the Building and Fire Research Laboratory at NIST studied the burning of crude oil under the sponsorship of the US Minerals Management Service. The aim of the work was to assess the feasibility of using burning as a means to remove spilled oil from the sea surface. As part of the effort, Rehm and Baum developed a special application of the LES model called ALOFT. The model was a spin-off of the two-dimensional LES enclosure model, in which a three-dimensional steady-state plume was computed as a two-dimensional evolution of the lateral wind field generated by a large fire blown in a steady wind. The ALOFT model is based on large eddy simulation in that it attempts to resolve the relevant scales of a large, bent-over plume. Validation work was performed by simulating the plumes from several large experimental burns of crude oil in which aerial and ground sampling of smoke particulate was performed [21]. Yamada [22] performed a validation of the ALOFT model for 10 m oil tank fire. The results indicate that the prediction of the plume cross section 500 m from the fire agree well with the experimental observations.

2.2 Validation of FDS since 2000

There is an on-going effort at NIST and elsewhere to validate FDS as new capabilities are added. To date, most of the validation work has evaluated the model's ability to predict the transport of heat and exhaust products from a fire through an enclosure. In these studies, the heat release rate is usually prescribed, along with the production rates of various products of combustion. More recently, validation efforts have moved beyond just transport issues to consider fire growth, flame spread, suppression, sprinkler/detector activation, and other fire-specific phenomena.

The validation work discussed below can be organized into several categories: Comparisons with full-scale tests conducted especially for the chosen evaluation, comparisons with previously published full-scale test data, comparisons with standard tests, comparisons with documented fire experience, and comparisons with engineering correlations. There is no single method by which the predictions and measurements are compared. Formal, rigorous validation exercises are time-consuming and expensive. Most validation exercises are done simply to assess if the model can be used for a very specific purpose. While not comprehensive on their own, these studies collectively constitute a valuable assessment of the model.

2.2.1 Comparison with Full-Scale Tests Conducted Specifically for the Chosen Evaluation

As part of the NIST investigation of the World Trade Center fires and collapse, a series of large scale fire experiments were performed specifically to validate FDS [23]. The tests were performed in a rectangular compartment 7.2 m long by 3.6 m wide by 3.8 m tall. The fires were fueled by heptane for some tests and a heptane/toluene mixture for the others. The results of the experiments and simulations are included in detail in this Guide.

A second set of experiments to validate FDS for use in the World Trade Center investigation is documented in Ref. [24]. The experiments are not described as part of this Guide. The intent of these tests was

to evaluate the ability of the model to simulate the growth of a fire burning three office workstations within a compartment of dimensions 11 m by 7 m by 4 m, open at one end to mimic the ventilation of windows similar to those in the WTC towers. Six tests were performed with various initial conditions exploring the effect of jet fuel spray and ceiling tiles covering the surface of the desks and carpet. Measurements were made of the heat release rate and compartment gas temperatures at four locations using vertical thermocouple arrays. Six different material samples were tested in the NIST cone calorimeter: desk, chair, paper, computer case, privacy panel, and carpet. Data for the carpet, desk and privacy panel were input directly into FDS, with the other three materials lumped together to form an idealized fuel type. Open burns of single workstations were used to calibrate the simplified fuel package. Details of the modeling are contained in Ref. [25].

2.2.2 Comparison with Engineering Correlations

There are several examples of fire flows that have been extensively studied, so much so that a set of engineering correlations combining the results of many experiments have been developed. These correlations are useful to modelers because of their simplicity. The most studied phenomena include fire plumes, ceiling jets, and flame heights.

Although much of the early validation work before FDS was released involved fire plumes, it remains an active area of interest. One study by Chow and Yin [26] surveys the performance of various models in predicting plume temperatures and entrainment for a 470 kW fire with a diameter of 1 m and an unbounded ceiling. They compare the FDS results with various correlations and a RANS (Reynolds-Averaged Navier-Stokes) model.

Battaglia *et al.* [27] used FDS to simulate fire whirls. First, the model was shown to reproduce the McCaffrey correlation of a fire plume, then it was shown to reproduce qualitatively certain features of fire whirls. At the time, FDS used Lagrangian elements to introduce heat from the fire (no longer used), and this combustion model could not replicate the extreme stretching of the core of the flame zone.

Quintiere and Ma [28, 29] compared predicted flame heights and plume centerline temperatures to empirical correlations. For plume temperature, the Heskestad correlation [30] was chosen. Favorable agreement was found in the plume region, but the results near the flame region were found to be grid-dependent, especially for low Q^* fires. At this same time, researchers at NIST were reaching similar conclusions, and it was noticed by both teams that a critical parameter for the model is $D^*/\delta x$, where D^* is the characteristic fire diameter and δx is the grid cell size. If this parameter is sufficiently large, the fire can be considered well-resolved and agreement with various flame height correlations was found. If the parameter is not large enough, the fire is not well-resolved and adjustments must be made to the combustion routine to account for it.

2.2.3 Comparisons with Previously Published Full-Scale Test Data

Experiments conducted solely for model validation are somewhat rare. More common are validation studies that use data from past experiments. This section contains brief descriptions of work published comparing FDS with past experiments or correlations of experimental data.

Pool Fires

Xin *et al.* [31] used FDS to model a 1 m diameter methane pool fire. The computational domain was 2 m by 2 m by 4 m with a uniform grid size of 2.5 cm. The predicted results were compared to experimental data and found to qualitatively and quantitatively reproduce the velocity field. The same authors performed a similar study of a 7.1 cm methane burner [32] and a helium plume [33].

Hostikka *et al.* [34] modeled small pool fires of methane, natural gas and methanol to test the FDS radiation solver for low-sooting fires. They conclude that the predicted radiative fluxes are higher than measured values, especially at small heat release rates, due to an over-prediction of the gas temperature. These tests are also included in the Heat Flux section of this report.

Hietaniemi, Hostikka and Vaari [35] consider heptane pool fires of various diameters. Predictions of the burning rate as a function of diameter follow the trend observed in a number of experimental studies. Their results show an improvement in the model over the earlier work with methanol fires, due to improvements in the radiation routine and the fact that heptane is more sooty than methanol, simplifying the treatment of radiation. The authors point out that reliable predictions of the burning rate of liquid fuels require roughly twice as fine a grid spanning the burner than would be necessary to predict plume velocities and temperatures. The reason for this is the prediction of the heat feedback to the burning surface necessary to *predict* rather than to *specify* the burning rate.

Air and Gas Movement in the Absence of Fire

The low Mach number assumption in FDS is appropriate not only to fire, but to most building ventilation scenarios. An example of how the model can be used to assess indoor air quality is presented by Musser *et al.* [36]. The test compartment was a displacement ventilation test room that contained computers, furniture, and lighting fixtures as well as heated rectangular boxes intended to represent occupants. A detailed description of the test configuration is given by Yuan *et al.* [37]. The room is ventilated with cool supply air introduced via a diffuser that is mounted on a side wall near the floor. The air rises as it is warmed by heat sources and exits through a return duct located in the upper portion of the room. The flow pattern is intended to remove contaminants by sweeping them upward at the source and removing them from the room. Sulphur hexafluoride, SF₆, was introduced into the compartment during the experiment as a tracer gas near the breathing zone of the occupants. Temperature, tracer concentration, and velocity were measured during the experiments. For temperature, the two finest grids (50 by 36 by 24 and 64 by 45 by 30) produced results in which the agreement between the measurement and prediction was considered “acceptable.” The agreement for the tracer concentrations were not as good. It was suggested that the difference could be related to the way the source of the tracer gas was modeled. The comparison of velocity data was deemed “reasonable,” given the limitations of the velocity probes at low velocities.

In another study, Musser and Tan [38] used FDS to assess the design of ventilation systems for facilities in which train locomotives operate. Although there is only a limited amount of validation, the study is useful in demonstrating a practical use of FDS for a non-fire scenario.

Mniszewski [39] used FDS to model the release of flammable gases in simple enclosures and open areas. In this work, the gases were not ignited.

Kerber and Walton provided a comparison between FDS version 1 and experiments on positive pressure ventilation in a full-scale enclosure without a fire. The model predictions of velocity were within 10 % to 20 % of the experimental values [40].

Wind Engineering

Most applications of FDS involve fires within buildings. However, it can be used to model thermal plumes in the open and wind impinging on the exterior of a building. Rehm, McGrattan, Baum and Simiu [41] used the LES solver to estimate surface pressures on simple rectangular blocks in a crosswind, and compared these estimates to experimental measurements. In a subsequent paper [42], they considered the qualitative effects of multiple buildings and trees on a wind field.

A different approach to wind was taken by Wang and Joulain [43]. They considered a small fire in a wind tunnel 0.4 m wide and 0.7 m tall with flow speeds of 0.5 m/s to 2.5 m/s. Much of the comparison

with experiment is qualitative, including flame shape, lean, length. They also use the model to determine the predominant modes of heat transfer for different operating conditions. To assess the combustion, they implemented an “eddy break-up” combustion model [44] and compared it to the mixture fraction approach used by FDS. The two models performed better or worse, depending on the operating conditions. Some of the weaknesses of the mixture fraction model as implemented in FDS version 2 were addressed in subsequent versions.

Chang and Meroney [45] compared the results of FDS with the commercial CFD package FLUENT in simulating the transport of pollutants from steady point sources in an idealized urban environment. FLUENT employs a variety of RANS (Reynolds Averaged Navier-Stokes) closure methods, whereas FDS employs large eddy simulation (LES). The results of the numerical models were compared with wind tunnel measurements within a 1:50 scale physical model of an urban street “canyon.”

Growing Fires

Vettori [46] modeled two different fire growth rates in an obstructed ceiling geometry. The rectangular compartment was 9.2 m by 5.6 m by 2.4 m with a hollow steel door to the outside that remained closed during the tests. An open wooden stairway led to an upper floor with the same dimensions as the fire compartment below. Wooden joists measuring 0.038 m by 0.24 m were spaced at 0.41 m intervals across the ceiling and were supported by a single steel beam that spanned the width of the room. A rectangular methane gas burner measuring 0.7 m by 1.0 m by 0.31 m was placed in the corner of the chamber. Slow and fast burning fires that reached 1055 kW in 600 s and 150 s, respectively, were monitored. Four vertical arrays of Type K thermocouples were used to measure temperatures during the tests. The FDS model used four grid refinements and piecewise-linear grid spacing for each fire growth rate (slow and fast). For the fast growing fire, the predicted temperatures were within 20 % of the measured values and within 10 % for the slow growing fire. In general, finer grids produced better agreement.

In a follow-up report, Vettori [47] extended his study to include sloped ceilings, with and without obstructions. He found that the difference between predicted and measured sprinkler activation times varied between 4 % and 26 % for all cases studied. He also noted that FDS was able to predict the first activation of a sprinkler twice as far from the fire as another; caused presumably by the re-direction of smoke and heat by the beams on the ceiling.

Floyd [48, 49] validated FDS by comparing the modeling results with measurements from fire tests at the Heiss-Dampf Reaktor (HDR) facility. The structure was originally the containment building for a nuclear power reactor in Germany. The cylindrical structure was 20 m in diameter and 50 m in height topped by a hemispherical dome 10 m in radius. The building was divided into eight levels. The total volume of the building was approximately 11,000 m³. From 1984 to 1991, four fire test series were performed within the HDR facility. The T51 test series consisted of eleven propane gas tests and three wood crib tests. To avoid permanently damaging the test facility, a special set of test rooms were constructed, consisting of a fire room with a narrow door, a long corridor wrapping around the reactor vessel shield wall, and a curtained area centered beneath a maintenance hatch. The fire room walls were lined with fire brick. The doorway and corridor walls had the same construction as the test chamber. Six gas burners were mounted in the fire room. The fuel source was propane gas mixed with 10 % air fed at a constant rate to one of the six burners. The FDS model predicted the layer height and temperature of the space to within 10 % of the experimental values [48].

FDS predictions of fire growth and smoke movement in large spaces were presented by Kashef [50]. The experiments were conducted at the National Research Council Canada. The tests were performed in a compartment with dimensions of 9 m by 6 m by 5.5 m with 32 exhaust inlets and a single supply fan. A burner generated fires ranging in size from 15 kW to 1000 kW.

Flame Spread

Although FDS simulations have been compared to actual and experimental large-scale fires, it is difficult to *quantify* the accuracy because of the uncertainty associated with material properties. Most quantified validation work associated with flame spread have been for small, laminar flames with length scales ranging from millimeters to a few centimeters.

For example, FDS (or its core algorithms) have been used at a grid resolution of roughly 1 mm to look at flames spreading over paper in a micro-gravity environment [51, 52, 53, 54, 55, 56], as well as "g-jitter" effects aboard spacecraft [57]. Simulations have been compared to experiments performed aboard the Space Shuttle. The flames are laminar and relatively simple in structure, and the materials are relatively well-characterized.

The flame spread calculations from FDS were compared to the vertical flame spread over a 5 m slab of PMMA performed by Factory Mutual Research Corporation (FMRC). The predicted flame spread rate was within 0.3 m/s for any point in time during the analysis. The comparison at the quasi-steady burning rate once the full slab was burning shows that FDS over-estimated the burning rate [28, 29].

A charring model was implemented in FDS by Hostikka and McGrattan [58]. The model is a simplification of work done at NIST by Ritchie *et al.* [59]. The charring model was first used to predict the burning rate of a small wooden sample in the cone calorimeter. The results were more favorable for higher imposed heat fluxes. For low imposed fluxes, the heat transfer at the edge of the sample was more pronounced, and more difficult to model accurately. Full-scale room tests with wood paneling were modeled, but the results were judged to be grid-dependent. This was likely a consequence of the gas phase spatial resolution, rather than the solid phase. The authors concluded that it is difficult to predict the growth rate of a fire in a wood-lined room without "tuning" the pyrolysis rate coefficients. For real wood products, it is unlikely that all of the necessary properties can be obtained easily. Thus, grid sensitivity and uncertain material properties make *blind* predictions of fire growth on real materials beyond the reach of the current version of the model. However, the model can still be used for a qualitative assessment of fire behavior as long as the uncertainty in the flame spread rate is recognized.

Sprinklers, Mist System, and Suppression by Water

A significant validation effort for sprinkler activation and suppression was a project entitled the International Fire Sprinkler, Smoke and Heat Vent, Draft Curtain Fire Test Project organized by the National Fire Protection Research Foundation [60]. Thirty-nine large scale fire tests were conducted at Underwriters Laboratories in Northbrook, IL. The tests were aimed at evaluating the performance of various fire protection systems in large buildings with flat ceilings, like warehouses and "big box" retail stores. All the tests were conducted under a 30 m by 30 m adjustable-height platform in a 37 m by 37 m by 15 m high test bay. At the time, FDS had not been publicly released and was referred to as the Industrial Fire Simulator (IFS), but it was essentially the same as FDS version 1. The first series of heptane spray burner fires have been simulated with the latest version of FDS and are included in this Guide under the heading "UL/NFPRF Test Series." Most of the full-scale experiments performed during the project used a heptane spray burner to generate controlled fires of 1 MW to 10 MW. However, five experiments were performed with 6 m high racks containing the Factory Mutual Standard Plastic Commodity, or Group A Plastic. To model these fires, bench scale experiments were performed to characterize the burning behavior of the commodity, and larger test fires provided validation data with which to test the model predictions of the burning rate and flame spread behavior [61, 62]. Two to four tier configurations were evaluated. For the period of time prior to application of water, the simulated heat release rate was within 20 % of the experimental heat release rates. It should be noted that the model was very sensitive to the thermal parameters and the numerical grid when used to model the fire growth in the piled commodity tests.

High rack storage fires of pool chemicals were modeled by Olenick *et al.* [63] to determine the validity of sprinkler activation predictions of FDS. The model was compared to full-scale fires conducted in January, 2000 at Southwest Research Institute in San Antonio, Texas.

FDS has been used to study the behavior of a fire undergoing suppression by a water mist system. Kim and Ryou [64, 65] compared FDS predictions to results of compartment fire tests with and without the application of a water mist. The cooling and oxygen dilution were predicted to within about 10 % of the measurements, but the simulations failed to predict the complete extinguishment of a hexane pool fire. The authors suggest that this is a result of the combustion model rather than the spray or droplet model.

Another study of water mist suppression using FDS was conducted by Hume at the University of Canterbury, Christchurch, New Zealand [66]. Full-scale experiments were performed in which a fine water mist was combined with a displacement ventilation system to protect occupants and electrical equipment in the event of a fire. Simulations of these experiments with FDS showed qualitative agreement, but the version of the model used in the study (version 3) was not able to predict accurately the decrease in heat release rate of the fire.

Hostikka and McGrattan [67] evaluated the absorption of thermal radiation by water sprays. They considered two sets of experimental data and concluded that FDS has the ability to predict the attenuation of thermal radiation “when the hydrodynamic interaction between the droplets is weak.” However, modeling interacting sprays would require a more costly coalescence model. They also note that the results of the model were sensitive to grid size, angular discretization, and droplet sampling.

Airflows in Fire Compartments

Friday studied the use of FDS in large scale mechanically ventilated spaces. The ventilated enclosure was provided with air injection rates of 1 to 12 air changes per hour and a fire with heat release rates ranging from 0.5 MW to 2 MW. The test measurements and model output were compared to assess the accuracy of FDS [68]. These simulations have been repeated with the latest version of FDS and reported in this Guide under the heading “FM/SNL Test Series.”

Zhang *et al.* [69] utilized the FDS model to predict turbulence characteristics of the flow and temperature fields due to fire in a compartment. The experimental data was acquired through tests that replicated a half-scale ISO Room Fire Test. Two cases were explored – the heat source in the center of the room and the heat source adjacent to a wall. In both cases, the heat source was a heating element with an output of 12 kW/m². The predicted intensity of the temperature fluctuation “agree[d] very well” at all points except those directly adjacent to the burner. The turbulent heat flux was found to be larger in the region above the heat source.

Tunnel Fires

Cochard [70] used FDS to study the ventilation within a tunnel. He compared the model results with a full-scale tunnel fire experiment conducted as part of the Massachusetts Highway Department Memorial Tunnel Fire Ventilation Test Program. The test consisted of a single point supply of fresh air through a 28 m² opening in a 135 m tunnel. The ventilation was started 2 min after the ignition of a 40 MW fire. Fifteen temperature measurement trees were placed within the tunnel and replicated within the model. Depending on location, the difference between predicted and measured temperature rise ranged from 10 % to 20 %.

McGrattan and Hamins [71] also applied FDS to simulate two of the Memorial Tunnel Fire Tests as validation for the use of the model in studying an actual fire in the Howard Street Tunnel, Baltimore, Maryland, July 2001. The experiments chosen for the comparison were unventilated. One experiment was a 20 MW fire; the other a 50 MW fire. FDS predictions of peak near-ceiling temperatures were within 50 °C of the measured peak temperatures, which were 600 °C and 800 °C, respectively.

Piergoirgio *et al.* [72] provided a qualitative analysis of FDS applied to a truck fire within a tunnel. The goal of their analysis was to describe the spread of the toxic gases within the tunnels, to determine the places not involved in the spreading of combustion products and to quantify the oxygen, carbon monoxide and hydrochloric acid concentrations during the fire.

Edwards *et al.* [73, 74] used FDS to determine the critical air velocity for smoke reversal in a tunnel as a function of the fire intensity, and his results compared favorably with experimental results. In a further study, Edwards and Hwang [75] applied FDS to study fire spread along combustibles in a ventilated mine entry. Analyses such as these are intended for planning and implementation of ventilation changes during mine fire fighting and rescue operations.

Smoke Detection

The ability of version 1 of FDS to accurately predict smoke detector activation was studied by D'Souza [76]. The smoke transport model within FDS was tested and compared with UL 217 test data. The second step in this research was to further validate the model with full-scale multi-compartment fire tests. The results indicated that FDS is capable of predicting smoke detector activation when used with smoke detector lag correlations that correct for the time delay associated with smoke having to penetrate the detector housing. A follow-up paper by Zhang *et al.* [77] describes the implementation and validation of the smoke detector algorithm currently incorporated in FDS.

Another study of smoke detector activation was carried out by Brammer at the University of Canterbury, New Zealand [78]. Two fire tests from a series performed in a two-story residence were simulated, and smoke detector activation times were predicted using three different methods. The methods consisted of either a temperature correlation, a time-lagged function of the optical density, or a thermal device much like a heat detector. The purpose was to identify ways to reliably predict smoke detector activation using typical model output like temperature and smoke concentration. It was remarked that simulating the early stage of the fire is critical to reliable prediction.

Cleary [79] also provided a comparison between FDS computed gas velocity, temperature and concentrations at various detector locations. The research concluded that multi-room fire simulations with the FDS model can accurately predict the conditions that a sensor might experience during a real fire event. The FDS model was able to predict the smoke and gas concentrations, heat, and flow velocities at various detector locations to within 15 % of measurements.

Combustion Model

A few studies have been performed comparing direct numerical simulations (DNS) of a simple burner flame to laboratory experiments [80]. Another study compared DNS calculations of a counterflow diffusion flames to experimental measurements and the results of a one-dimensional multi-step kinetics model [81].

Bundy, Dillon and Hamins [82, 83] studied the use of FDS in providing data and correlations for fire investigators to support their investigations. A paraffin wax candle was placed within a 0.61 m by 0.61 m by 0.76 m plexi-glass enclosure. The chamber was raised 20 mm off the surface to reveal 44 uniformly spaced 6 mm diameter holes. The holes provided oxygen to the flame without subjecting the flame to a draft. A 150 mm hole was provided at the top of the enclosure to allow for the heat and combustion products to exit the space. The heat flux from the candle flame was modeled with FDS. The model provides a prediction of the heat flux of the candle at a height of 56 mm above the base of the flame with an accuracy of 5 %. The flux is under predicted by 16 % at 76 mm above the base of the flame. The remainder of the predictions show flux measurements were under-predicted by 15 % to 40 % of the measured values.

Floyd *et al.* [84, 49] compared the radiation model of FDS version 2 with full-scale data from the Virginia Tech Fire Research Laboratory (VTFRL). The test compartment was outfitted with equipment capable

of taking temperature, air velocity, gas concentrations, unburned hydrocarbon and heat flux measurements. The test facility consisted of a single compartment geometrically similar to the ISO 9705 standard compartment with dimensions of 1.2 m by 1.8 m by 1.2 m in height. The ceiling and walls were constructed of fiberboard over a steel shell with a floor of concrete. Three baseline experiments were completed with fires ranging in size from 90 kW to 440 kW. Overall, FDS predicted the temperatures to within 15 % of the measured temperatures. The FDS velocity measurements followed the trend of the test data but did not replicate it. The outgoing velocities were under-predicted by 30 % to 40 % and the incoming velocities were over-predicted by 40 %. FDS predicted the heat flux gauge response to within 10 % of the measured values. The radiation model in FDS predicted the measured fluxes to within 15 %.

Xin and Gore [85] compared FDS predictions and measurements of the spectral radiation intensities of small fires. The fuel flow rates for methane and ethylene burners were selected so that the Froude numbers matched that of liquid toluene pool fires. The heat release rate was 4.2 kW for the methane flame and 3.4 kW for the ethylene flame. Line of sight spectral radiation intensities were measured at six downstream locations. The spectral radiation intensity calculations were performed by post-processing the transient scalar distributions provided by FDS.

Zhang *et al.* [86] compared the experimental results of a circular methane gas burner to predictions computed by FDS. The compartment was 2.8 m by 2.8 m by 2.2 m high with natural ventilation from a standard door.

2.2.4 Comparison with Standard Tests

Standard fire tests are performed at various testing laboratories and universities around the world. While most were not designed as validation tools, they nevertheless can be used as relatively simple, well characterized fire experiments.

An extensive amount of validation work with FDS version 4 has been performed by Hietaniemi, Hostikka, and Vaari at VTT, Finland [35]. The case studies are comprised of fire experiments ranging in scale from the cone calorimeter (ISO 5660-1, 2002) to full-scale fire tests such as the room corner test (ISO 9705, 1993). Comparisons are also made between FDS 4 results and data obtained in the SBI (Single Burning Item) Euro-classification test apparatus (EN 13823, 2002) as well as data obtained in two *ad hoc* experimental configurations: one is similar to the room corner test but has only partial linings and the other is a space to study fires in building cavities. In the study of upholstered furniture, the experimental configurations are the cone and furniture calorimeters, and the ISO room. For liquid pool fires, comparison is made to data obtained by numerous researchers. The burning materials include spruce timber, MDF (Medium Density Fiber) board, PVC wall carpet, upholstered furniture, cables with plastic sheathing, and heptane.

The scope of the VTT work is considerable. Assessing the accuracy of the model must be done on a case by case basis. In some cases, predictions of the burning rate of the material were based solely on its fundamental properties, as in the heptane pool fire simulations. In other cases, some properties of the material are unknown, as in the spruce timber simulations. Thus, some of the simulations are true predictions, some are calibrations. The intent of the authors was to provide guidance to engineers using the model as to appropriate grid sizes and material properties. In many cases, the numerical grid was made fairly coarse to account for the fact that in practice, FDS is used to model large spaces of which the fuel may only comprise a small fraction.

2.2.5 Comparison with Documented Fire Experience

Documented fire experience includes known behavior of materials in fires, eyewitness accounts of real fires, observed post fire conditions, and other means. To date, several actual fires have been reconstructed using FDS. One case study performed by NIST is documented in Ref. [87]. Two fire fighters were killed and one

severely injured in a townhouse fire in Washington, D.C. during the evening of May 30, 1999. Questions arose about the injuries the fire fighters had sustained, the lack of thermal damage in the living room where a fallen fire fighter was found and why the fire fighters never opened their hose lines to protect themselves or to extinguish the fire.

To answer some of the questions, a rectangular volume of 10 m by 6 m by 5.1 m was divided into 76,500 cells in the FDS model. The FDS results that best replicated the observed fire behavior indicated that the opening of the basement sliding glass door provided oxygen to a pre-heated, under-ventilated fire. Flashover was estimated to occur in less than 60 s following the entry of fire fighters into the basement. The resulting fire gases flowed up the basement stairs and moved across the living room ceiling towards the back wall of the townhouse. These hot gases came in direct contact with the fire fighters who were killed. The hot gases traversed the townhouse in less than 2 s, giving the fire fighters little time to respond. The model showed that the oxygen level was too low to support flaming and, therefore, the fire fighters did not have a visual cue of the thermal conditions until it was too late. Results of the FDS study were shared with the D.C. fire department and have been made available via a multi-media CD-ROM to other fire departments across the country.

Another case study performed at NIST involved a fire in a Houston restaurant [88]. On the morning of February 14, 2000, a fire started in the office area of a fast food restaurant. Two fire fighters died when the roof collapsed. The FDS model was used to simulate the fire. The fuel was assumed to be the contents of a typical office, and the fire was assumed to have a slowly growing heat release rate peaking at 6 MW. Multiple vents were modeled and the time at which they opened replicated the fire fighters' actions after arrival. The model provided a visual representation of the fire during the initial phases until the collapse of the roof.

NIST also performed a case study on a fire that killed three children and three fire fighters on the morning of December 22, 1999 [89]. The fire started on top of a stove in a two-story residence. FDS was used to simulate the fire. The fuel packages consisted of several furniture items in the kitchen and living room with heat release rates reaching 5.2 MW. The model results indicated the critical event in the fire was flashover of the kitchen. The fire became a multi-room event after flashover with temperatures increasing to over 600 °C. The hot gases spread quickly from the living room to the stairway on the second floor trapping the fire fighters.

Outside of NIST, FDS has been used to investigate many actual fires, but very few of these studies are documented in the literature. Exceptions include a study by Rein *et al.* [90] looking at several fire events using an analytical fire growth model, the NIST zone model CFAST, and FDS. A similar study was performed several years earlier by Spearpoint *et al.* [91] as a class exercise at the University of Maryland. During the SFPE Professional Development Week in the fall of 2001, a workshop was held in which several engineers related their experiences using FDS as a forensic tool [92]. The role of carbon monoxide in the deaths of three fire fighters was studied by Christensen and Icove [93].

Chapter 3

Description of Experiments

This chapter contains a brief description of the experiments that were used for model validation. Only enough detail is included here to provide a general understanding of the model simulations. Anyone wishing to use the experimental measurements for validation ought to consult the cited test reports for a comprehensive description.

3.1 VTT Large Hall Tests

The experiments are described in Ref. [94]. The series consisted of 8 experiments, but because of replicates only three unique fire scenarios. The experiments were undertaken to study the movement of smoke in a large hall with a sloped ceiling. The tests were conducted inside the VTT Fire Test Hall, with dimensions of 19 m high by 27 m long by 14 m wide. Each test involved a single heptane pool fire, ranging from 2 MW to 4 MW. Four types of predicted output were used in the present evaluation – the HGL temperature and depth, average flame height and the plume temperature. Three vertical arrays of thermocouples (TC), plus two thermocouples in the plume, were compared to FDS predictions. The HGL temperature and height were reduced from an average of the three TC arrays using the standard algorithm described in Chapter 4. The ceiling jet temperature was not considered, because the ceiling in the test hall is not flat, and the standard model algorithm is not appropriate for this geometry.

The VTT test report lacks some information needed to model the experiments, which is why some information was based on private communications with the principal investigator, Simo Hostikka.

Surface Materials: The walls and ceiling of the test hall consist of a 1 mm thick layer of sheet metal on top of a 5 cm layer of mineral wool. The floor was constructed of concrete. The report does not provide thermal properties of these materials.

Natural Ventilation: In Cases 1 and 2, all doors were closed, and ventilation was restricted to infiltration through the building envelope. Precise information on air infiltration during these tests is not available. The scientists who conducted the experiments recommend a leakage area of about 2 m^2 , distributed uniformly throughout the enclosure. By contrast, in Case 3, the doors located in each end wall (Doors 1 and 2, respectively) were open to the external ambient environment. These doors are each 0.8 m wide by 4 m high, and are located such that their centers are 9.3 m from the south wall.

Mechanical Ventilation: The test hall has a single mechanical exhaust duct, located in the roof space, running along the center of the building. This duct had a circular section with a diameter of 1 m, and opened horizontally to the hall at a distance of 12 m from the floor and 10.5 m from the west wall. Mechanical exhaust ventilation was operational for Case 3, with a constant volume flow rate of $11 \text{ m}^3/\text{s}$ drawn through the exhaust duct.

Heat Release Rate: Each test used a single liquid fuel pan with its center located 16 m from the west wall and 7.4 m from the south wall. For all tests, the fuel was heptane in a circular steel pan that was partially filled with water. The pan had a diameter of 1.17 m for Case 1 and 1.6 m for Cases 2 and 3. In each case, the fuel surface was 1 m above the floor. The trays were placed on load cells, and the HRR was calculated from the mass loss rate. For the three cases, the fuel mass loss rate was averaged from individual replicate tests. In the HRR estimation, the heat of combustion (taken as 44,600 kJ/kg) and the combustion efficiency for n-heptane was used. Hostikka suggests a value of 0.8 for the combustion efficiency. Tewarson reports a value of 0.93 for a 10 cm pool fire [95]. For the calculations reported in the current study, a combustion efficiency of 0.85 is assumed. In general, an uncertainty of 15 % has been assumed for the reported HRR of most of the large scale fire experiments used.

Radiative Fraction: The radiative fraction was assumed to be 0.35, similar to many smoky hydrocarbons.

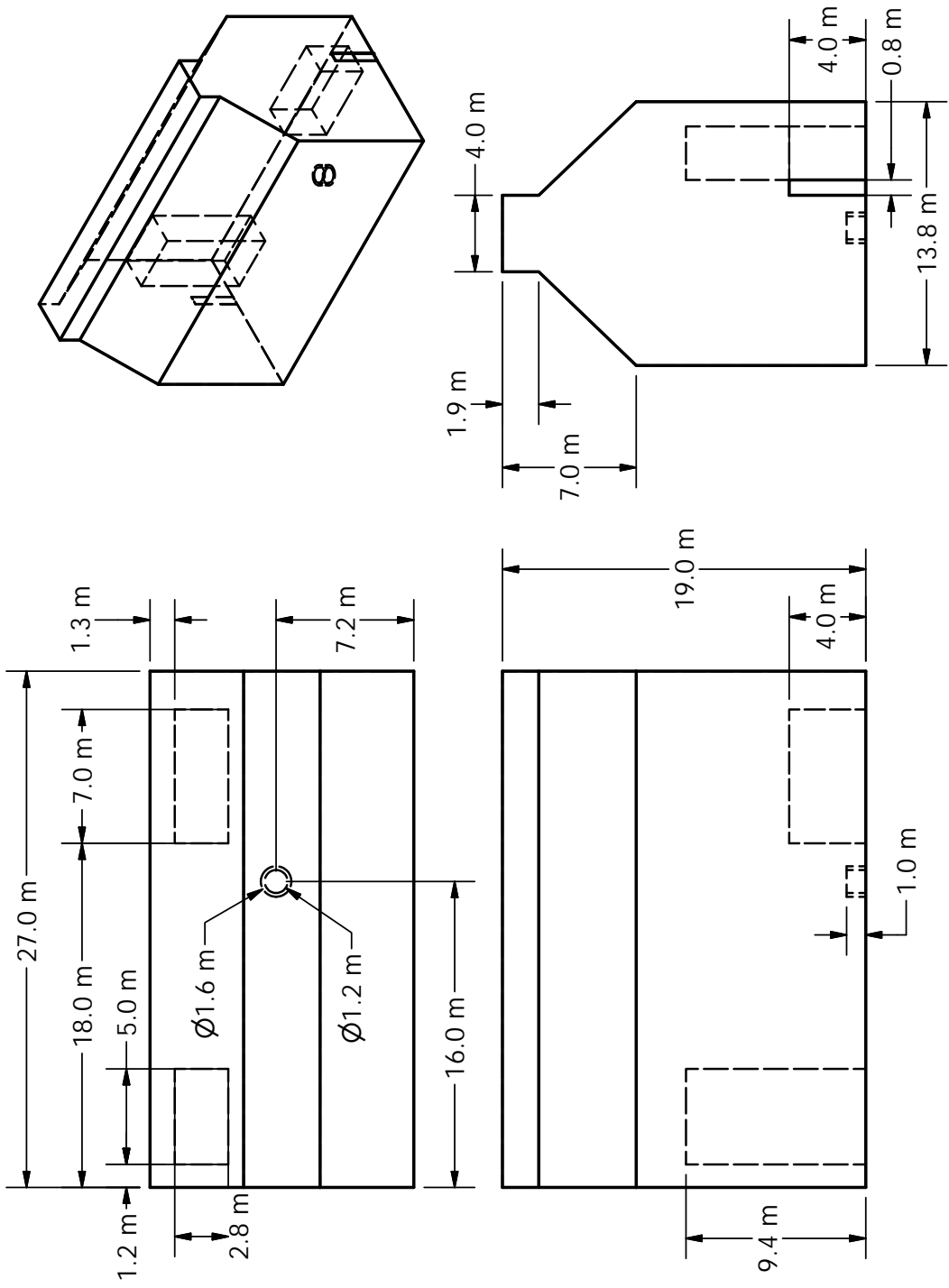


Figure 3.1: Geometry of the VTT Large Fire Test Hall.

3.2 UL/NFPRF Sprinkler, Vent, and Draft Curtain Study

In January, 1997, a series of 22 heptane spray burner experiments was conducted at the Large Scale Fire Test Facility at Underwriters Laboratories (UL) in Northbrook, Illinois [96]. The objective of the experiments was to characterize the temperature and flow field for fire scenarios with a controlled heat release rate in the presence of sprinklers, draft curtains and a single smoke & heat vent. The Large Scale Fire Test Facility at UL contains a 37 m by 37 m (120 ft by 120 ft) main fire test cell, equipped with a 30.5 m by 30.5 m (100 ft by 100 ft) adjustable height ceiling. The layout of the experiments is shown in Fig. 3.2. One 1.2 m by 2.4 m (4 ft by 8 ft) vent was installed among 49 upright sprinklers on a 3 m by 3 m (10 ft by 10 ft) spacing.

Ceiling: The ceiling was raised to a height of 7.6 m and instrumented with thermocouples and other measurement devices. The ceiling was constructed of 0.6 m by 1.2 m by 1.6 cm UL fire-rated Armstrong Ceramaguard (Item 602B) ceiling tiles. The manufacturer reported the thermal properties of the material to be: specific heat 753 J/(kg·K), thermal conductivity 0.0611 W/(m·K), and density 313 kg/m³.

Draft Curtains: Sheet metal, 1.2 mm thick and 1.8 m deep, was suspended from the ceiling for 16 of the 22 tests, enclosing an area of about 450 m² and 49 sprinklers.

Sprinklers: Central ELO-231 (Extra Large Orifice) uprights were used for all the tests. The orifice diameter of this sprinkler is reported by the manufacturer to be nominally 1.6 cm (0.64 in), the reference actuation temperature is reported by the manufacturer to be 74°C (165°F). The RTI (Response Time Index) and C-factor (Conductivity factor) were reported by UL to be $148 \text{ (m}\cdot\text{s)}^{\frac{1}{2}}$ and $0.7 \text{ (m/s)}^{\frac{1}{2}}$, respectively [96]. When installed, the sprinkler deflector was located 8 cm below the ceiling. The thermal element of the sprinkler was located 11 cm below the ceiling. The sprinklers were installed with nominal 3 m by 3 m (exact 10 ft by 10 ft) spacing in a system designed to deliver a constant 0.34 L/(s·m²) (0.50 gpm/ft²) discharge density when supplied by a 131 kPa (19 psi) discharge pressure

Vent: A single UL listed double leaf fire vent with steel covers and steel curb was installed in the adjustable height ceiling in the position shown in Fig. 3.2. The vent is designed to open manually or automatically. The vent doors were recessed into the ceiling about 0.3 m (1 ft).

Heat Release Rate: The heptane spray burner consisted of a 1 m by 1 m square of 1.3 cm pipe supported by four cement blocks 0.6 m off the floor. Four atomizing spray nozzles were used to provide a free spray of heptane that was then ignited. For all but one of the tests, the total heat release rate from the fire was manually ramped up following a “t-squared” curve to a steady-state in 75 s (150 s was used in Test I-16). The fire growth curve was followed until a specified fire size was reached or the first sprinkler activated. After either of these events, the fire size was maintained at that level until conditions reached roughly a steady state, *i.e.* the temperatures recorded near the ceilings remained steady and no more sprinkler activations occurred. The heat release rate from the burner was confirmed by placing it under the large product calorimeter at UL, ramping up the flow of heptane in the same manner as in the tests, and measuring the total and convective heat release rates. It was found that the convective heat release rate was 0.65 ± 0.02 of the total.

Instrumentation: The instrumentation for the tests consisted of thermocouples, gas analysis equipment, and pressure transducers. The locations of the instrumentation are referenced in the plan view of the facility (Fig. 3.2). Temperature measurements were recorded at 104 locations. Type K 0.0625 in diameter Inconel sheathed thermocouples were positioned to measure (i) temperatures near the ceiling, (ii) temperatures of the ceiling jet, and (iii) temperatures near the vent.

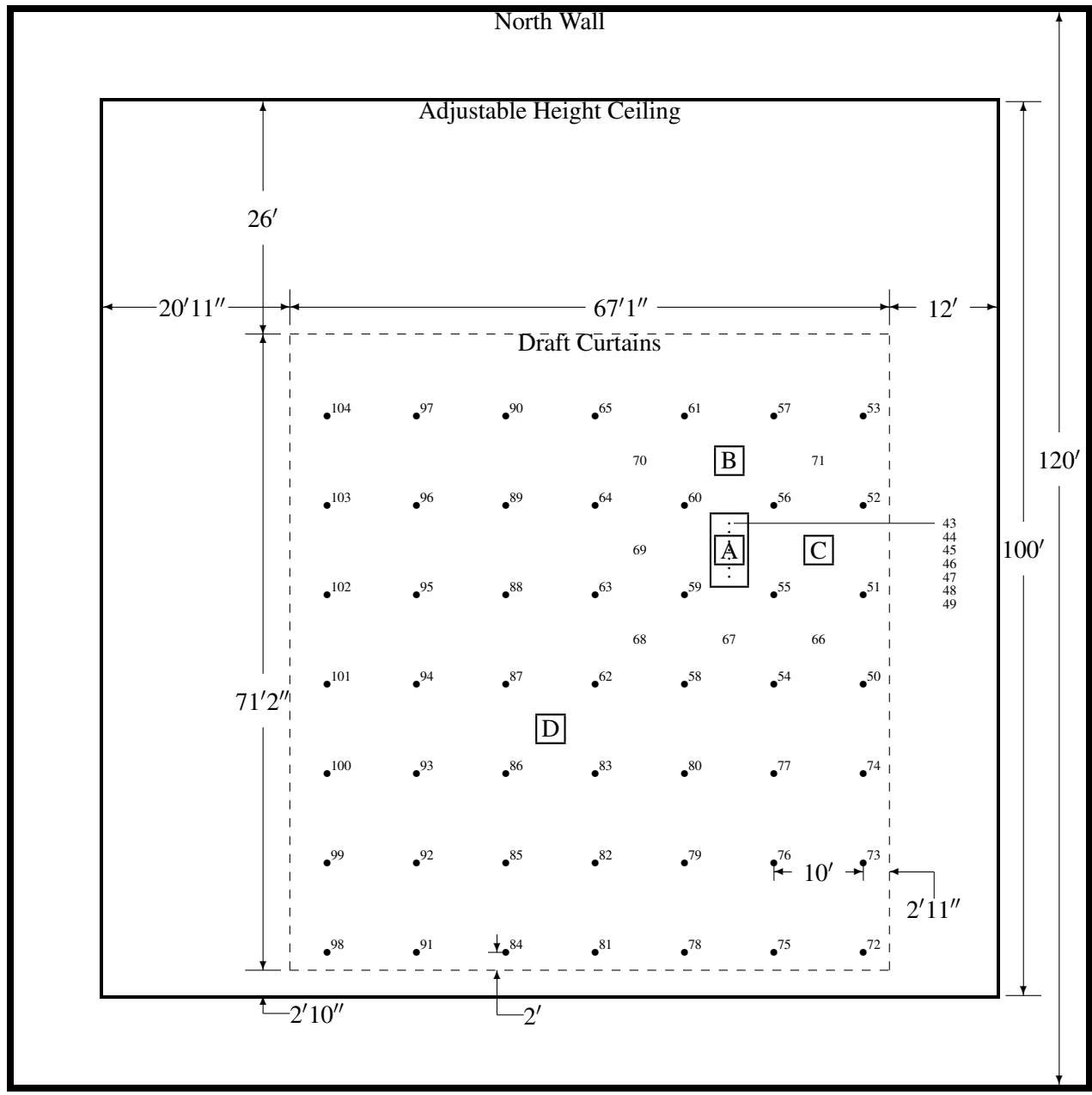


Figure 3.2: Plan view of the UL/NFPRF Experiments. The sprinklers are indicated by the solid circles and are spaced 3 m apart. The number beside each sprinkler location indicates the channel number of the nearest thermocouple. The vent dimensions are 4 ft by 8 ft. The boxed letters A, B, C and D indicate burner positions. Corresponding to each burner position is a vertical array of thermocouples. Thermocouples 1–9 hang 7, 22, 36, 50, 64, 78, 92, 106 and 120 in from the ceiling, respectively, above Position A. Thermocouples 10 and 11 are positioned above and below the ceiling tile directly above Position B, followed by 12–20 that hang at the same levels below the ceiling as 1–9. The same pattern is followed at Positions C and D, with thermocouples 21–31 at C and 32–42 at D.

3.3 NIST/NRC Test Series

These experiments, sponsored by the US NRC and conducted at NIST, consisted of 15 large-scale experiments performed in June 2003. All 15 tests were included in the validation study. The experiments are documented in Ref. [97]. The fire sizes ranged from 350 kW to 2.2 MW in a compartment with dimensions 21.7 m by 7.1 m by 3.8 m high, designed to represent a compartment in a nuclear power plant containing power and control cables. The walls and ceiling were covered with two layers of marinate boards, each layer 0.0125 m thick. The floor was covered with one layer of gypsum board on top of a layer of plywood. Thermo-physical and optical properties of the marinate and other materials used in the compartment are given in Ref. [97]. The room had one door and a mechanical air injection and extraction system. Ventilation conditions, the fire size, and fire location were varied. Numerous measurements (approximately 350 per test) were made including gas and surface temperatures, heat fluxes and gas velocities.

Following are some notes provided by Anthony Hamins, who conducted the experiments:

Natural Ventilation: The compartment had a 2 m by 2 m door in the middle of the west wall. Some of the tests had a closed door and no mechanical ventilation (Tests 2, 7, 8, 13, and 17), and in those tests the measured compartment leakage was an important consideration. The test report lists leakage areas based on measurements performed prior to Tests 1, 2, 7, 8, and 13. For the closed door tests, the leakage area used in the simulations was based on the last available measurement. The chronological order of the tests differed from the numerical order. For Test 4, the leakage area measured before Test 2 was used. For Tests 10 and 16, the leakage area measured before Test 7 was used.

Mechanical Ventilation: The mechanical ventilation and exhaust was used during Tests 4, 5, 10, and 16, providing about 5 air changes per hour. The door was closed during Test 4 and open during Tests 5, 10, and 16. The supply duct was positioned on the south wall, about 2 m off the floor. An exhaust duct of equal area to the supply duct was positioned on the opposite wall at a comparable location. The flow rates through the supply and exhaust ducts were measured in detail during breaks in the testing, in the absence of a fire. During the tests, the flows were monitored with single bi-directional probes during the tests themselves.

Heat Release Rate: A single nozzle was used to spray liquid hydrocarbon fuels onto a 1 m by 2 m fire pan that was about 0.1 m deep. The test plan originally called for the use of two nozzles to provide the fuel spray. Experimental observation suggested that the fire was less unsteady with the use of a single nozzle. In addition, it was observed that the actual extent of the liquid pool was well-approximated by a 1 m circle in the center of the pan. For safety reasons, the fuel flow was terminated when the lower-layer oxygen concentration dropped to approximately 15 % by volume. The fuel used in 14 of the tests was heptane, while toluene was used for one test. The HRR was determined using oxygen consumption calorimetry. The recommended uncertainty values were 17 % for all of the tests.

Radiative Fraction: The value of the radiative fraction and its uncertainty were reported as 0.44 and 0.40 for heptane and toluene, respectively.

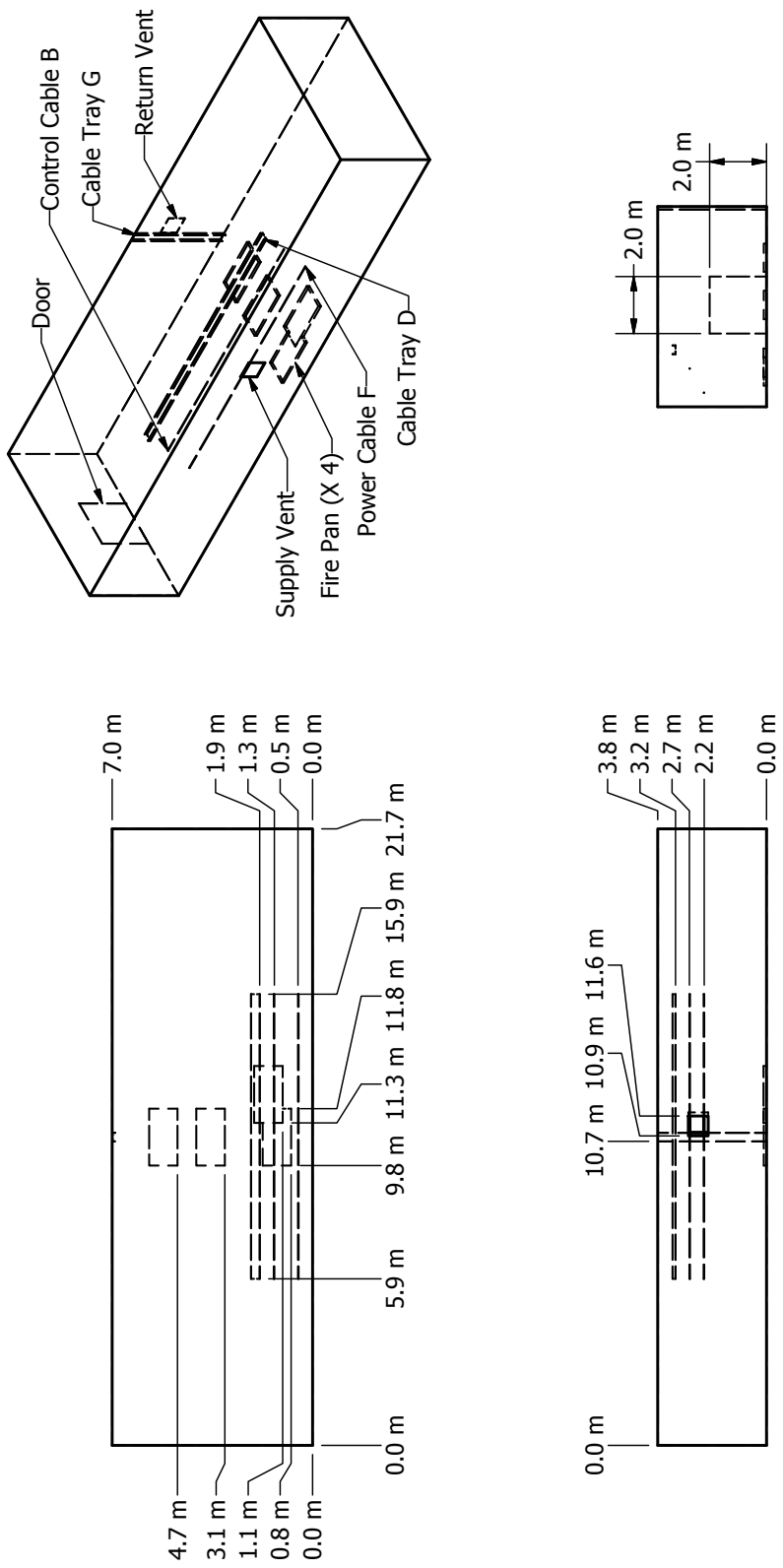


Figure 3.3: Geometry of the NIST/NRC Experiments.

3.4 WTC Spray Burner Test Series

As part of its investigation of the World Trade Center disaster, the Building and Fire Research Laboratory at NIST conducted several series of fire experiments to both gain insight into the observed fire behavior and also to validate FDS for use in reconstructing the fires. The first series of experiments involved a relatively simple compartment with a liquid spray burner and various structural elements with varying amounts of sprayed fire-resistive materials (SFRM). A complete description of the experiments can be found in the NIST WTC report NCSTAR 1-5B [23]. The overall enclosure was rectangular, as were the vents and most of the obstructions. The compartment walls and ceiling were made of 2.54 cm thick marinite. The manufacturer provided the thermal properties of the material used in the calculation. The density was 737 kg/m³, conductivity 0.12 W/m/K. The specific heat ranged from 1.17 kJ/kg/K at 93 °C to 1.42 kJ/kg/K at 425 °C. This value was assumed for higher temperatures. The steel used to construct the column and truss flanges was 0.64 cm thick. The density of the steel was assumed to be 7,860 kg/m³; its specific heat 0.45 kJ/kg/K.

Two fuels were used in the tests. The properties of the fuels were obtained from measurements made on a series of unconfined burns that are referenced in the test report. The first fuel was a blend of heptane isomers, C₇H₁₆. Its soot yield was set at a constant 1.5 %. The second fuel was a mixture (40 % - 60 % by volume) of toluene, C₇H₈, and heptane. Because FDS only considers the burning of a single hydrocarbon fuel, the mixture was taken to be C₇H₁₂ with a soot yield of 11.2 %. The radiative fraction for the heptane blend was 0.44; for the heptane/toluene mixture it was 0.39. The heat release rate of the simulated burner was set to that which was measured in the experiments. The spray burner was modeled using reported properties of the nozzle and liquid fuel droplets.

3.5 FM/SNL Test Series

The Factory Mutual and Sandia National Laboratories (FM/SNL) test series was a series of 25 fire tests conducted in 1985 for the U.S. Nuclear Regulatory Commission (NRC) by Factory Mutual Research Corporation (FMRC), under the direction of Sandia National Laboratories (SNL) [98, 99]. The primary purpose of these tests was to provide data with which to validate computer models for various types of compartments typical of nuclear power plants. The experiments were conducted in an enclosure measuring approximately 18 m long x 12 m wide x 6 m high, constructed at the FMRC fire test facility in Rhode Island. All of the tests involved forced ventilation to simulate typical power plant operations. Four of the tests were conducted with a full-scale control room mockup in place. Parameters varied during the experiments included fire intensity, enclosure ventilation rate, and fire location.

The current study used data from three experiments (Tests 4, 5, and 21). In these tests, the fire source was a propylene gas burner with a diameter of approximately 0.9 m, with its rim located approximately 0.1 m above the floor. For Tests 4 and 5, the burner was positioned on the longitudinal axis centerline, 6.1 m from the nearest wall. For Test 21, the fire source was placed within a simulated electrical cabinet.

Following is supplemental information provided by the test director, Steve Nowlen of Sandia National Laboratory:

Heat Release Rate: The HRR was determined using oxygen consumption calorimetry in the exhaust stack with a correction applied for the carbon dioxide in the upper layer of the compartment. The uncertainty of the fuel mass flow was not documented. All three tests selected for this study had the same target peak heat release rate of 516 kW following a 4 min “t-squared” growth profile. The test report contains time histories of the measured HRR, for which the average, sustained HRR following the ramp up for Tests 4, 5, and 21 have been estimated as 510 kW, 480 kW, and 470 kW, respectively. Once reached, the peak HRR was maintained essentially constant during a steady-burn period of 6 min in Tests 4 and

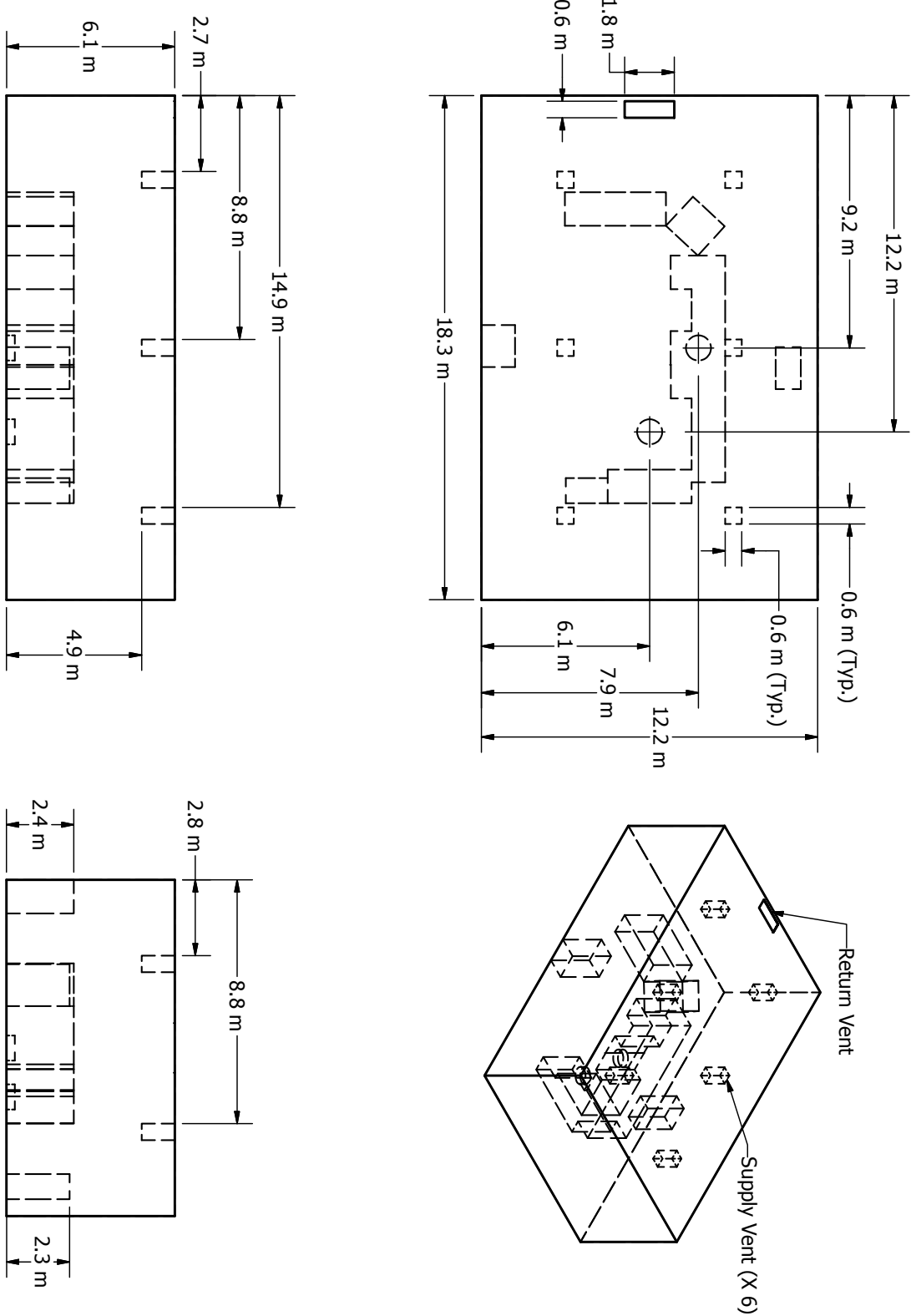
5, and 16 min in Test 21. Note that in Test 21, Nowlen reports a “significant” loss of effluent from the exhaust hood that could lead to an under-estimate of the HRR towards the end of the experiment.

Radiative Fraction: The radiative fraction was not measured during the experiment, but in this study it is assumed to equal 0.35, which is typical for a smoky hydrocarbons. It was further assumed that the radiative fraction was about the same in Test 21 as the other tests, as fuel burning must have occurred outside of the electrical cabinet in which the burner was placed.

Measurements: Four types of measurements were conducted during the FM/SNL test series that are used in the current model evaluation study, including the HGL temperature and depth, and the ceiling jet and plume temperatures. Aspirated thermocouples (TCs) were used to make all of the temperature measurements. Generally, aspirated TC measurements are preferable to bare-bead TC measurements, as systematic radiative exchange measurement error is reduced.

HGL Depth and Temperature: Data from all of the vertical TC trees were used when reducing the HGL height and temperature. For the FM/SNL Tests 4 and 5, Sectors 1, 2, and 3 were used, all weighted evenly. For Test 21, Sectors 1 and 3 were used, evenly weighted. Sector 2 was partially within the fire plume in Test 21.

Figure 3.4: Geometry of the FM/SNL Experiments.



3.6 NBS Multi-Room Test Series

The National Bureau of Standards (NBS, which is now called the National Institute of Standards and Technology, NIST) Multi-Room Test Series consisted of 45 fire tests representing 9 different sets of conditions were conducted in a three-room suite. The experiments were conducted in 1985 and are described in detail in Ref. [100]. The suite consisted of two relatively small rooms, connected via a relatively long corridor. The fire source, a gas burner, was located against the rear wall of one of the small compartments. Fire tests of 100 kW, 300 kW and 500 kW were conducted. For the current study, only three 100 kW fire experiments have been used, including Test 100A from Set 1, Test 100O from Set 2, and Test 100Z from Set 4. These tests were selected because they had been used in prior validation studies, and because these tests had the steadiest values of measured heat release rate during the steady-burn period.

Following is additional information provided by the test director, Richard Peacock of NIST:

Heat Release Rate: In the two tests for which the door was open, the HRR during the steady-burn period measured via oxygen consumption calorimetry was 110 kW with an uncertainty of about 15 %, consistent with the replicate measurements made during the experimental series and the uncertainty typical of oxygen consumption calorimetry. It was assumed that the closed door test (Test 100O) had the same HRR as the open door tests.

Radiative Fraction: Natural gas was used as the fuel in Test 100A. In Tests 100O and 100Z, acetylene was added to the natural gas to increase the smoke yield, and as a consequence, the radiative fraction increased. The radiative fraction of natural gas has been studied previously, whereas the radiative fraction of the acetylene/natural gas mixture has not been studied. The radiative fraction for the natural gas fire was assigned a value of 0.20, whereas a value of 0.30 was assigned for the natural gas/acetylene fires.

Measurements: Only two types of measurements conducted during the NBS test series were used in the evaluation considered here, because there was less confidence in the other measurements. The measurements considered here were the HGL temperature and depth, in which bare bead TCs were used to make these measurements. Single point measurements of temperature within the burn room were not used in the evaluation of plume or ceiling jet algorithms. This is because the geometry was not consistent in either case with the assumptions used in the model algorithms of plumes or jets. Specifically, the burner was mounted against a wall, and the room width-to-height ratio was less than that assumed by the various ceiling jet correlations.

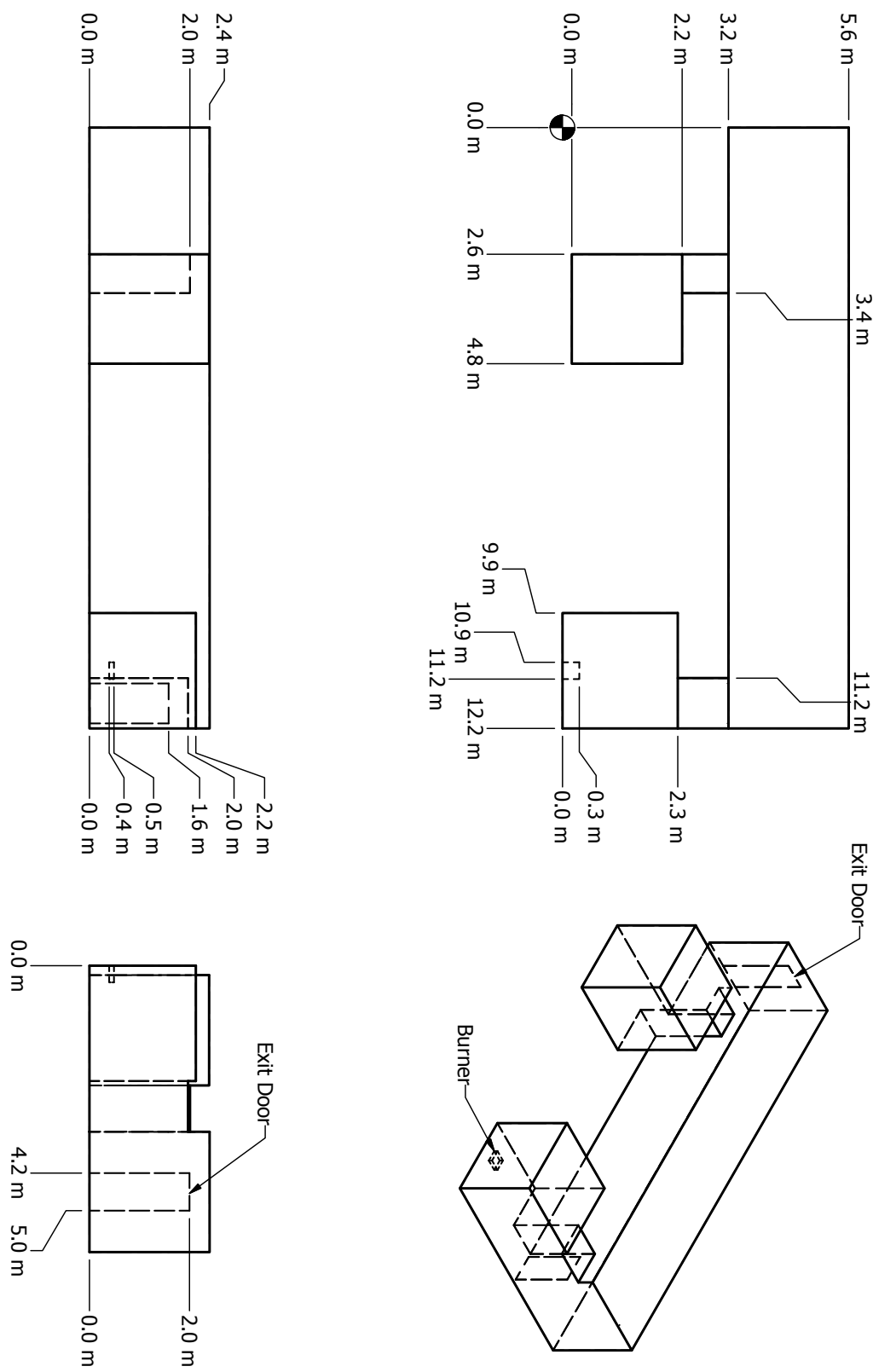


Figure 3.5: Geometry of the NBS Multi-Room Experiments.

3.7 Steckler Compartment Experiments

Steckler, Quintiere and Rinkinen performed a set of 55 compartment fire tests at NBS in 1979. The compartment was 2.8 m by 2.8 m by 2.18 m high, with a single door of various widths, or alternatively a single window with various heights. A 30 cm diameter methane burner was used to generate fires with heat release rates of 31.6 kW, 62.9 kW, 105.3 kW and 158 kW. Vertical profiles of velocity and temperature were measured in the doorway, along with a single vertical profile of temperature within the compartment. A full description and results are reported in Reference [102]. The basic test matrix is listed in Table 3.1.

Table 3.1: Summary of Steckler compartment experiments.

Test	Opening Width (m)	Opening Height (m)	HRR \dot{Q} (kW)	Burner Location	Test	Opening Width (m)	Opening Height (m)	HRR \dot{Q} (kW)	Burner Location
10	0.24	1.83	62.9	Center	224	0.74	0.92	62.9	Back Corner
11	0.36	1.83	62.9	Center	324	0.74	0.92	62.9	Back Corner
12	0.49	1.83	62.9	Center	220	0.74	1.83	31.6	Back Corner
612	0.49	1.83	62.9	Center	221	0.74	1.83	105.3	Back Corner
13	0.62	1.83	62.9	Center	514	0.24	1.83	62.9	Back Wall
14	0.74	1.83	62.9	Center	544	0.36	1.83	62.9	Back Wall
18	0.74	1.83	62.9	Center	512	0.49	1.83	62.9	Back Wall
710	0.74	1.83	62.9	Center	542	0.62	1.83	62.9	Back Wall
810	0.74	1.83	62.9	Center	610	0.74	1.83	62.9	Back Wall
16	0.86	1.83	62.9	Center	510	0.74	1.83	62.9	Back Wall
17	0.99	1.83	62.9	Center	540	0.86	1.83	62.9	Back Wall
22	0.74	1.38	62.9	Center	517	0.99	1.83	62.9	Back Wall
23	0.74	0.92	62.9	Center	622	0.74	1.38	62.9	Back Wall
30	0.74	0.92	62.9	Center	522	0.74	1.38	62.9	Back Wall
41	0.74	0.46	62.9	Center	524	0.74	0.92	62.9	Back Wall
19	0.74	1.83	31.6	Center	541	0.74	0.46	62.9	Back Wall
20	0.74	1.83	105.3	Center	520	0.74	1.83	31.6	Back Wall
21	0.74	1.83	158.0	Center	521	0.74	1.83	105.3	Back Wall
114	0.24	1.83	62.9	Back Corner	513	0.74	1.83	158.0	Back Wall
144	0.36	1.83	62.9	Back Corner	160	0.74	1.83	62.9	Center*
212	0.49	1.83	62.9	Back Corner	163	0.74	1.83	62.9	Back Corner*
242	0.62	1.83	62.9	Back Corner	164	0.74	1.83	62.9	Back Wall*
410	0.74	1.83	62.9	Back Corner	165	0.74	1.83	62.9	Left Wall*
210	0.74	1.83	62.9	Back Corner	162	0.74	1.83	62.9	Right Wall*
310	0.74	1.83	62.9	Back Corner	167	0.74	1.83	62.9	Front Center*
240	0.86	1.83	62.9	Back Corner	161	0.74	1.83	62.9	Doorway*
116	0.99	1.83	62.9	Back Corner	166	0.74	1.83	62.9	Front Corner*
122	0.74	1.38	62.9	Back Corner					* Raised burner

3.8 McCaffrey Plume Experiments

In 1979, at the National Bureau of Standards (now NIST), Bernard McCaffrey measured centerline temperature and velocity profiles above a porous, refractory burner. There were five distinct heat release rates, ranging from 14 kW to 57 kW. The fuel was natural gas. The burner was square, 0.3 m on each side. The results of the experiments are reported in Reference [101].

3.9 Smyth Slot Burner Experiment

Kermit Smyth *et al.* conducted diffusion flame experiments at NIST using a methane/air Wolfhard-Parker slot burner. The experiments are described in detail in Refs. [103, 104]. The Wolfhard-Parker slot burner consists of an 8 mm wide central slot flowing fuel surrounded by two 16 mm wide slots flowing dry air with 1 mm separations between the slots. The slots are 41 mm in length. Measurements were made of all major species and a number of minor species along with temperature and velocity. Experimental uncertainties have been reported as 5 % for temperature and 10 % to 20 % for the major species.

3.10 Beyler Hood Experiments

Craig Beyler performed a large number of experiments involving a variety of fuels, fire sizes, burner diameters, and burner distances beneath a hood [105]. The hood consisted of concentric cylinders separated by an air gap. The inner cylinder was shorter than the outer and this allowed combustion products to be removed uniformly from the hood perimeter. The exhaust gases were then analyzed to determine species concentrations. The burner could be raised and lowered with respect to the bottom edge of the hood. Based on the published measurement uncertainties, species errors are estimated at 6 %.

3.11 NIST Reduced Scale Enclosure Experiments

The CO production test series used the NIST Reduced Scale Enclosure (RSE) [106]. The RSE is a 40 % scaled version of the ISO 9705 compartment. It measures 0.98 m wide by 1.46 m deep by 0.98 m tall. The compartment contains a door centered on the small face that measures 0.48 m wide by 0.81 m tall. A 15 cm diameter natural gas burner was positioned in the center of the compartment. The burner was on a stand so that its top was 15 cm above the floor. Species measurements were made inside the upper layer of the compartment at the front near the door and near the rear of the compartment.

3.12 Hamins Methane Burner Experiments

Anthony Hamins *et al.* performed a series of tests on circular gas burners measuring the radial and vertical radiative heat flux profiles outside the flame region. The tests are described in [34]. Tests at three burner diameters, 0.10 m, 0.38 m and 1.0 m are used for validation.

3.13 NRL/HAI Wall Heat Flux Measurements

Back, Beyler, DiNenno and Tatem [107] measured the heat flux from 9 different sized propane fires set up against a wall composed of gypsum board. The experiments were sponsored by the Naval Research Laboratory and conducted by Hughes Associates, Inc., of Baltimore, Maryland. The square sand burner ranged in size from 0.28 m to 0.70 m, and the fires ranged in size from 50 kW to 520 kW.

3.14 Experimental Uncertainty

The documentation of the experiments described in this chapter have varying descriptions of the uncertainty in the reported measurements. However, in order to assess the accuracy of FDS, there must be some estimate of the combined effect of the uncertainty in the reported input parameters, like the heat release rate of the fire, and the reported measurement of the quantity of interest, like the hot gas layer (HGL) temperature.

In the US Nuclear Regulatory Commission Verification and Validation study [108], Hamins estimates the combined uncertainty of the quantities of interest for the large scale fire experiments under consideration (VTT, NIST/NRC, NBS Multi-Room, FM/SNL). The results are summarized in Table 3.2. These values were obtained by estimating the uncertainty of the HRR in large scale fire experiments to be on the order of 15 %. Using well-known empirical relationships between the predicted quantities and the HRR (and other relevant input parameters), Hamins estimates the uncertainty in the predicted quantities based on the uncertainty of the reported HRR. For example, the HGL temperature rise is roughly proportional to the HRR raised to the two-thirds power, thus a 15 % uncertainty in the HRR leads to a 10 % uncertainty in the FDS prediction. Combining this value (via a quadrature) with the uncertainty in the HGL temperature measurement itself leads to a combined uncertainty of 14 %.

Table 3.2: Summary of Hamins' uncertainty estimates.

Quantity	Combined Uncertainty (%)
HGL Temperature	14
HGL Depth	13
Ceiling Jet Temperature	16
Plume Temperature	14
Gas Concentrations	9
Smoke Concentration	33
Pressure with Ventilation	80
Pressure without Ventilation	40
Heat Flux	20
Surface Temperature	14

Chapter 4

HGL Temperature and Depth

FDS, like any CFD model, does not perform a direct calculation of the HGL temperature or height. These are constructs unique to two-zone models. Nevertheless, FDS does make predictions of gas temperature at the same locations as the thermocouples in the experiments, and these values can be reduced in the same manner as the experimental measurements to produce an “average” HGL temperature and height. Regardless of the validity of the reduction method, the FDS predictions of the HGL temperature and height ought to be representative of the accuracy of its predictions of the individual thermocouple measurements that are used in the HGL reduction. The temperature measurements from all six test series are used to compute an HGL temperature and height with which to compare to FDS. The same layer reduction method is used for five of the six test series. Only the NBS Multi-Room series uses another method.

A brief description of each test series is included below, followed by graphs comparing the predicted and measured HGL temperature and layer height.

4.1 HGL Reduction Method

Fire protection engineers often need to estimate the location of the interface between the hot, smoke-laden upper layer and the cooler lower layer in a burning compartment. Relatively simple fire models, often referred to as *two-zone models*, compute this quantity directly, along with the average temperature of the upper and lower layers. In a computational fluid dynamics (CFD) model like FDS, there are not two distinct zones, but rather a continuous profile of temperature. Nevertheless, there are methods that have been developed to estimate layer height and average temperatures from a continuous vertical profile of temperature. One such method [109] is as follows: Consider a continuous function $T(z)$ defining temperature T as a function of height above the floor z , where $z = 0$ is the floor and $z = H$ is the ceiling. Define T_u as the upper layer temperature, T_l as the lower layer temperature, and z_{int} as the interface height. Compute the quantities:

$$(H - z_{int}) T_u + z_{int} T_l = \int_0^H T(z) dz = I_1$$
$$(H - z_{int}) \frac{1}{T_u} + z_{int} \frac{1}{T_l} = \int_0^H \frac{1}{T(z)} dz = I_2$$

Solve for z_{int} :

$$z_{int} = \frac{T_l(I_1 I_2 - H^2)}{I_1 + I_2 T_l^2 - 2 T_l H} \quad (4.1)$$

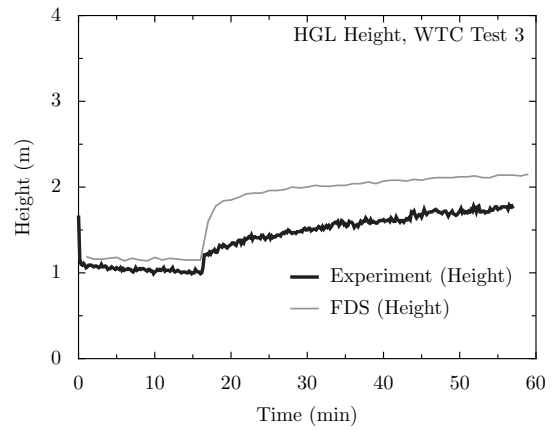
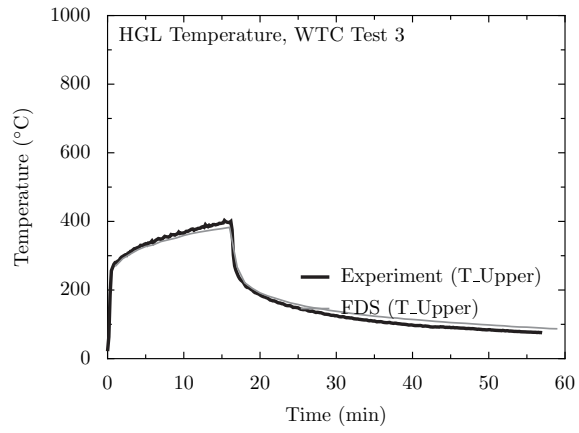
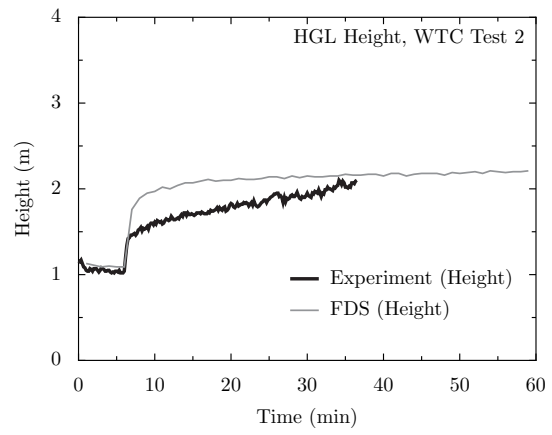
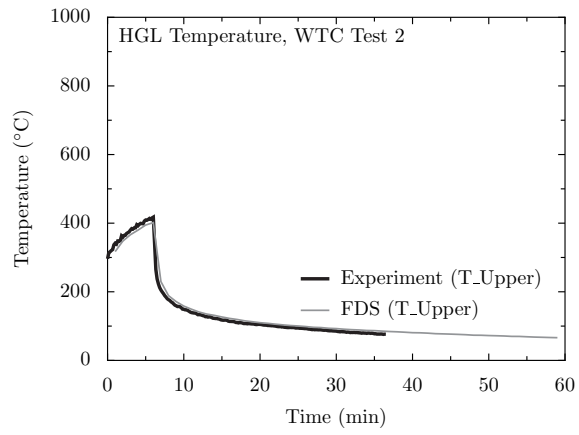
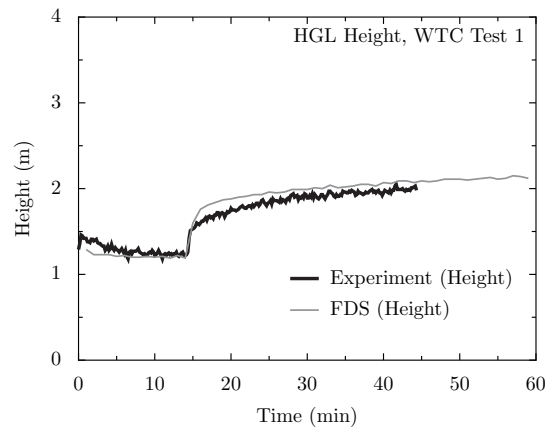
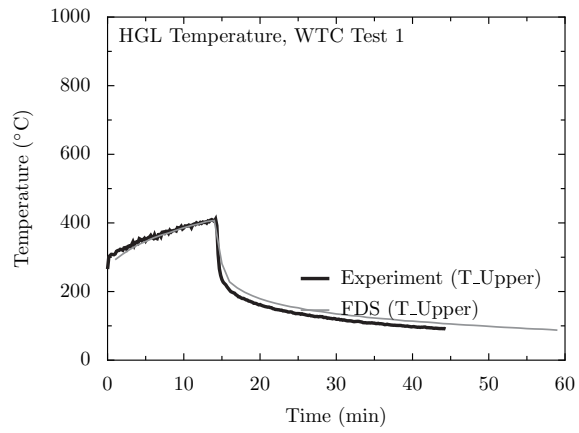
Let T_l be the temperature in the lowest mesh cell and, using Simpson's Rule, perform the numerical integration of I_1 and I_2 . T_u is defined as the average upper layer temperature via

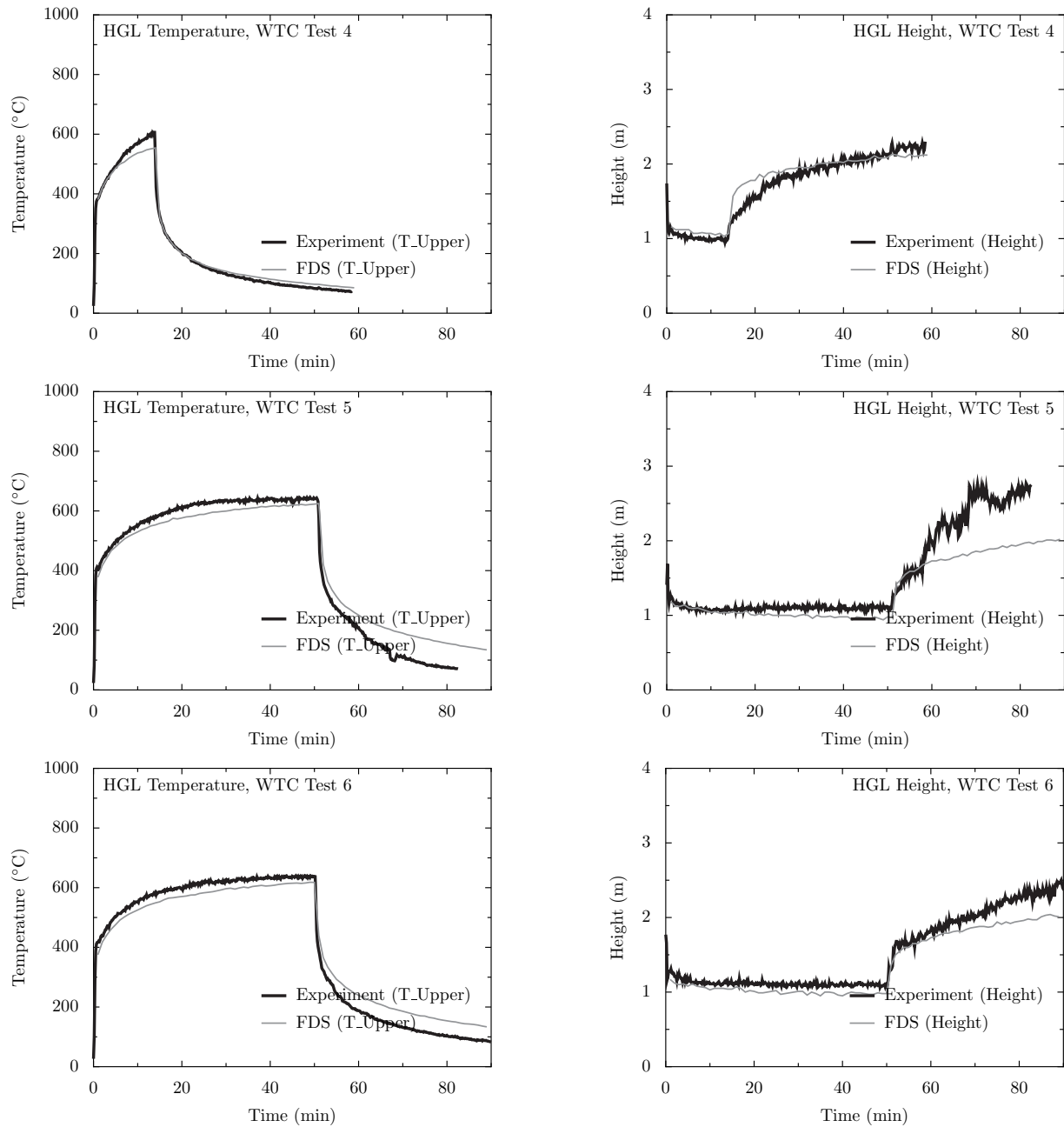
$$(H - z_{int}) T_u = \int_{z_{int}}^H T(z) dz \quad (4.2)$$

Further discussion of similar procedures can be found in Ref. [110].

4.2 WTC Test Series

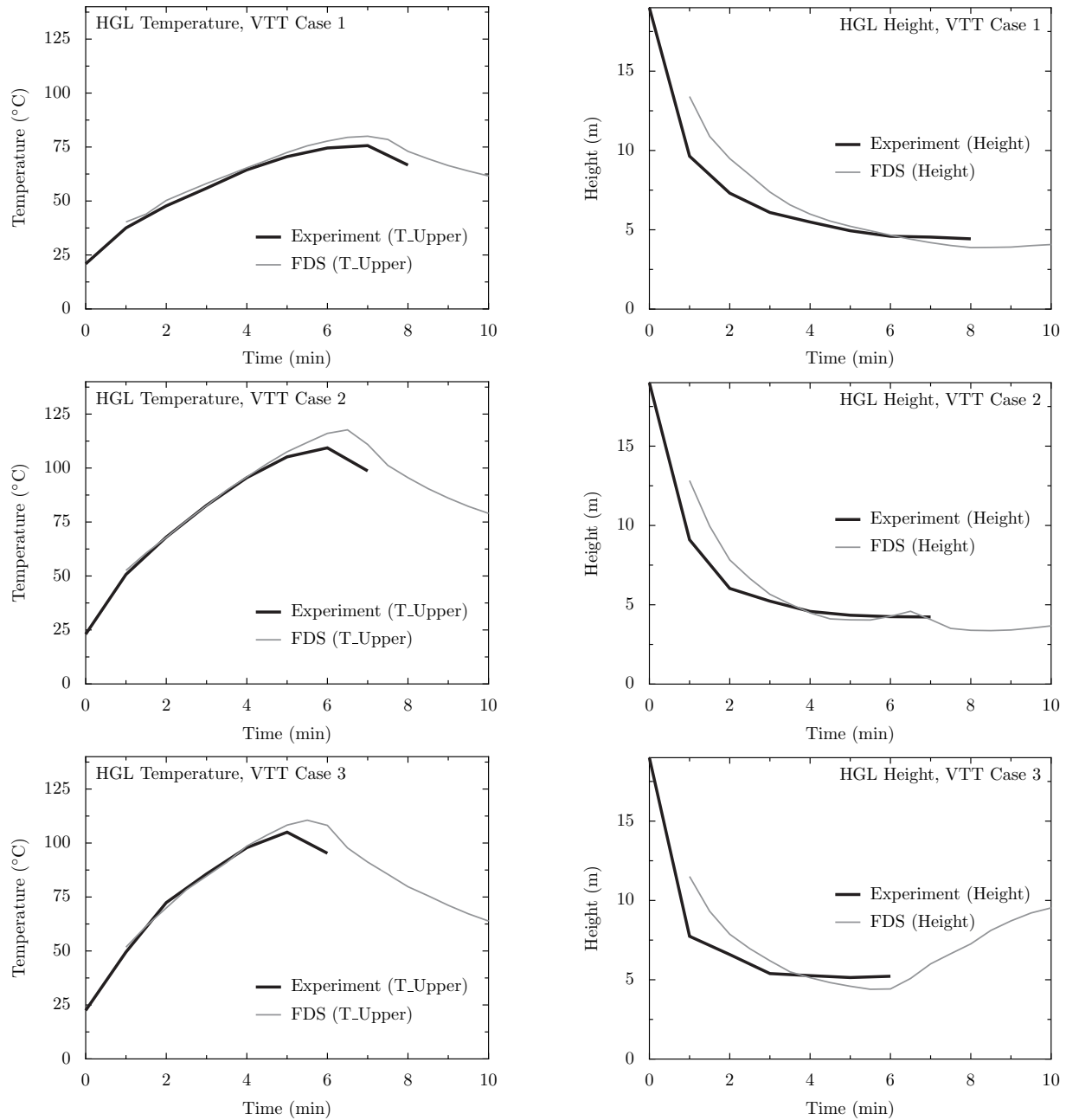
The HGL temperature and height for the WTC experiments were calculated from two TC trees, one that was approximately 3 m to the west and one 2 m to the east of the fire pan. Each tree consisted of 15 thermocouples, the highest point being 5 cm below the ceiling.





4.3 VTT Test Series

The HGL temperature and height are calculated from the (1 min) averaged gas temperatures from three vertical thermocouple arrays using the standard reduction method. There are 10 thermocouples in each vertical array, spaced 2 m apart in the lower two-thirds of the hall, and 1 m apart near the ceiling.

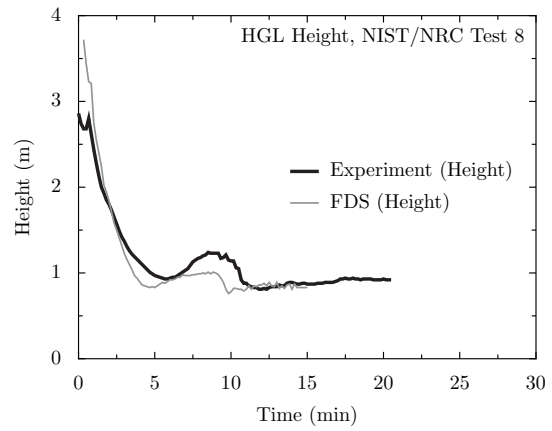
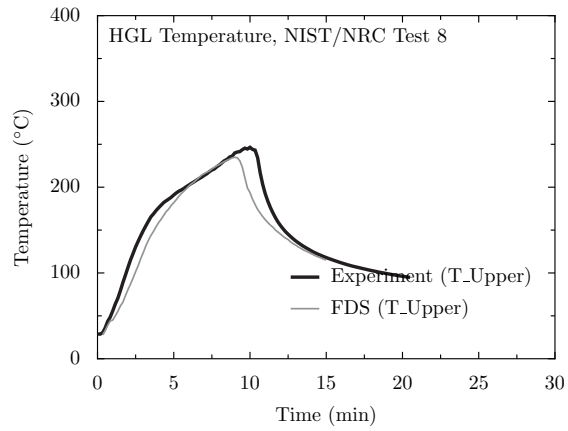
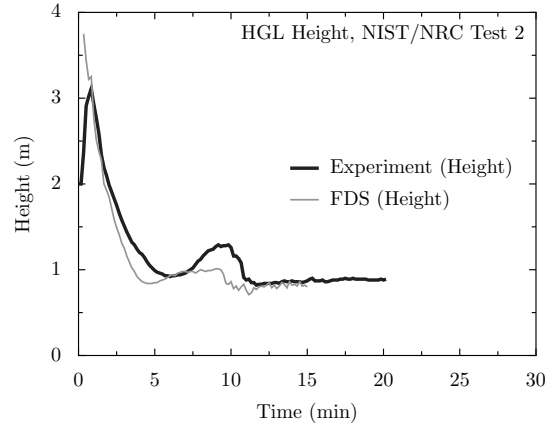
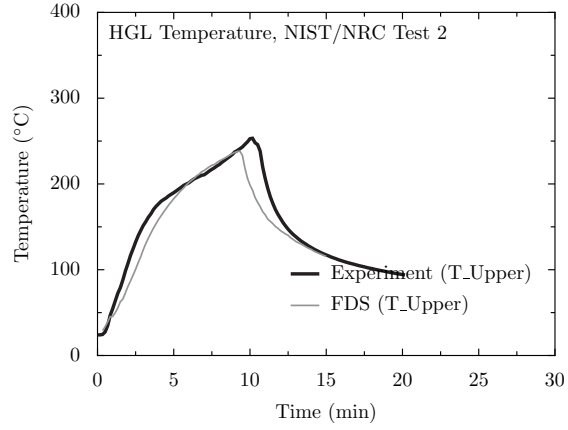
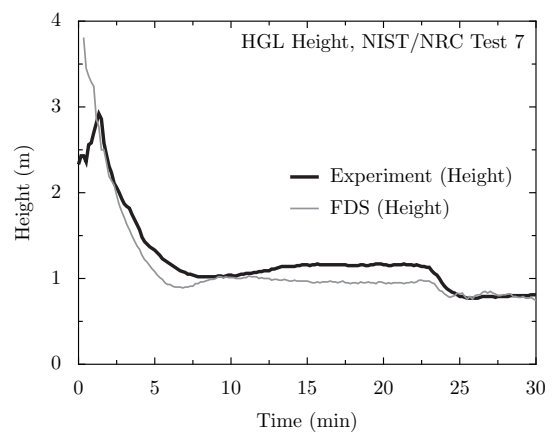
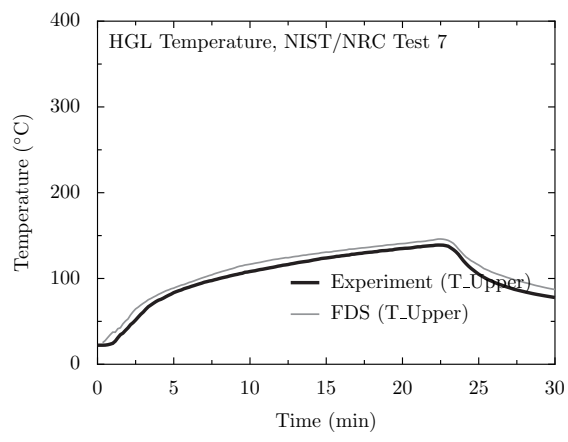
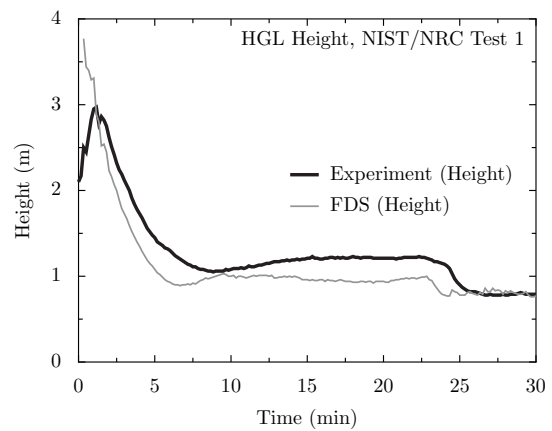
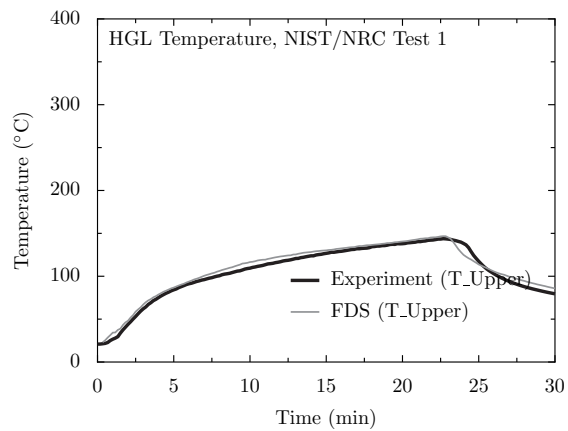


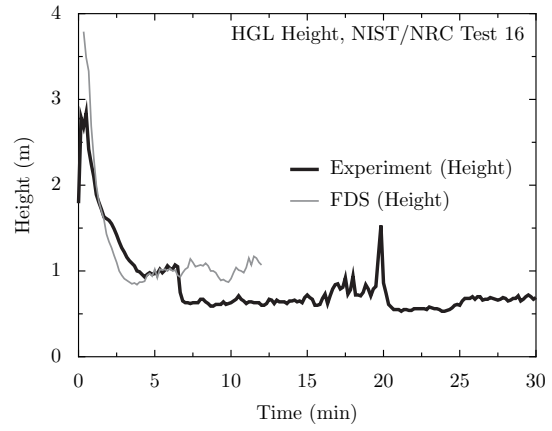
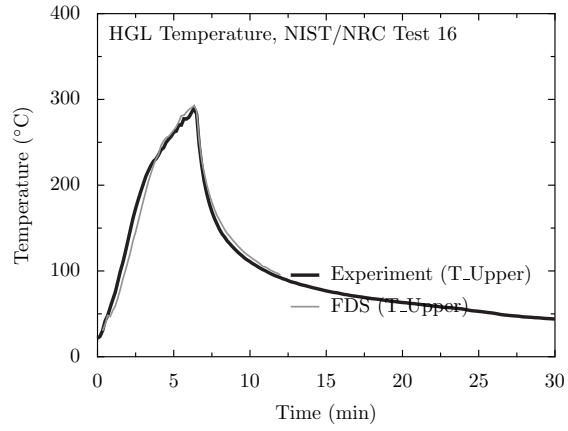
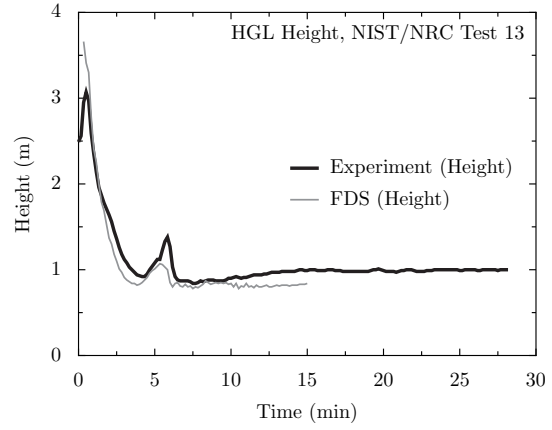
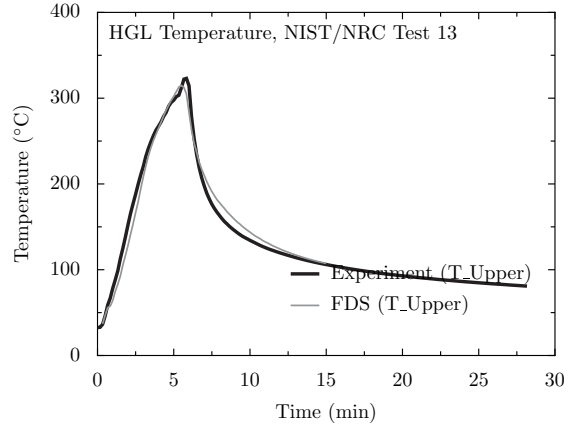
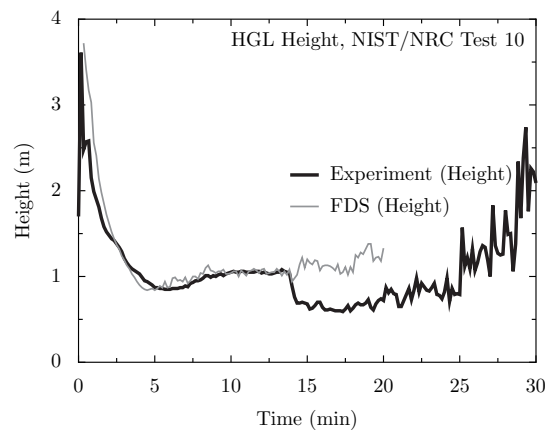
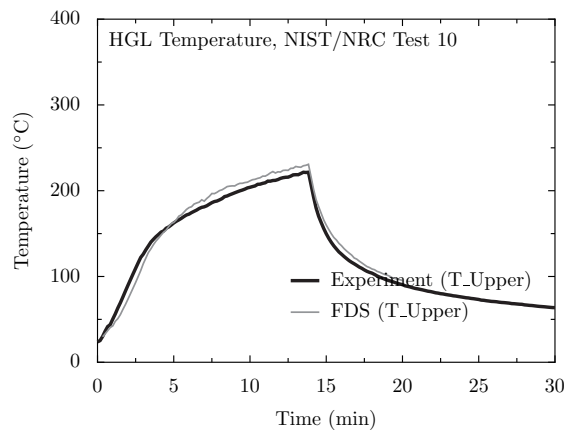
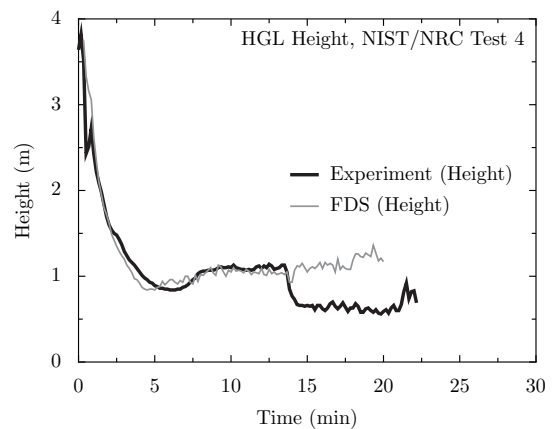
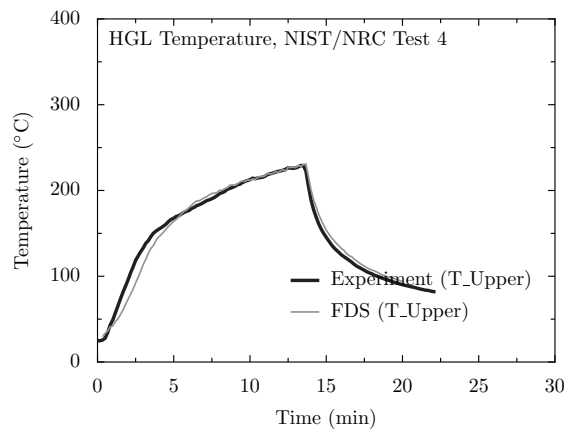
4.4 NIST/NRC Test Series

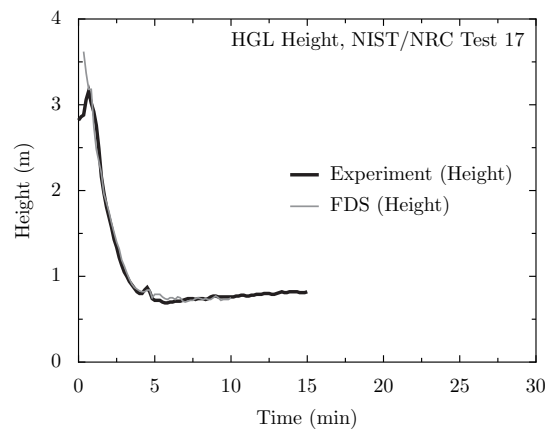
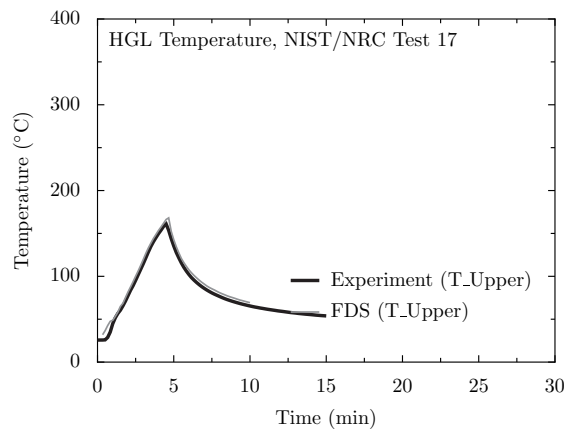
The NIST/NRC series consisted of 15 liquid spray fire tests with different heat release rates, pan locations, and ventilation conditions. Gas temperatures were measured using seven floor-to-ceiling thermocouple arrays (or “trees”) distributed throughout the compartment. The average hot gas layer temperature and height are calculated using thermocouple Trees 1, 2, 3, 5, 6 and 7. Tree 4 was not used because one of its thermocouples (TC 4-9) malfunctioned during most of the experiments.

A few observations about the simulations:

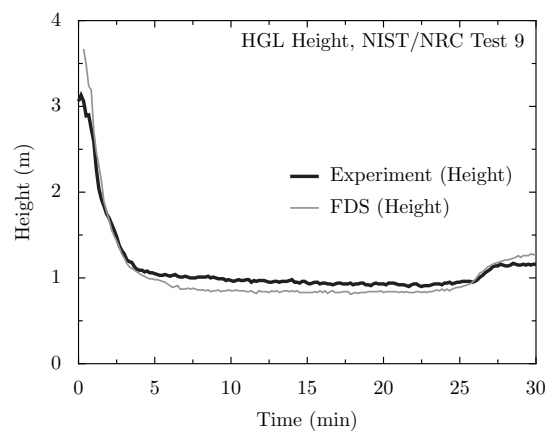
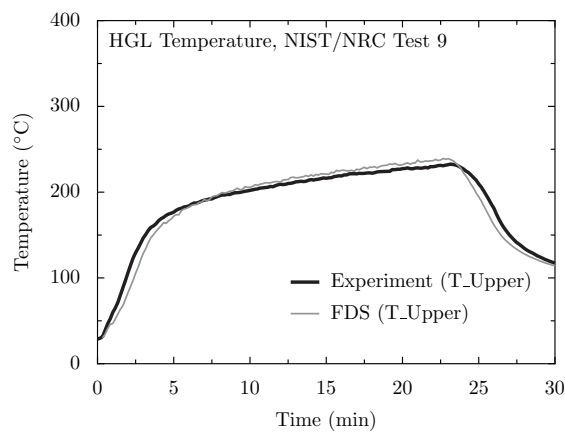
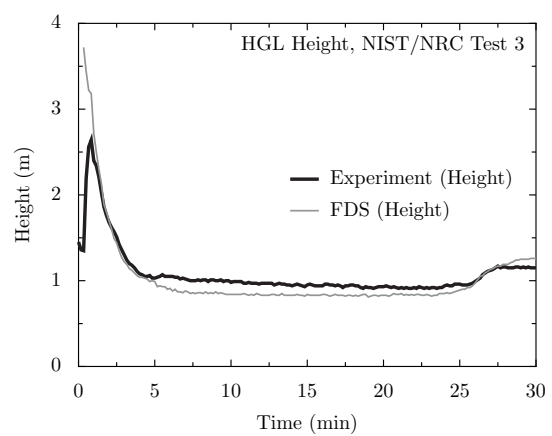
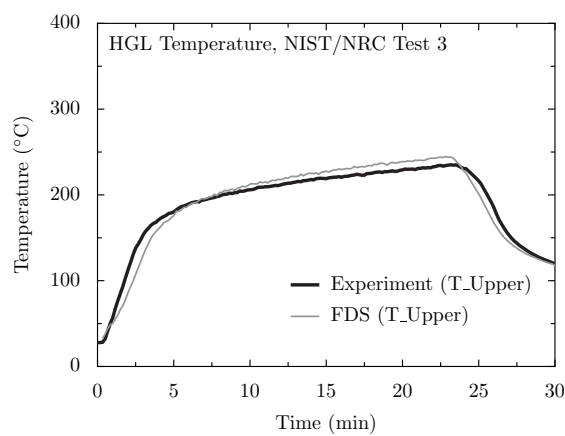
- During Tests 4, 5, 10 and 16 a fan blew air into the compartment through a vent in the south wall. The measured velocity profile of the fan is not uniform, with the bulk of the air blowing from the lower third of the duct towards the ceiling at a roughly 45° angle. The exact flow pattern is difficult to replicate in the model, thus, the results for Tests 4, 5, 10 and 16 should be evaluated with this in mind. The effect of the fan on the hot gas layer is small, but it does have a some effect on target temperatures near the vent.
- For all of the tests involving a fan, the predicted HGL height rises after the fire is extinguished, while the measured HGL drops. This appears to be a curious artifact of the layer reduction algorithm. It is not included in the calculation of the relative difference.
- In the closed door tests, the hot gas layer descends all the way to the floor. However, the reduction method, used on both the measured and predicted temperatures, does not account for the formation of a single layer, and therefore does not indicate that the layer drops all the way to the floor. This is neither a flaw in the measurements nor in FDS, but rather in the layer reduction method.
- The HGL reduction method produces spurious results in the first few minutes of each test because no clear layer has yet formed. These early times are not included in the relative difference calculation.

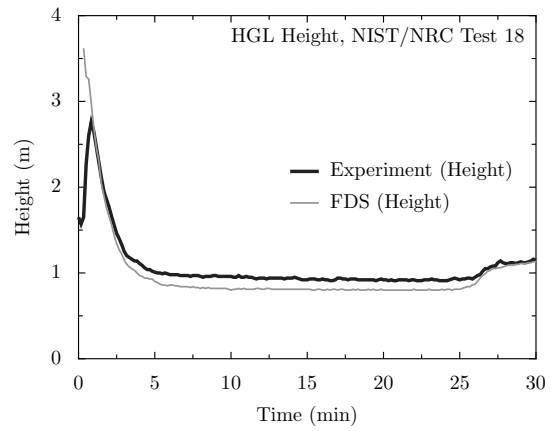
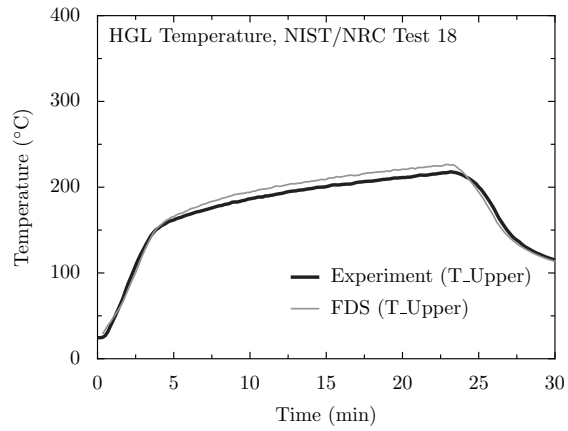
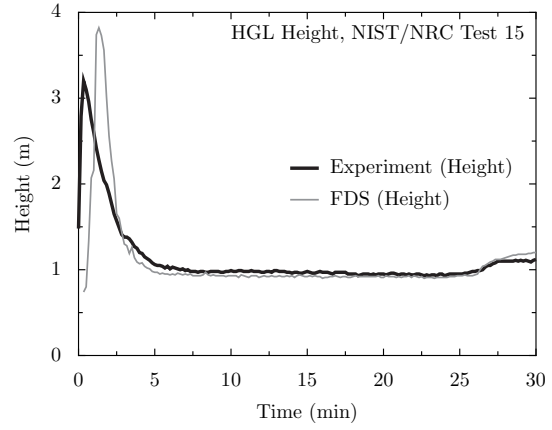
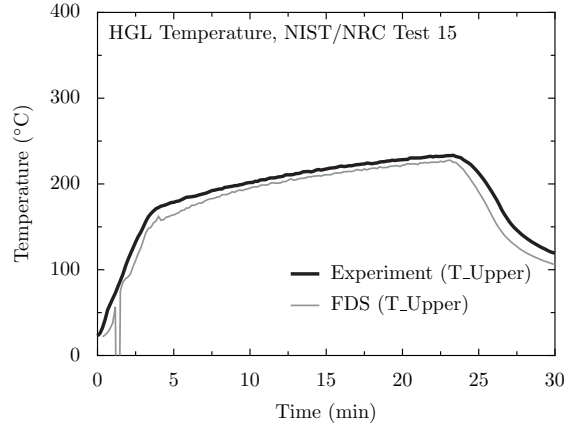
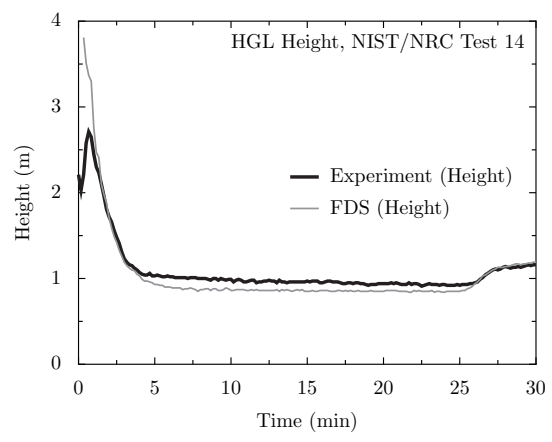
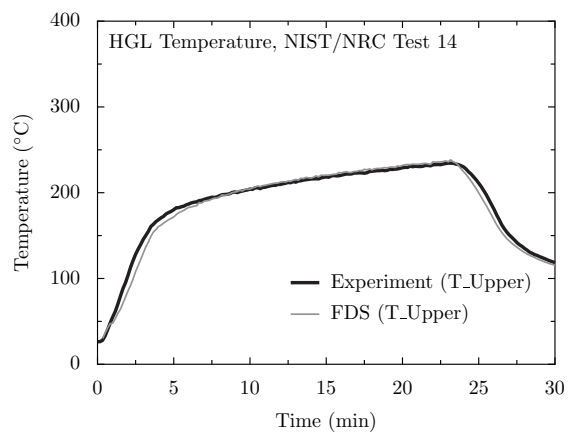
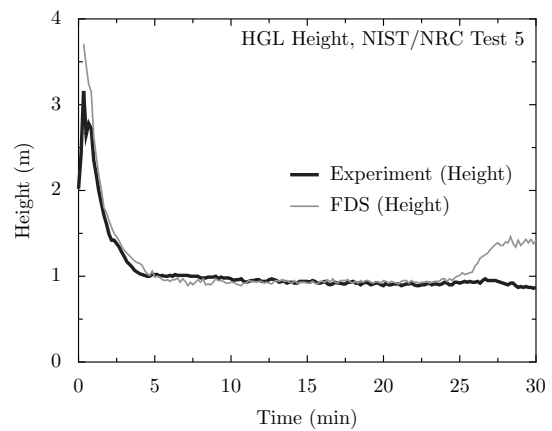
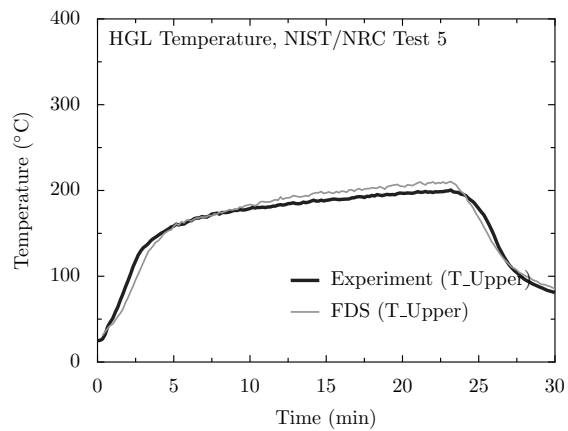






Open door tests to follow



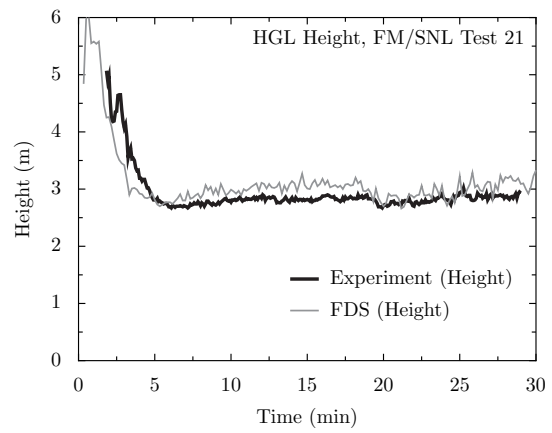
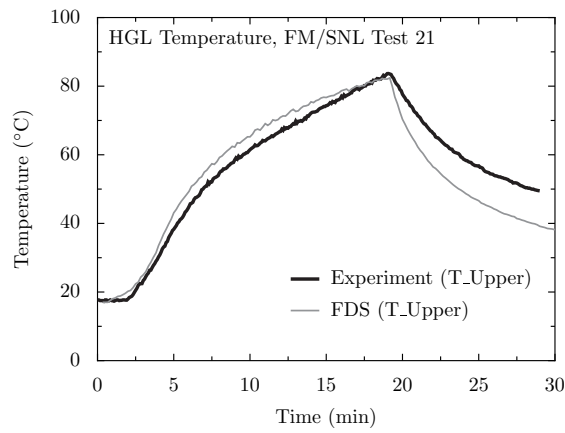
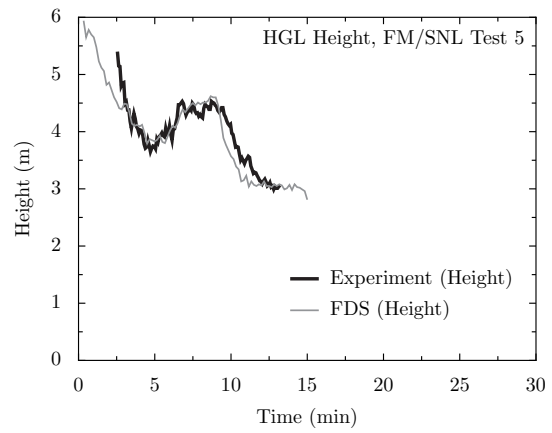
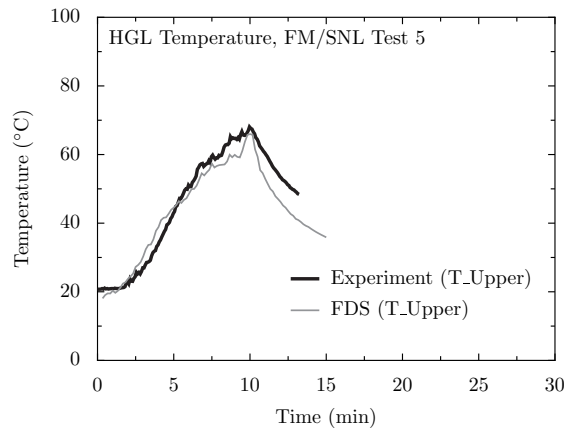
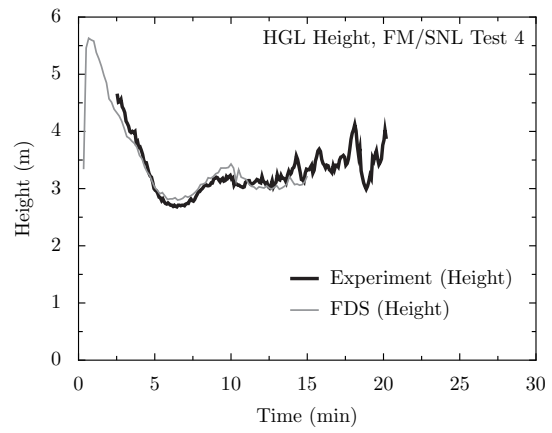
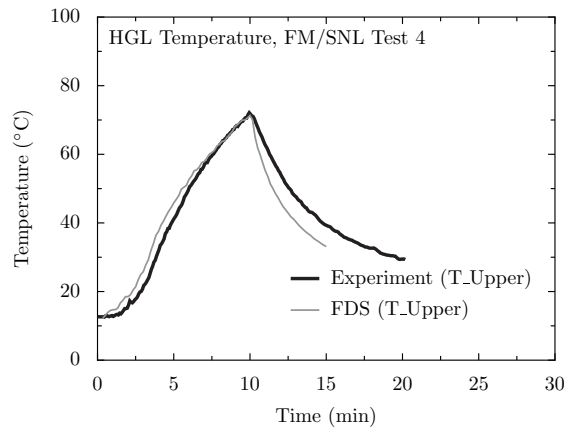


4.5 FM/SNL Test Series

Tests 4, 5, and 21 from the FM/SNL test series were selected for comparison. The hot gas layer temperature and height are calculated using the standard method. The thermocouple arrays that are referred to as Sectors 1, 2 and 3 are averaged (with an equal weighting for each) for Tests 4 and 5. For Test 21, only Sectors 1 and 3 are used, as Sector 2 falls within the smoke plume.

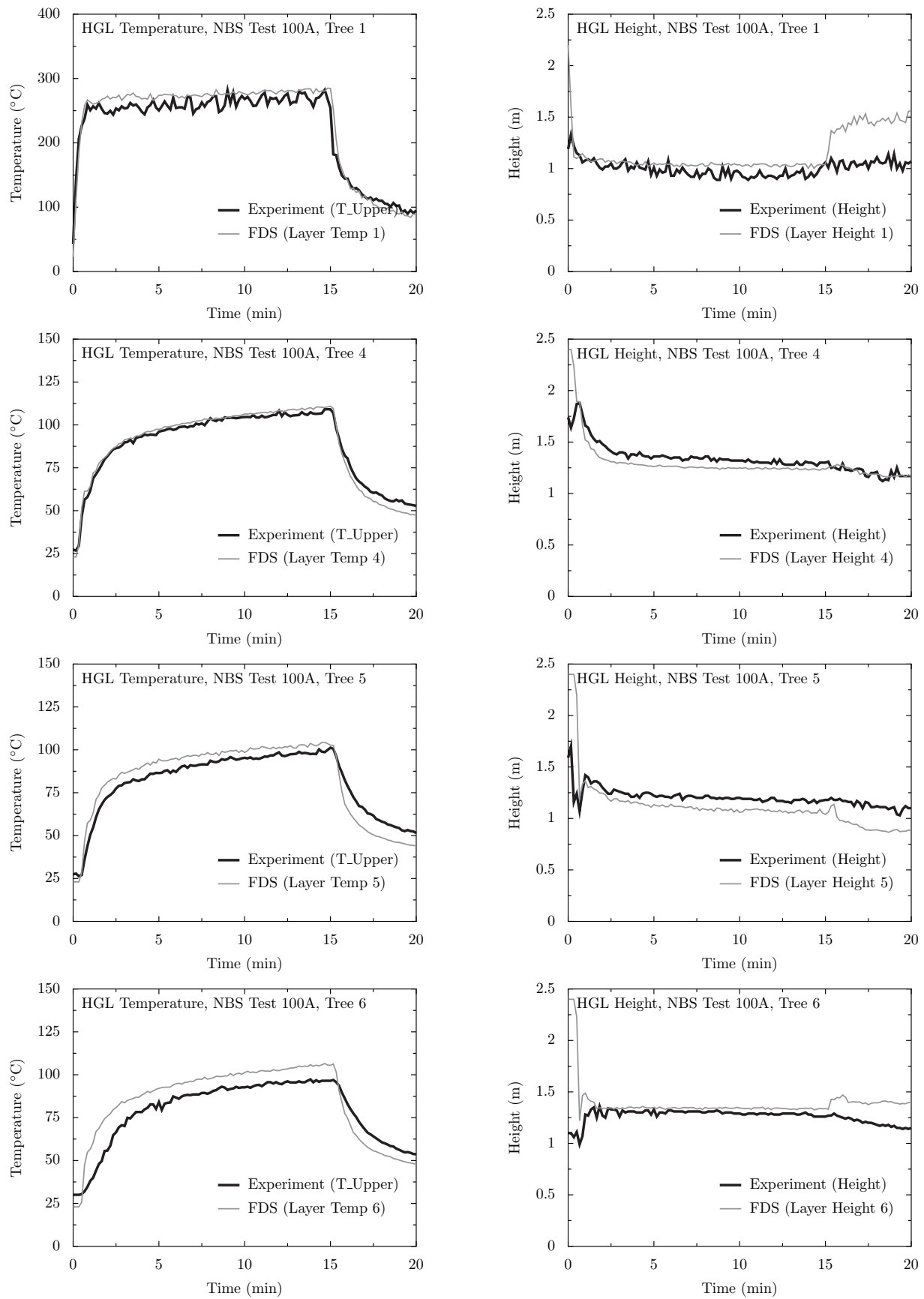
Note the following:

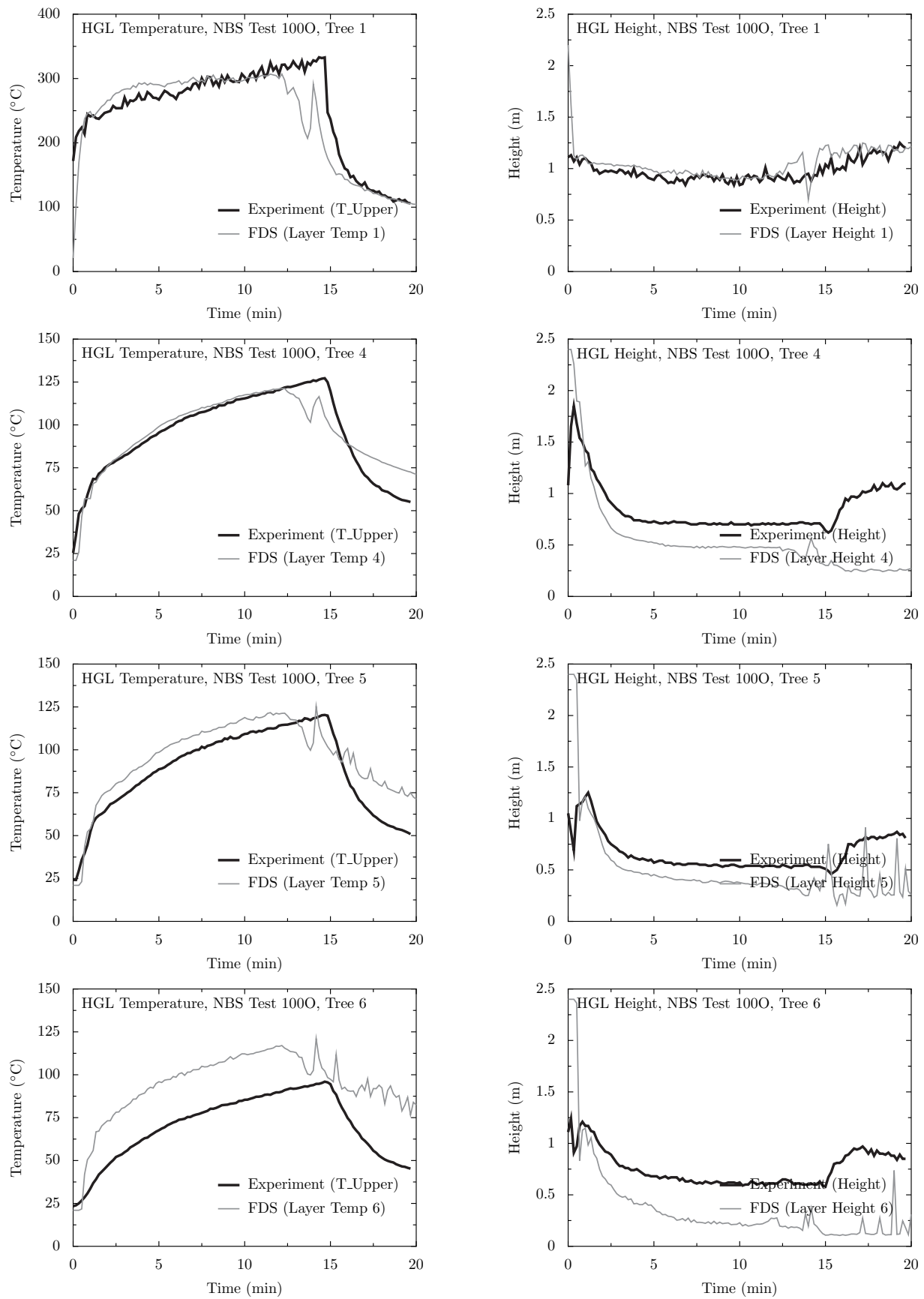
- The HGL heights, both the measured and predicted, are somewhat noisy due to the effect of ventilation ducts in the upper layer.
- The ventilation was turned off after 9 min in Test 5, the effect of which was a slight increase in both the measured and predicted HGL temperature.
- The measured HGL temperature is noticeably greater than the prediction in Test 21. This is possibly due to an increase in the HRR towards the end of the test. The simulations all used fixed HRRs after the 4 min ramp up.

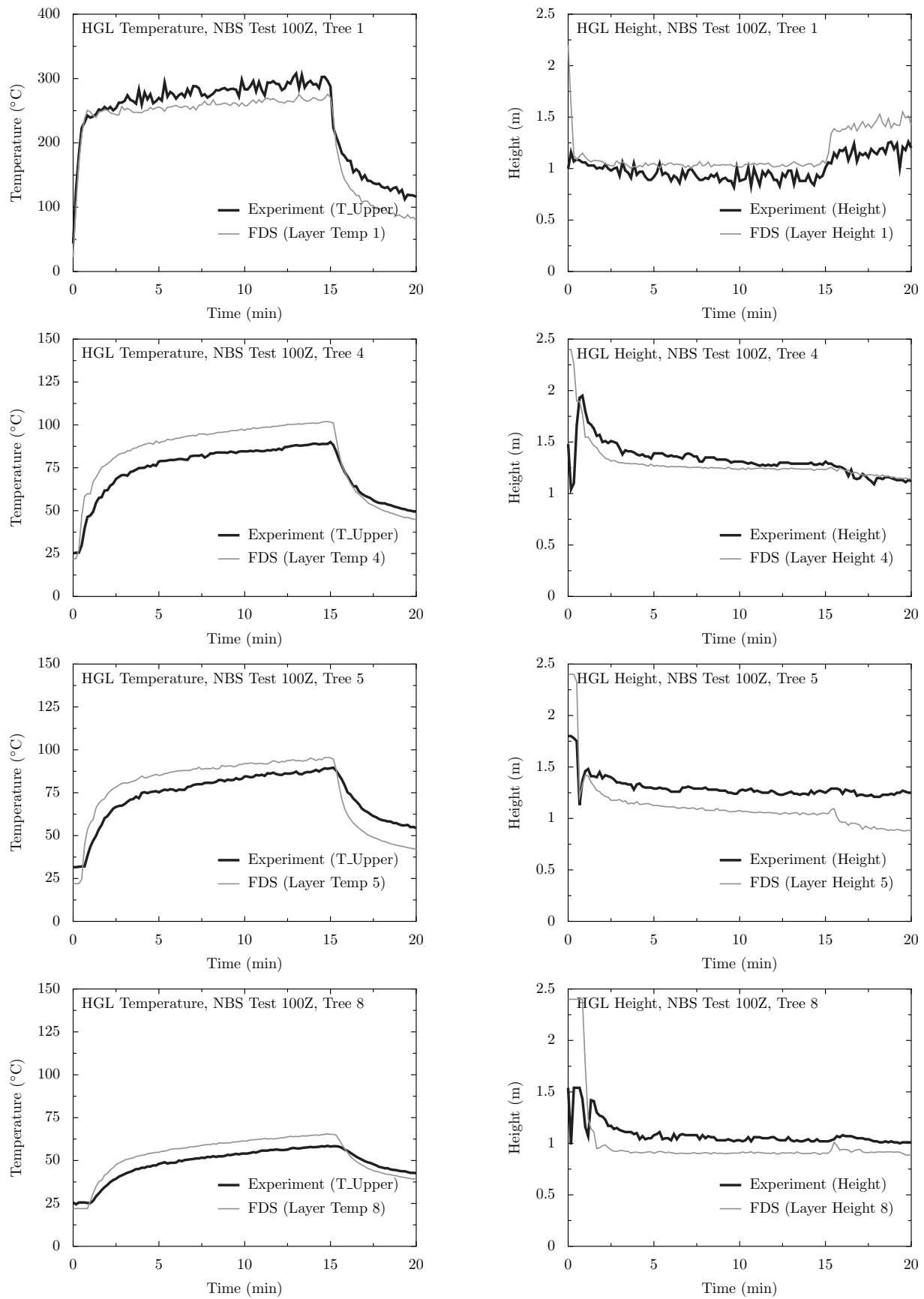


4.6 NBS Multi-Room Test Series

This series of experiments consists of two relatively small rooms connected by a long corridor. The fire is located in one of the rooms. Eight vertical arrays of thermocouples are positioned throughout the test space: one in the burn room, one near the door of the burn room, three in the corridor, one in the exit to the outside at the far end of the corridor, one near the door of the other or “target” room, and one inside the target room. Four of the eight arrays have been selected for comparison with model prediction: the array in the burn room (BR), the array in the middle of the corridor (18 ft from the BR), the array at the far end of the corridor (38 ft from the BR), and the array in the target room (TR). In Tests 100A and 100O, the target room is closed, in which case the array in the exit (EXI) doorway is used. The test director reduced the layer information individually for the eight thermocouple arrays using an alternative method. These results are included in the original data sets. However, for the current validation study, the selected TC trees were reduced using the conventional method common to all the experiments considered. The results are presented below.







4.7 Summary of Hot Gas Layer Temperature and Height

A summary scatter plot of the HGL predictions is given in Fig. 4.1. Most of the predictions fall within the experimental uncertainty bounds. Note, however, that both of these quantities represent spatial averages. At any given point in the compartment, a specific prediction of temperature may not fall within the uncertainty bounds. Point to point comparisons of temperature can be found in the chapters for plumes and ceiling jets.

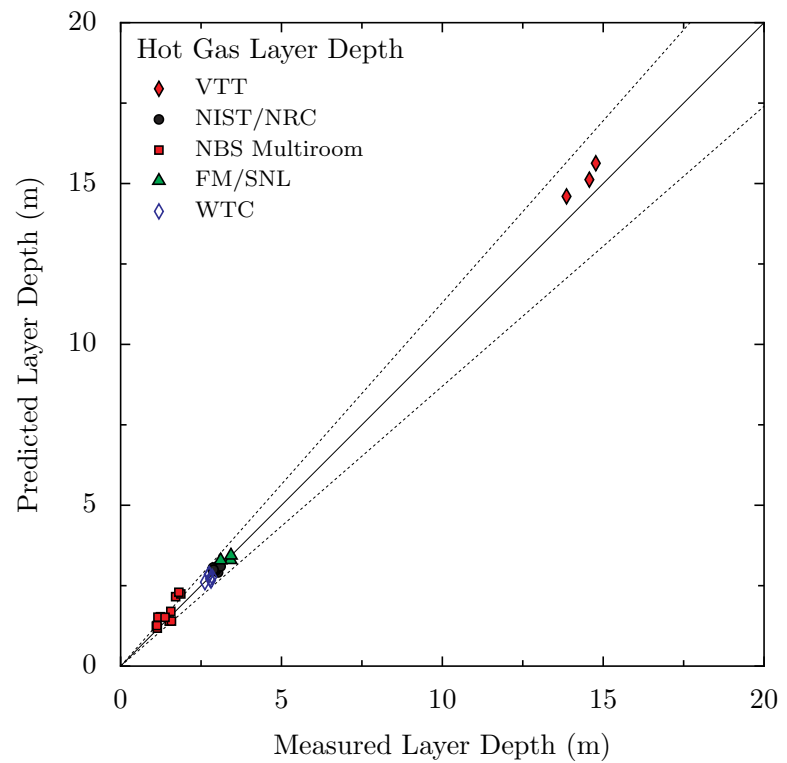
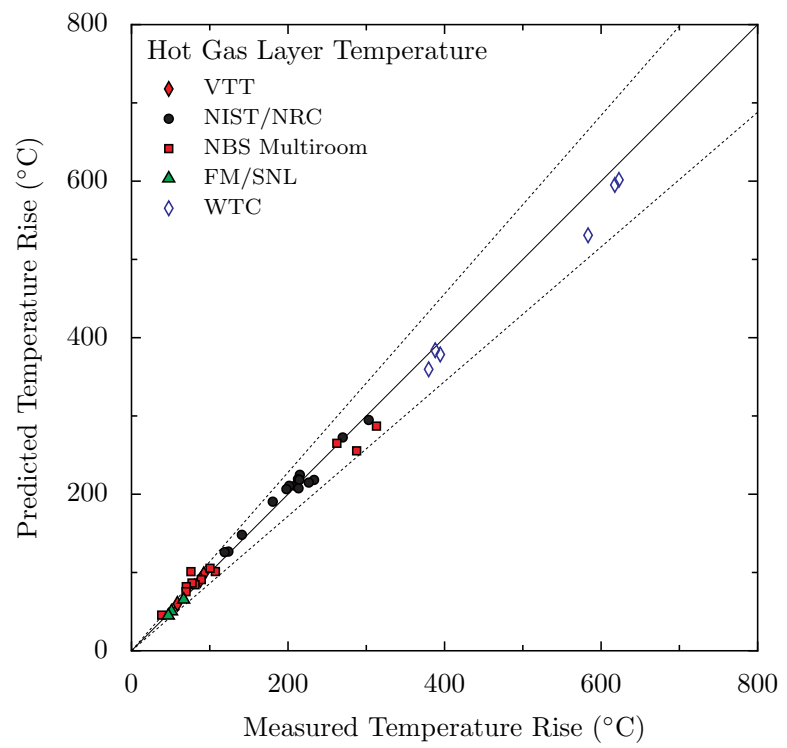
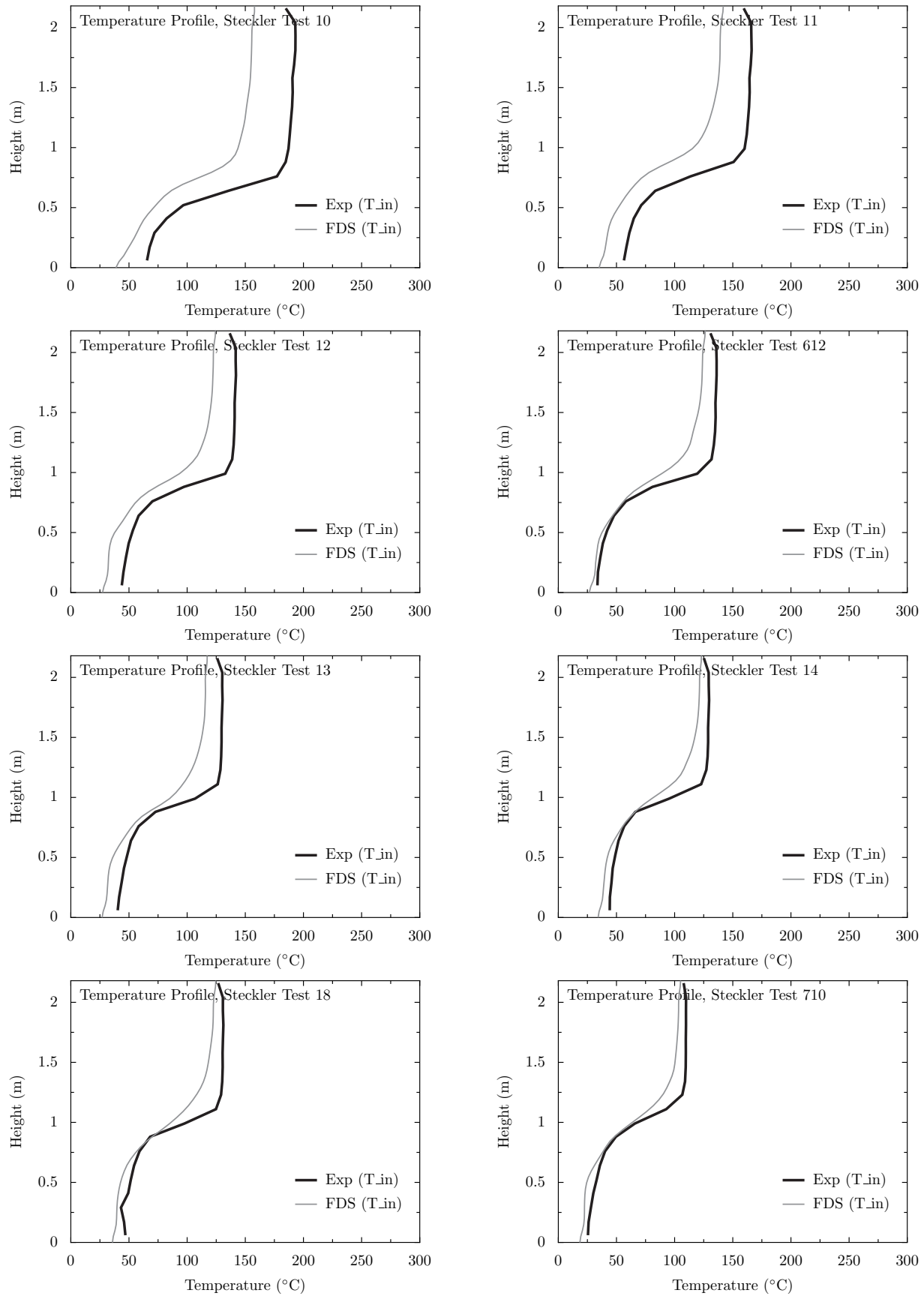
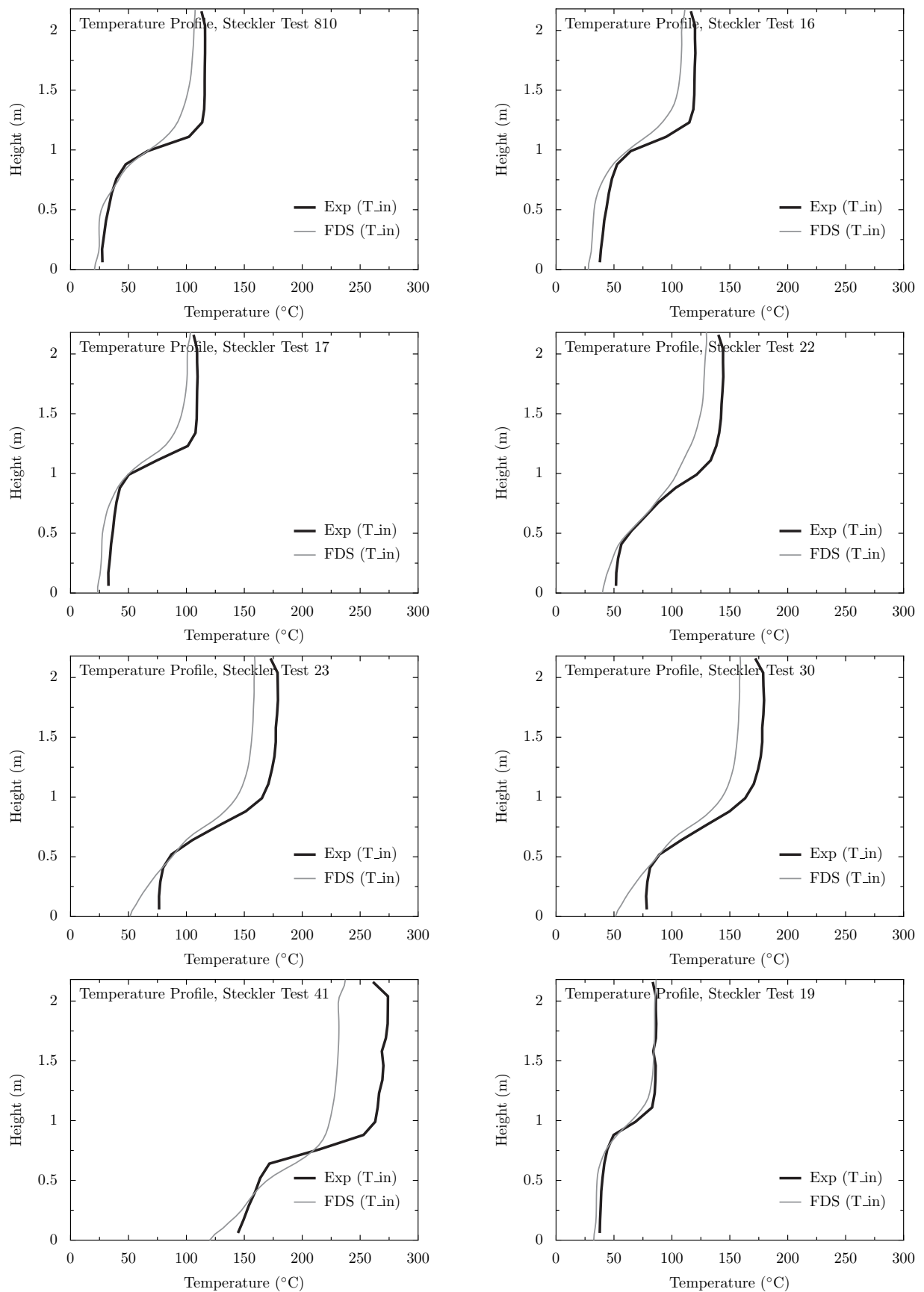


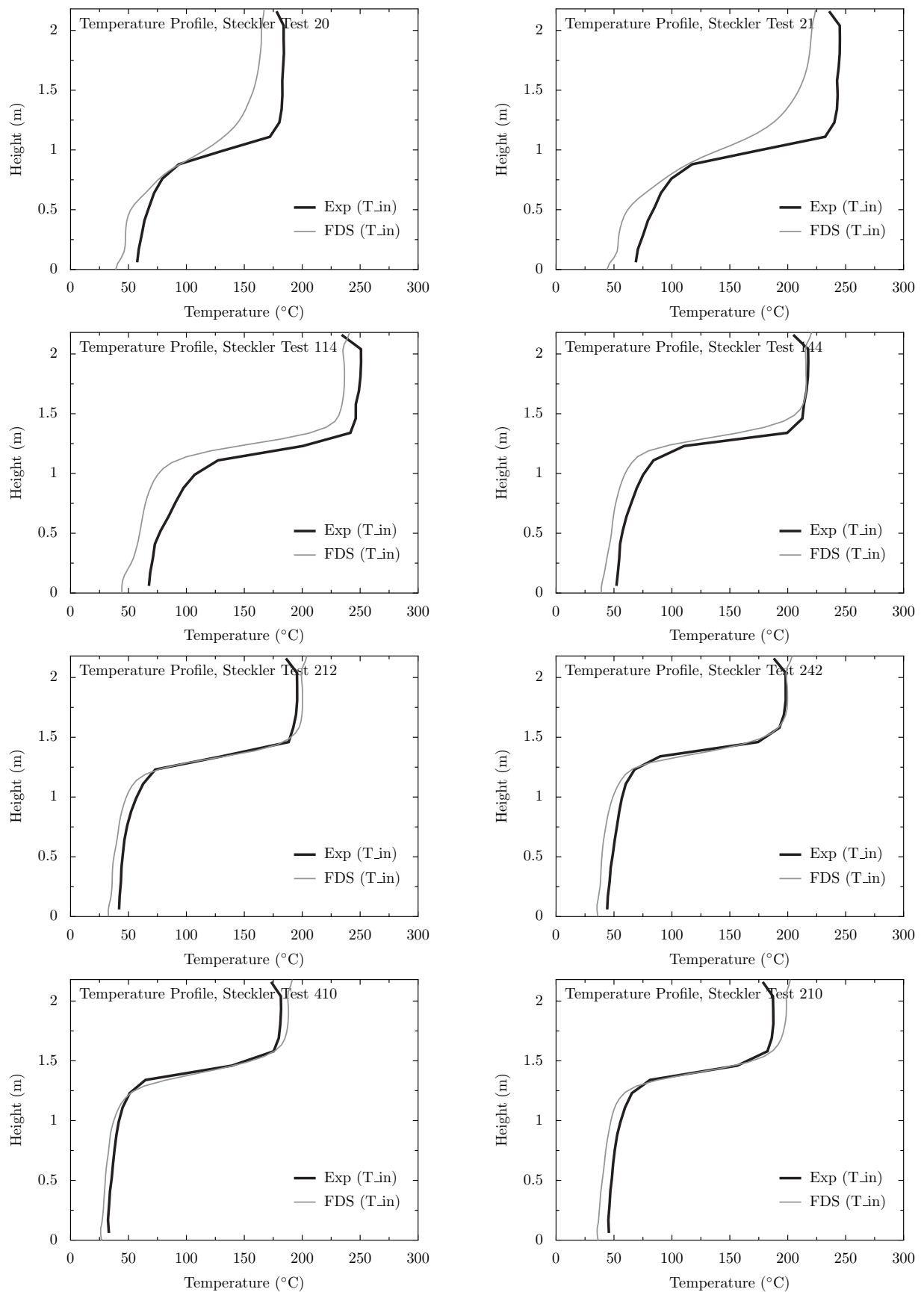
Figure 4.1: Summary of the HGL temperature and height predictions for the VTT, NIST/NRC, WTC, NBS and FM/SNL series.

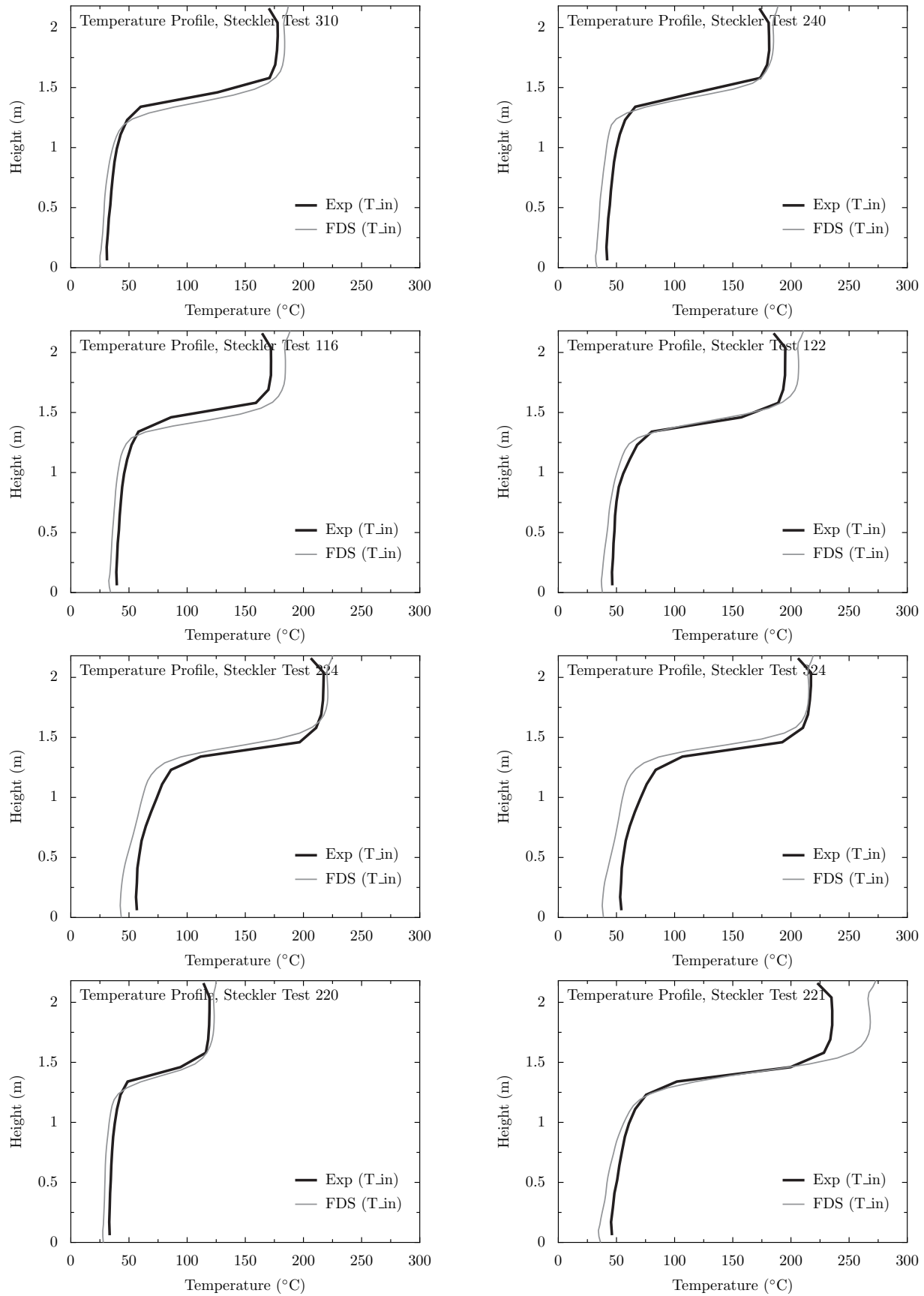
4.8 Steckler Compartment Experiments

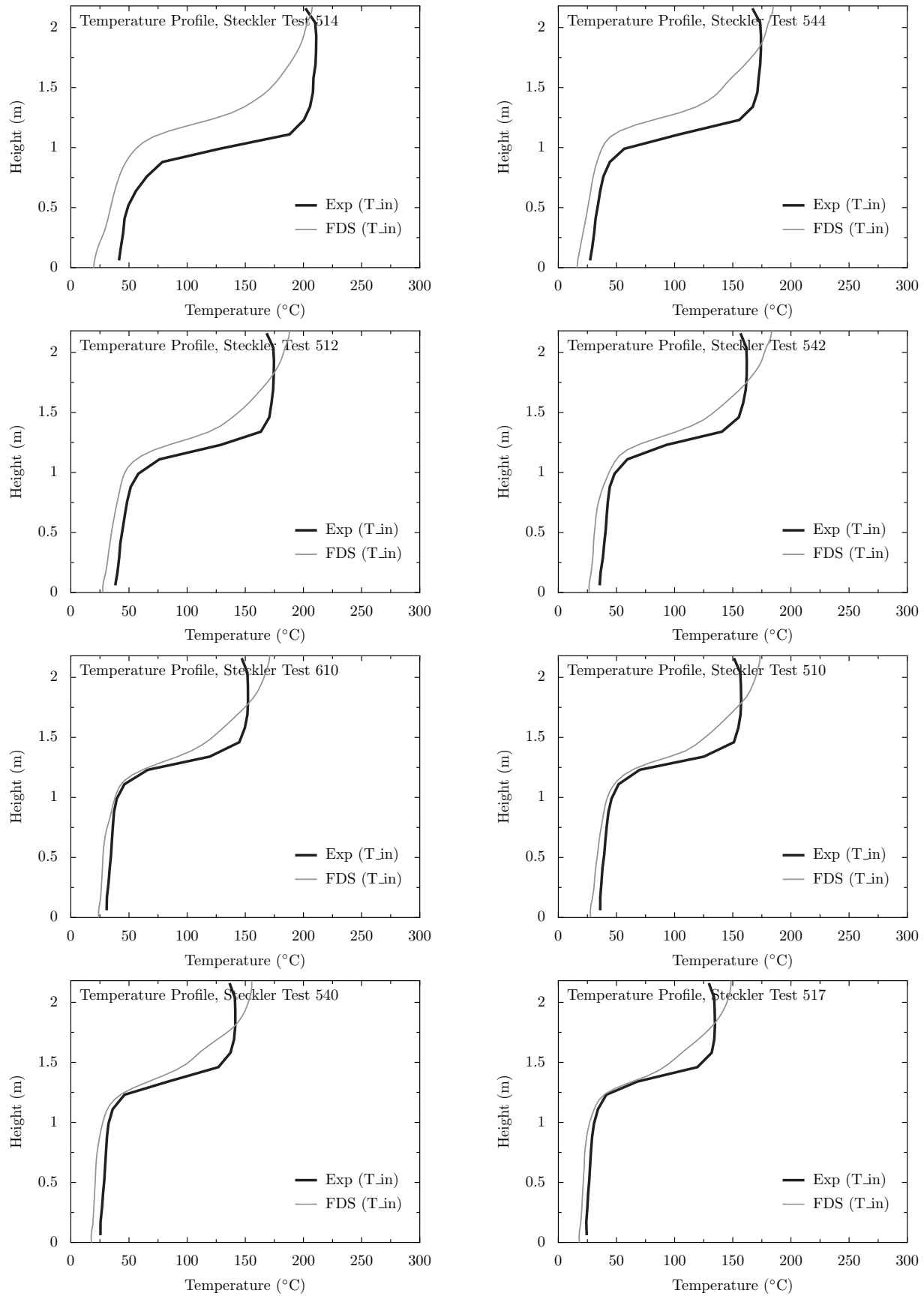
Steckler *et al.* [102] mapped the doorway/window flows in 55 compartment fire experiments. The test matrix is presented in Table 3.1. Shown on the following pages are the temperature profiles inside the compartment compared with model predictions. The FDS simulations were uniformly gridded with cells of 5 cm on each side. To quantify the difference between prediction and measurement, the maximum temperatures were compared.

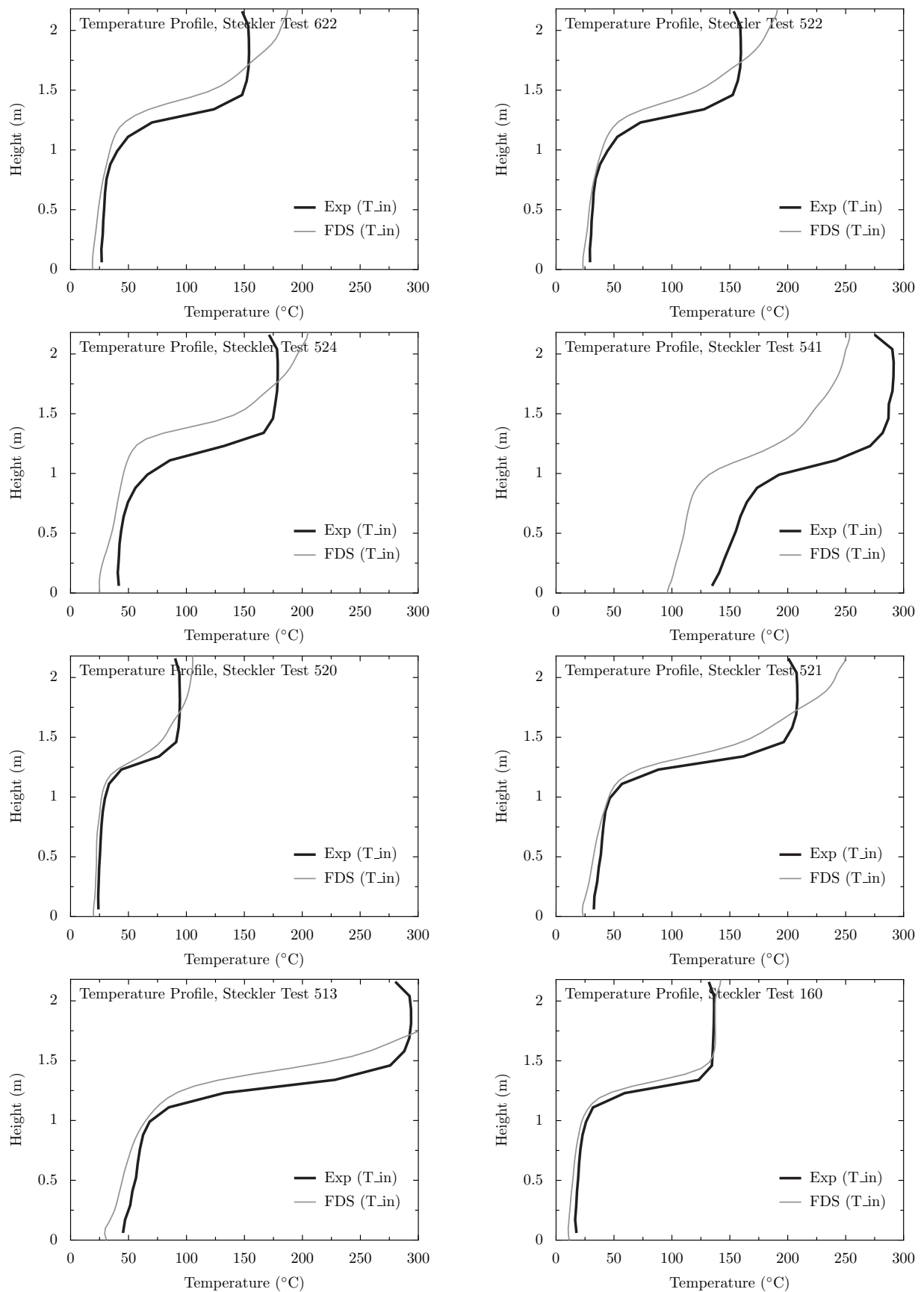


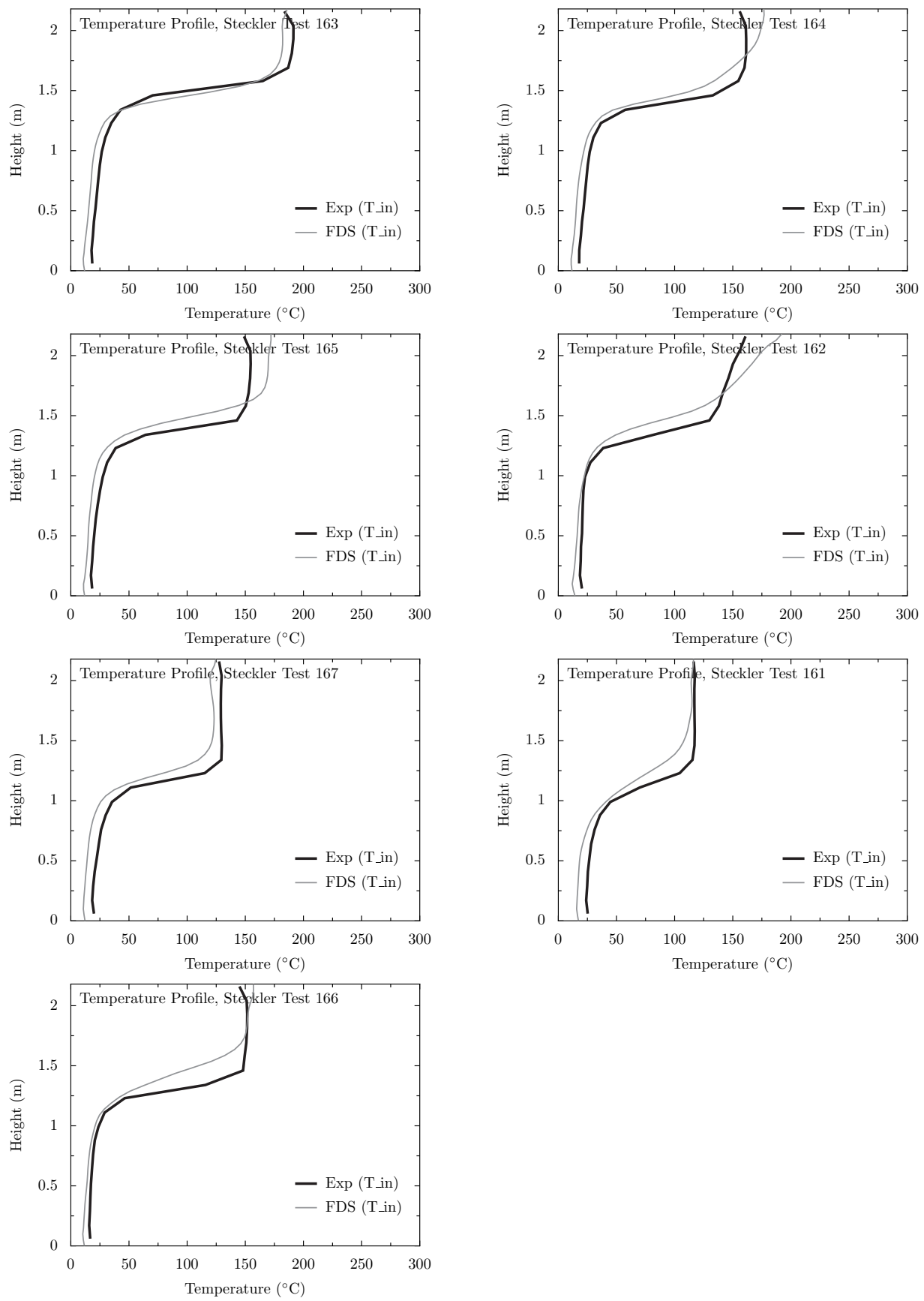












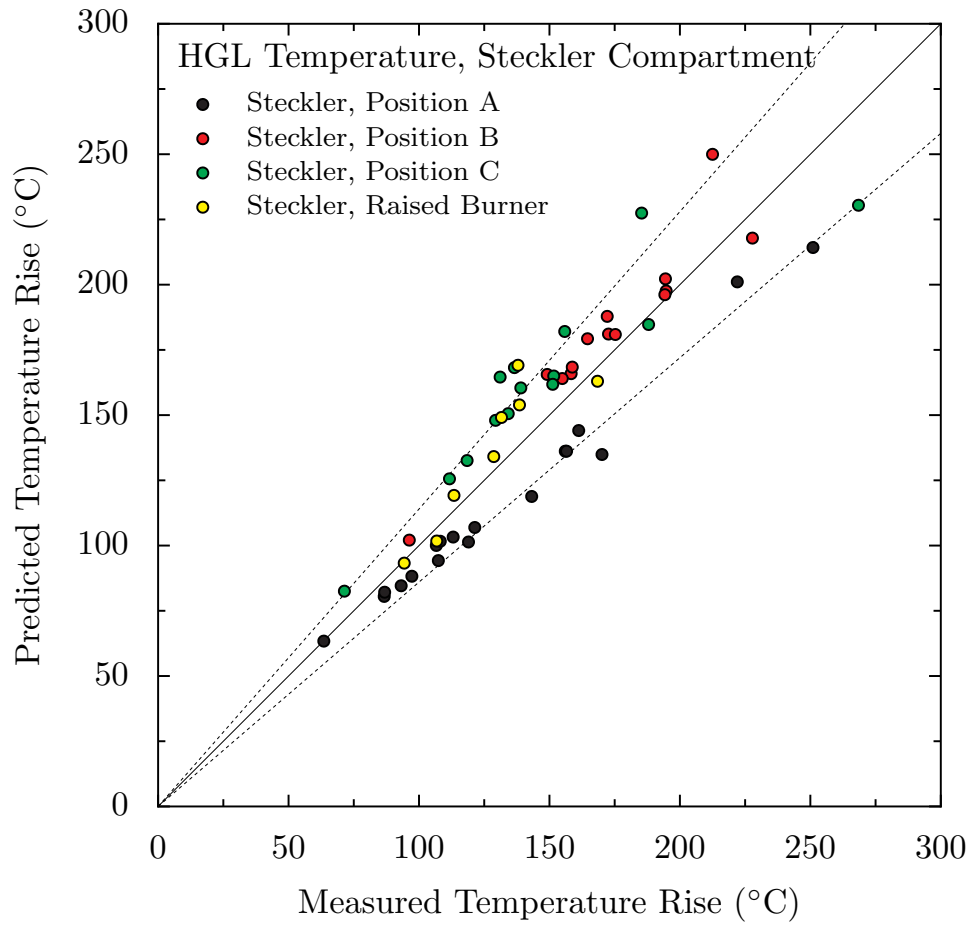


Figure 4.2: Summary of peak temperature predictions for the Steckler Compartment Experiments.

Chapter 5

Fire Plumes

For FDS simulations involving buoyant plumes, a measure of how well the flow field is resolved is given by the non-dimensional expression $D^*/\delta x$, where D^* is a characteristic fire diameter

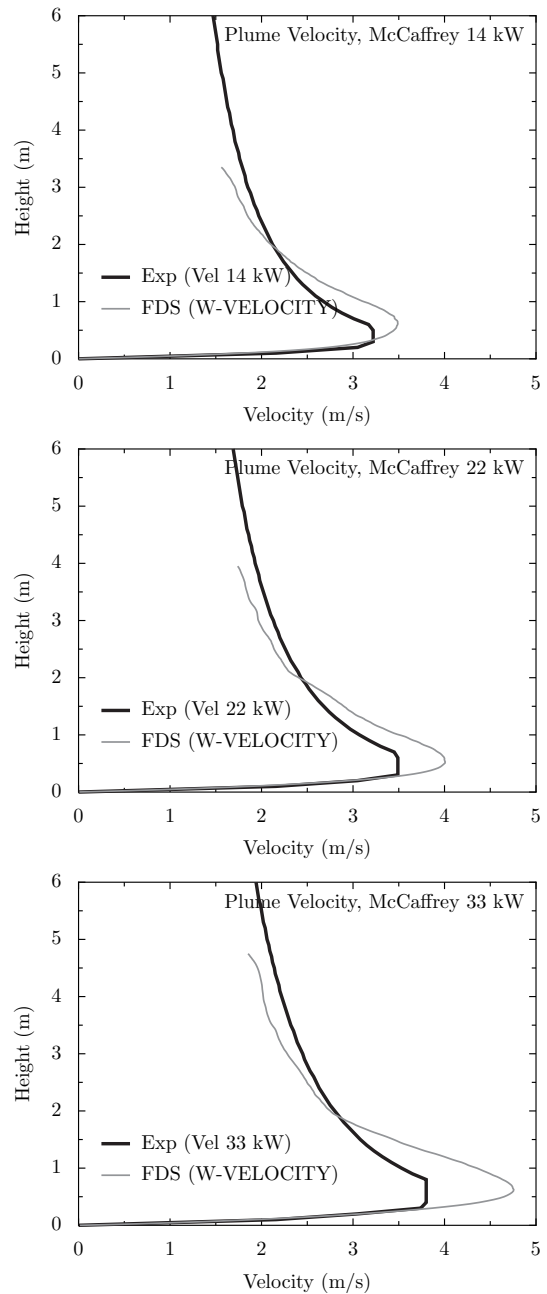
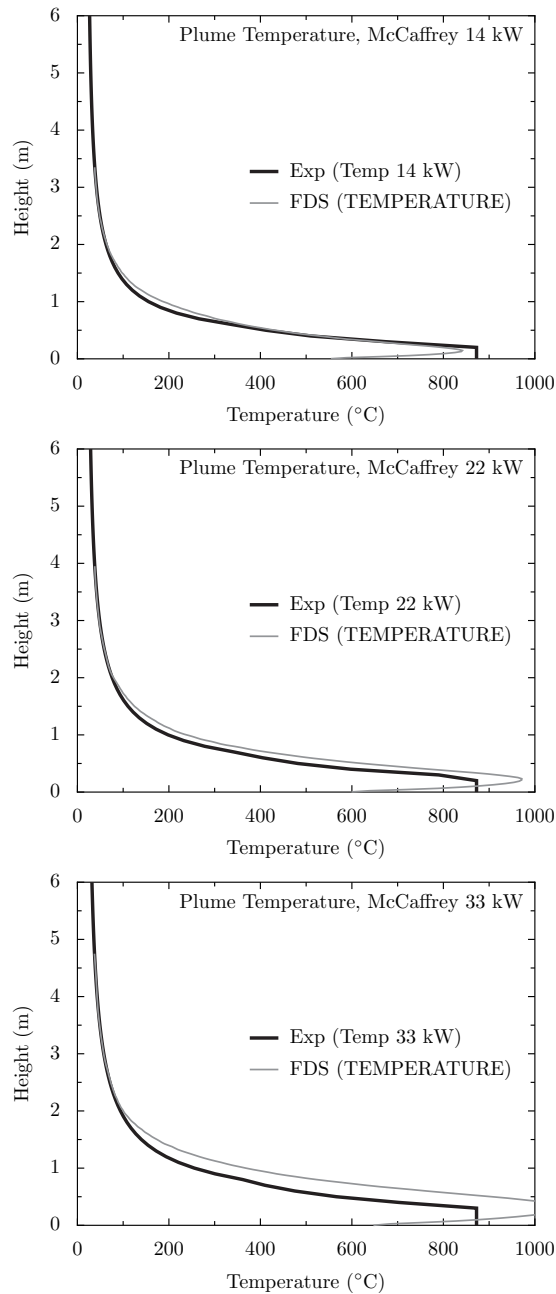
$$D^* = \left(\frac{\dot{Q}}{\rho_\infty c_p T_\infty \sqrt{g}} \right)^{\frac{2}{5}} \quad (5.1)$$

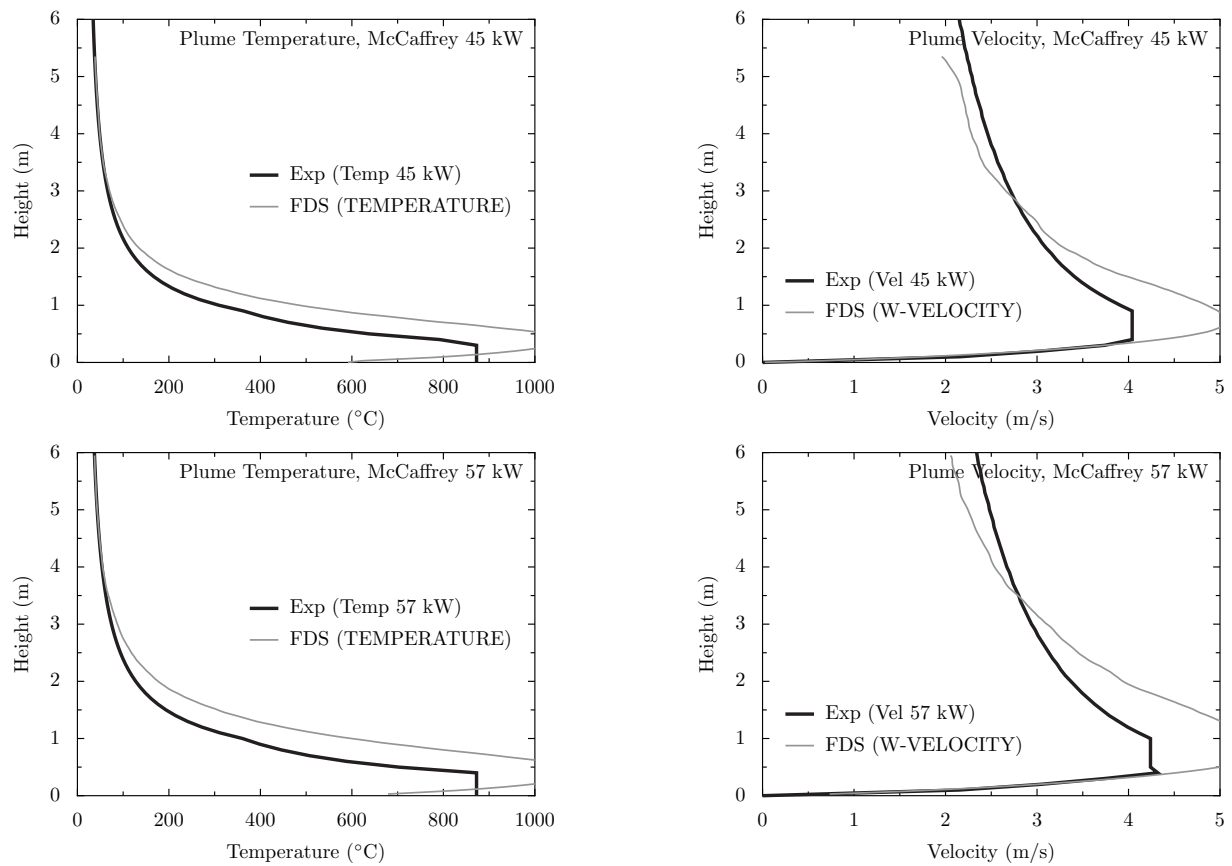
and δx is the nominal size of a mesh cell¹. The quantity $D^*/\delta x$ can be thought of as the number of computational cells spanning the characteristic (not necessarily the physical) diameter of the fire. The more cells spanning the fire, the better the resolution of the calculation. It is better to assess the quality of the mesh in terms of this non-dimensional parameter, rather than an absolute mesh cell size. For example, a cell size of 10 cm may be “adequate,” in some sense, for evaluating the spread of smoke and heat through a building from a sizable fire, but may not be appropriate to study a very small, smoldering source.

5.1 McCaffrey’s Plume Correlation

The following pages show the results of simulations of McCaffrey’s five fires with a grid resolution such that $D^*/\delta x = 10$. The mesh cells were all cubes, and no stretching was used.

¹The characteristic fire diameter is related to the characteristic fire size via the relation $Q^* = (D^*/D)^{5/2}$, where D is the physical diameter of the fire.





5.2 Heskestad's Flame Height Correlation

A widely used experimental correlation for flame height is given by the expression [30]:

$$\frac{L_f}{D} = 3.7 (Q^*)^{2/5} - 1.02 \quad (5.2)$$

where

$$Q^* = \frac{\dot{Q}}{\rho_\infty c_p T_\infty \sqrt{g} D^{5/2}} \quad (5.3)$$

is a non-dimensional quantity that relates the fire's heat release rate, \dot{Q} , with the diameter of its base, D . The greater the value of Q^* , the higher the flame height relative to its width. Table 5.1 lists the parameters for 16 FDS calculations of a fire in a 1 m by 1 m square pan², and Fig. 5.1 compares the FDS predictions with Heskestad's experimental correlation. Note that the flame height for the FDS simulations is defined as the distance above the pan, on average, at which 95 % of the fuel has been consumed. Note also that all the simulations used a cell size such that $D^*/\delta x = 10$.

Table 5.1: Summary of parameters for the flame height predictions.

Q^*	\dot{Q} (kW)	D^* (m)	δx (m)
0.1	151	0.45	0.045
0.2	303	0.59	0.059
0.5	756	0.86	0.086
1	1513	1.13	0.113
2	3025	1.49	0.149
5	7564	2.15	0.215
10	15127	2.84	0.284
20	30255	3.75	0.375
50	75636	5.40	0.540
100	151273	7.13	0.713
200	302545	9.41	0.941
500	756363	13.6	1.36
1000	1512725	17.9	1.79
2000	3025450	23.6	2.36
5000	7563625	34.1	3.41
10000	15127250	45.0	4.50

²The effective diameter, D , of a 1 m square pan is 1.13 m, obtained by equating the area of a square and circle.

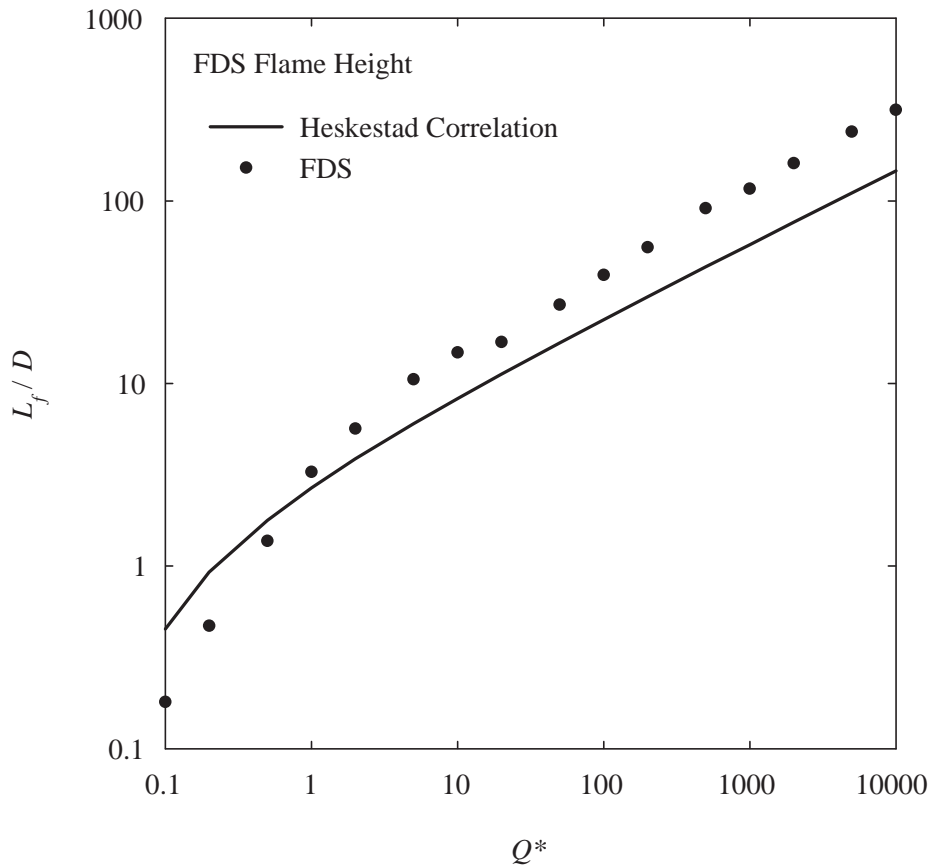


Figure 5.1: Comparison of FDS predictions of flame height from a 1 m square pan fire for Q^* values ranging from 0.1 to 10000.

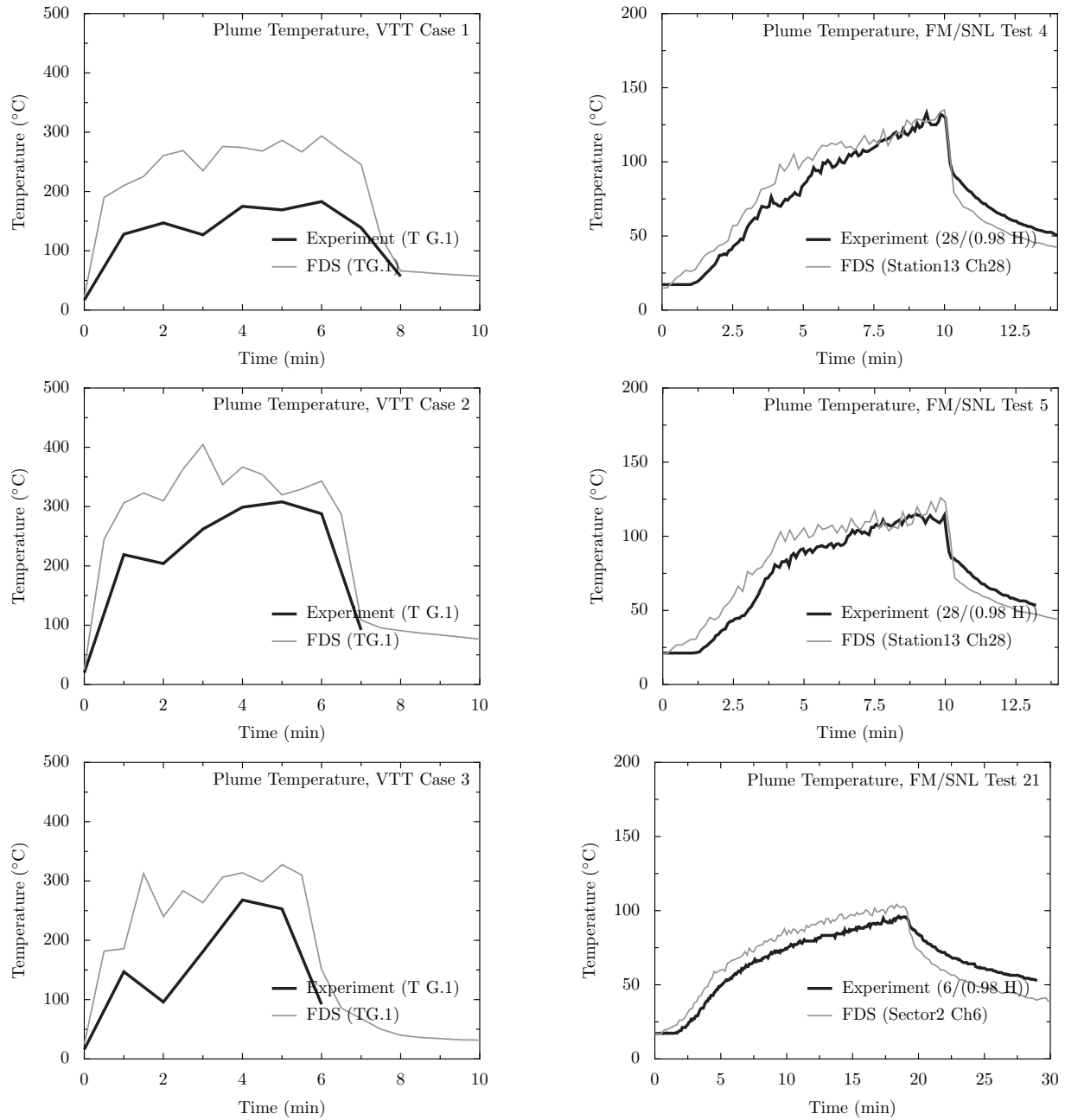
5.3 VTT Large Hall and FM/SNL Test Series

Plume temperature measurements are available from the VTT Large Hall and the FM/SNL series. For all the other full-scale experiments, the temperature above the fire has not been reported, or the fire plume leans because of the flow pattern within the compartment, or the fire is positioned against a wall. Only for the VTT and the FM/SNL series are the plumes relatively free from perturbations.

The VTT experiments consist of liquid fuel pan fires positioned in the middle of a large fire test hall. Plume temperatures are measured at two heights above the fire, 6 m and 12 m. The flames were observed to extend to about 4 m above the fire pan.

In the FM/SNL experiments, in Tests 4 and 5, thermocouples were positioned near the ceiling directly over the fire pan. In Test 21, the fire was positioned within an empty electrical cabinet, and the closest near ceiling thermocouple was used to assess the plume temperature prediction.

Comparisons of the predicted and measured plume temperatures for the VTT and FM/SNL tests are found on the following pages, including a summary plot at the end of the chapter.



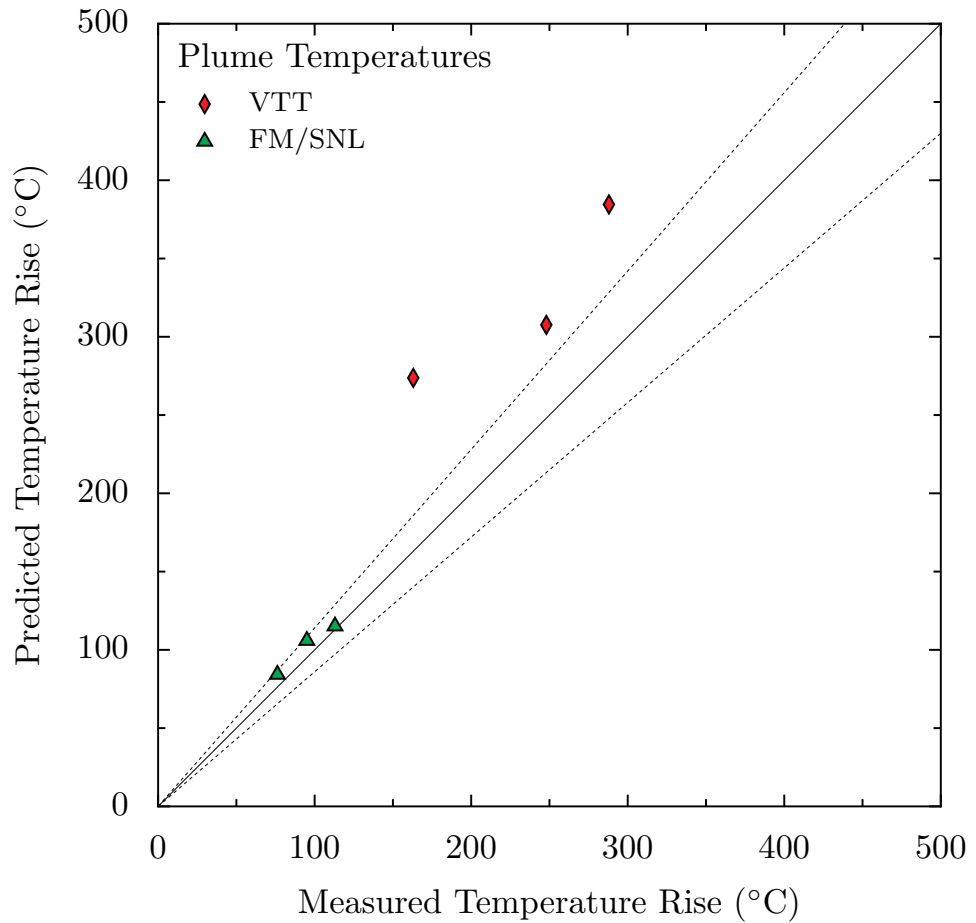


Figure 5.2: Summary of plume temperature predictions, VTT and FM/SNL test series.

Chapter 6

Ceiling Jets and Device Activation

FDS is a computational fluid dynamics (CFD) model and has no explicit ceiling jet model. Rather, temperatures throughout the fire compartment are computed directly from the governing conservation equations. Nevertheless, temperature measurements near the ceiling can be used to evaluate the model's ability to predict the flow of hot gases across a relatively flat ceiling. Measurements for this category are available from the NIST/NRC and the FM/SNL series.

6.1 WTC Test Series

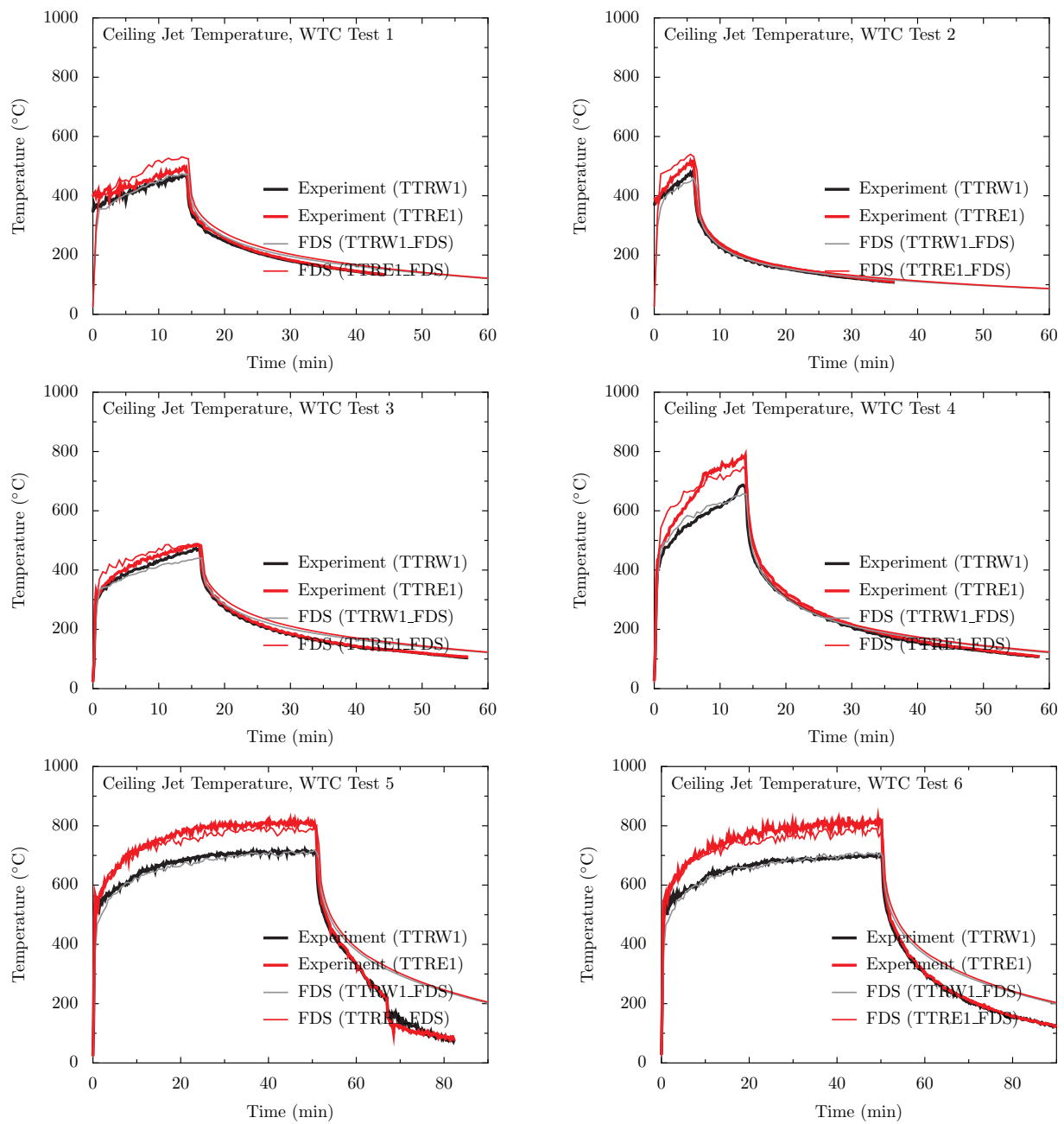
Aspirated thermocouples were positioned 3 m to the west (TTRW1) and 2 m to the east (TTRE1) of the fire pan, 18 cm below the ceiling.

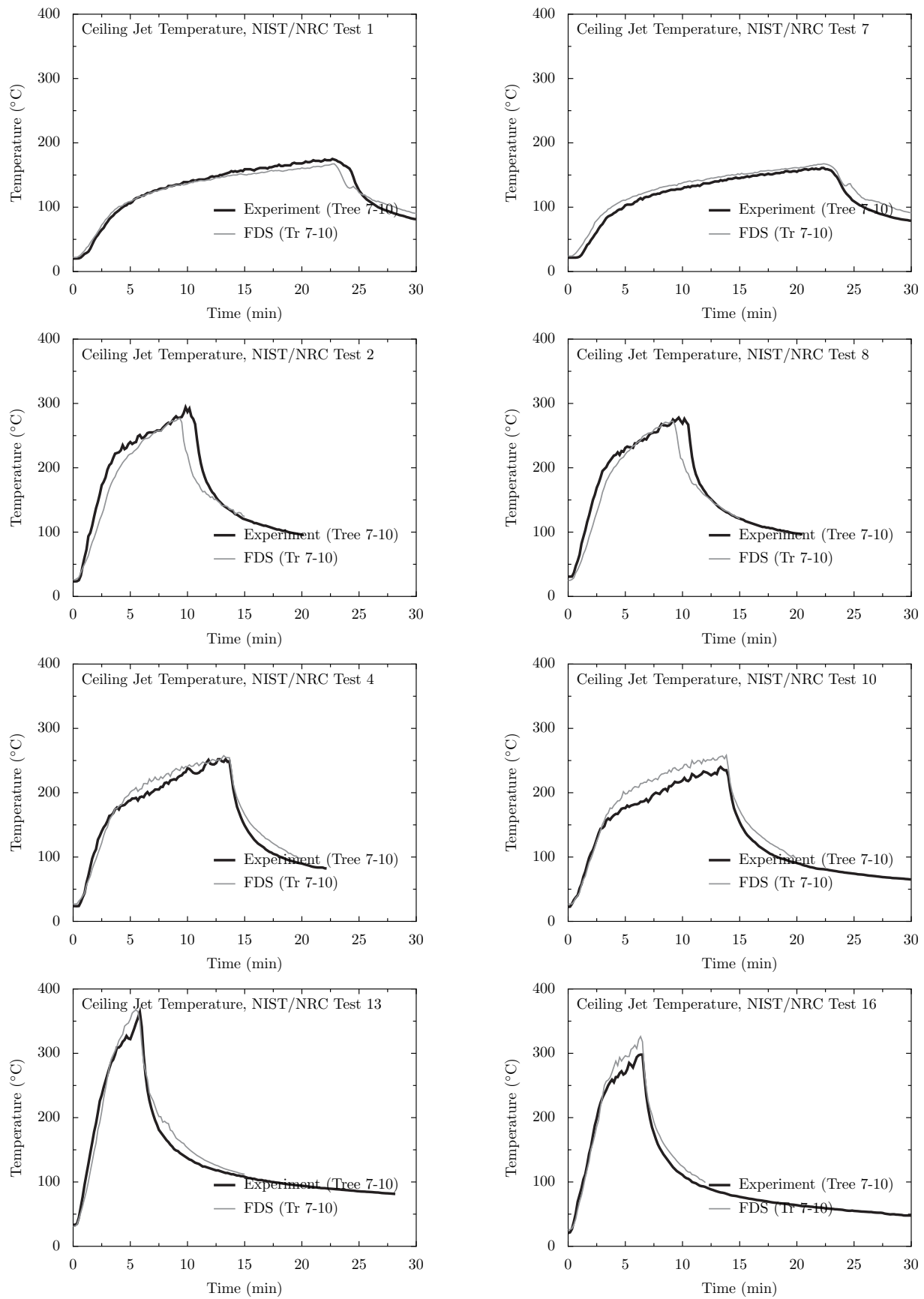
6.2 NIST/NRC Test Series

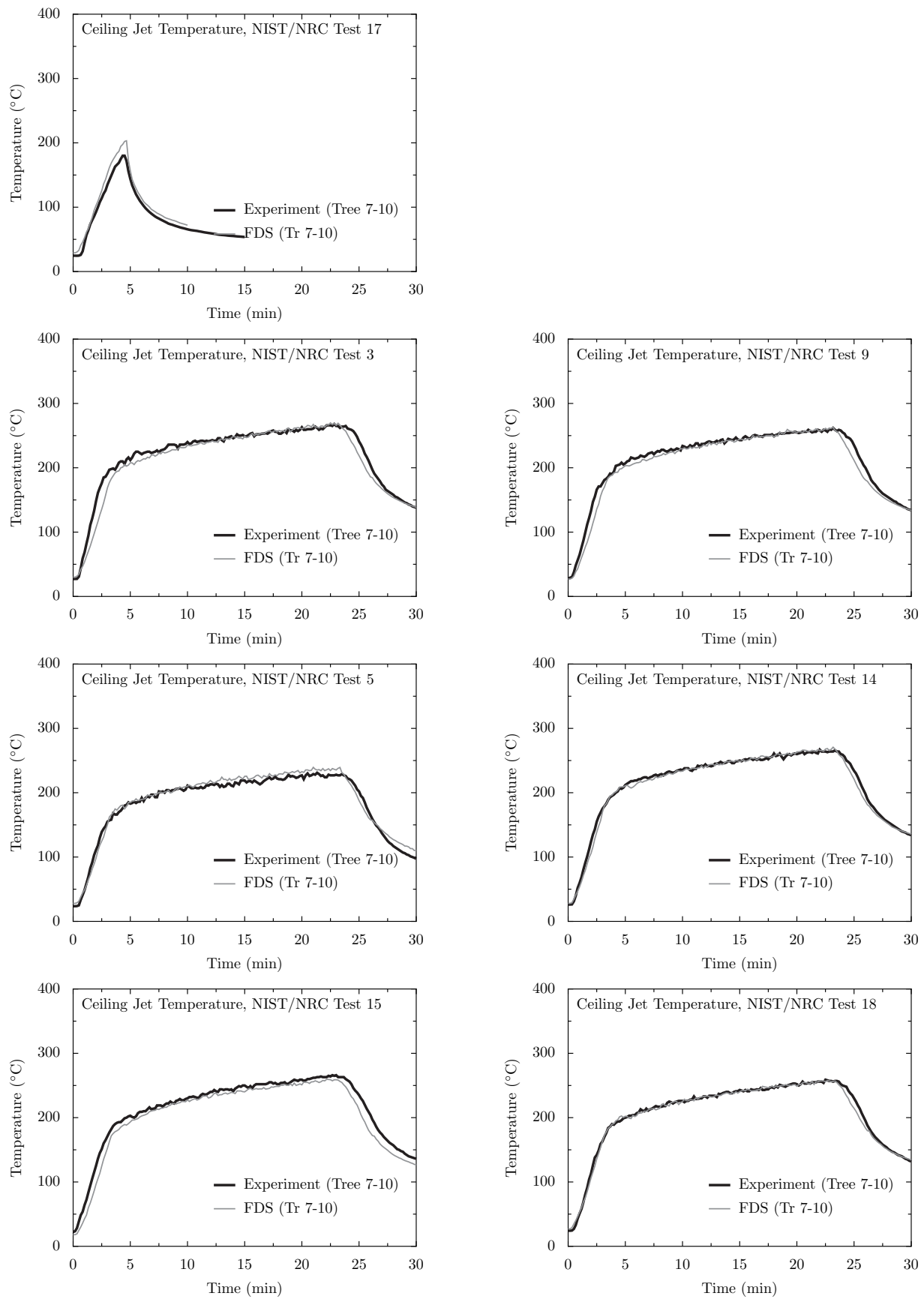
The thermocouple nearest the ceiling in Tree 7, located towards the back of the compartment, has been chosen as a surrogate for the ceiling jet temperature. Curiously, the difference between measured and predicted temperatures is noticeably greater for the open door tests. Certainly, the open door changes the flow pattern of the exhaust gases. However, the predicted HGL heights for the open door tests, shown in the previous section, do not show a noticeable difference from their closed door counterparts. The predicted HGL temperatures are only slightly less than those measured in the open door tests, due in large part to the contribution of Tree 7 in the layer reduction calculation.

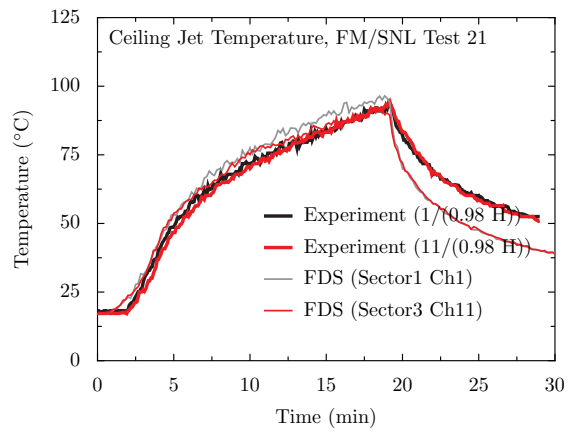
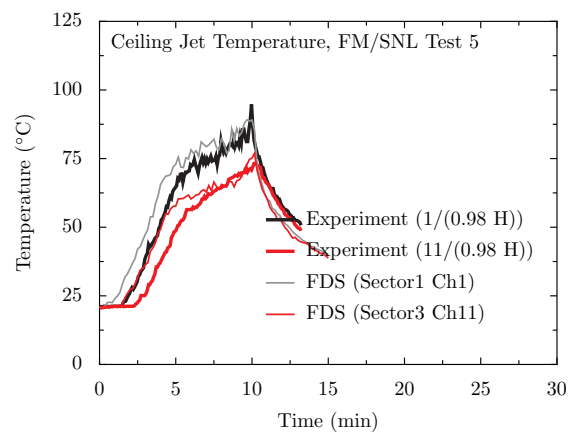
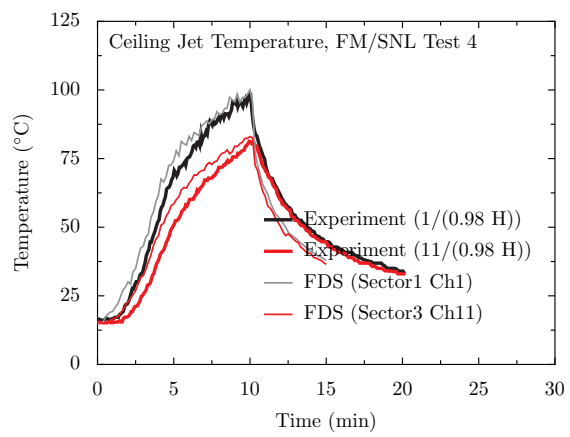
6.3 FM/SNL Test Series

The near-ceiling thermocouples in Sectors 1 and 3 have been chosen as surrogates for the ceiling jet temperature. The results are shown below. The only noticeable discrepancy is in Test 21, and it is the same pattern that was observed in the HGL temperature comparison for this test.









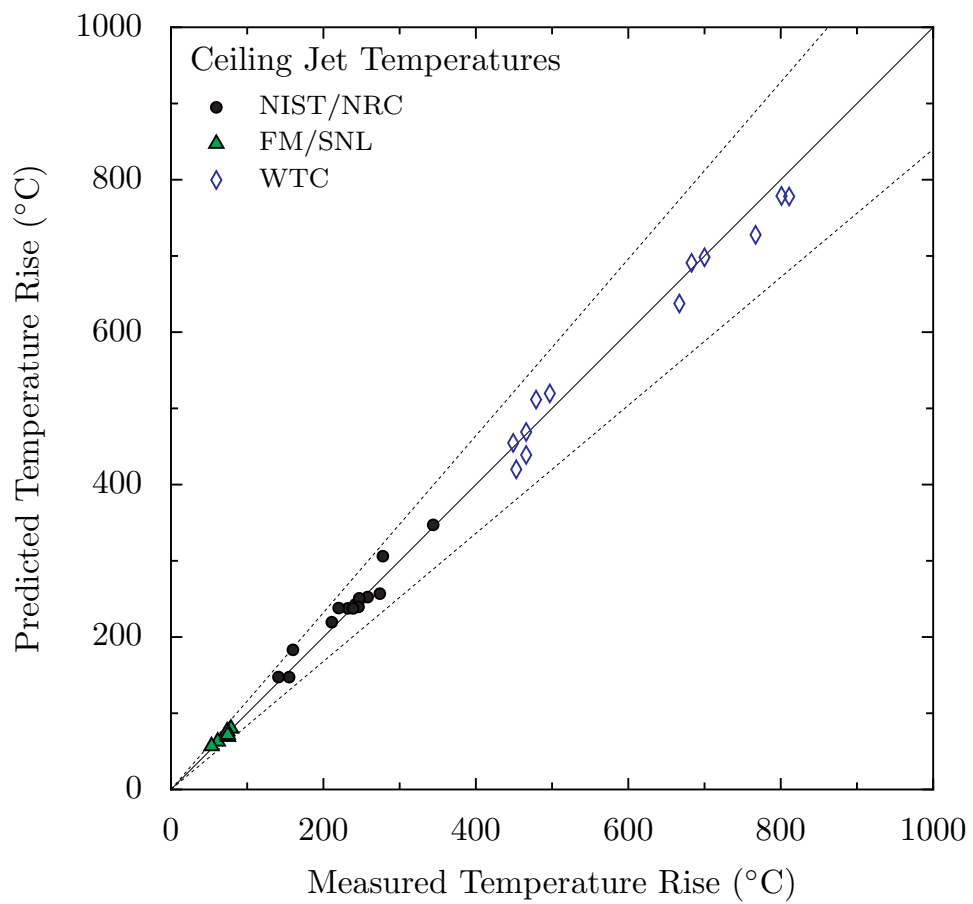


Figure 6.1: Summary of ceiling jet temperature predictions, WTC, NIST/NRC and FM/SNL test series.

6.4 UL/NFPRF Sprinkler, Vent, and Draft Curtain Experiments

The ceiling jet is an important fire phenomenon because of the presence of automatic fire protection devices at the ceiling, like sprinklers and smoke/heat vents. The results of the UL/NFPRF experiments provide useful data to assess the accuracy of FDS in predicting the velocity and temperature near the ceiling, and consequently the resulting activation of sprinklers. The UL/NFPRF test results (Series I) are summarized in Table 6.1, along with the predictions of FDS.

Heptane Spray Burner Test Series I								
Test No.	Burner Pos.	Vent Operation	First Act. (s)		Total Acts.		Draft Curtains	Heat Release Rate MW @ s
			Exp.	FDS	Exp.	FDS		
I-1	B	Closed	65	53	11	11	Yes	4.4 @ 50
I-2	B	Manual (0:40)	66	53	12	9	Yes	4.4 @ 50
I-3	B	Manual (1:30)	64	53	12	9	Yes	4.4 @ 50
I-4	C	Closed	60	52	10	11	Yes	4.4 @ 50
I-5	C	Manual (0:40)	72	52	9	8	Yes	4.4 @ 50
I-6	C	Manual (1:30)	62	52	8	8	Yes	4.4 @ 50
I-7	C	74°C link (DNO)	70	52	10	11	Yes	4.4 @ 50
I-8	B	74°C link (9:26)	60	53	11	11	Yes	4.4 @ 50
I-9	D	74°C link (DNO)	70	55	12	16	Yes	4.4 @ 50
I-10	D	Manual (0:40)	72	55	13	14	Yes	4.4 @ 50
I-11	D	74°C link (4:48)	N/A	N/A	N/A	N/A	Yes	4.4 @ 50
I-12	A	Closed	68	58	14	13	Yes	4.4 @ 50
I-13	A	74°C link (1:04)	69	59	5	11	Yes	6.0 @ 60
I-14	A	Manual (0:40)	74	127	7	7	Yes	5.8 @ 60
I-15	A	Manual (1:30)	64	59	5	13	Yes	5.8 @ 60
I-16	A	74°C link (1:46)	106	99	4	6	Yes	5.0 @ 110
I-17	B	100°C link (DNO)	58	54	4	6	No	4.6 @ 50
I-18	C	100°C link (DNO)	58	58	4	4	No	3.7 @ 50
I-19	A	100°C link (10:00)	56	60	10	4	No	4.6 @ 50
I-20	A	74°C link (1:20)	54	64	4	4	No	4.2 @ 50
I-21	C	74°C link (7:00)	58	52	10	4	No	4.6 @ 50
I-22	D	100°C link (DNO)	60	54	6	5	No	4.6 @ 50

Table 6.1: Results of the UL/NFPRF Experiments. Note that DNO means “Did Not Open”. Also note, the fires grew at a rate proportional to the square of the time until a certain flow rate of fuel was achieved at which time the flow rate was held steady. Thus, the “Heat Release Rate” was the size of the fire at the time when the fuel supply was leveled off.

Figure 6.2 displays graphically the difference between predicted and measured sprinkler activation times as a function of burner position. Note that there are no experimental uncertainty bounds on the plot because it is difficult to estimate the combined uncertainty related to the various parameters that are input into the model. For example, changing the median volumetric droplet size from 1000 μm to 750 μm led to a reduction of approximately 50 % in the number of predicted sprinkler activations due to the increased cooling of the smaller droplets. Consequently, three replicate experiments are compared to show how much variation one can expect in sprinkler activation times in repeat experiments.

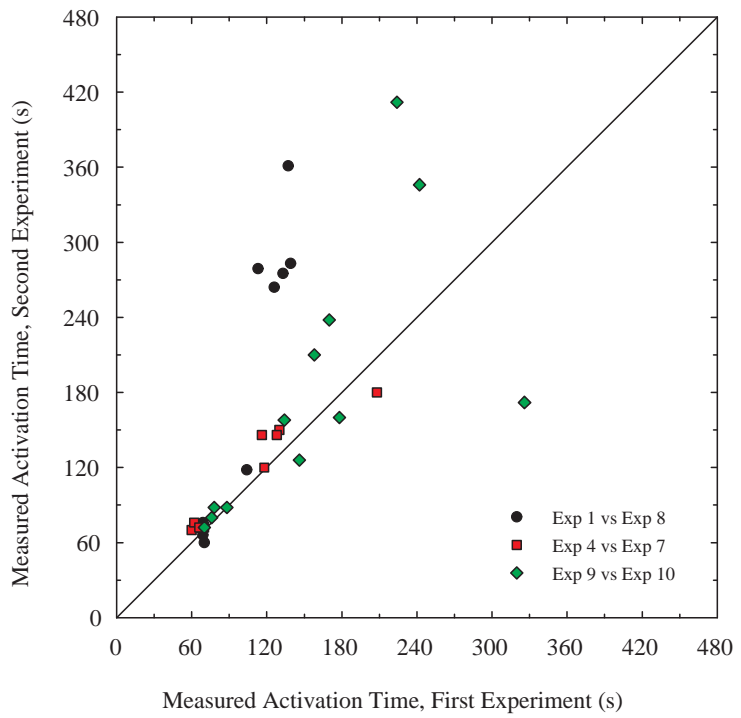
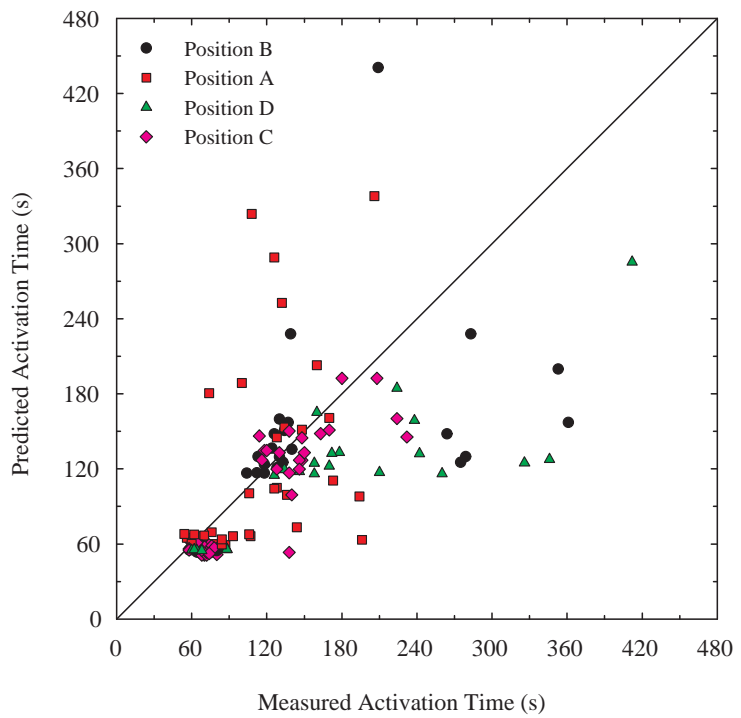


Figure 6.2: Above: Comparison of predicted and measured sprinkler activation times for the UL/NFPRF Series. Below: Comparison of activation times for three pairs of replicate experiments.

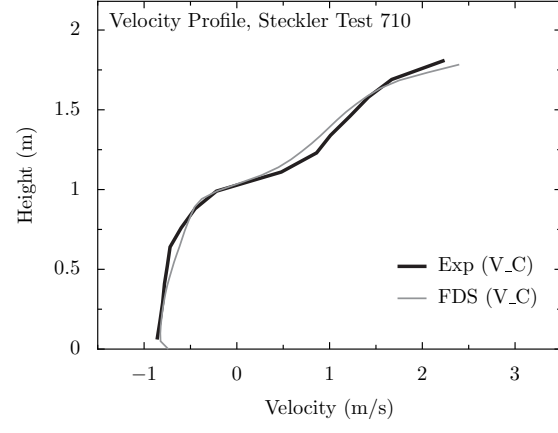
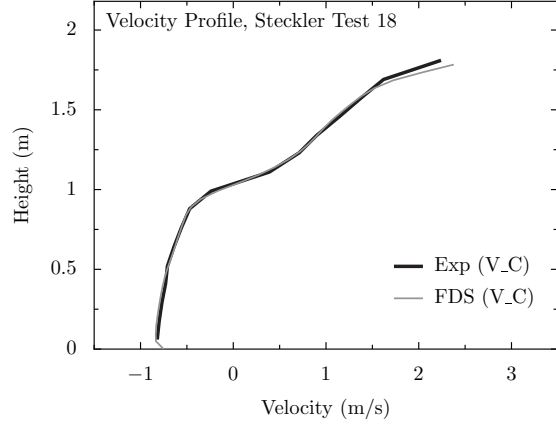
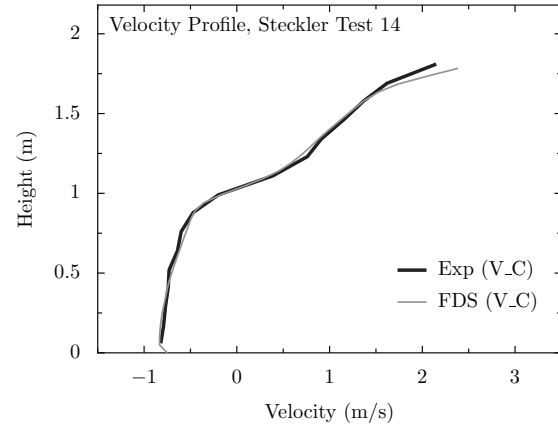
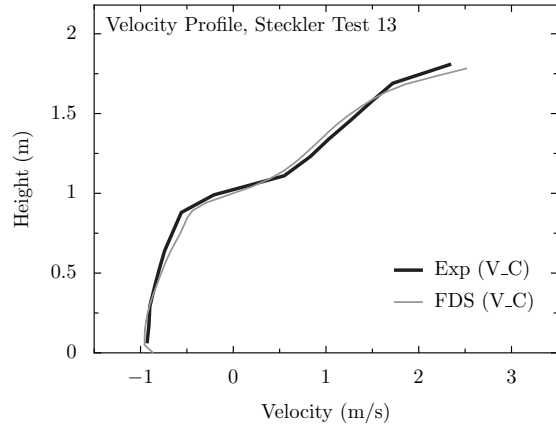
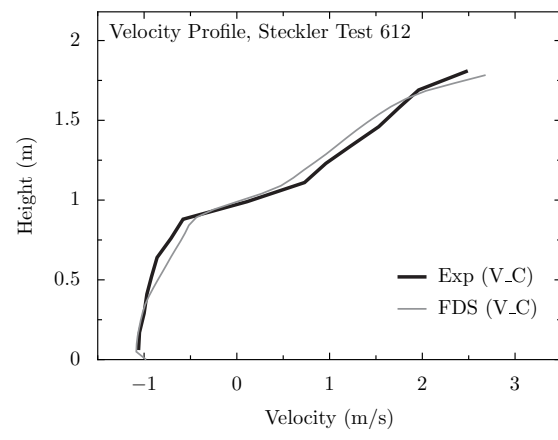
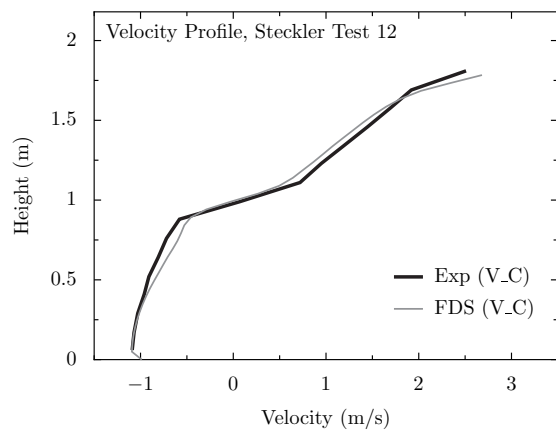
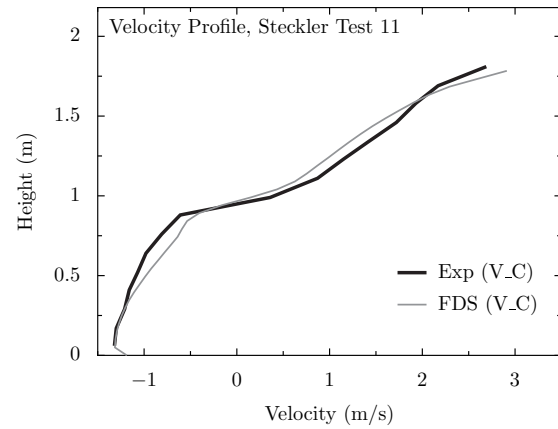
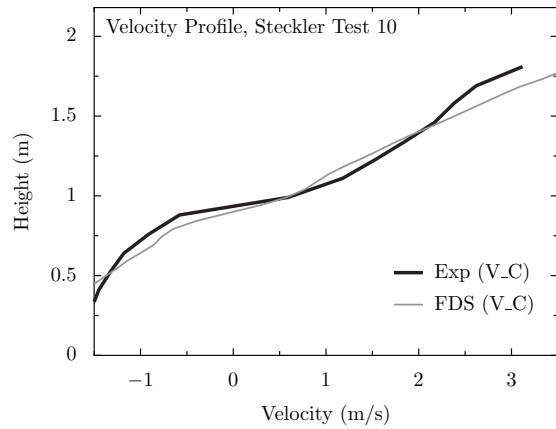
Chapter 7

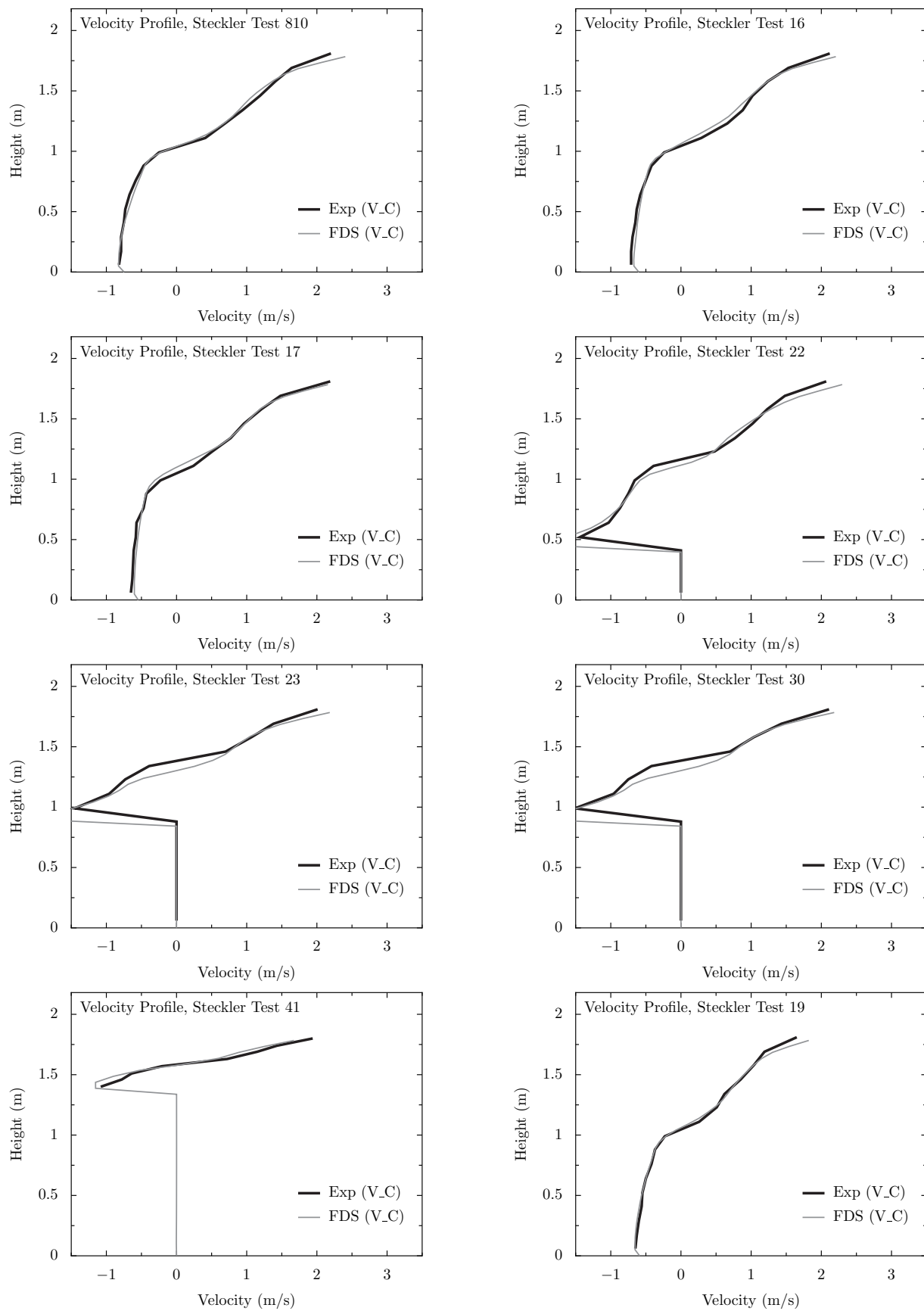
Gas Velocity

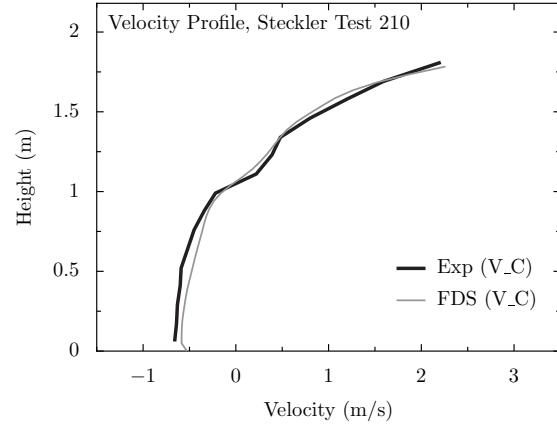
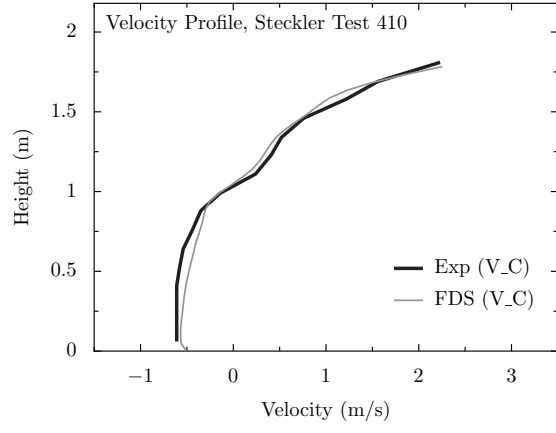
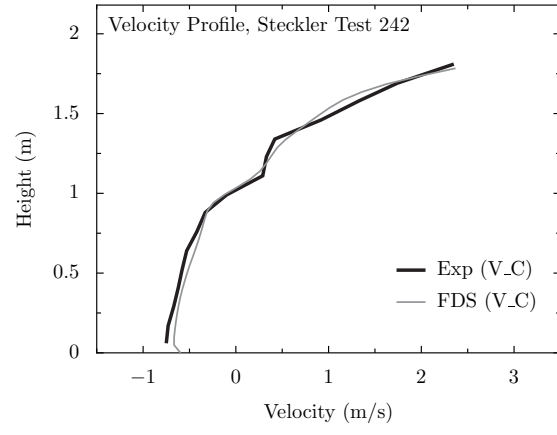
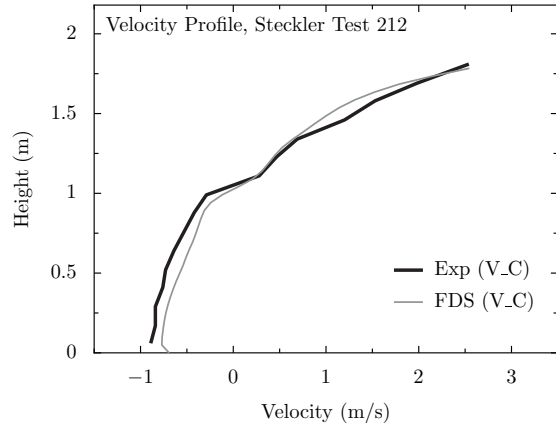
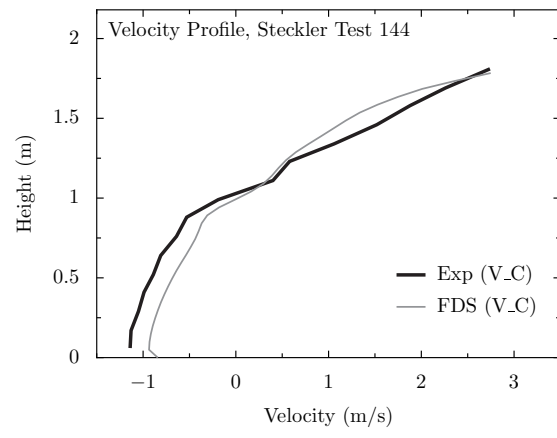
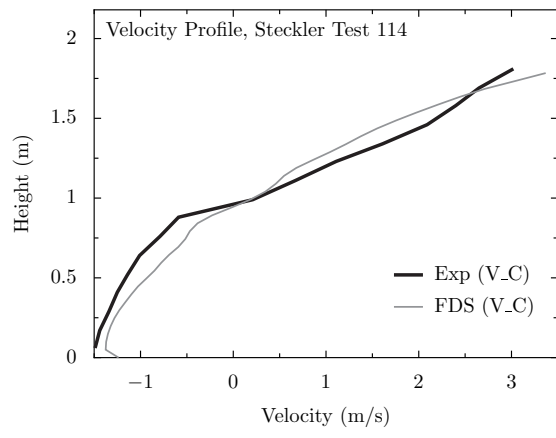
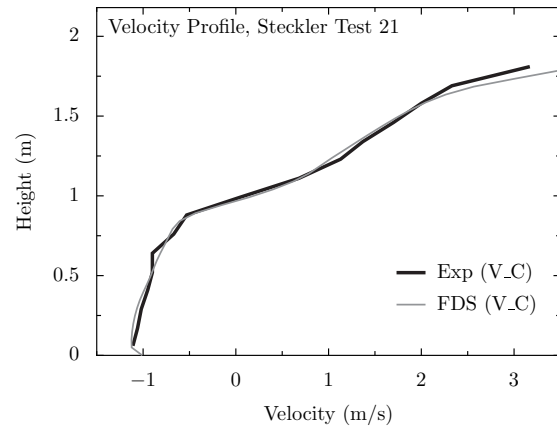
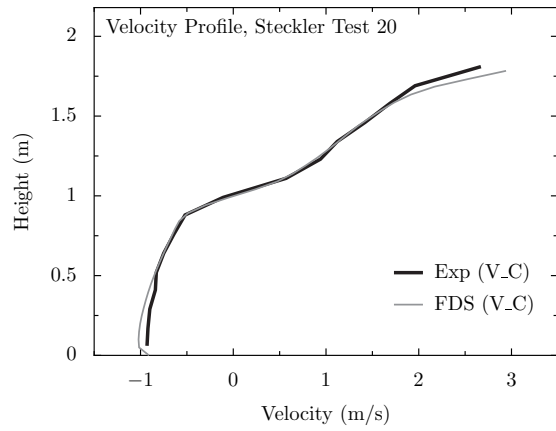
Gas velocity is often measured at compartment inlets and outlets as part of a global assessment of mass and energy conservation. This chapter contains measurements of gas velocity and related quantities.

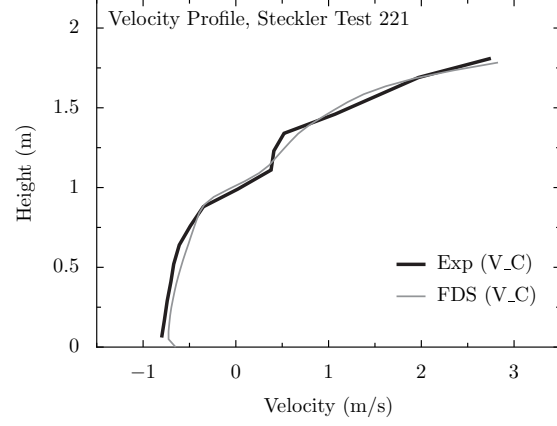
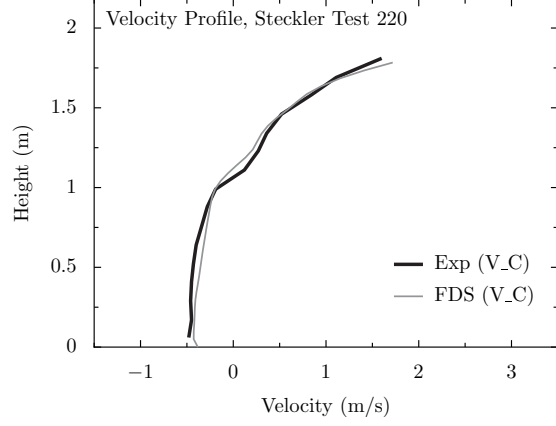
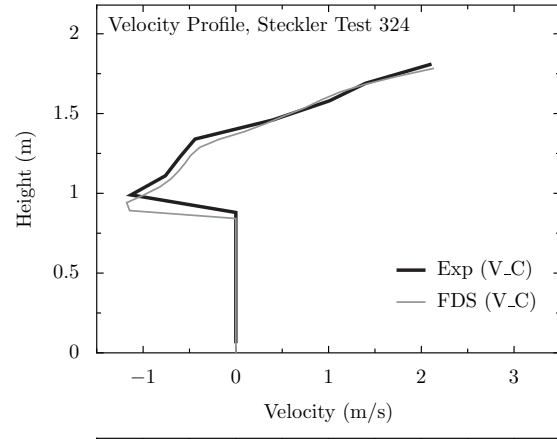
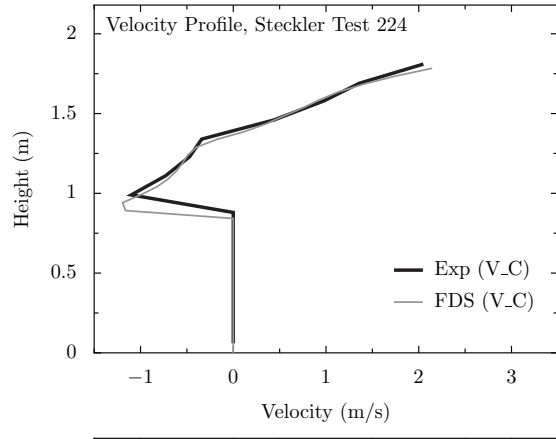
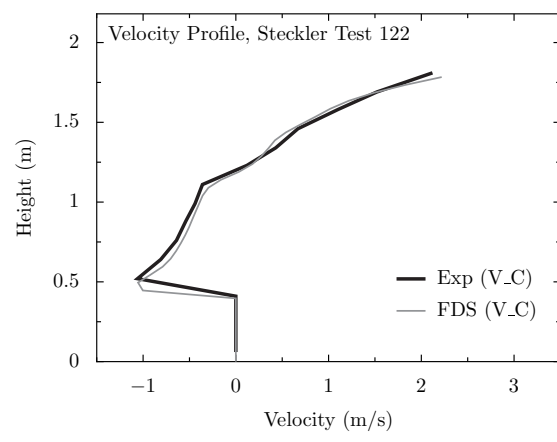
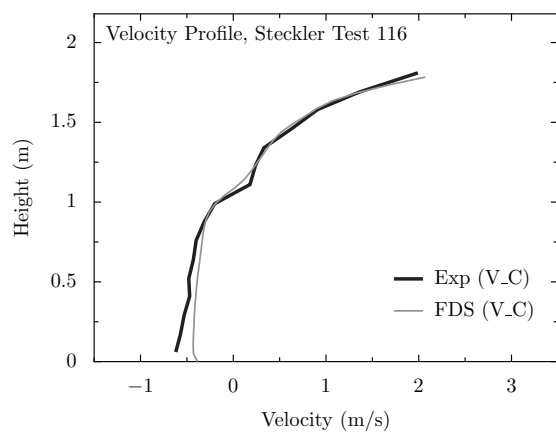
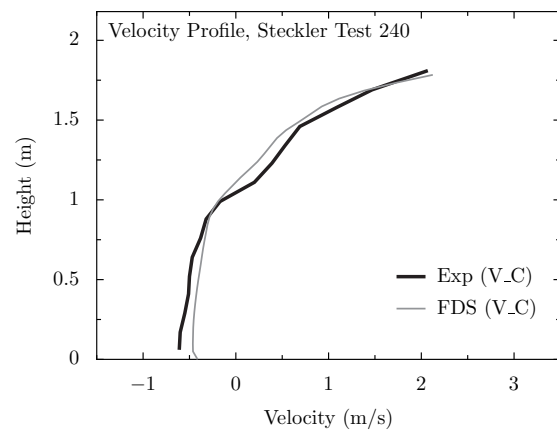
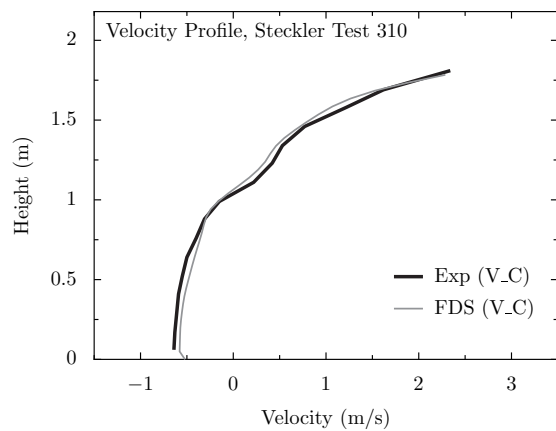
7.1 Steckler Compartment Doorway Velocity Profiles

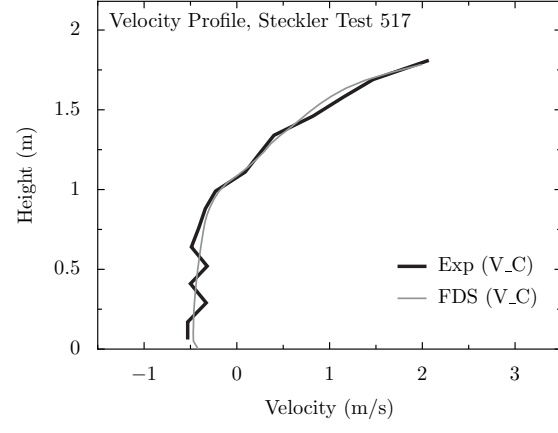
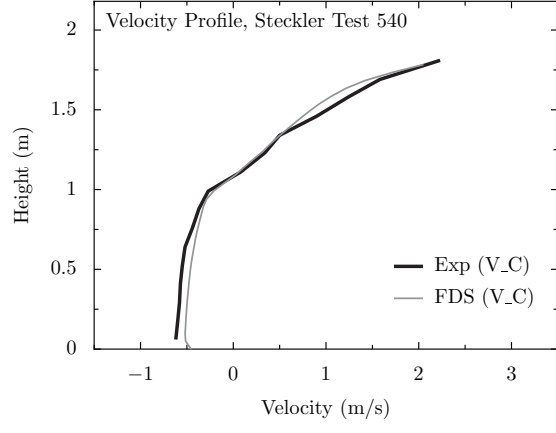
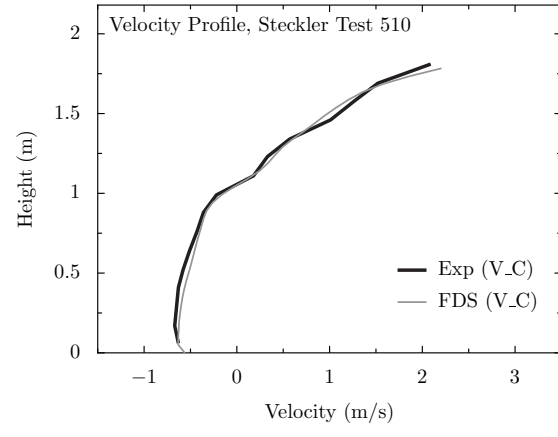
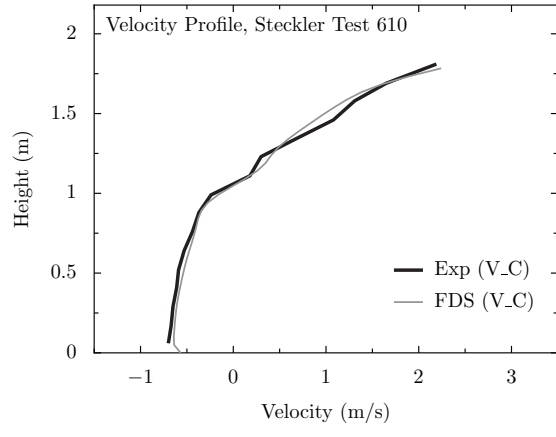
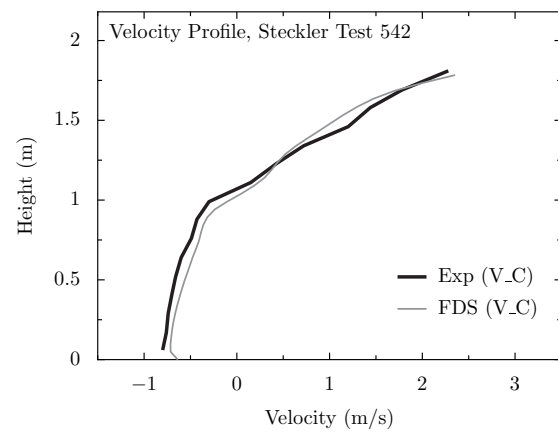
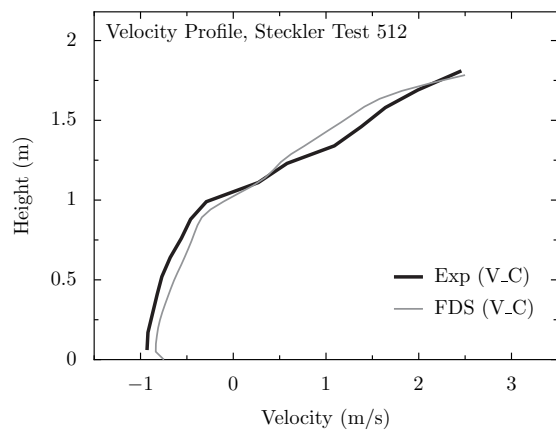
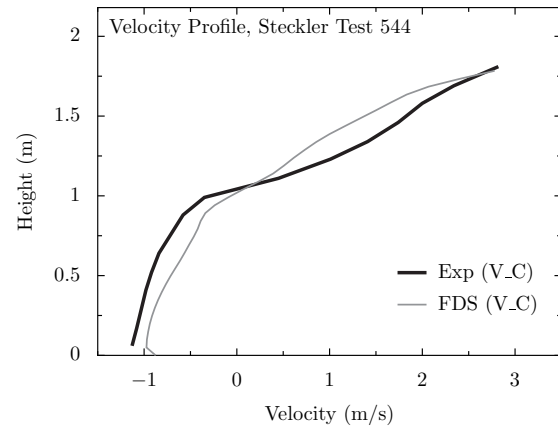
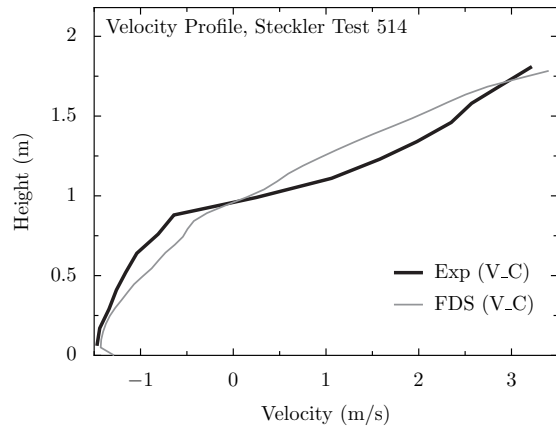
Steckler *et al.* [102] mapped the doorway/window flows in 55 compartment fire experiments. The test matrix is presented in Table 3.1. Shown on the following pages are the centerline profiles, compared with model predictions. Off-center profiles are not shown. The vertical spacing of the measurements was approximately 11 cm, with the uppermost velocity probe centered 5.7 cm below the 10 cm thick soffit. The FDS simulations were uniformly gridded with cells of 5 cm on each side. To quantify the difference between prediction and measurement, the maximum outward velocities, which always occurred at the uppermost measurement location, were compared.

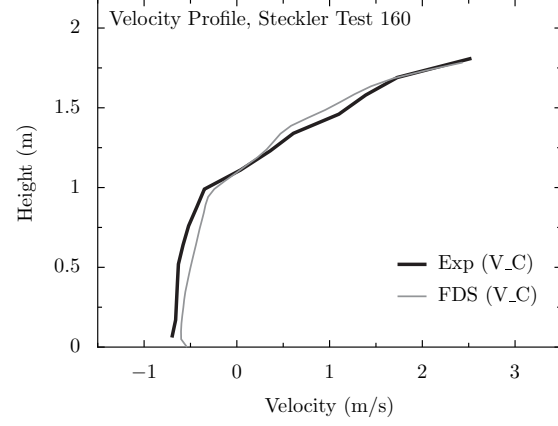
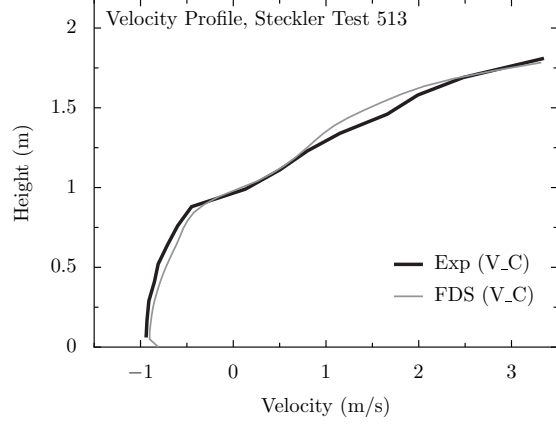
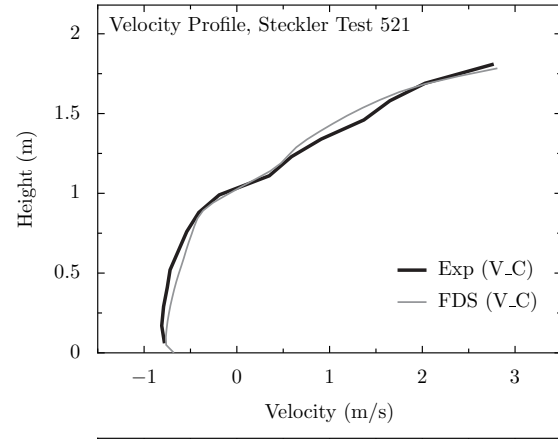
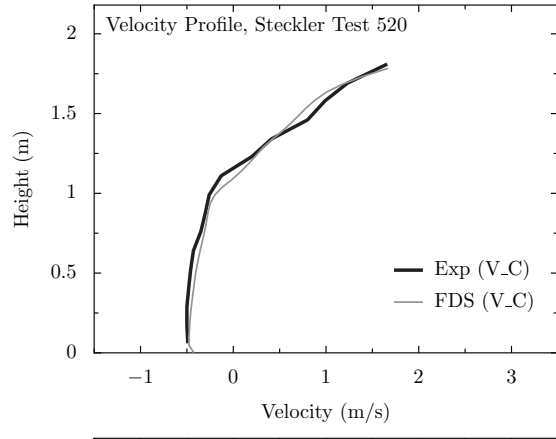
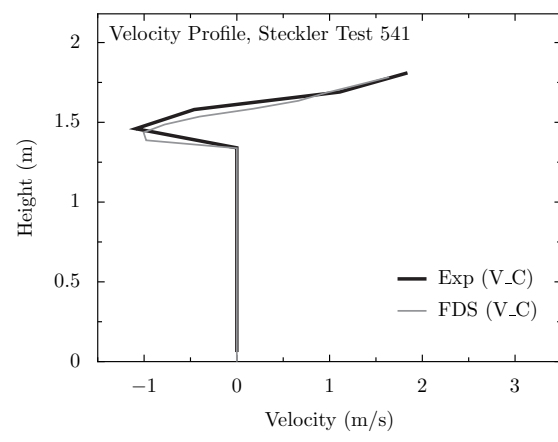
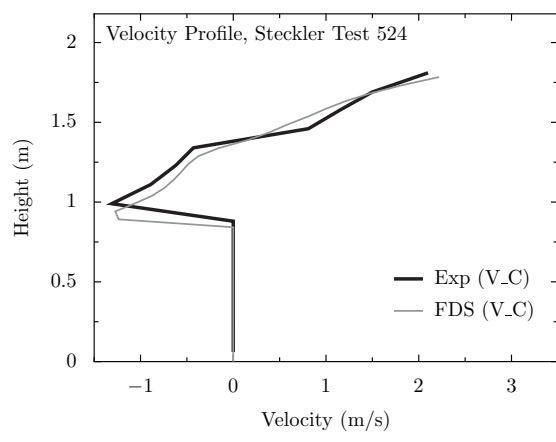
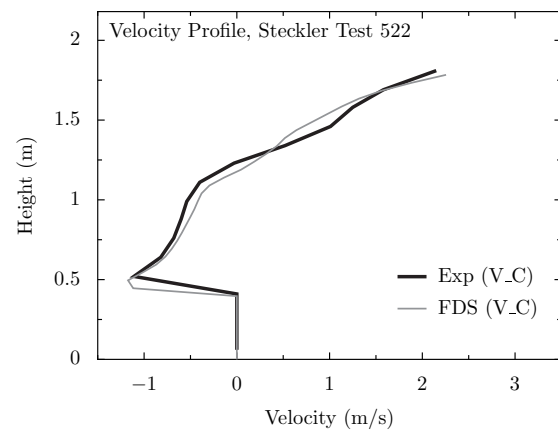
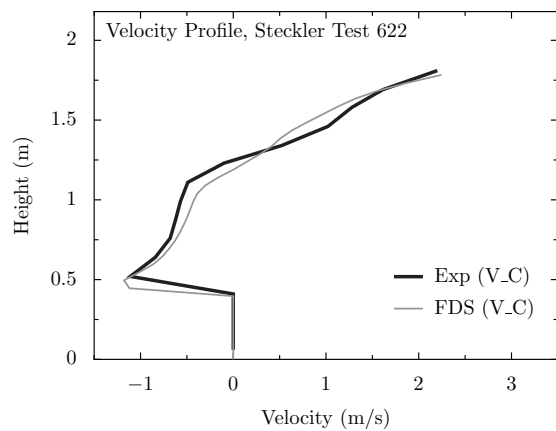


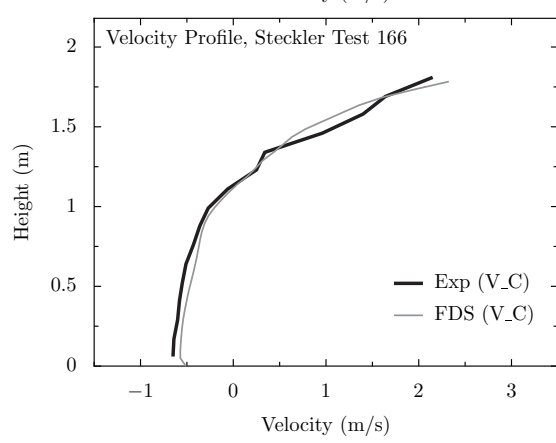
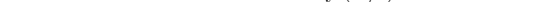
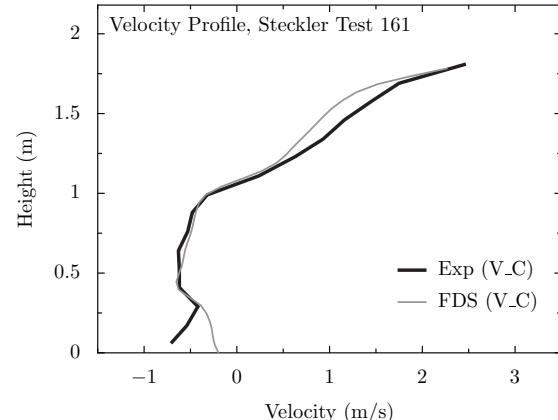
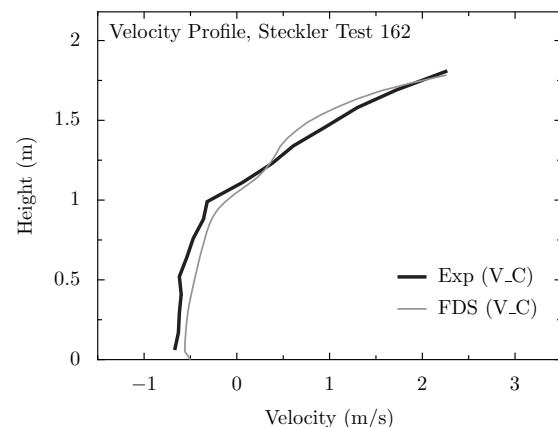
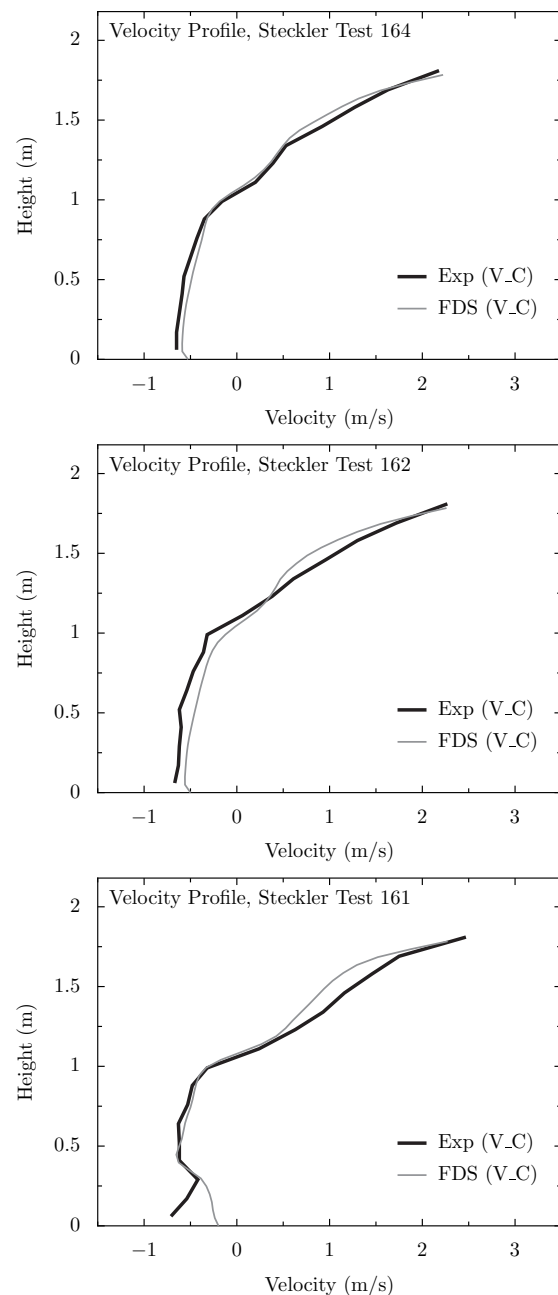
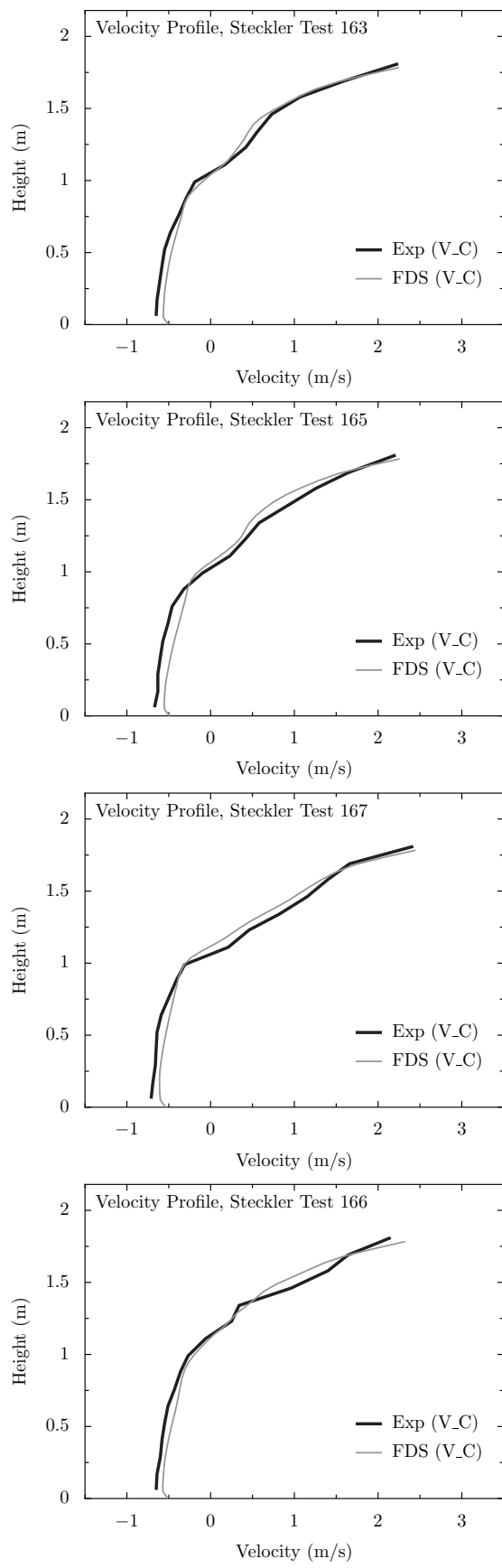












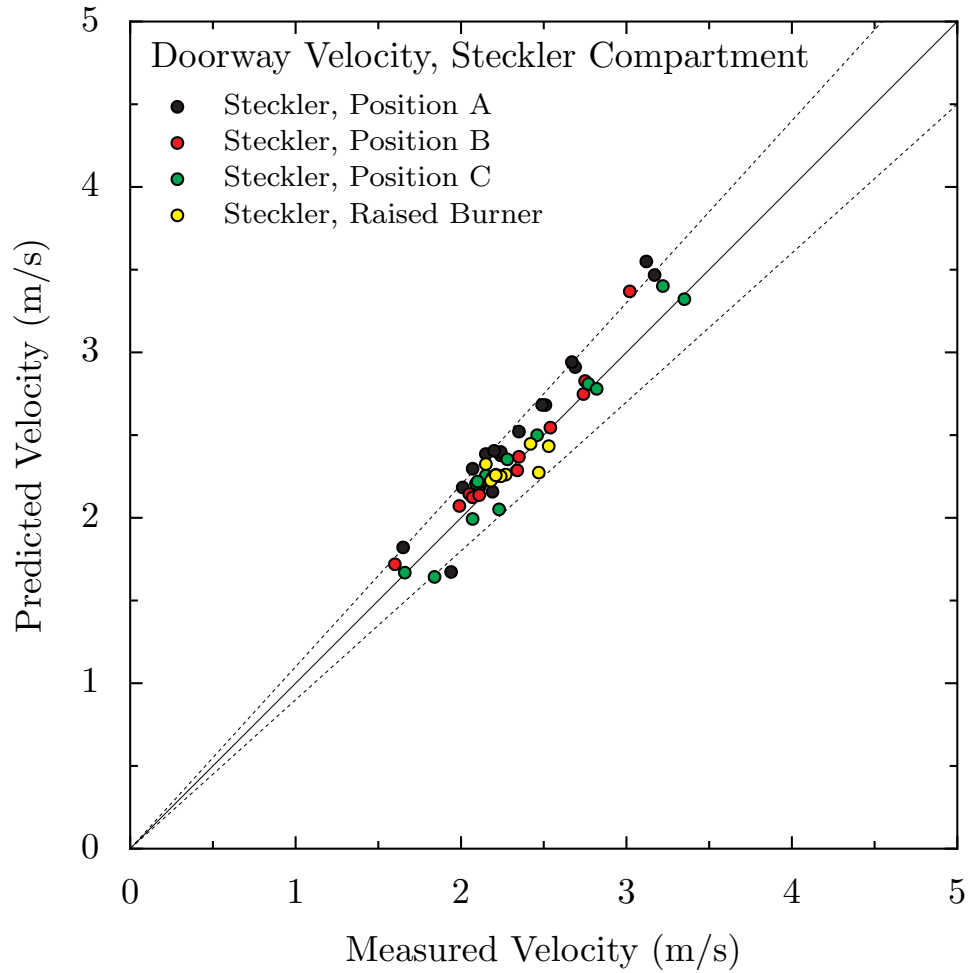


Figure 7.1: Summary of comparisons of predicted and measured maximum velocities in the doorway/window of the Steckler compartment experiments. The uncertainty in the measurements (dotted lines) were reported by Steckler to be about 10 %.

Chapter 8

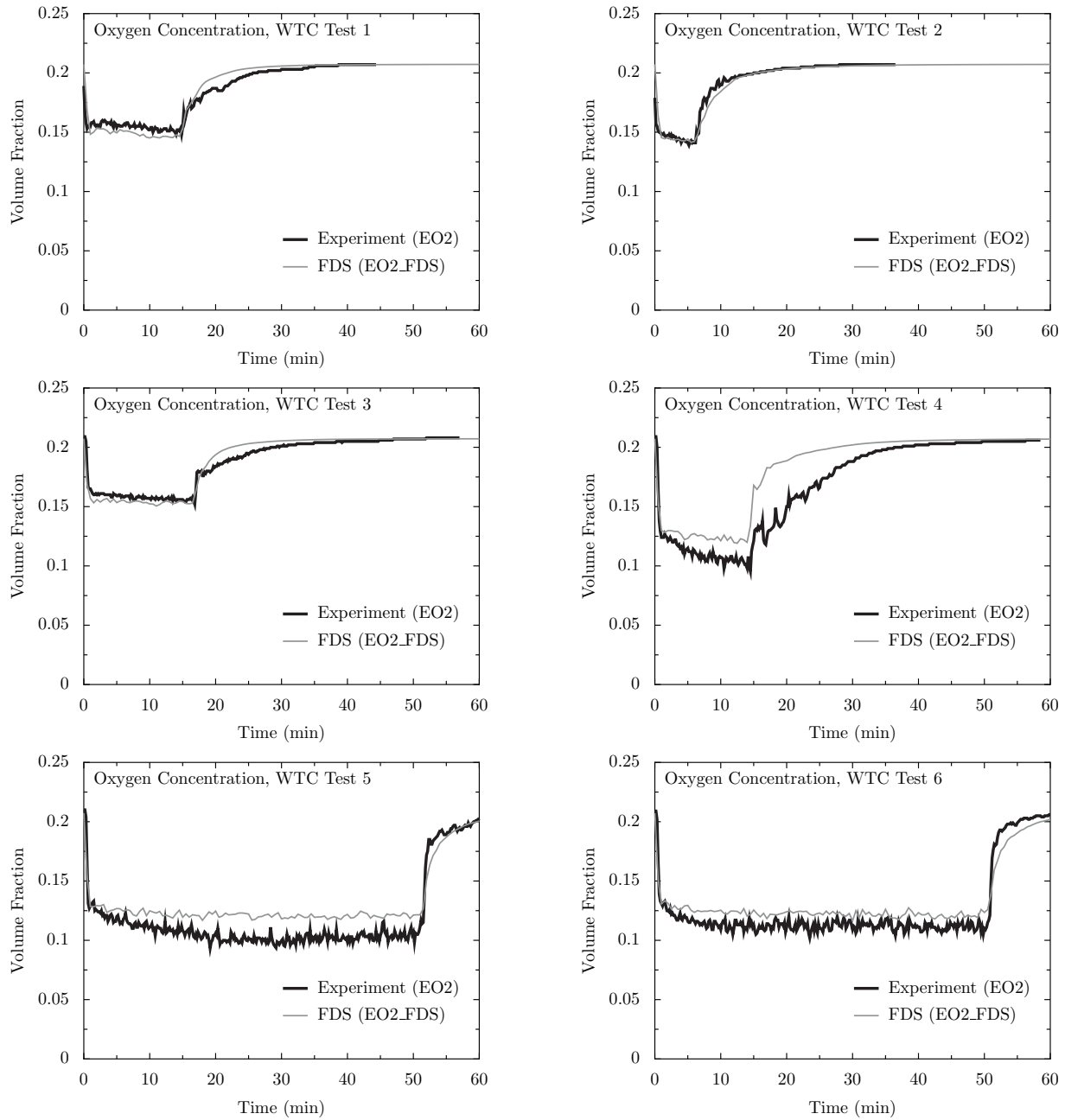
Gas Species and Smoke

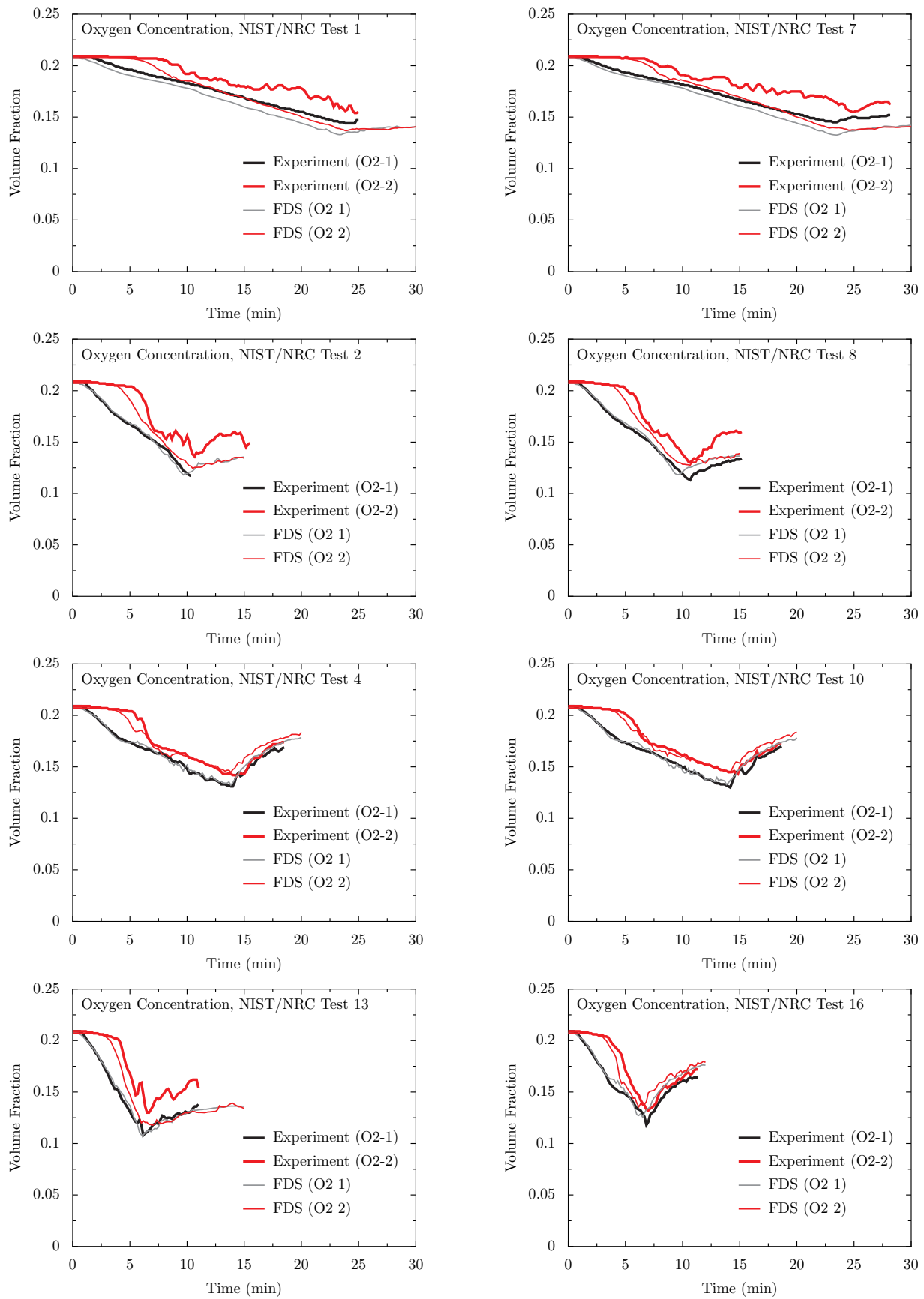
For most applications, FDS uses a single step chemical reaction whose products are tracked via a two-parameter mixture fraction model. The mixture fraction is a conserved scalar quantity that represents the mass fraction of one or more components of the gas at a given point in the flow field. By default, two components of the mixture fraction are explicitly computed. The first is the mass fraction of unburned fuel and the second is the mass fraction of burned fuel (i.e. the mass of the combustion products that originated as fuel). When the default model is used, O₂, CO₂ and smoke concentrations are obtained from the explicitly computed mixture fraction variables. Their yields are specified by the user and do not change.

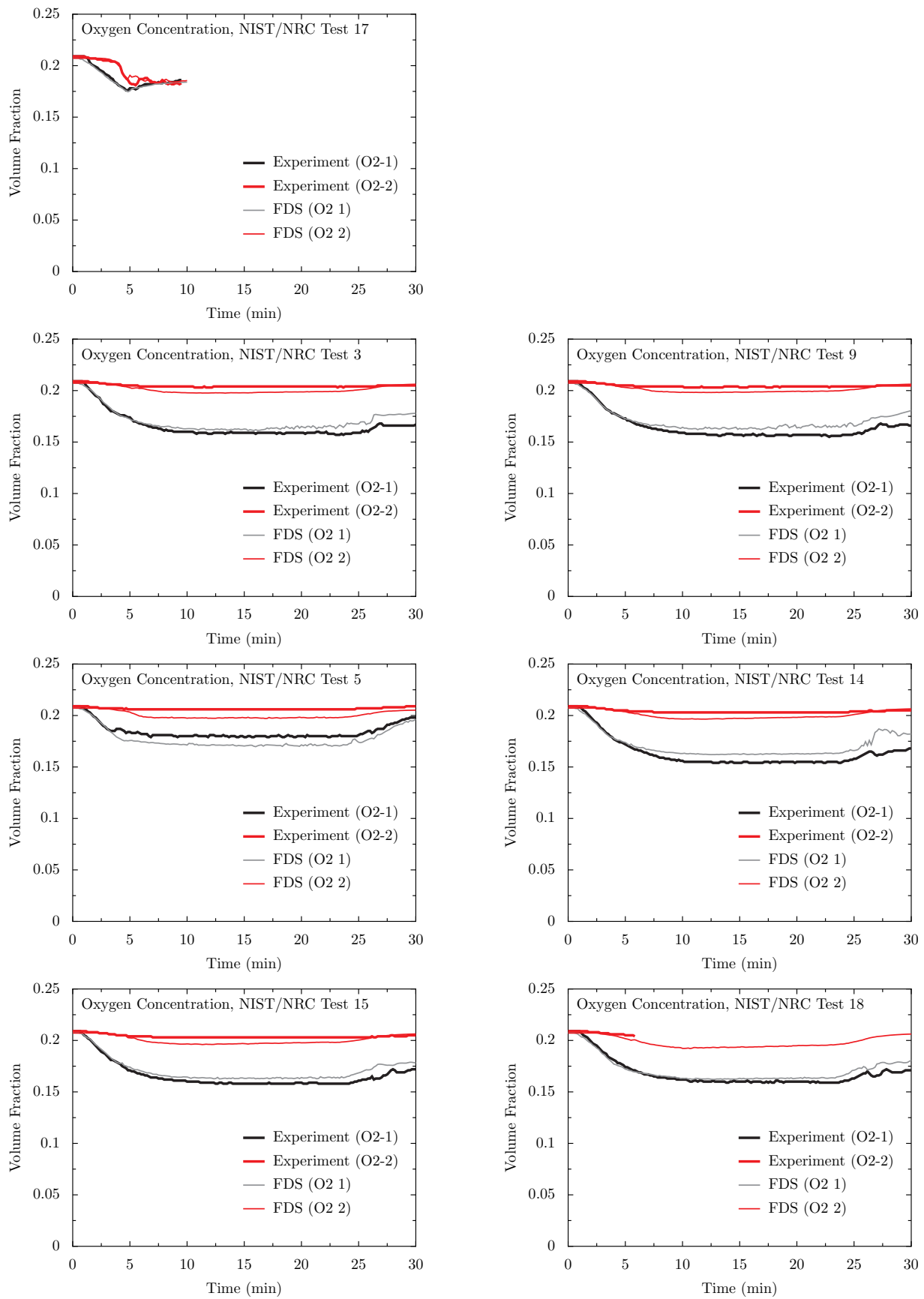
FDS has an optional two-step chemical reaction with a three parameter mixture fraction decomposition with the first step being oxidation of fuel to carbon monoxide and the second step the oxidation of carbon monoxide to carbon dioxide. The three mixture fraction components for the two step reaction are unburned fuel, mass of fuel that has completed the first reaction step, and the mass of fuel that has completed the second reaction step. The mass fractions of all of the major reactants and products can be derived from the mixture fraction parameters by means of “state relations.” Examples of this more detailed model can be found later in this chapter.

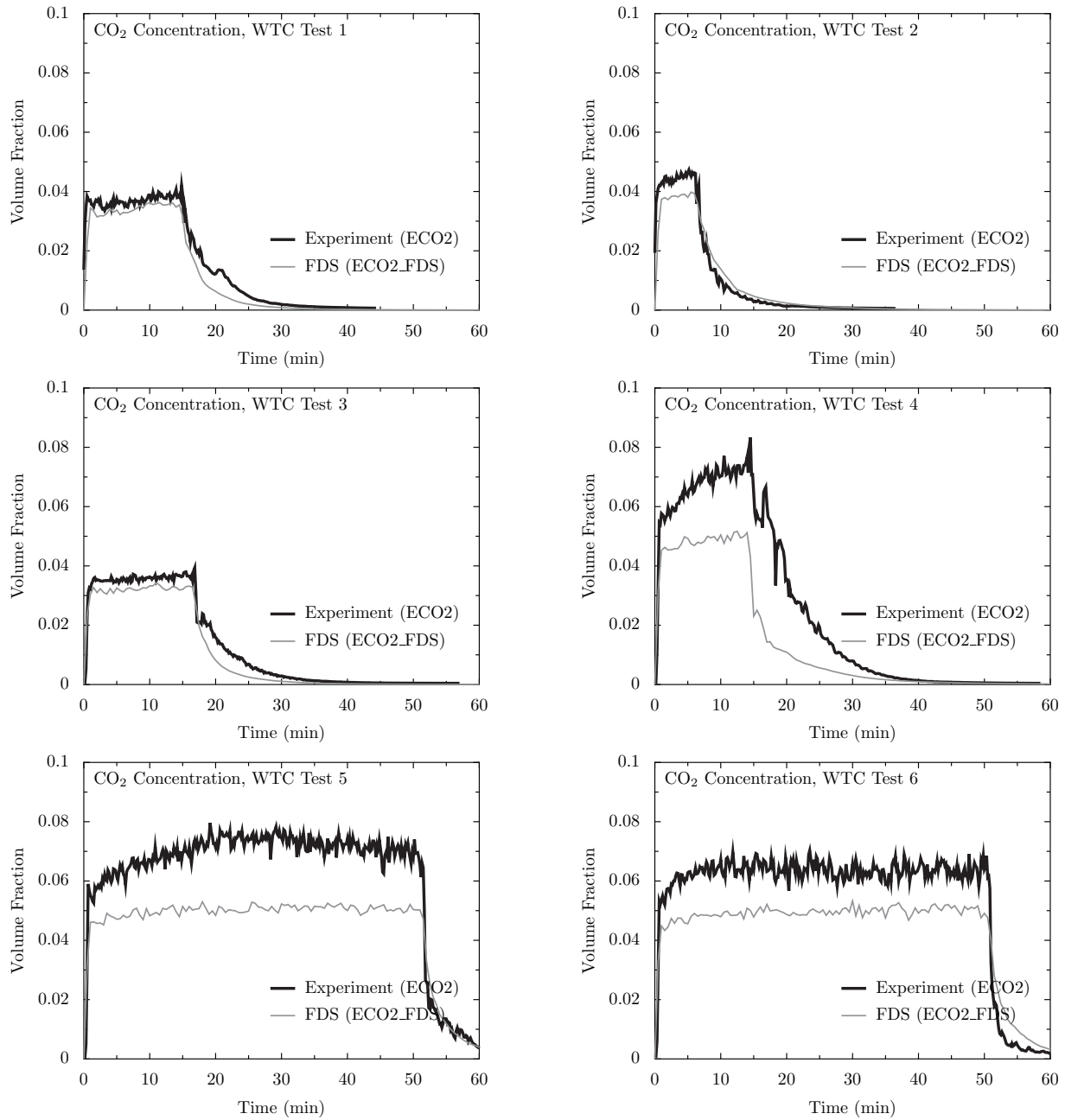
8.1 WTC and NIST/NRC Test Series, Oxygen and CO₂

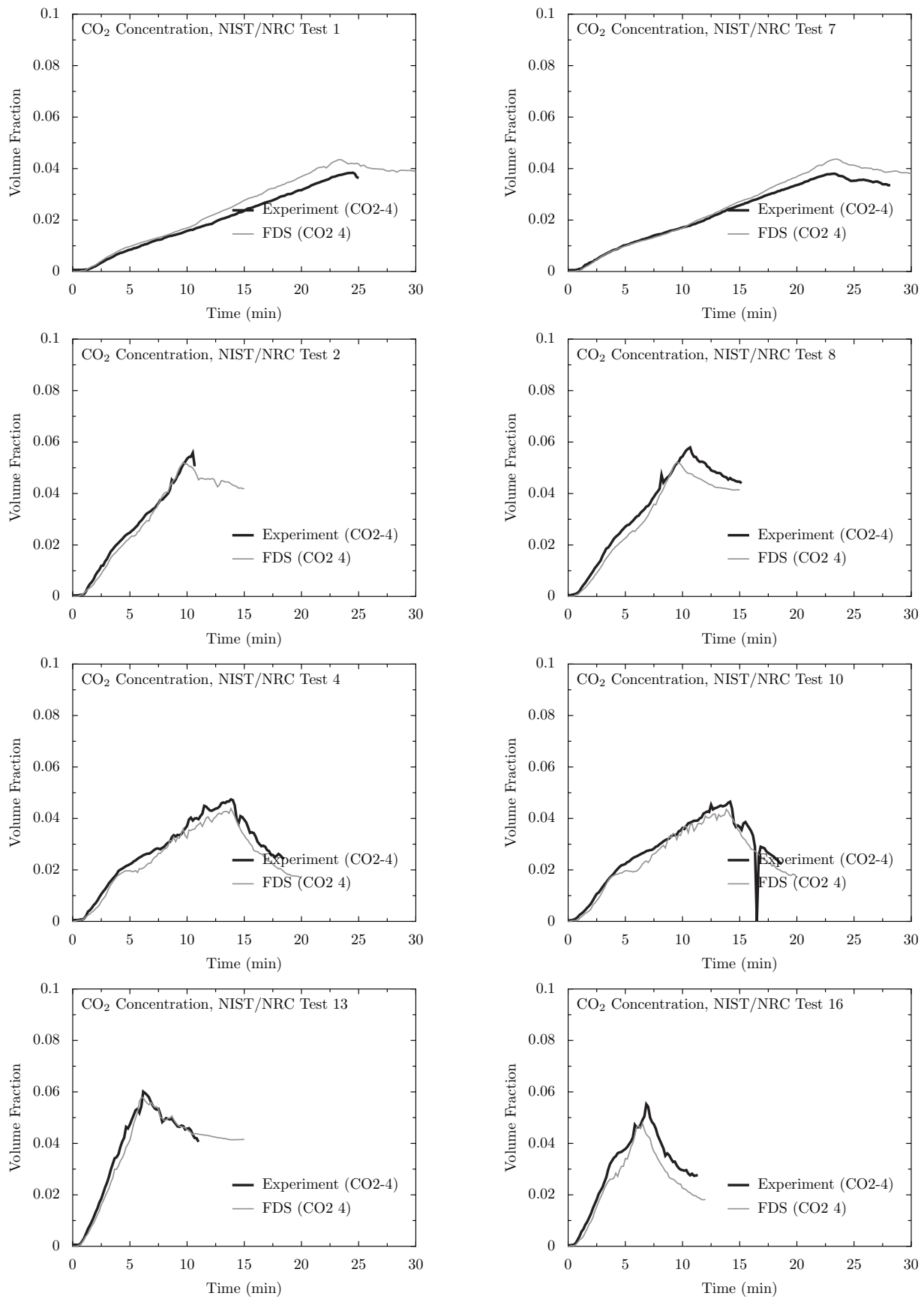
The following pages present comparisons of oxygen and carbon dioxide concentration predictions and measurements for the WTC and NIST/NRC series. In the WTC tests, there was only one measurement of each made near the ceiling of the compartment roughly 2 m from the seat of the fire. In the NIST/NRC tests, there were two oxygen measurements, one in the upper layer, one in the lower. There was only one carbon dioxide measurement in the upper layer.

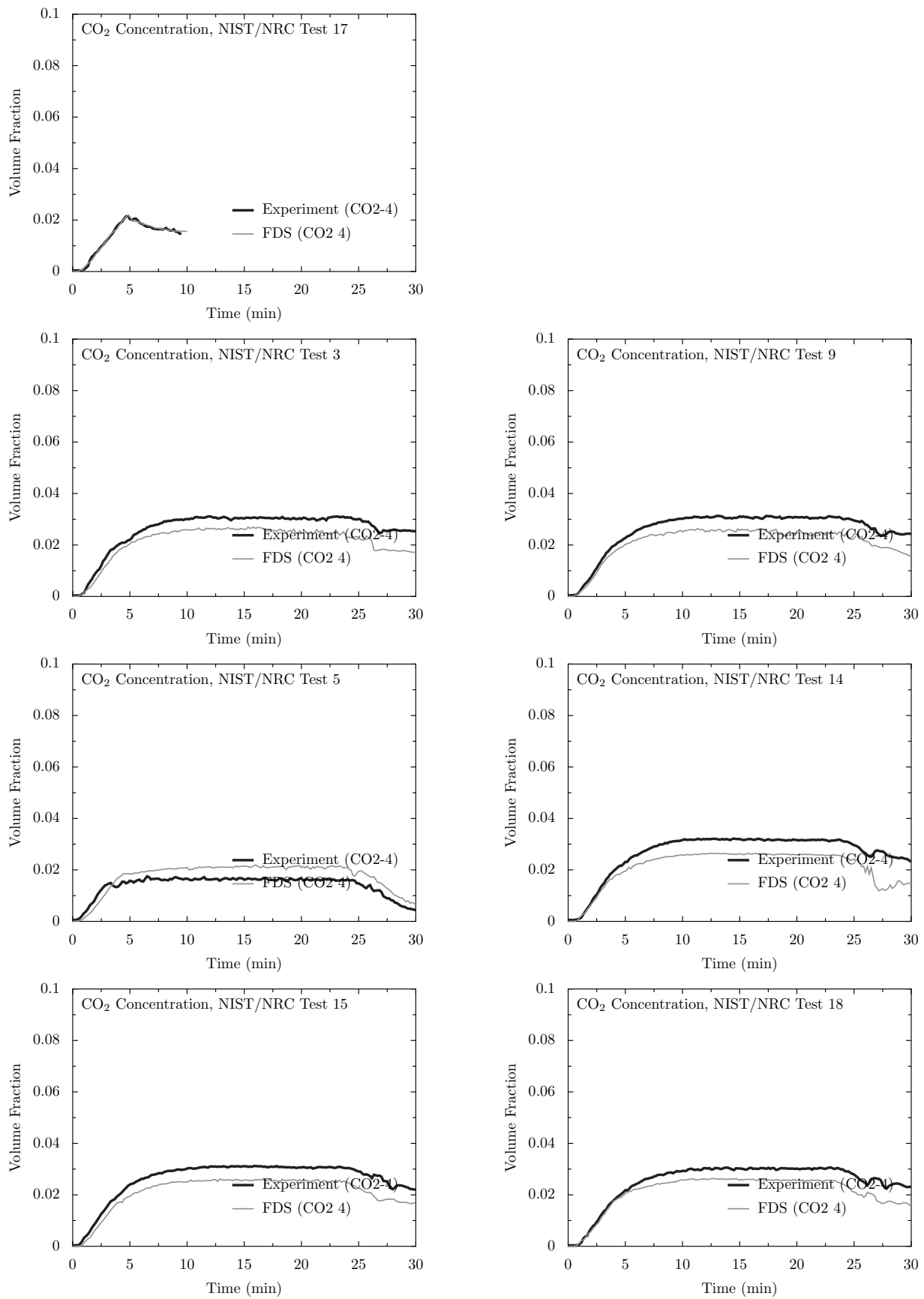












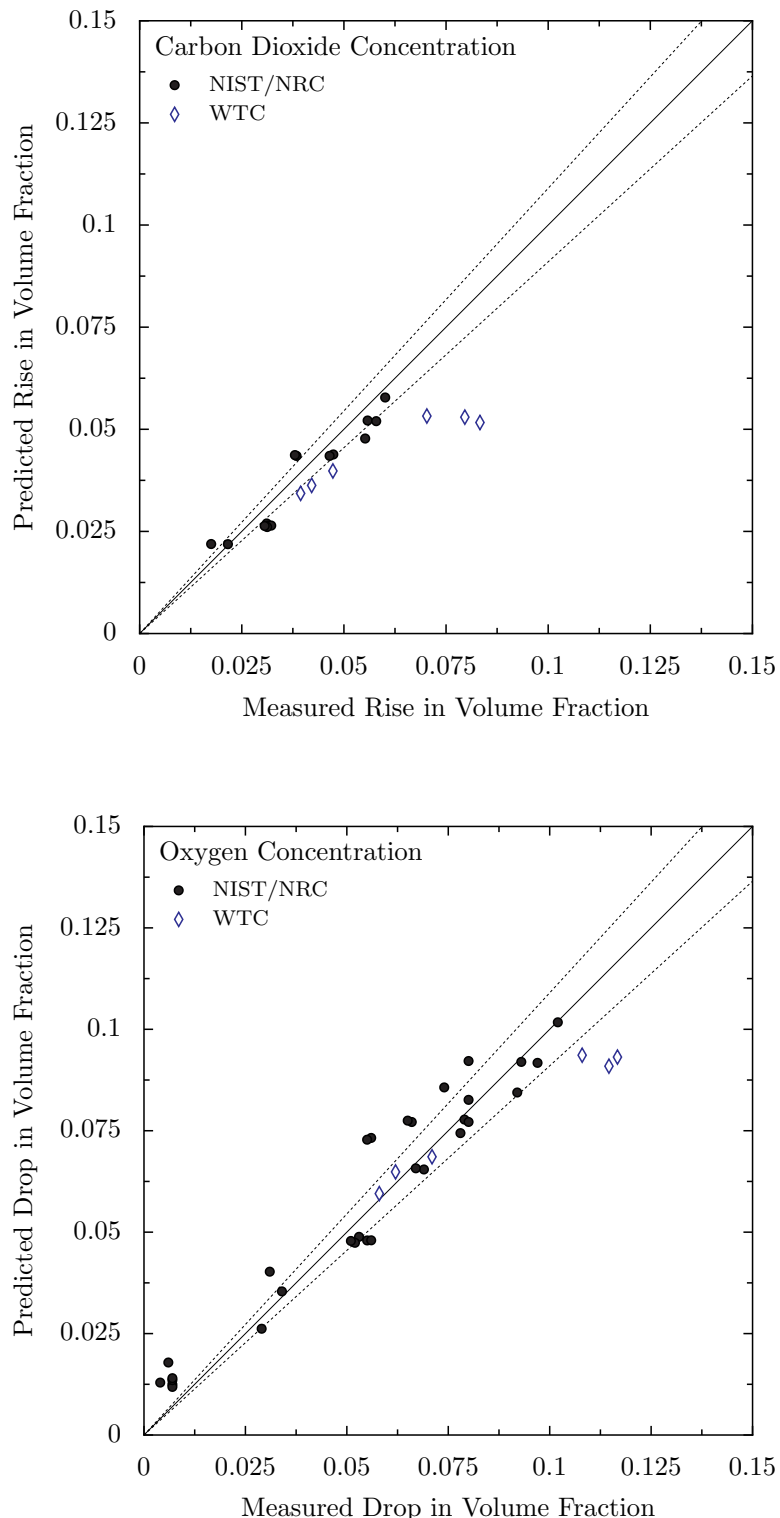
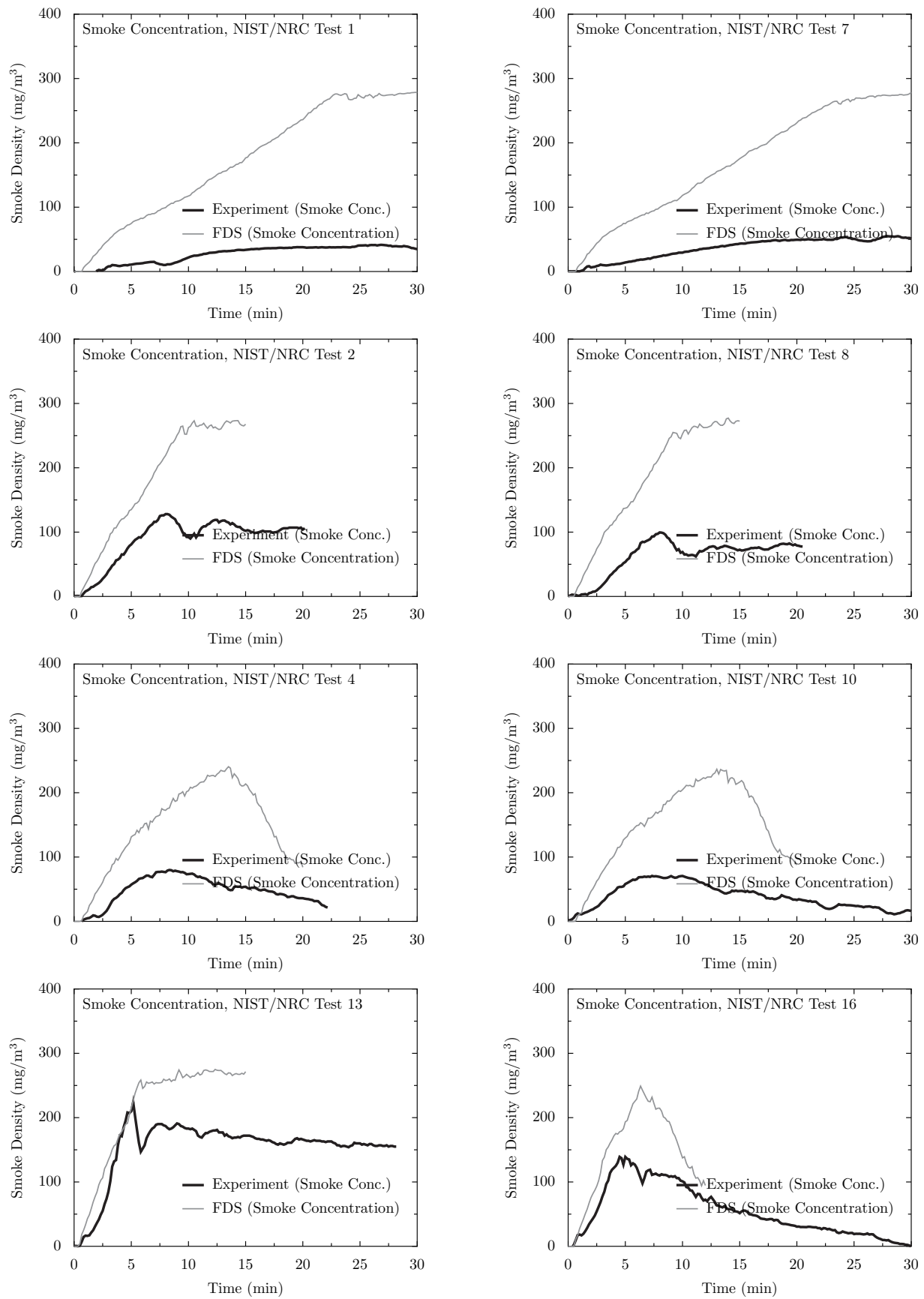
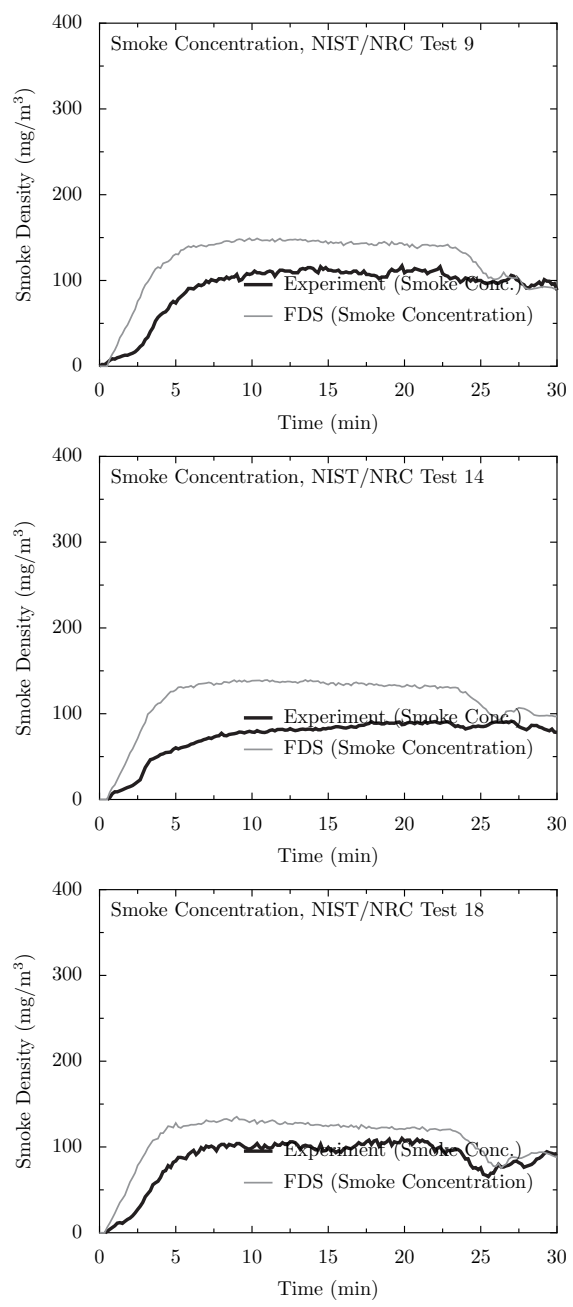
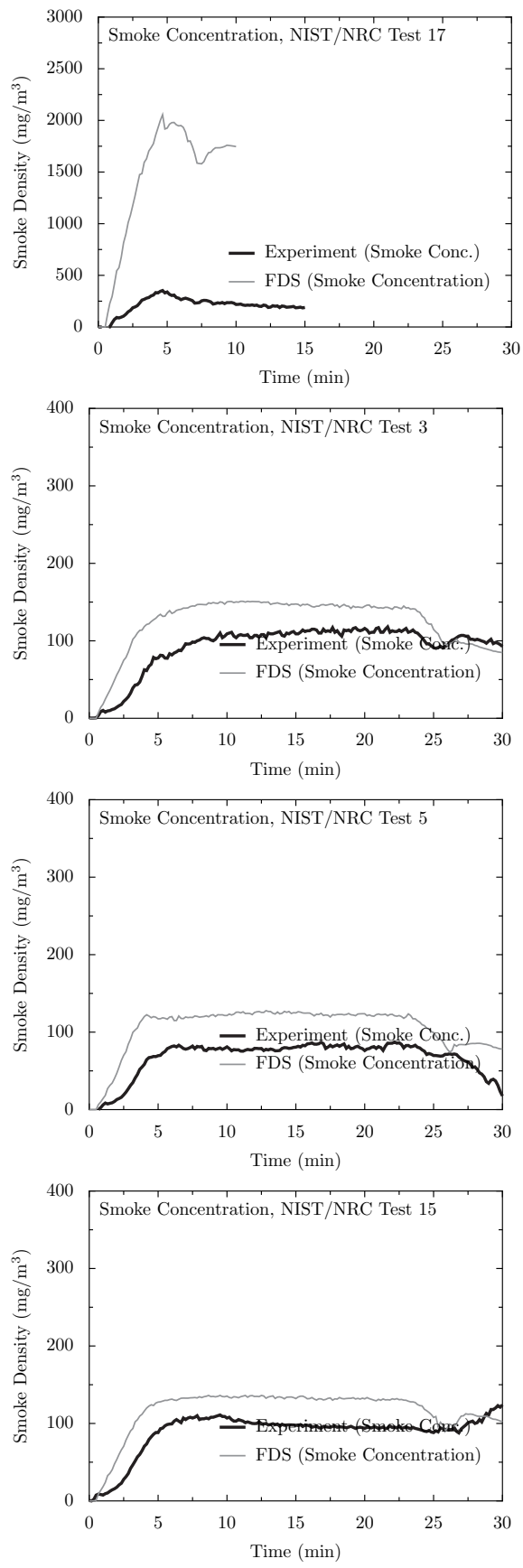


Figure 8.1: Summary of gas species predictions for the NIST/NRC and WTC test series.

8.2 NIST/NRC Test Series, Smoke

FDS treats smoke like all other combustion products, basically a tracer gas whose mass fraction is a function of the mixture fraction. To model smoke movement, the user need only prescribe the smoke yield, that is, the fraction of the fuel mass that is converted to smoke particulate. For the simulations of the NIST/NRC tests, the smoke yield is specified as one of the test parameters. The figures on the following pages contain comparisons of measured and predicted smoke concentration at one measuring station in the upper layer. There are two obvious trends in the figures: first, the predicted concentrations are about 50 % higher than the measured in the open door tests. Second, the predicted concentrations are roughly three times the measured concentrations in the closed door tests. As a contrast, Figure displays the time history of CO concentration for 6 of the NIST/NRC tests. Like smoke, the CO is specified in FDS via a fixed yield, measured along with smoke and reported in the test document. The large differences between model and measurement seen in the smoke data do not appear in the CO data.





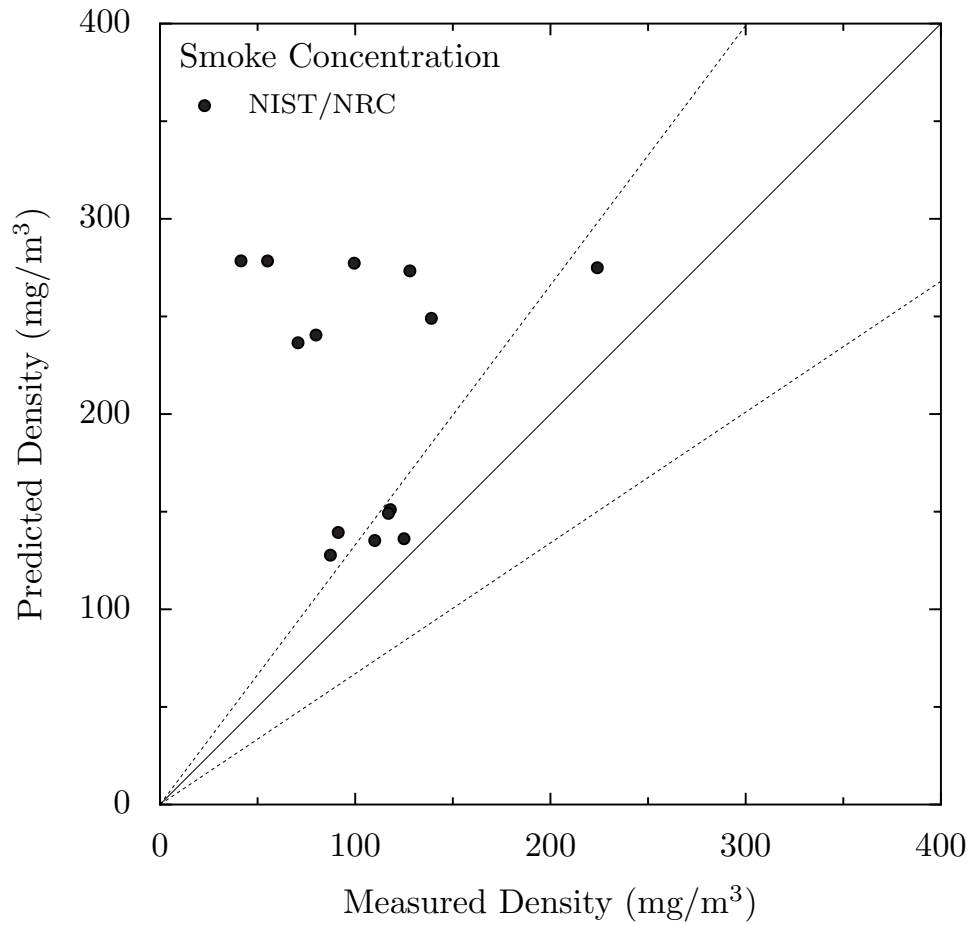


Figure 8.2: Summary of smoke concentration predictions for the NIST/NRC test series.

8.3 Smyth Slot Burner Experiment

The two-step, CO production model in FDS was used to simulate a methane/air slot burner diffusion flame. Figures 8.3 through 8.5 show predicted and measured temperatures at three elevations above the burner. The model predicts a flame that is slightly narrower and cooler than measured. The model also predicts higher centerline temperatures. These results are not surprising. The two-step combustion model considers the first step, $F \rightarrow CO$, to be infinitely fast, assuming that the local oxygen concentration satisfies a flammability criterion. This is true in the vicinity of the lip of the burner. In reality, the cold fuel and air streams do not react infinitely fast at this location and some oxygen penetrates the flame at the base, resulting in cooler gases being entrained into the core of the flame with a resulting drop in the centerline temperature.

Figures 8.3 through 8.5 also show predicted and measured values of CH_4 , O_2 , CO , and CO_2 at three elevations above the burner along. Note that the test data shows a small quantity of oxygen along the burner centerline which is not captured in the simulation. Along the centerline, the model predicts higher values of fuel and higher values of products than measured. The species profiles are also slightly narrower than measured, consistent with the temperature prediction. The reported uncertainty in the species concentration measurements ranges from 10 % to 20 %.

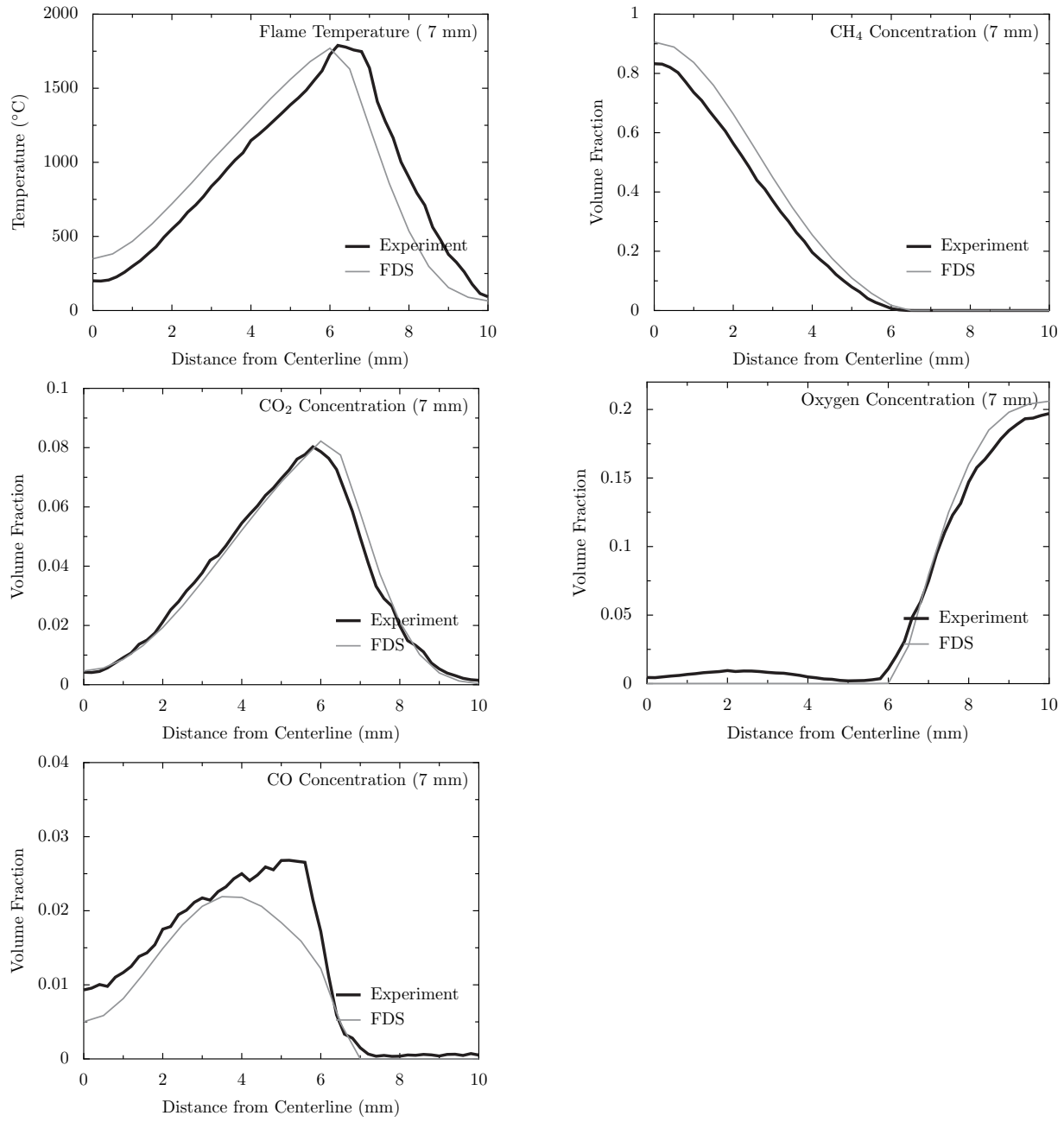


Figure 8.3: Predicted and measured temperature and gas species 7 mm above a methane-air slot burner.

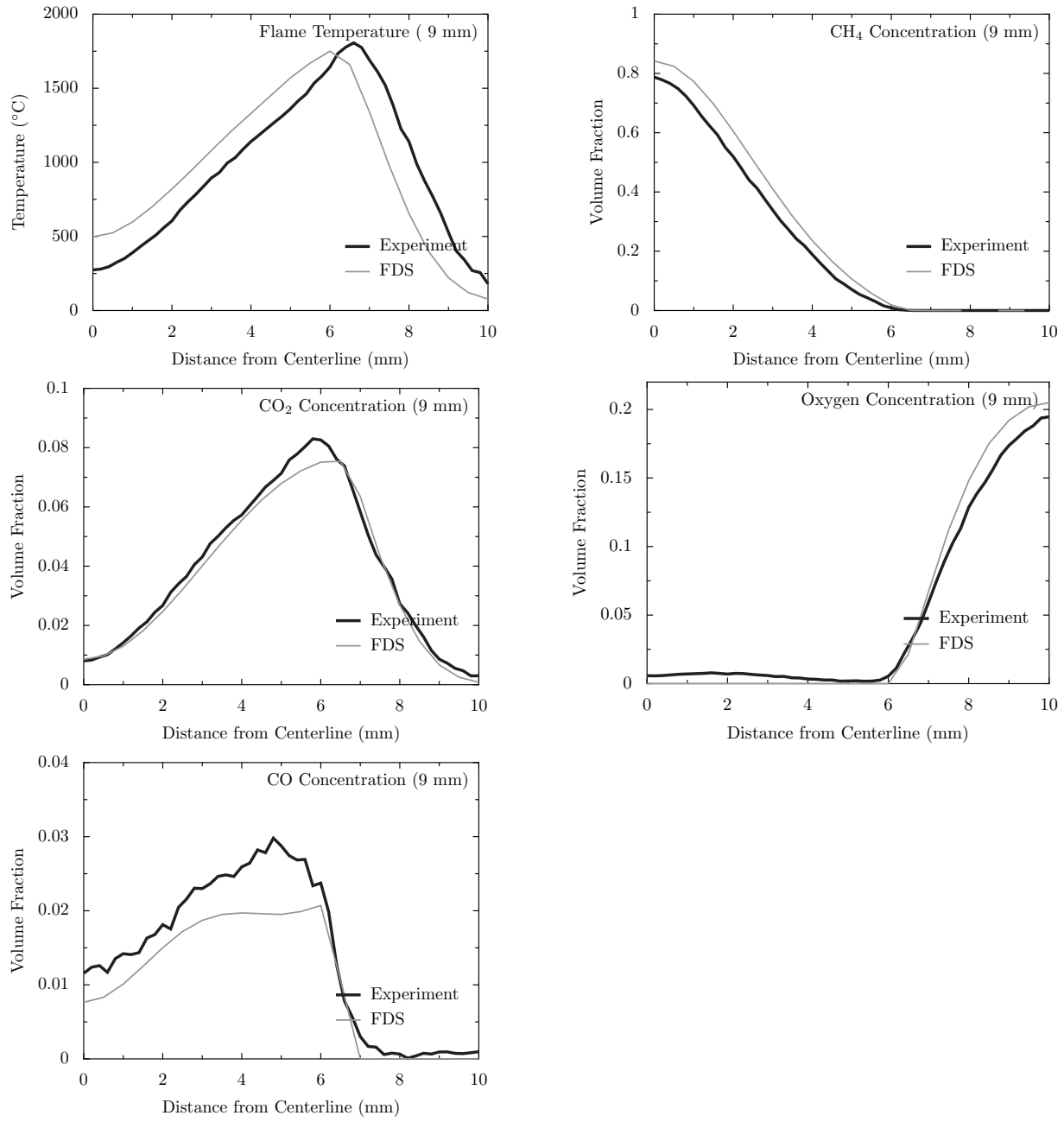


Figure 8.4: Predicted and measured temperature and gas species 9 mm above a methane-air slot burner.

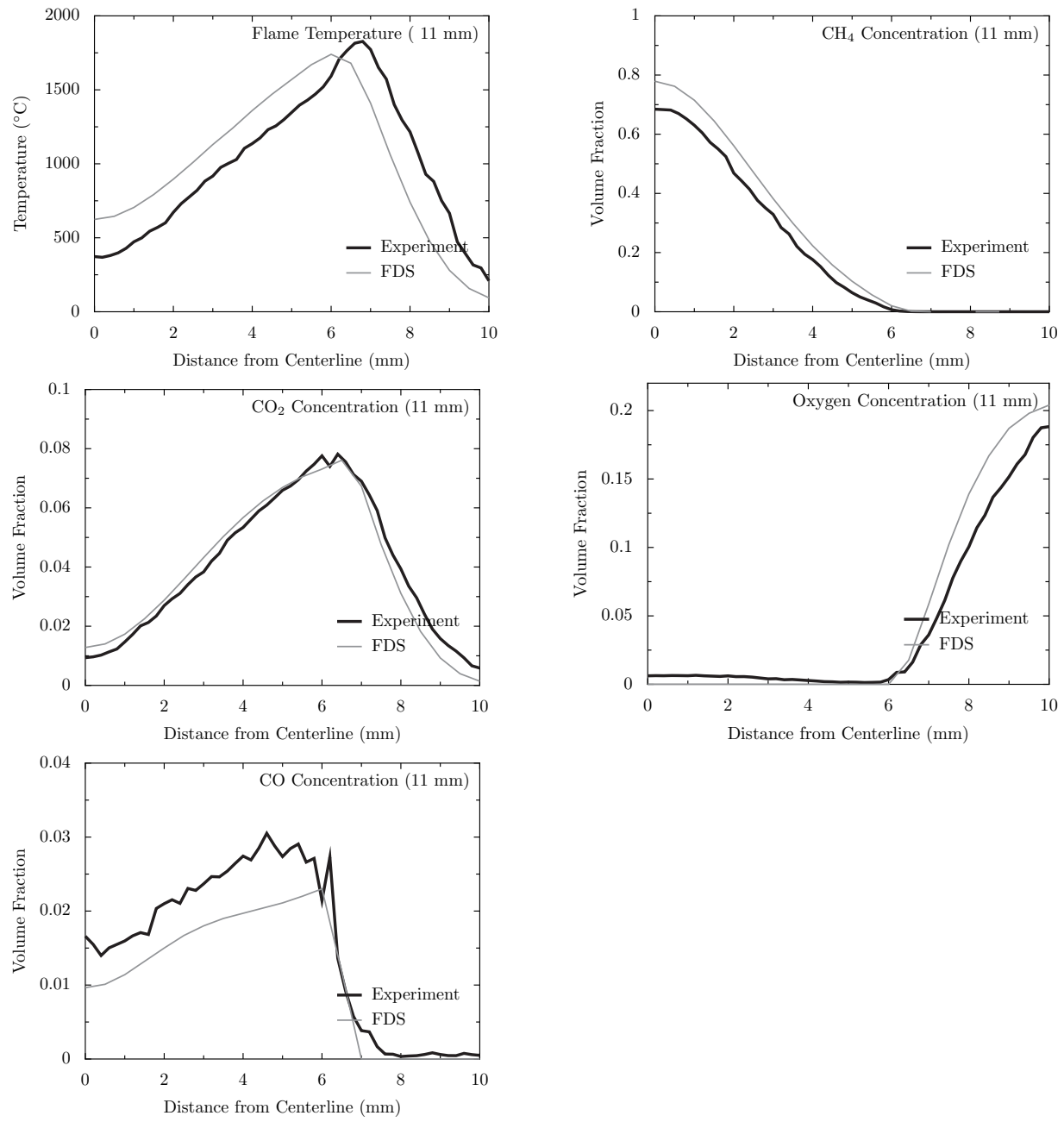


Figure 8.5: Predicted and measured temperature and gas species 11 mm above a methane-air slot burner.

8.4 Beyler Hood Experiments

Fig. 8.6 shows species predictions (using FDS 5.1.2) made by the two-step model compared with measured data for a range of fire sizes and burner positions. The dotted lines indicate the estimated measurement uncertainty. The model predicts the time-averaged species concentration at the hood exhaust vent. CO₂ predictions are within the measurement uncertainty for all but one of the simulations performed. For the well-ventilated fires (burner 10 cm below the edge of the hood), CO, CO₂, and unburned fuel predictions match the data. As the fires become under-ventilated, CO is over-predicted while fuel and O₂ are under-predicted. The most likely explanation for the discrepancy is that the model assumes fuel and oxygen react infinitely fast in the vicinity of near ambient conditions. This occurs at the lower edge of the hood where the vitiated layer is adjacent to the ambient air below the hood, and as a result layer burning is occurring in the model which depletes the fuel and O₂ and creates CO. This is not unexpected, and indicates that more work is required to establish the conditions under which combustion in the first step, conversion of fuel to CO, will be allowed.

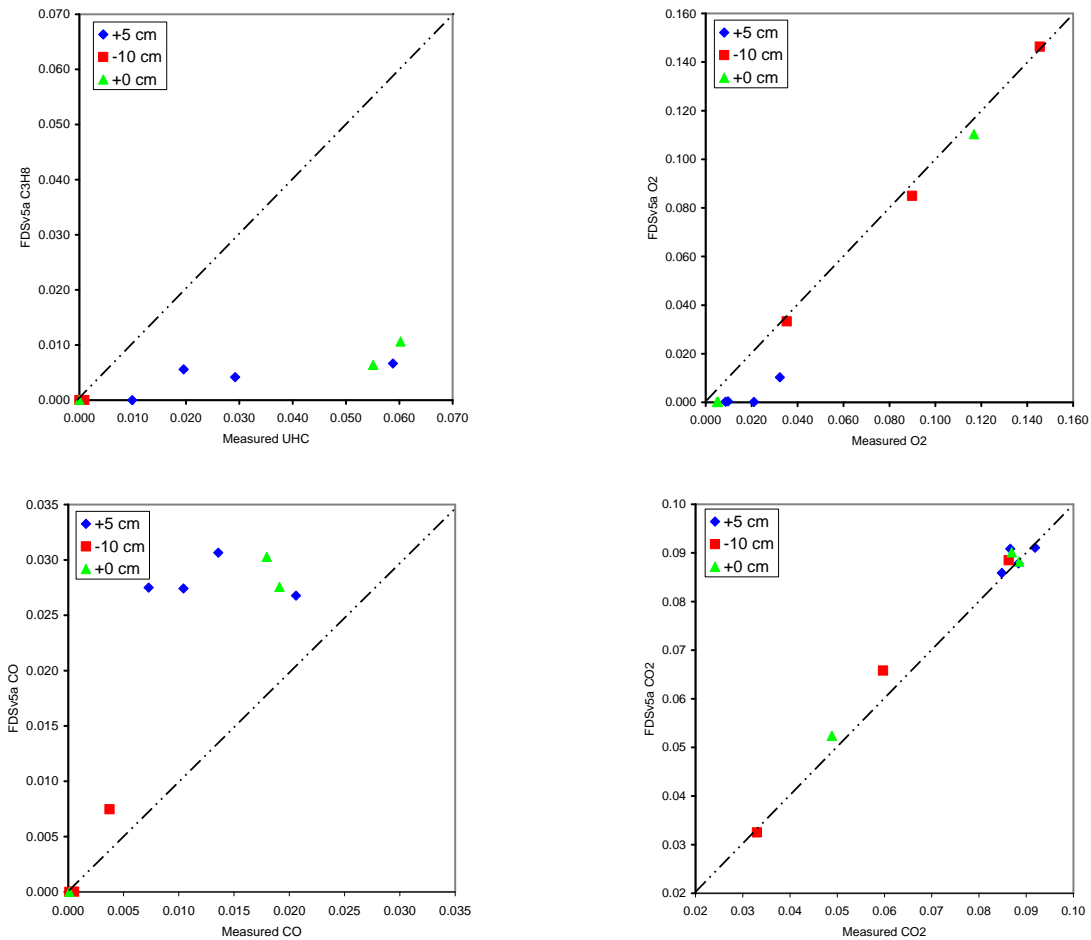


Figure 8.6: Comparison of measured and predicted species concentrations in the Beyler hood experiments, dotted lines show experimental uncertainty.

8.5 NIST Reduced Scale Enclosure (RSE) Test Series

The RSE natural gas experiments were selected to assess the CO production capability rather than soot production. Nine fire sizes were simulated: 50 kW, 75 kW, 100 kW, 150 kW, 200 kW, 300 kW, 400 kW, 500 kW, and 600 kW. The experiments were modeled using properties of the natural gas supplied to the test facility. The model geometry included the compartment interior along with a 0.6 m deep region outside the door. Figure 8.7 shows the measured and predicted CO₂ and CO concentrations. The measured values are from the test series performed by Bryner, Johnsson, and Pitts [106]. The model matches the data up to a fire size of 300 kW, including the location of the peak CO₂ concentration at 200 kW. For larger fires the model predicts more CO surviving in the upper layer than measured, along with correspondingly lower CO₂ levels. As the compartment becomes under-ventilated, the model under-predicts CO₂ and over-predicts CO. The relative error increases as the compartment becomes more under-ventilated. However, note that the under-prediction of CO₂ concentration in the rear (1.5 %) is equivalent to the over-prediction of CO (1.7 %). This implies that part of the model error results from the assumption of infinitely fast chemistry for the first step. Furthermore, since the model as implemented performs the two steps sequentially, higher CO is predicted where the first step consumes all of the available oxygen. Note that the figure below uses prediction made by FDS 5.1.3.

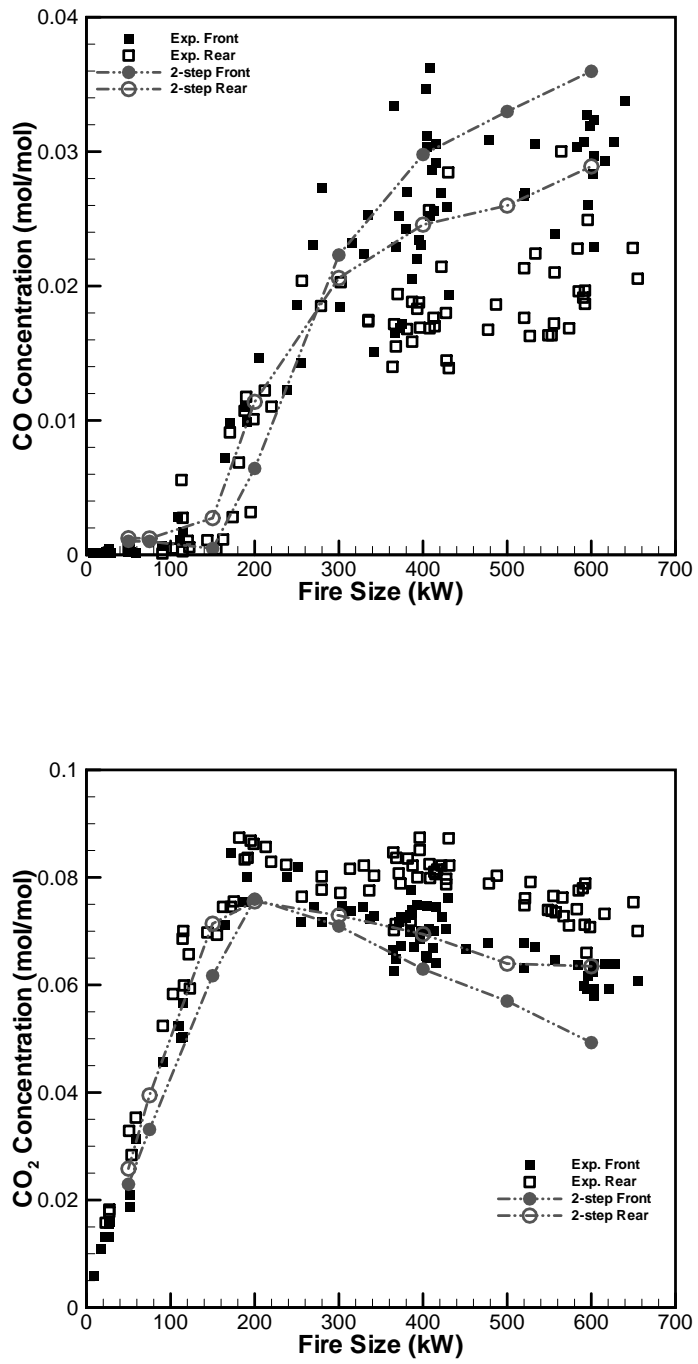


Figure 8.7: Summary of CO and CO₂ predictions for the Pitts reduced-scale enclosure experiments. Note that the calculations were performed using FDS version 5.1.3.

Chapter 9

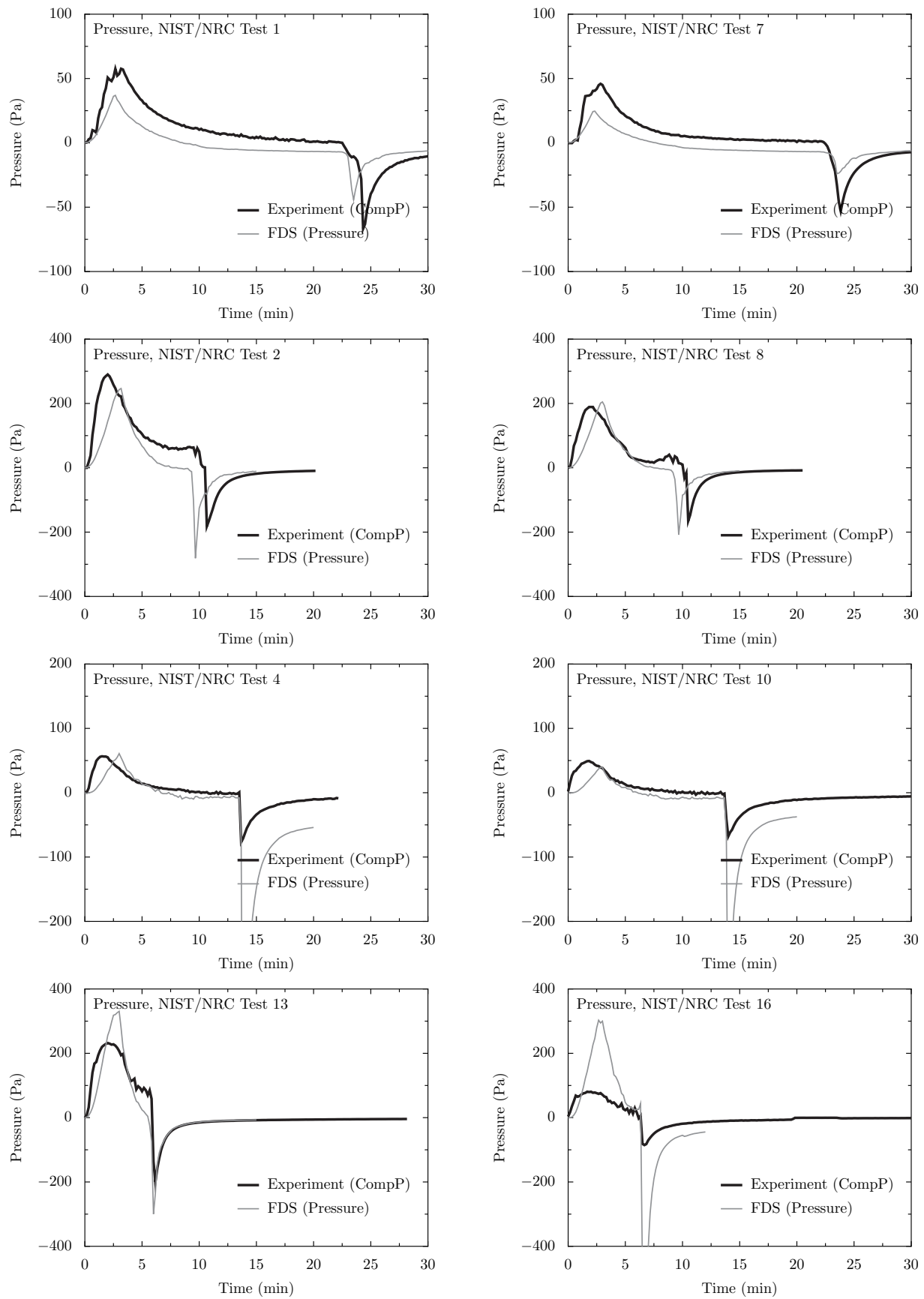
Compartment Pressure

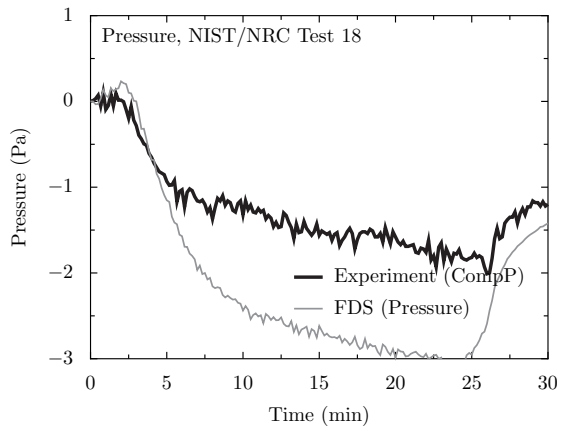
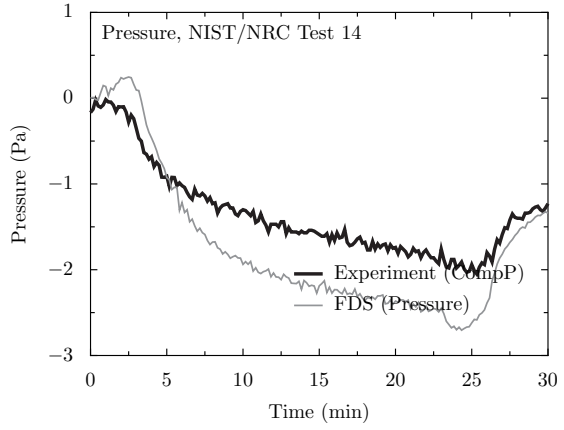
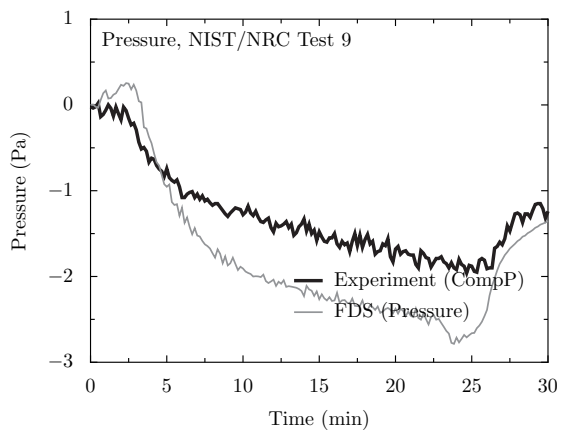
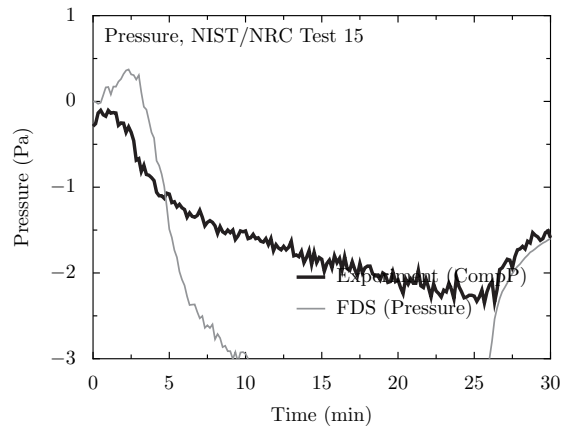
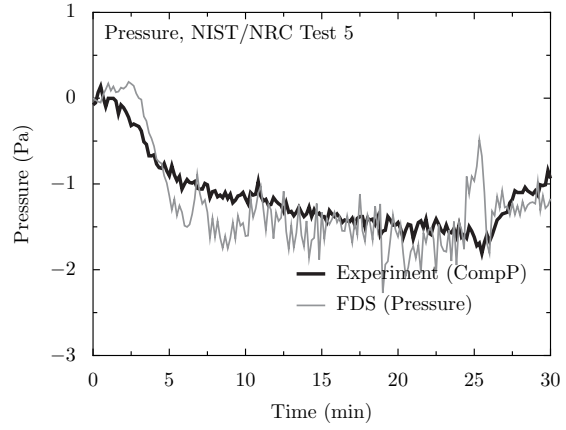
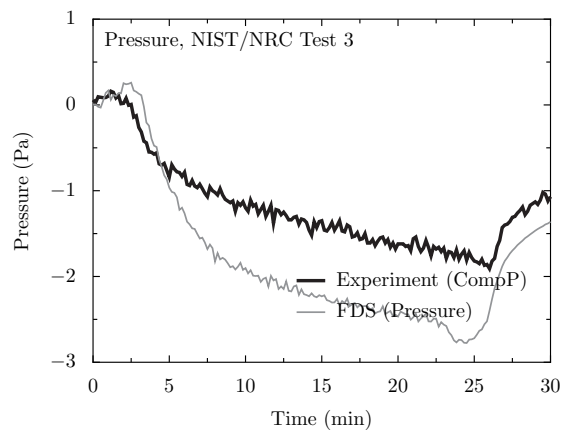
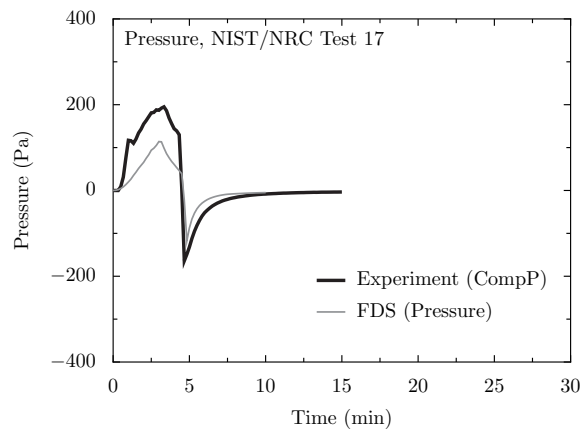
In FDS, the pressure is decomposed into a temporally-varying background pressure and a spatially-varying perturbation that drives the flow. The former can be thought of as the “over-pressure,” and it is essentially a check on global mass and energy balances; whereas the latter has most to do with momentum conservation. In real buildings, leakage and ventilation affect the compartment “over-pressure” along with the fire, which also affects the pressure perturbation.

9.1 NIST/NRC Test Series

Comparisons between measured and predicted pressures for the NIST/NRC Test Series are shown in on the following pages. For those tests in which the door to the compartment is open, the over-pressures are only a few Pascals, whereas when the door is closed, the over-pressures are several hundred Pascals. The pressure within the compartment was measured at a single point, near the floor. In the simulations of the closed door tests, the compartment was assumed to leak via a small uniform flow spread over the walls and ceiling. The flow rate was calculated based on the assumption that the leakage rate is proportional to the measured leakage area times the square root of compartment over-pressure.

Note that in the closed door tests, there is often a dramatic drop in the predicted compartment pressure. This is the result of the assumption in FDS that the heat release rate is decreased to zero in one second at the time in the experiment when the fuel flow was stopped for safety reasons. In reality, the fire did not extinguish immediately because there was an excess of fuel in the pan following the flow stoppage. For the purpose of model comparison, the peak over-pressures are differenced in the closed door tests, and the peak (albeit small) under-pressures are compared in the open door tests.





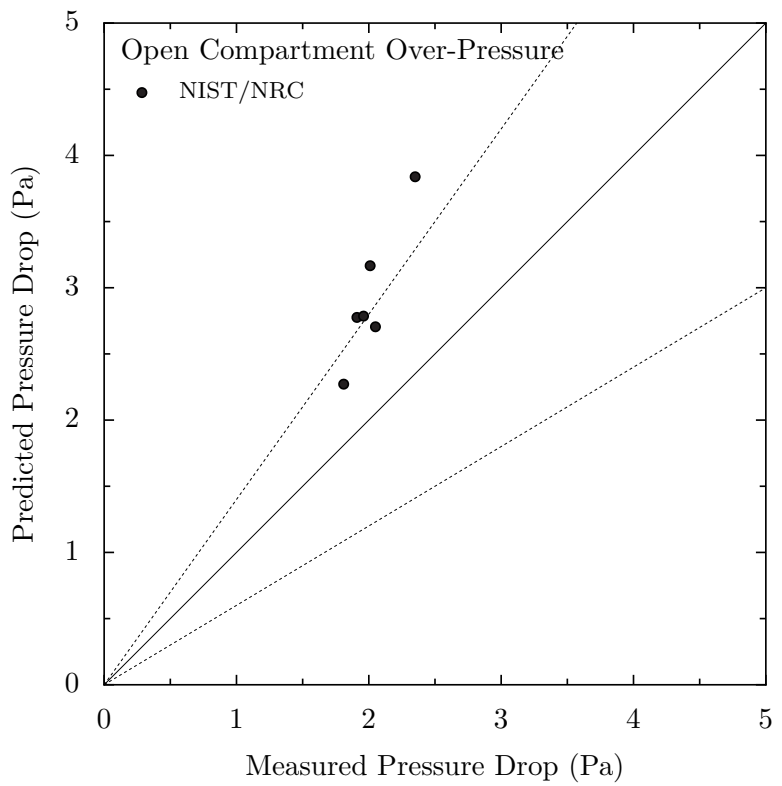
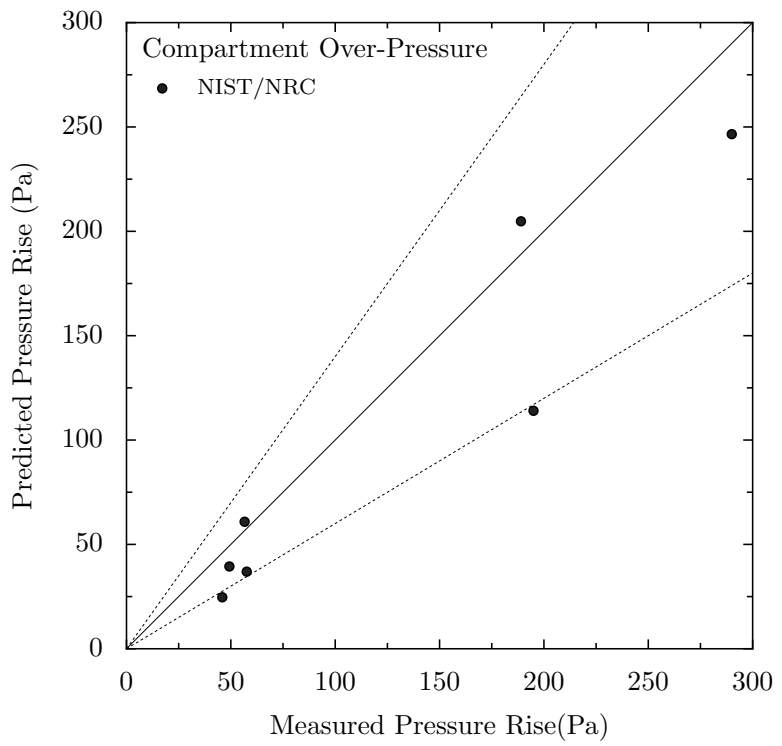


Figure 9.1: Summary of Pressure Results. The top graph shows the compartment “over-pressure” in closed door tests; the lower graph shows the small pressure perturbation in the open door tests.

Chapter 10

Surface Temperature

All solid surfaces in an FDS model are assigned thermal boundary conditions. Heat and mass transfer to and from solid surfaces is usually handled with empirical correlations, although it is possible to compute directly the heat and mass transfer when performing a Direct Numerical Simulation (DNS). Heat conduction into a solid surface is calculated via a one-dimensional solution of the heat equation in either cartesian or cylindrical coordinates. The latter is useful for cables.

10.1 WTC Test Series, Steel Structural Members and “Slug” Calorimeters

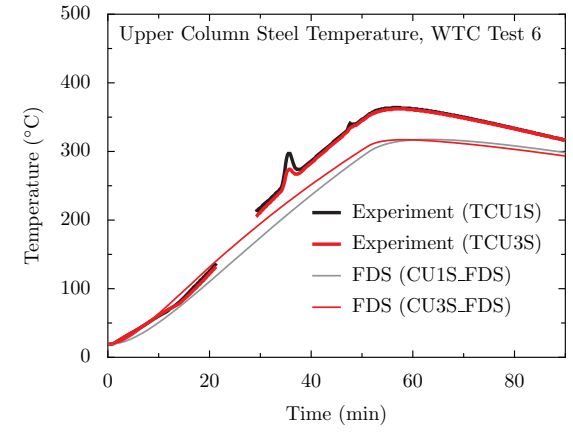
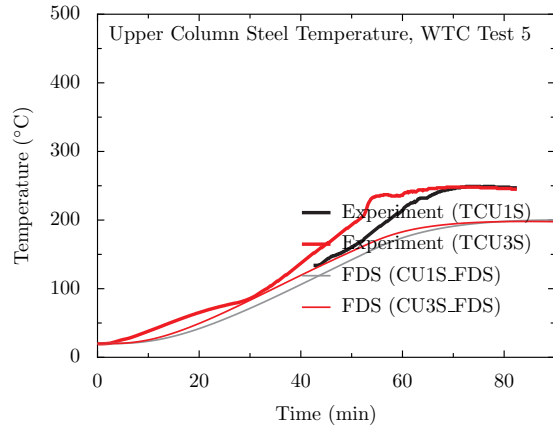
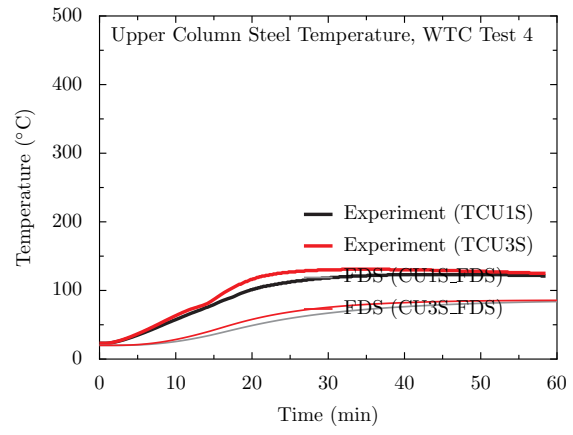
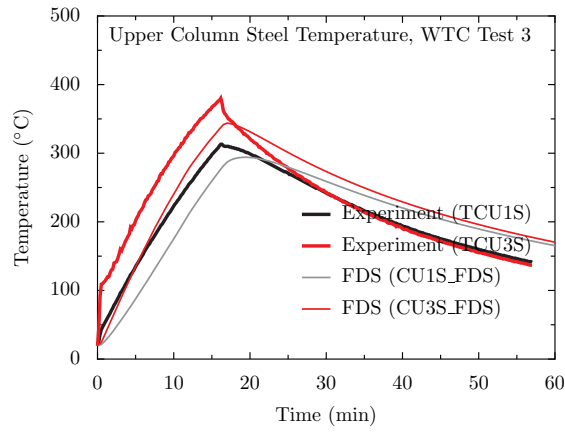
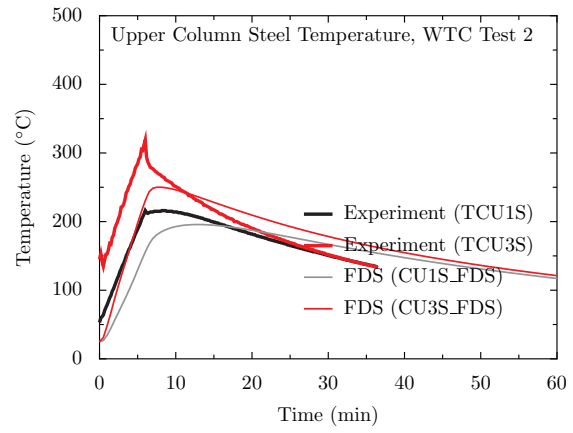
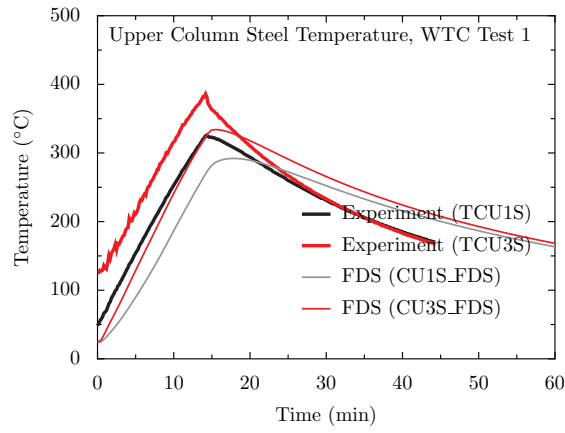
The compartment for the WTC experiments contained a hollow box column roughly 0.5 m from the fire pan, two trusses over the top of the pan, and one or two steel bars resting on the lower truss flanges. In Tests 1, 2 and 3, the steel was bare, and in Tests 4, 5 and 6, the steel was coated with various thicknesses of sprayed fire-resistive materials.

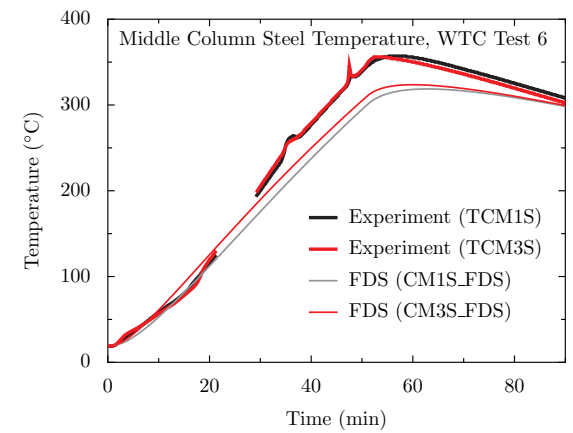
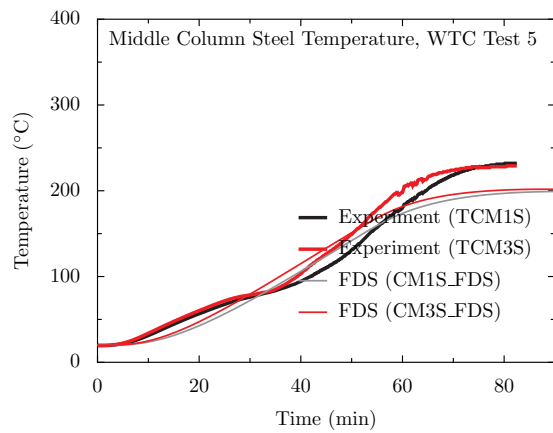
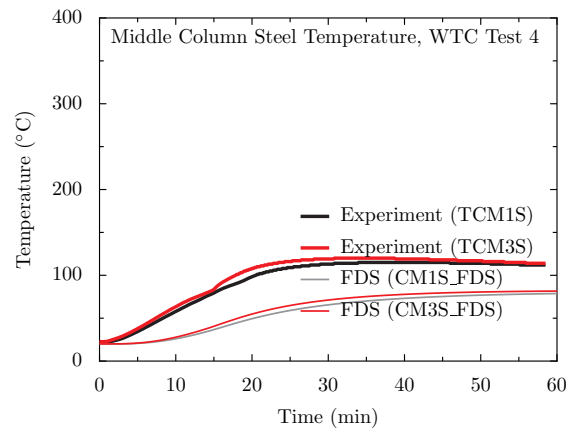
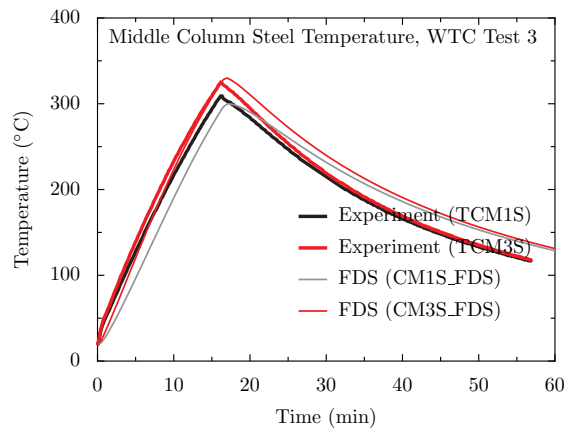
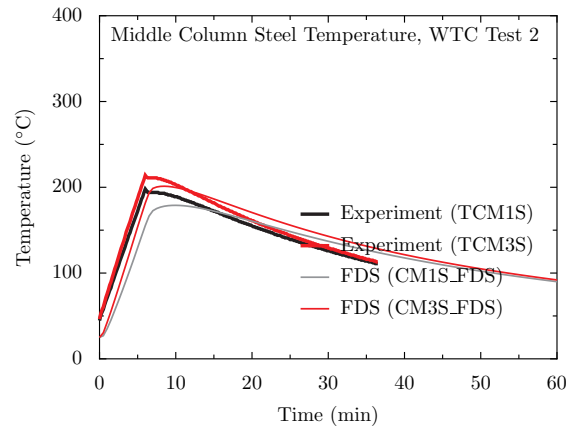
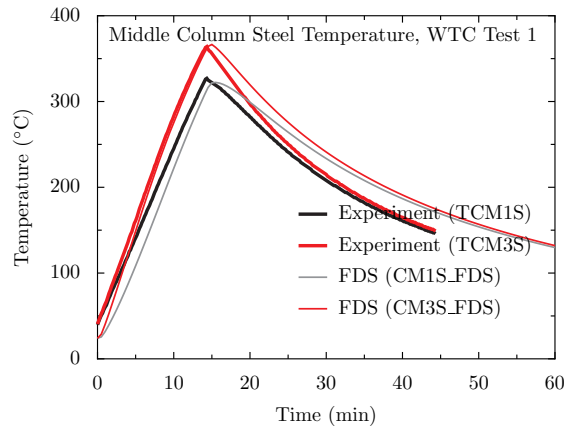
The column was instrumented near its base (about 0.5 m from the floor, middle (1.5 m), and upper (2.5 m)). Four measurements of steel (and insulation) temperatures were made at each location, for each of its four sides.

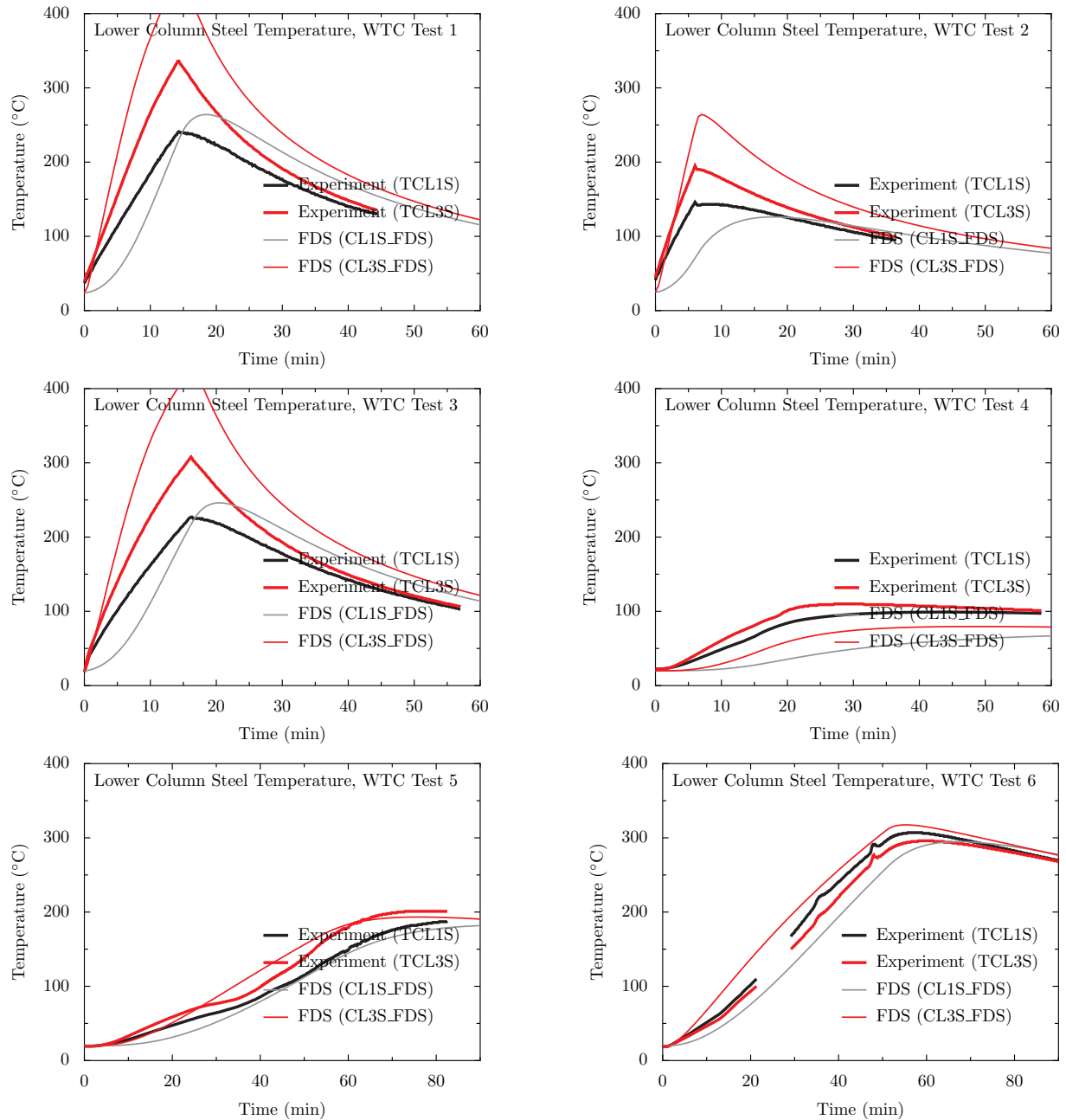
In FDS, these elements were modeled using thin sheet obstructions with a resolution of 10 cm.

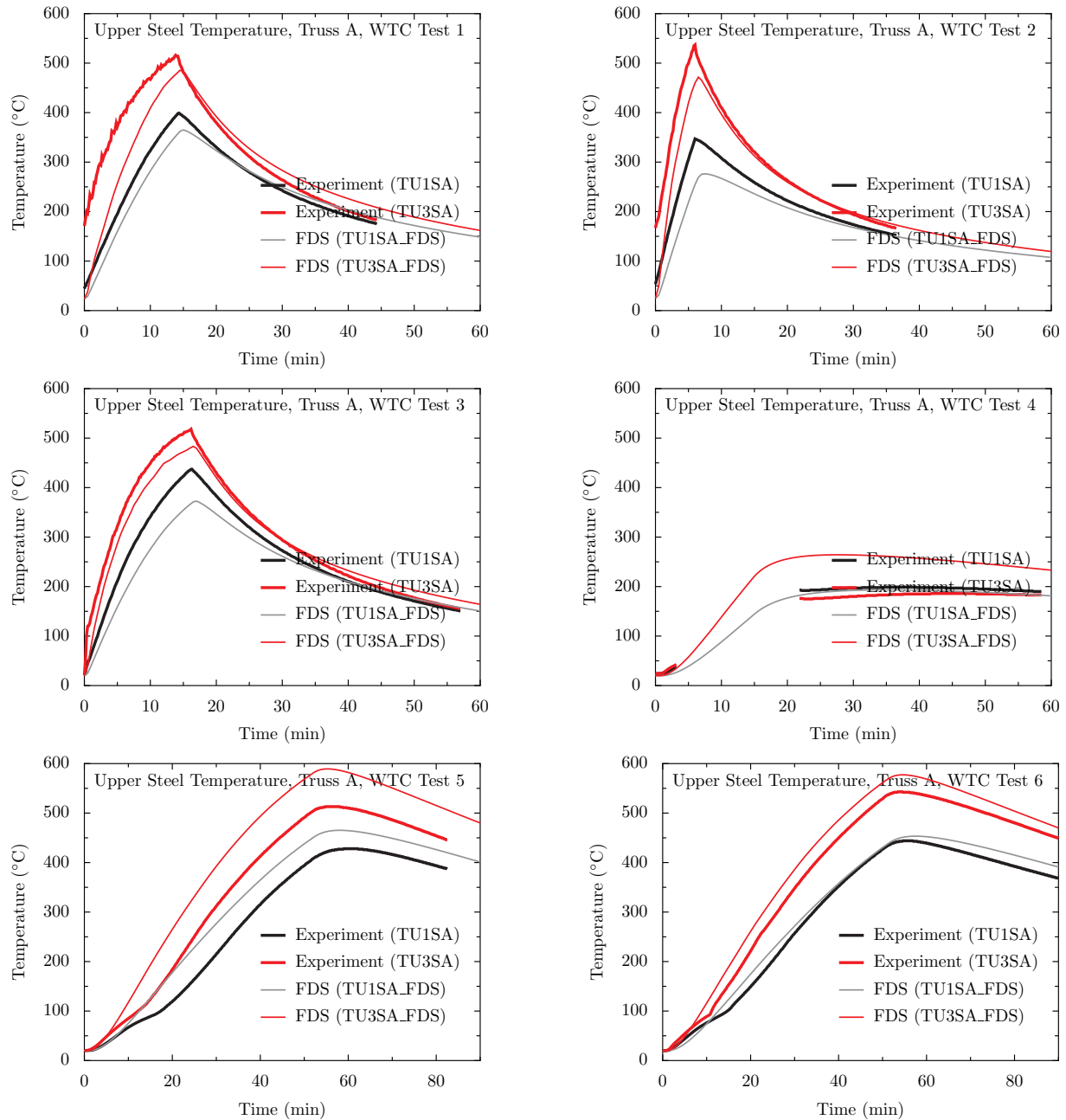
Five cylinders (“slugs”) of nickel 200 ($\geq 99\%$ nickel), 25.4 cm long and 10.2 cm in diameter, were positioned 50 cm north of the centerline in the WTC experiments. Slugs 1 through 5 were 2.92 m, 1.82 m, 0.57 m, 0.05 m, and 1.56 m, respectively, from the longitudinal axis of the fire pan. All the slugs were 50 cm north of the lateral axis. The fire pan measured 2 m by 1 m. Four thermocouples were inserted into each slug at various locations. All four temperatures for each slug were virtually indistinguishable.

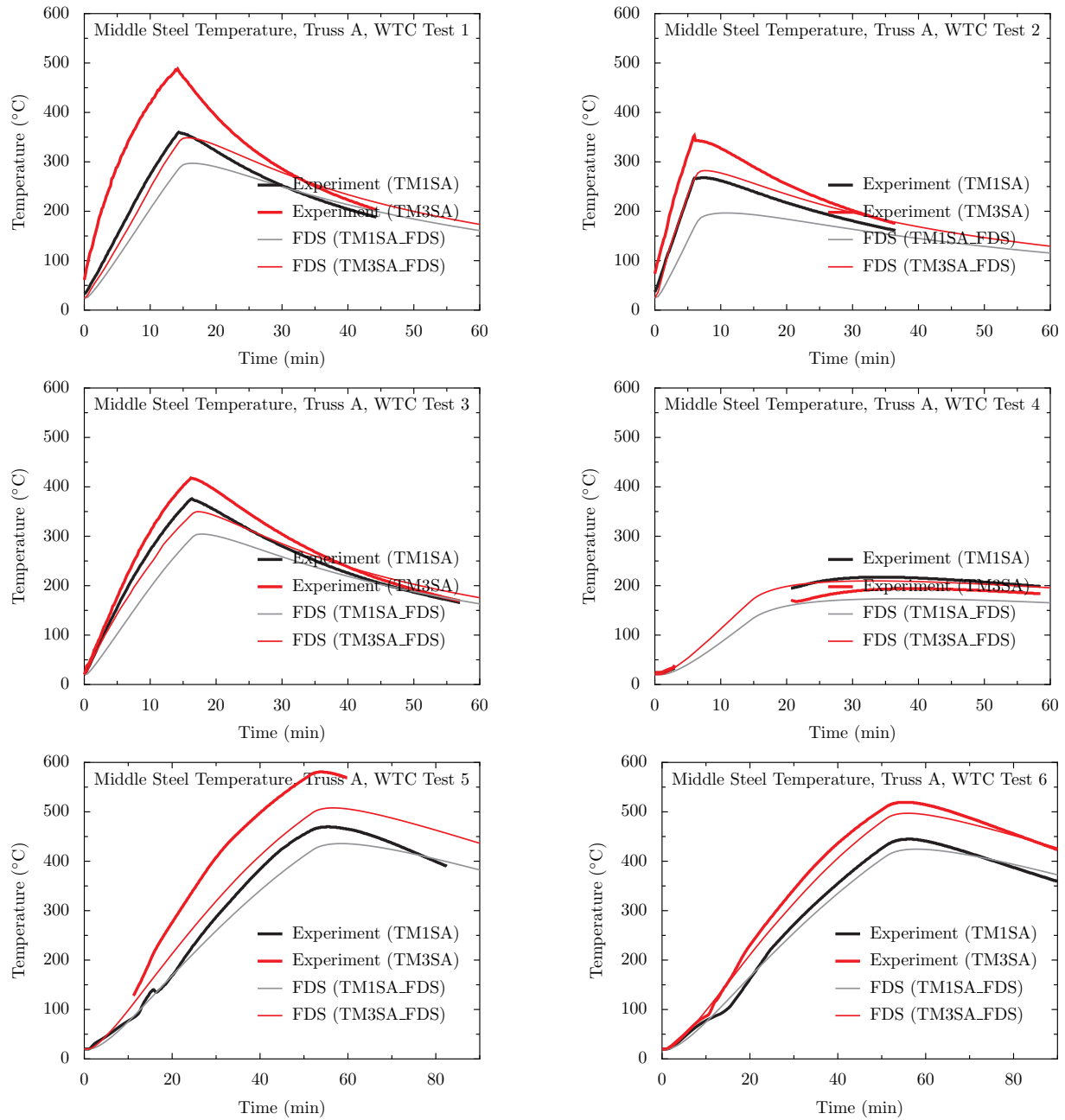
In FDS, rectangular obstructions were used to model the slugs, but the one-dimensional heat conduction calculation was performed using cylindrical coordinates.

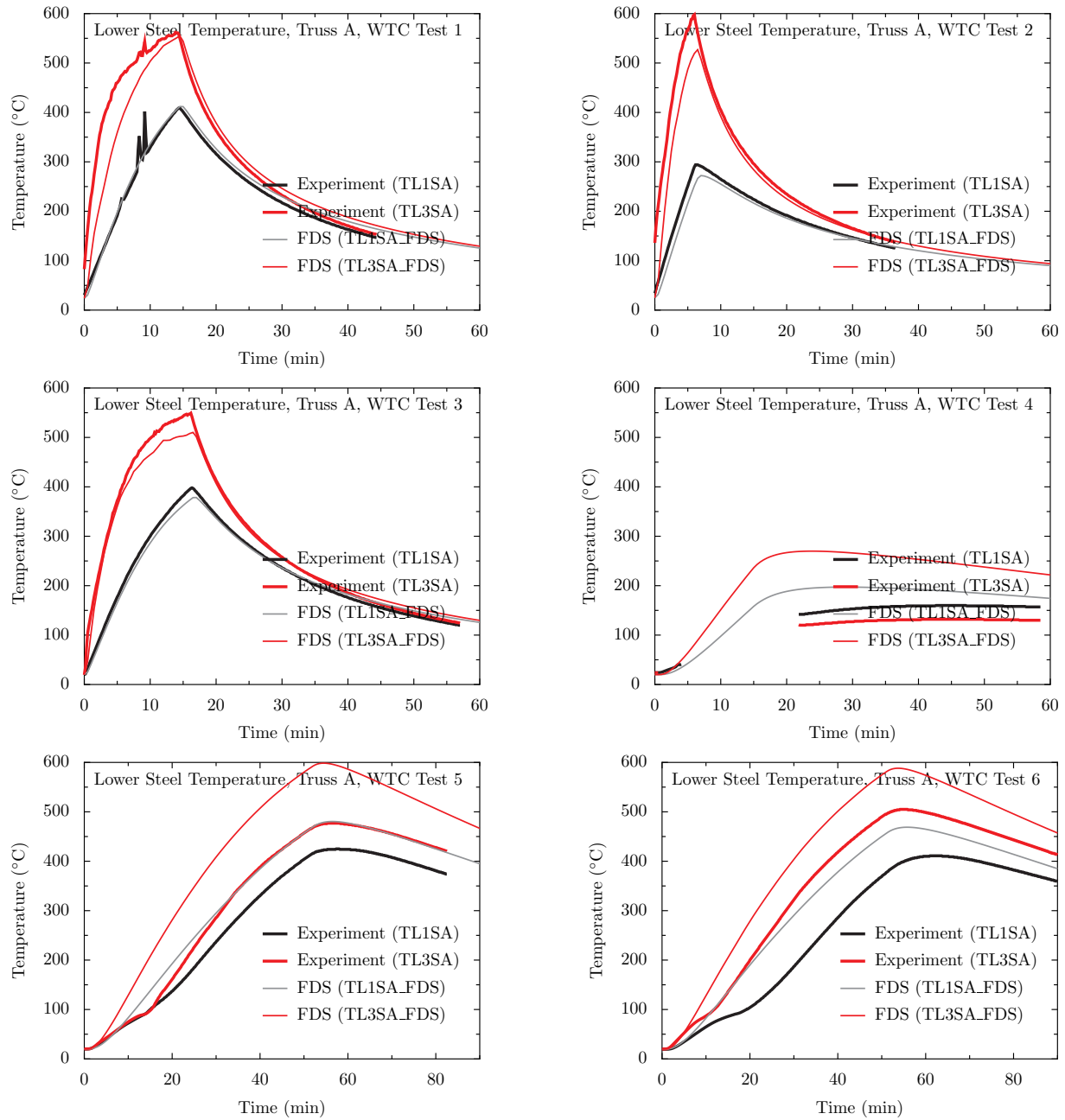


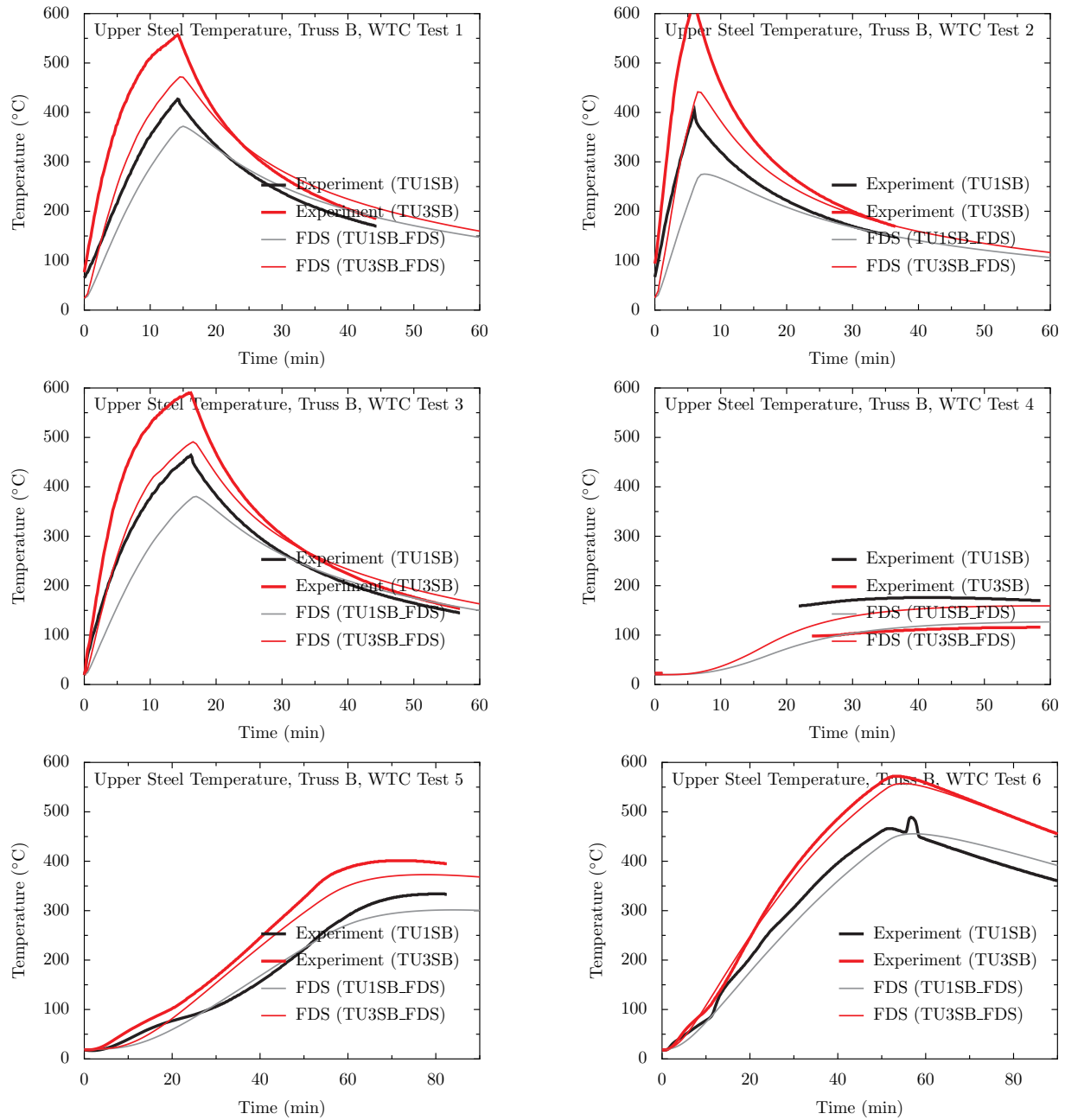


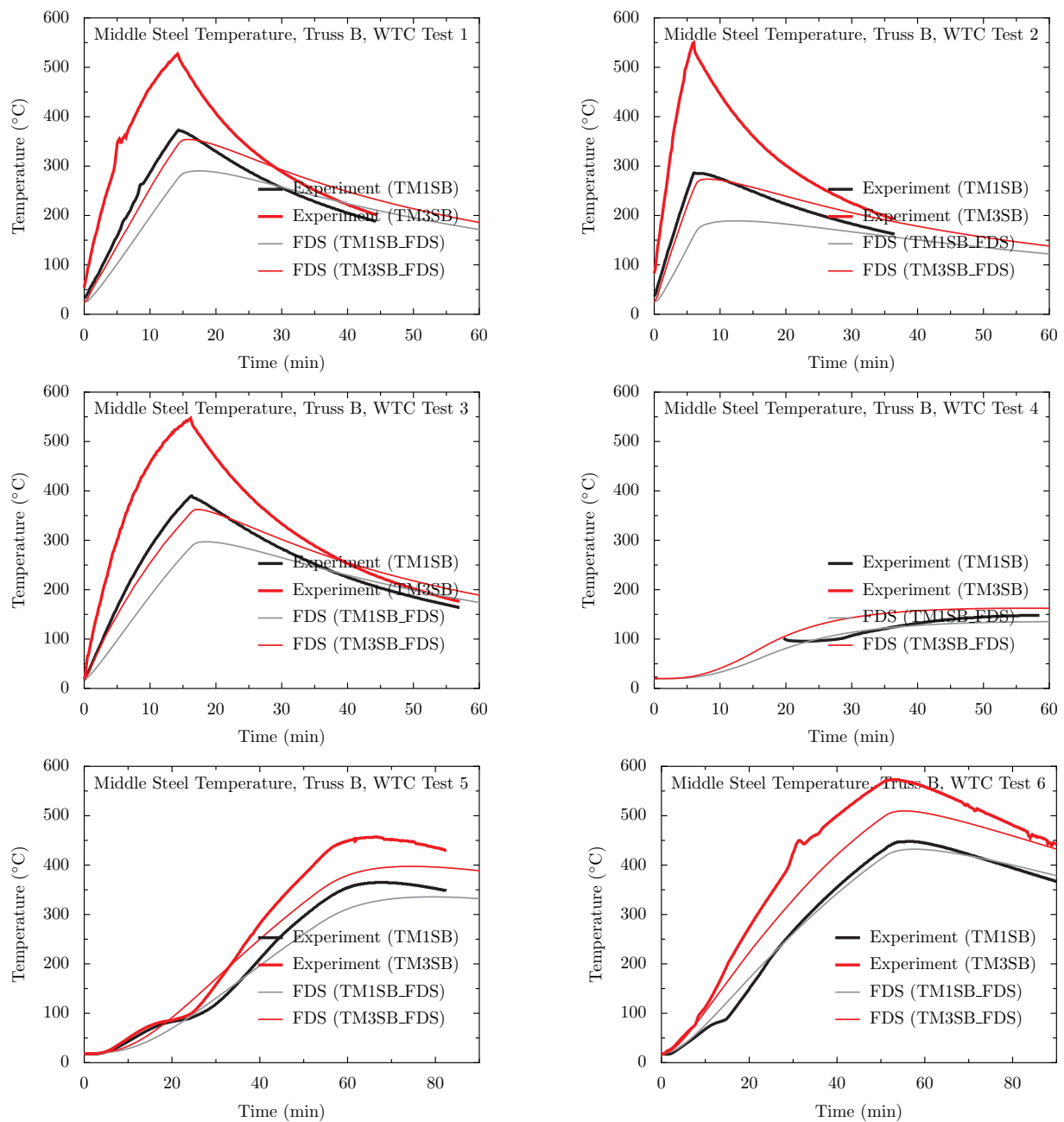


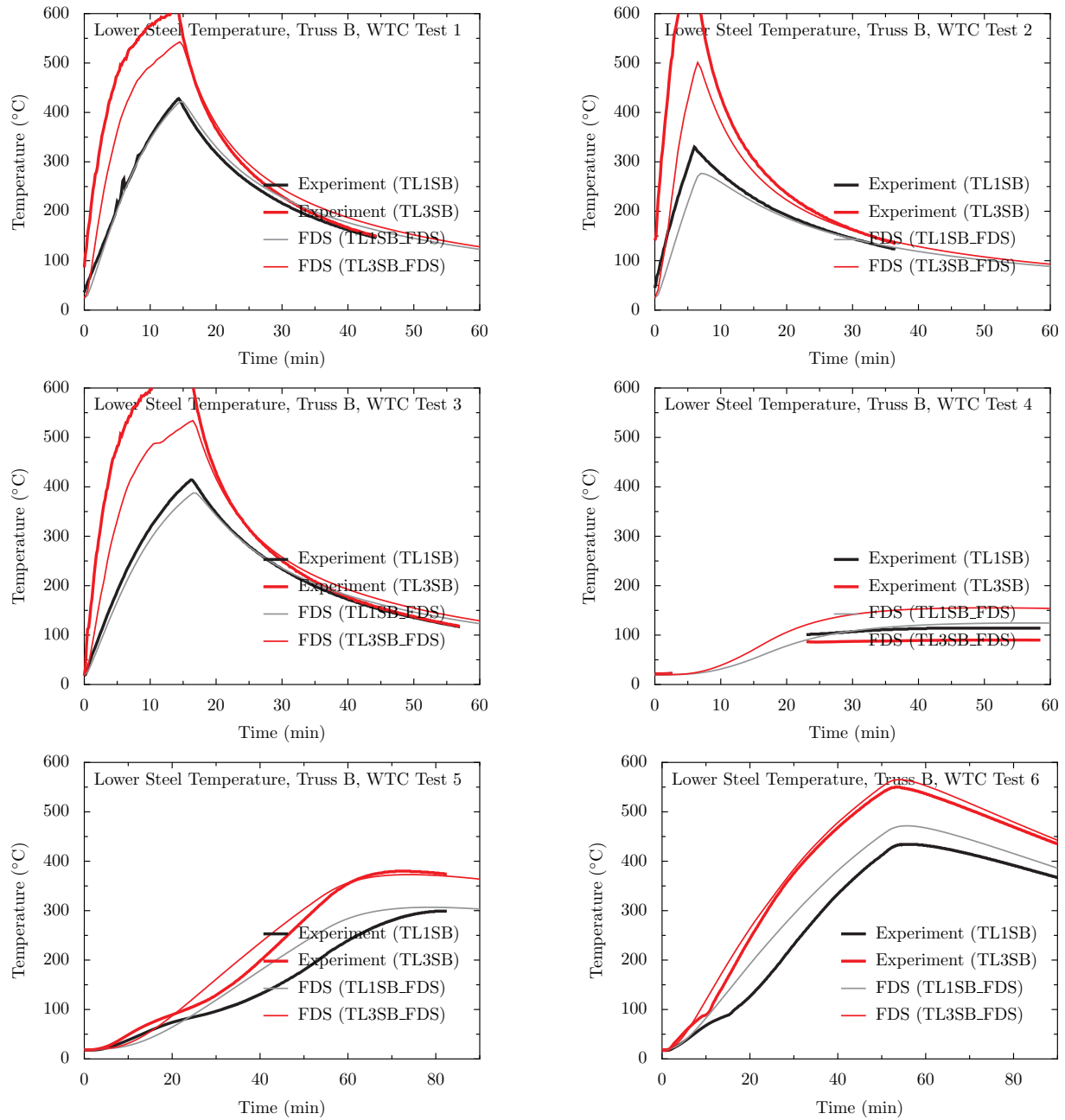


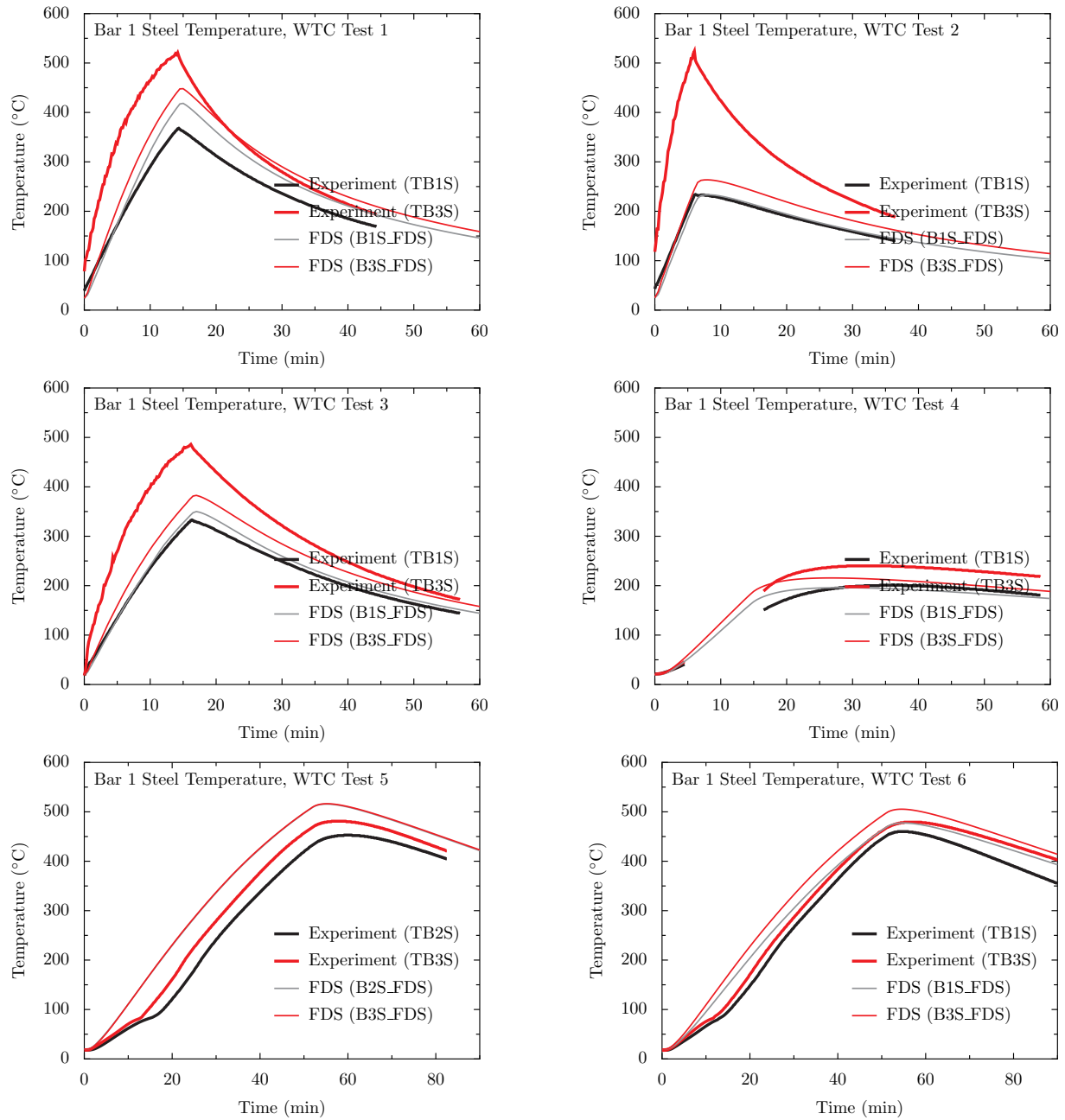


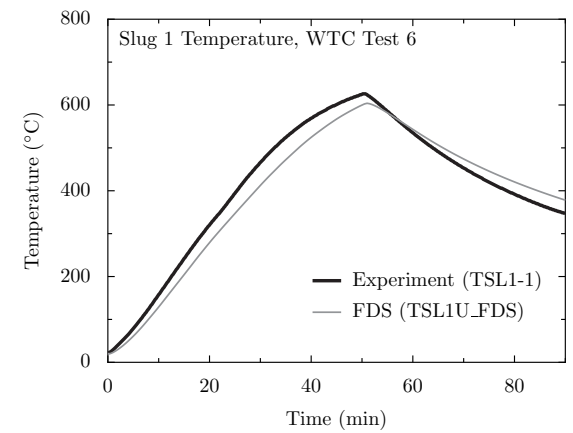
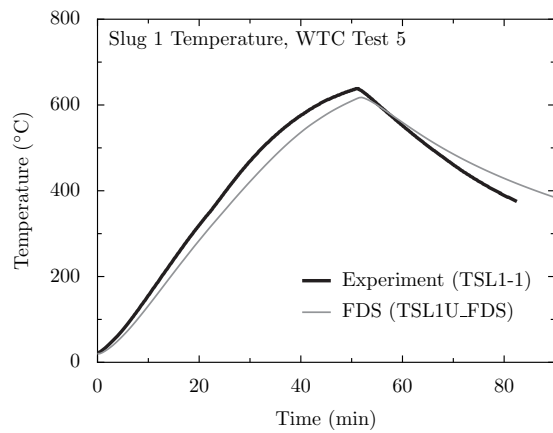
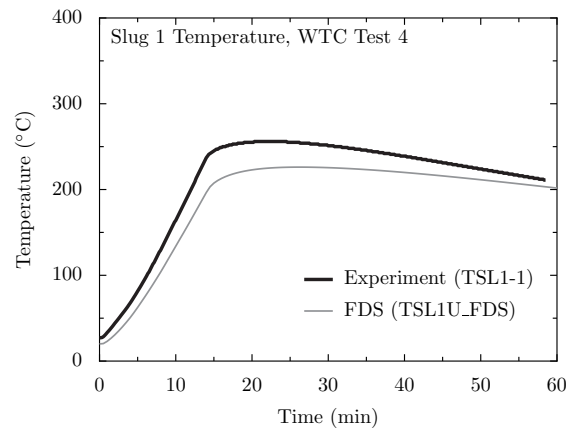
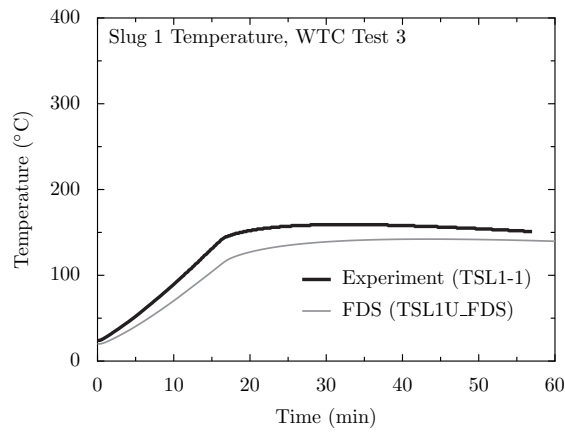
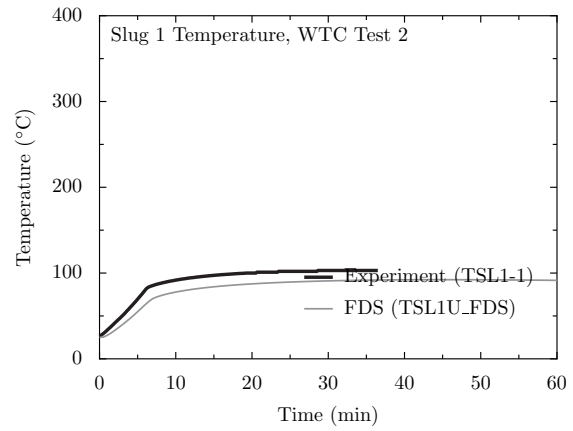
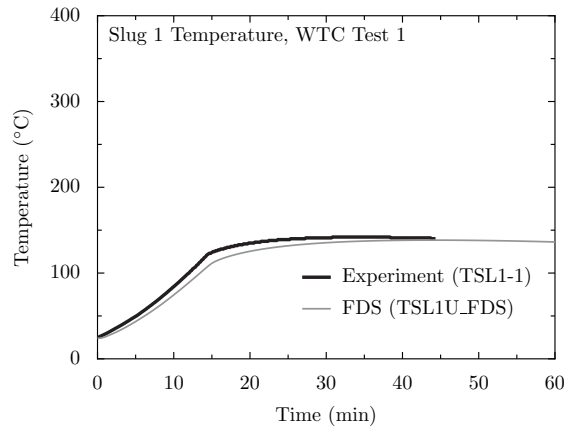


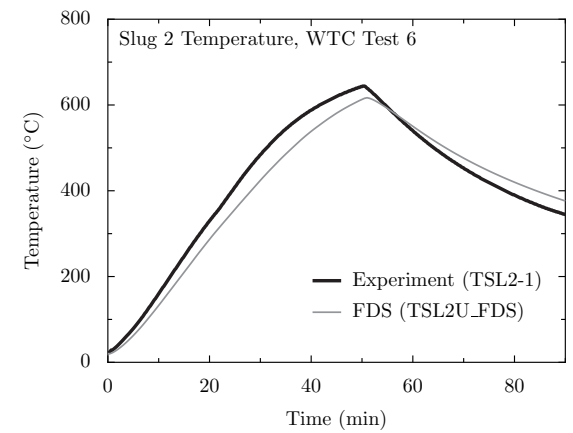
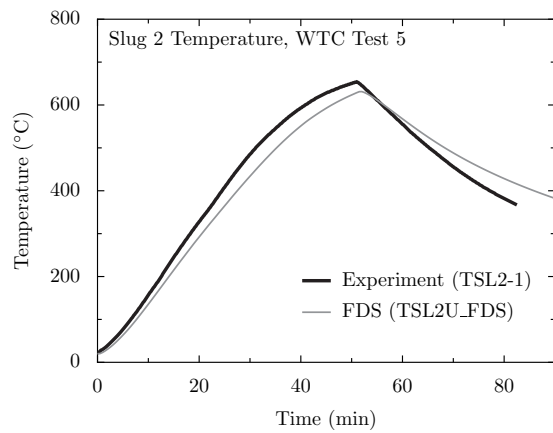
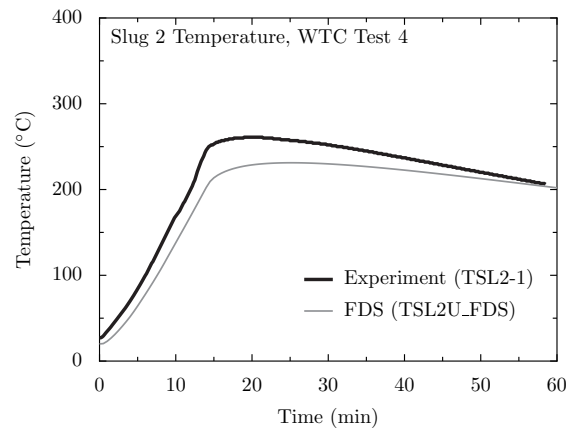
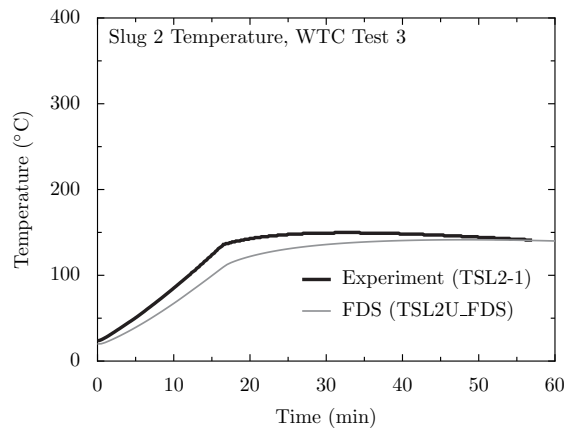
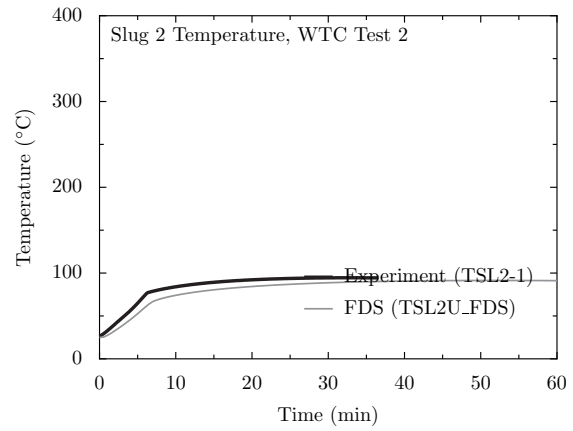
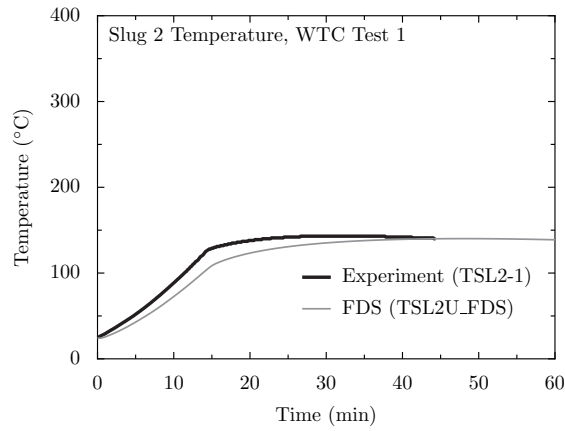


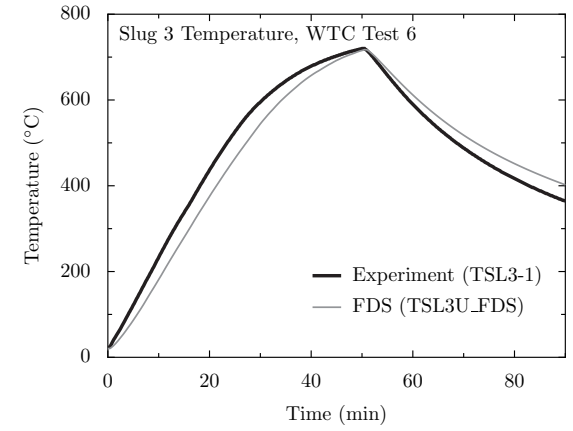
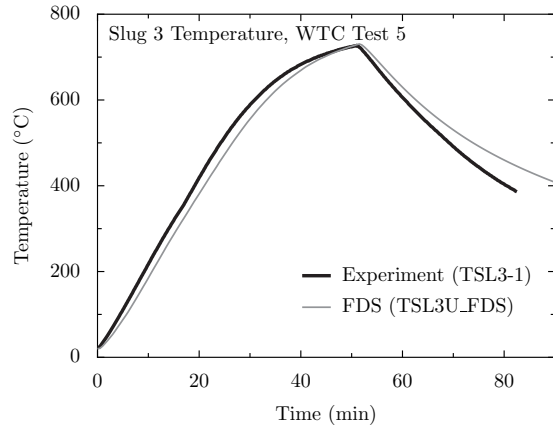
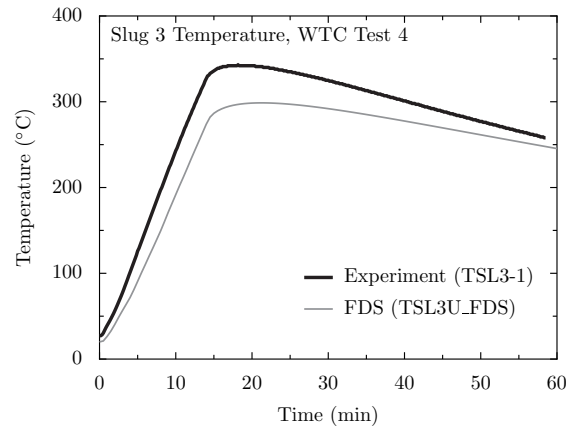
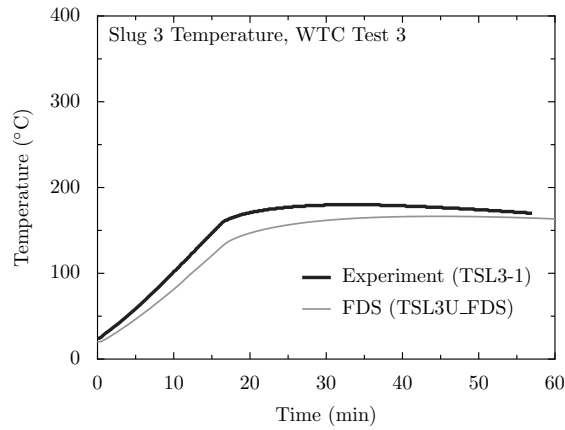
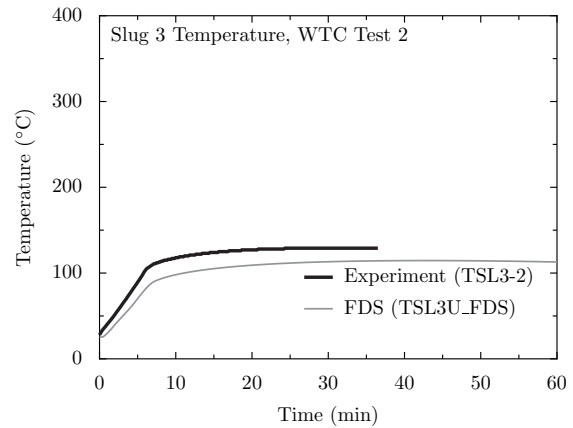
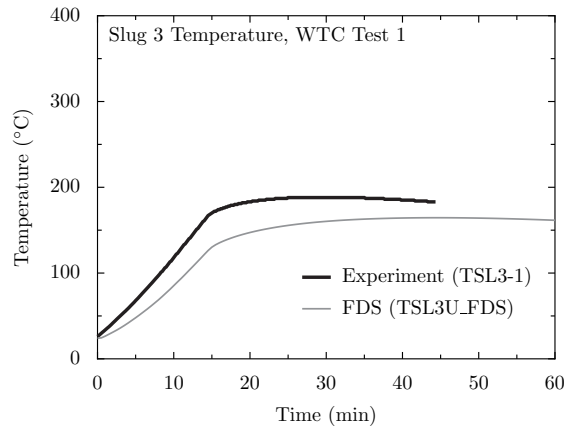


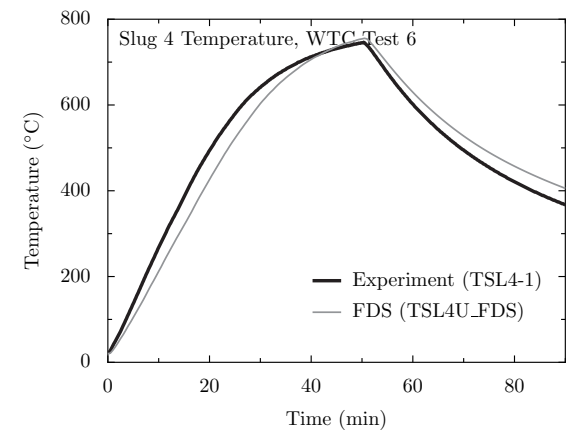
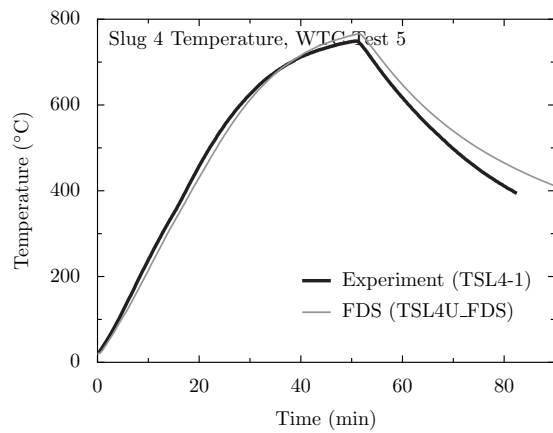
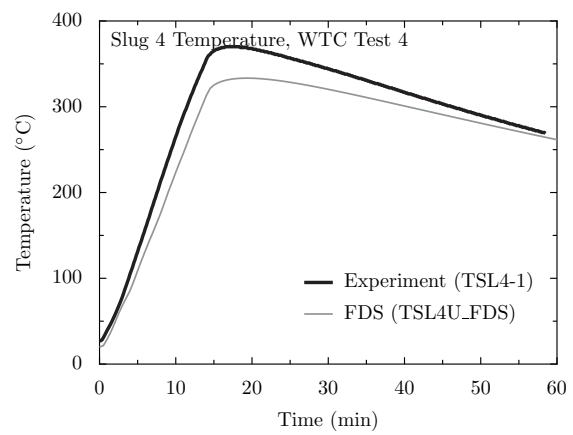
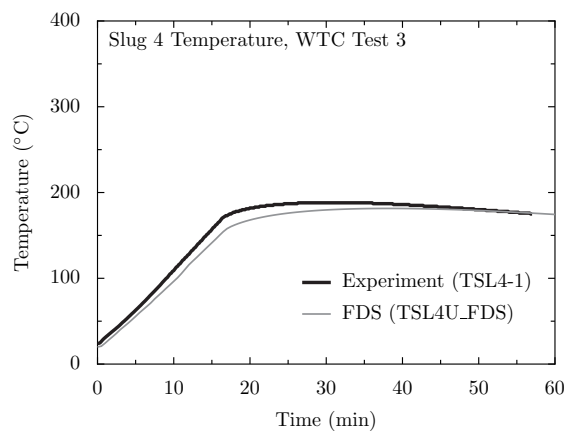
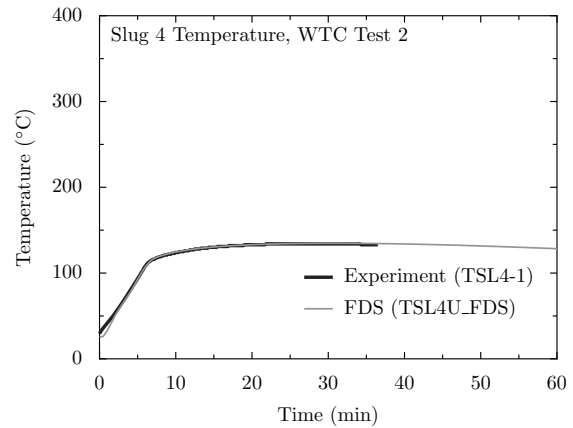
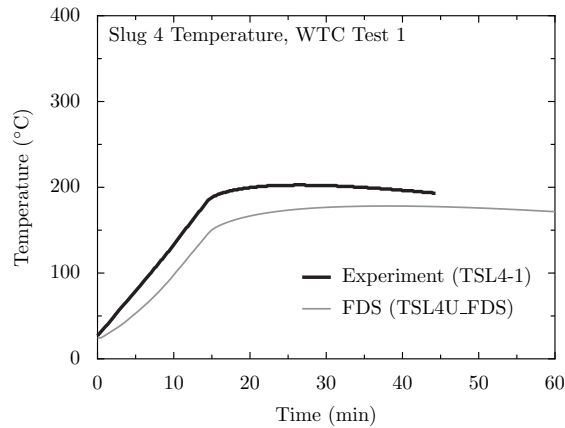


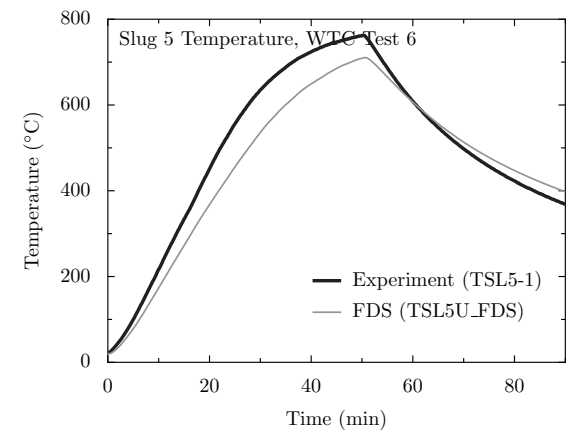
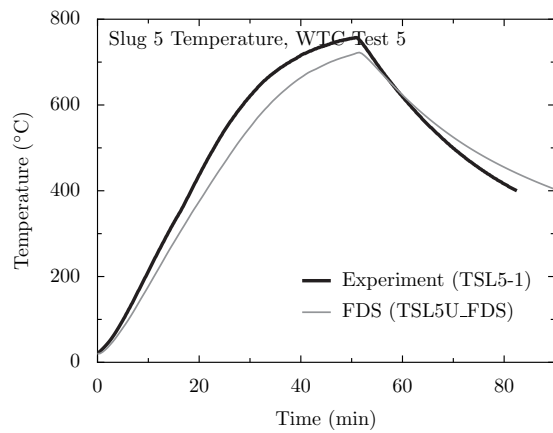
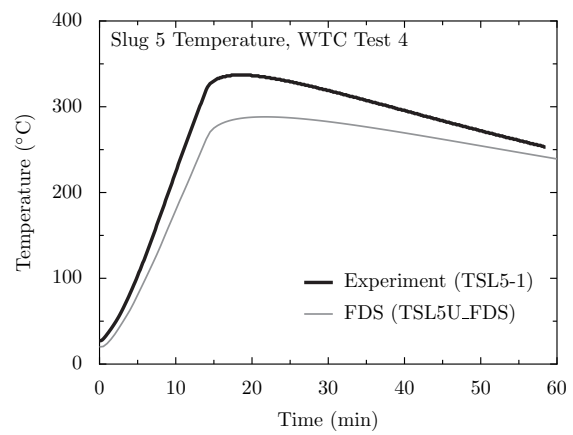
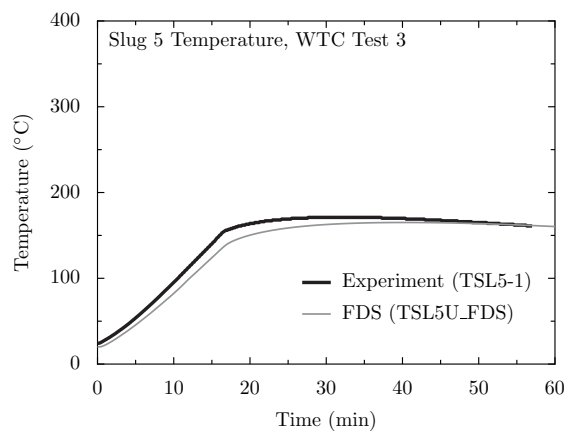
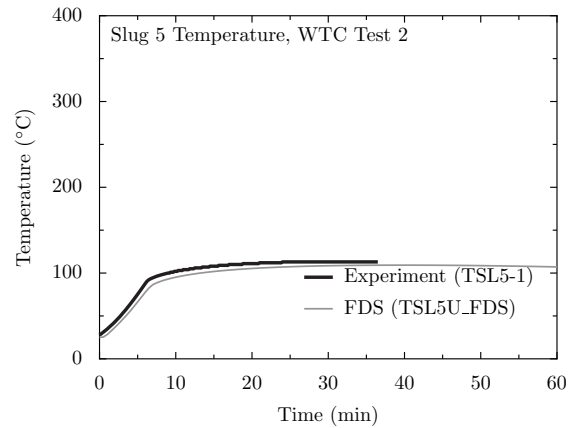
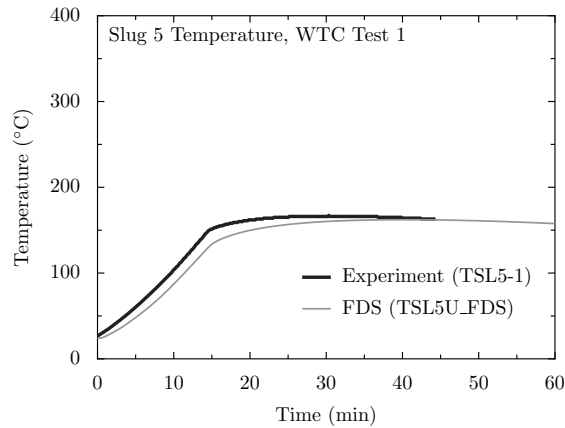












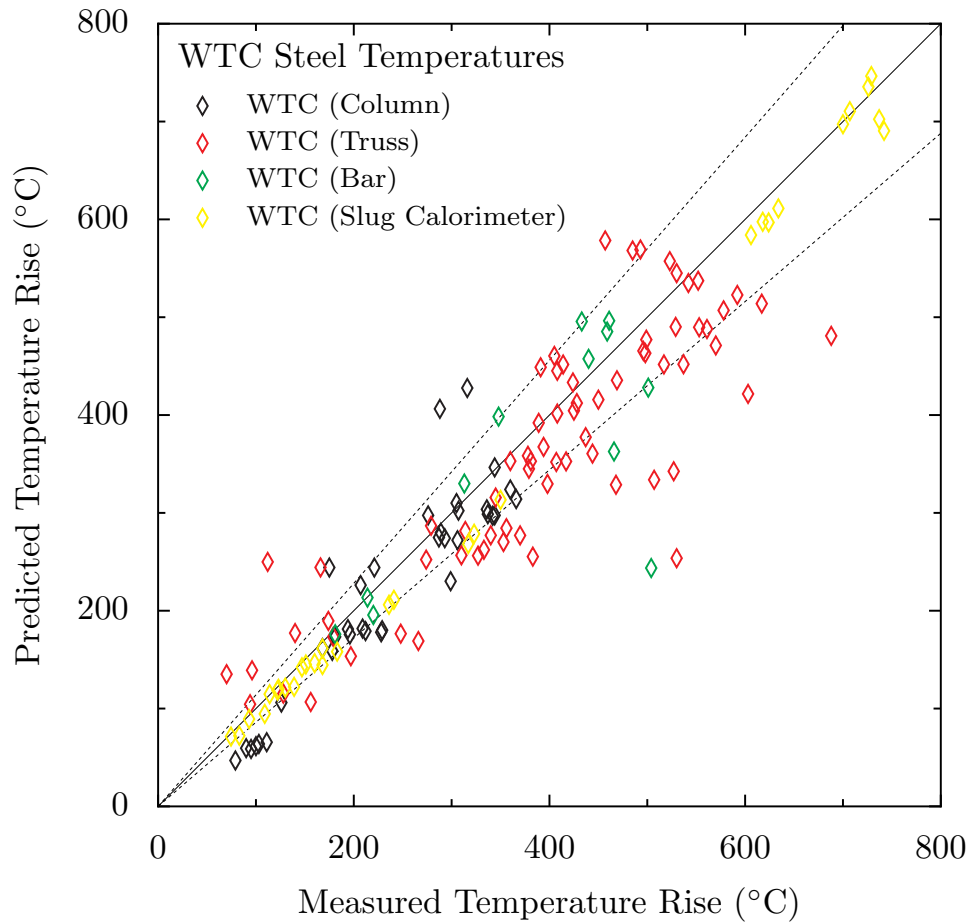
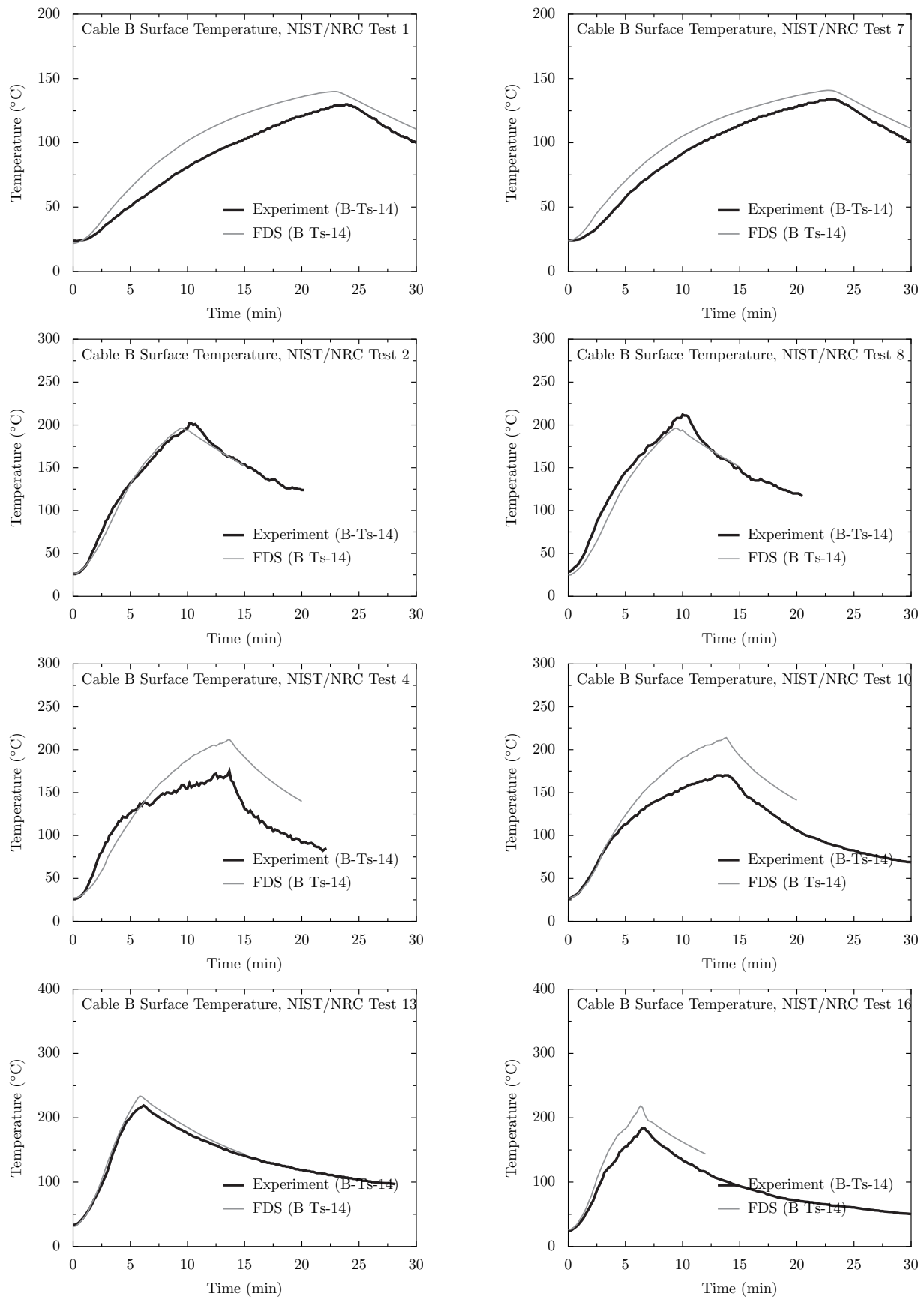
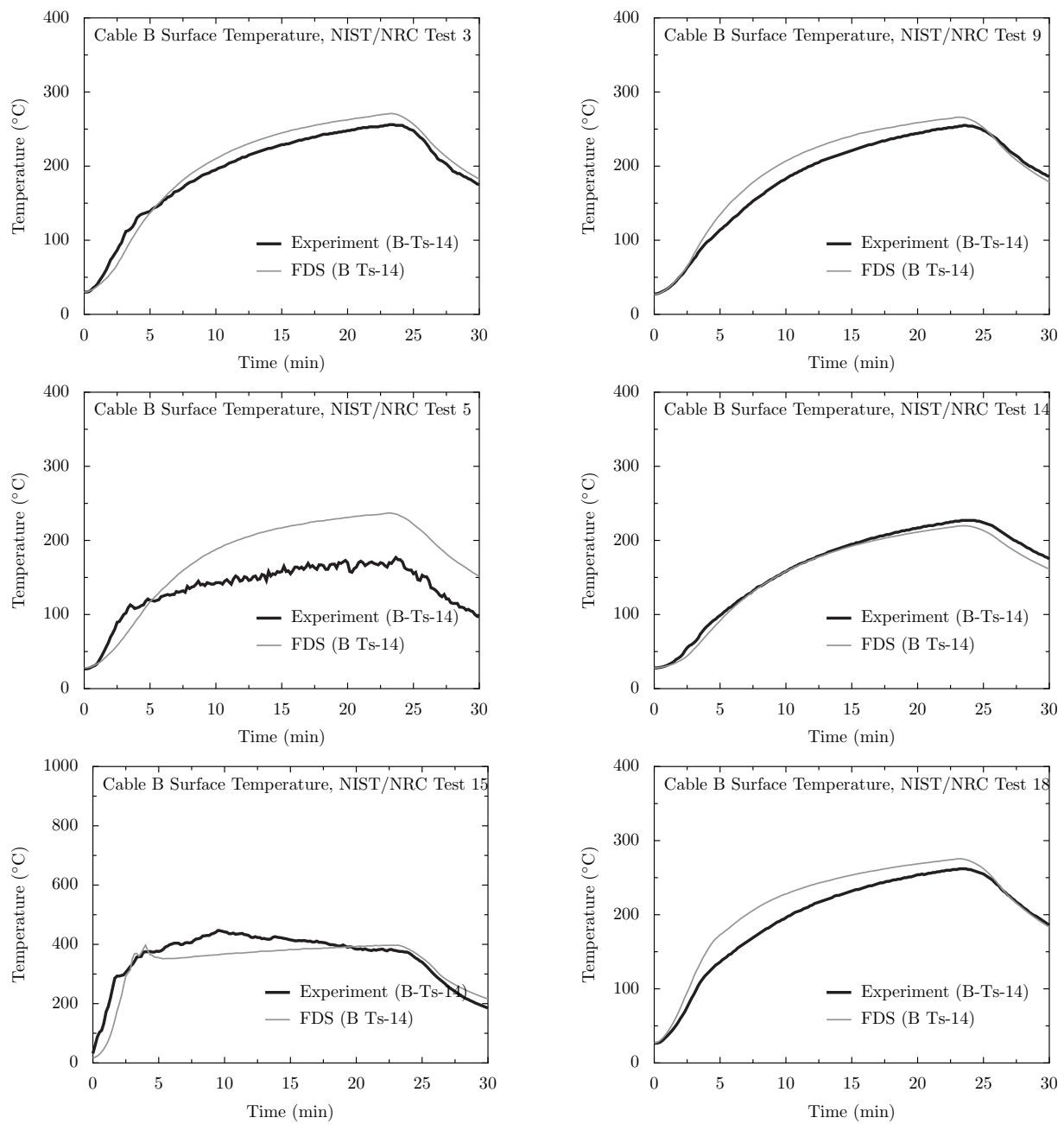


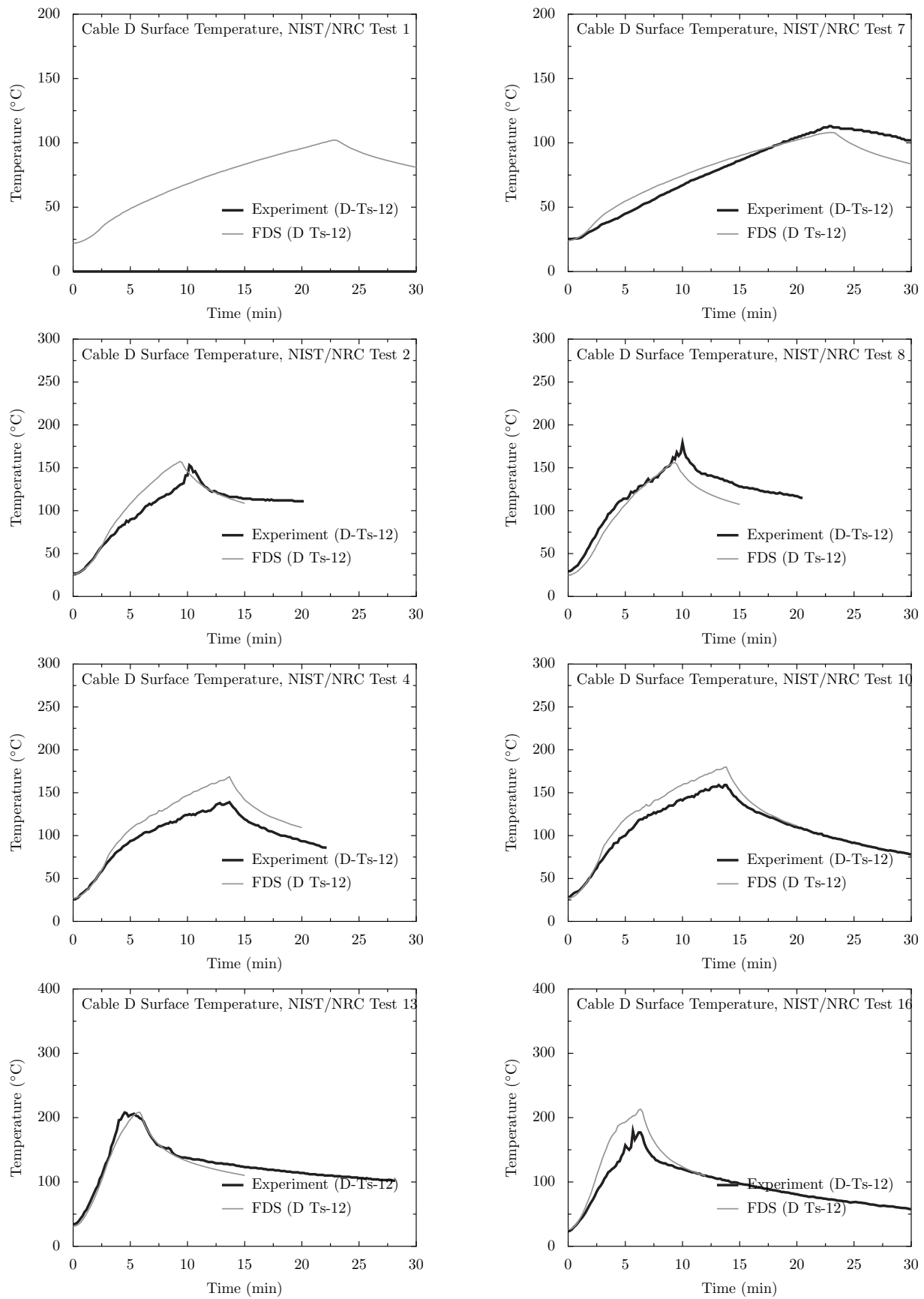
Figure 10.1: Summary of steel temperature predictions for the WTC test series.

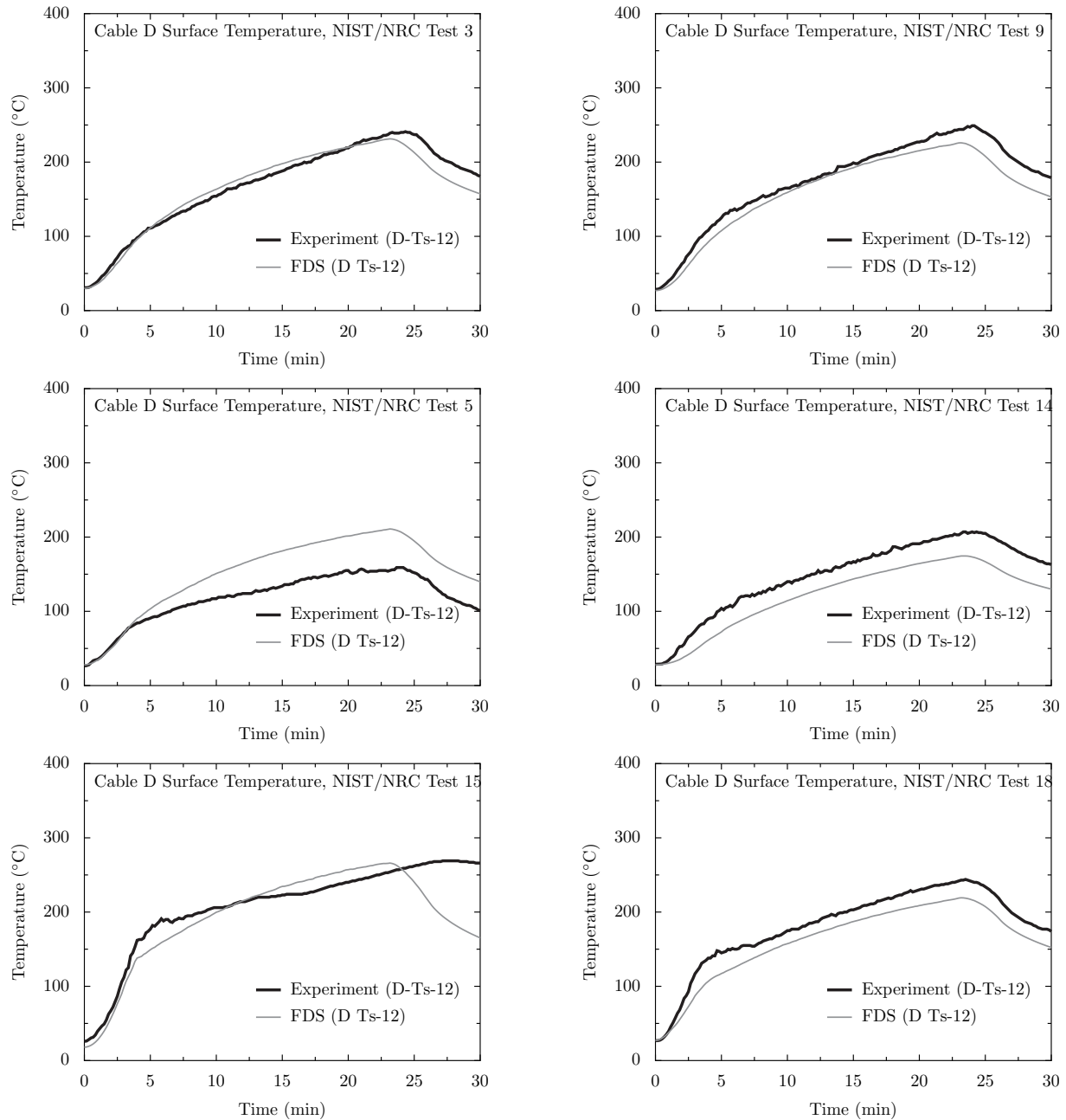
10.2 NIST/NRC Test Series, Cables

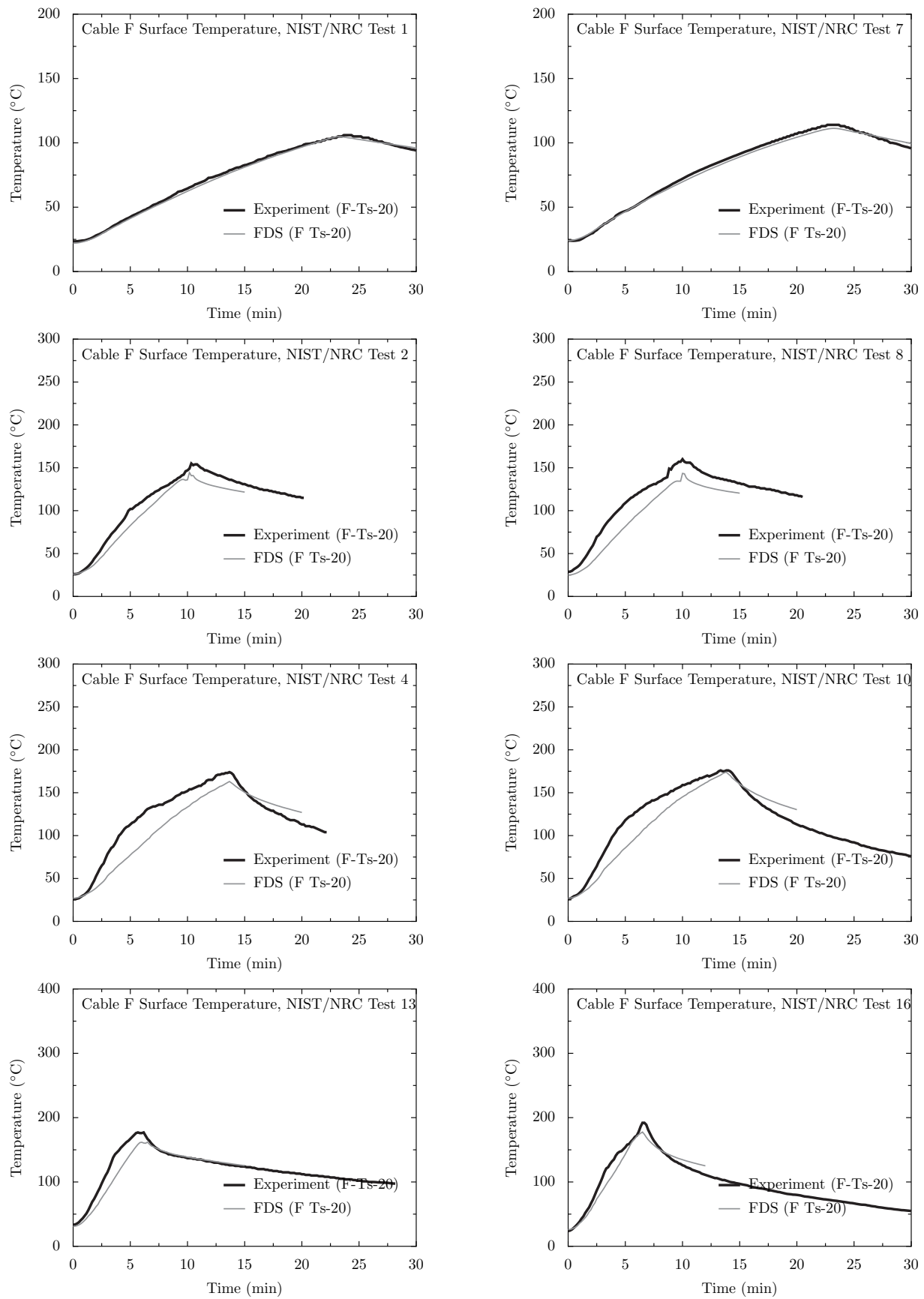
Cables in various types (power and control), and configurations (horizontal, vertical, in trays or free-hanging), were installed in the test compartment. For each of the four cable targets considered, measurements of the local gas temperature, surface temperature, radiative heat flux, and total heat flux are available. The following pages display comparisons of these quantities for Control Cable B, Horizontal Cable Tray D, Power Cable F and Vertical Cable Tray G. FDS does not have a detailed solid phase model that can account for the heat transfer within the bundled, cylindrical, non-homogenous cables. For the bundled cables within horizontal and vertical trays (Targets D and G), FDS assumes them to be rectangular slabs of thickness comparable to the diameter of the individual cables. For the free-hanging cables B and F, FDS assumes them to be cylinders of uniform composition into which it computes the radial heat transfer as a function of the heat flux to a designated location. The superposition of gas temperature, heat flux and surface temperature in the figures on the following pages provides information about how cables heat up in fires. Favorable or unfavorable predictions of cable surface temperatures can often be explained in terms of comparable errors in the prediction of the thermal environment in the vicinity of the cable.

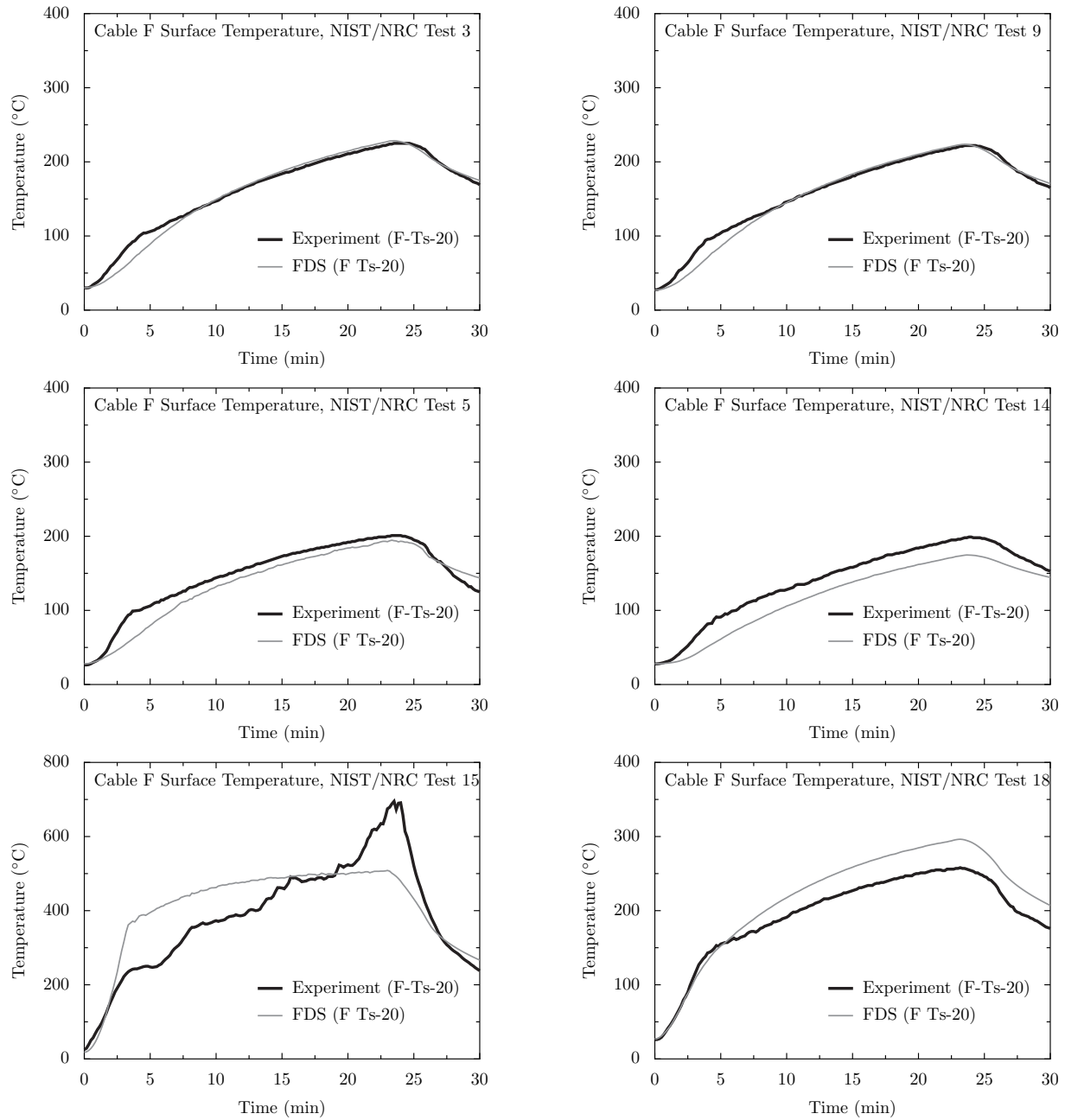


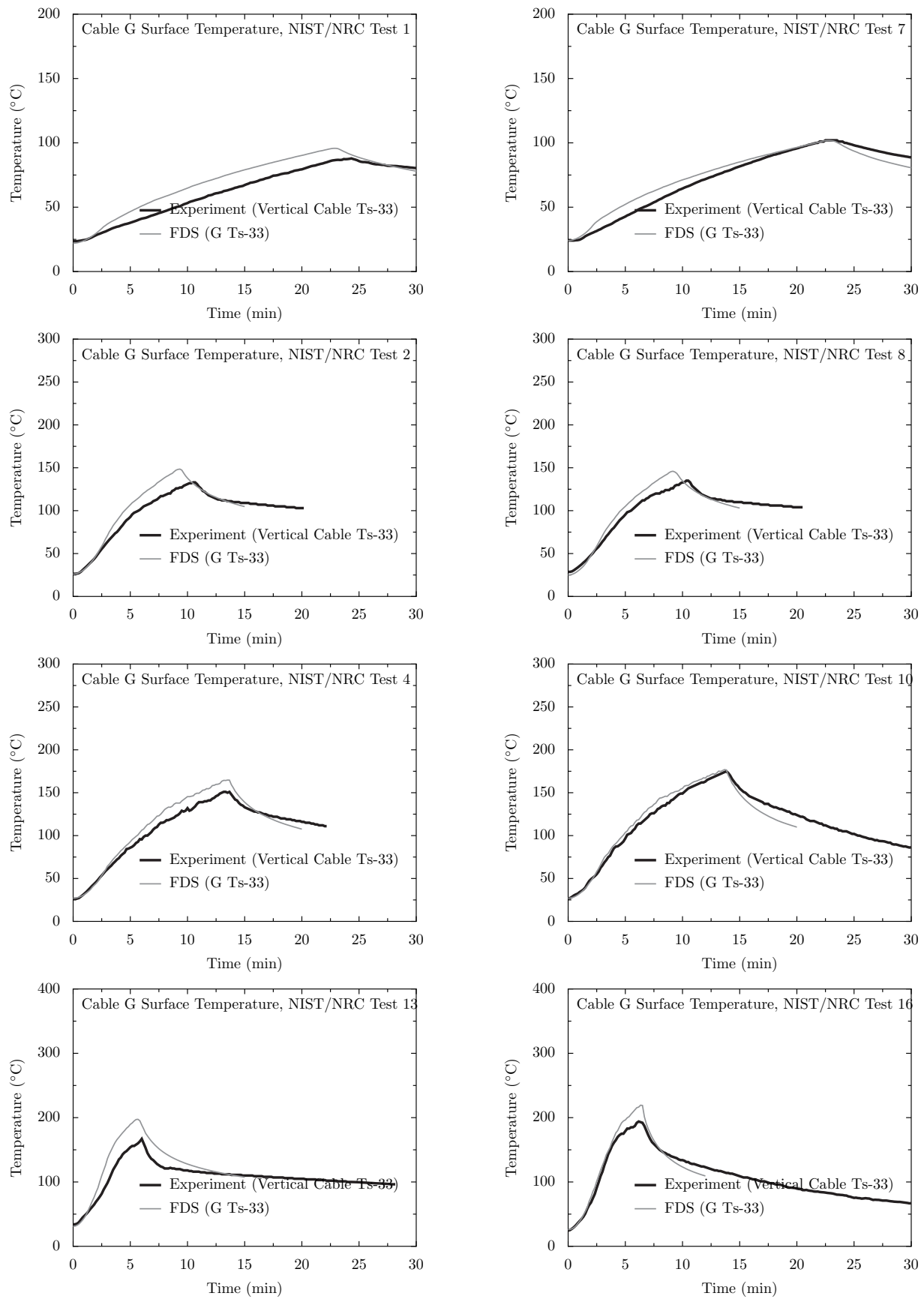


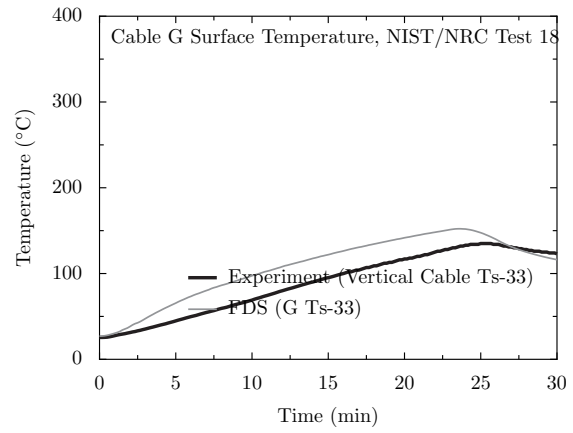
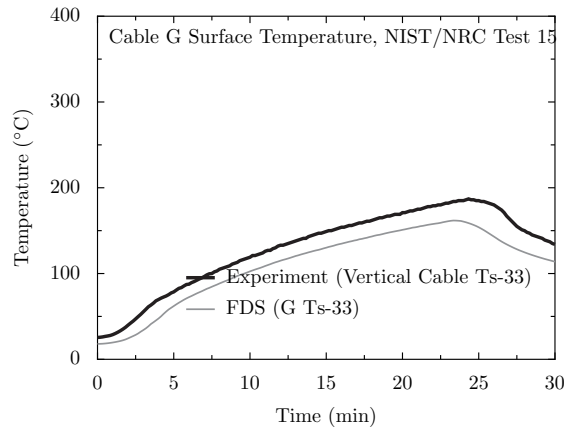
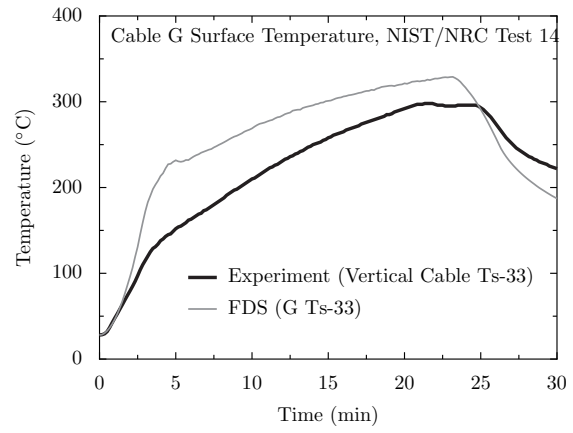
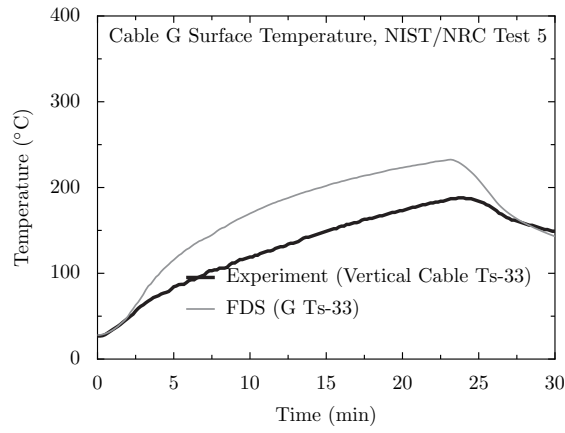
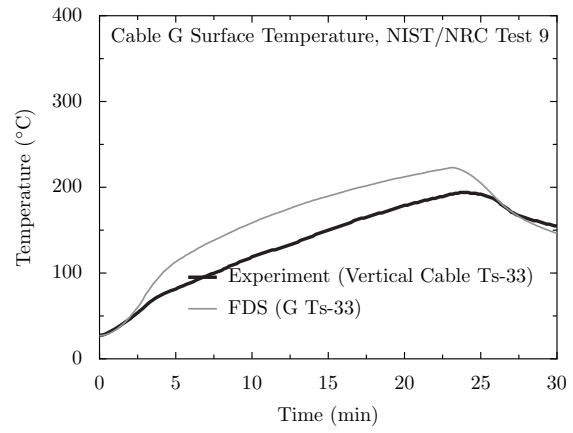
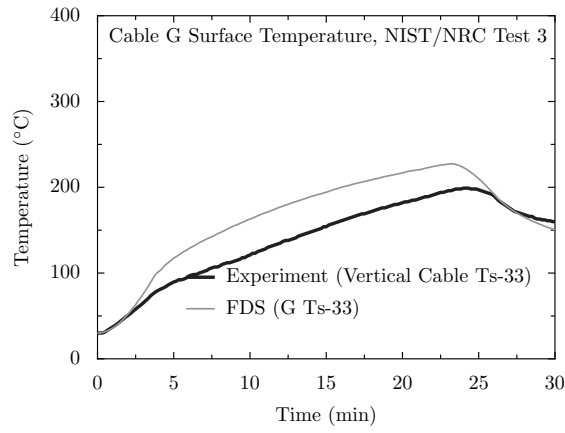












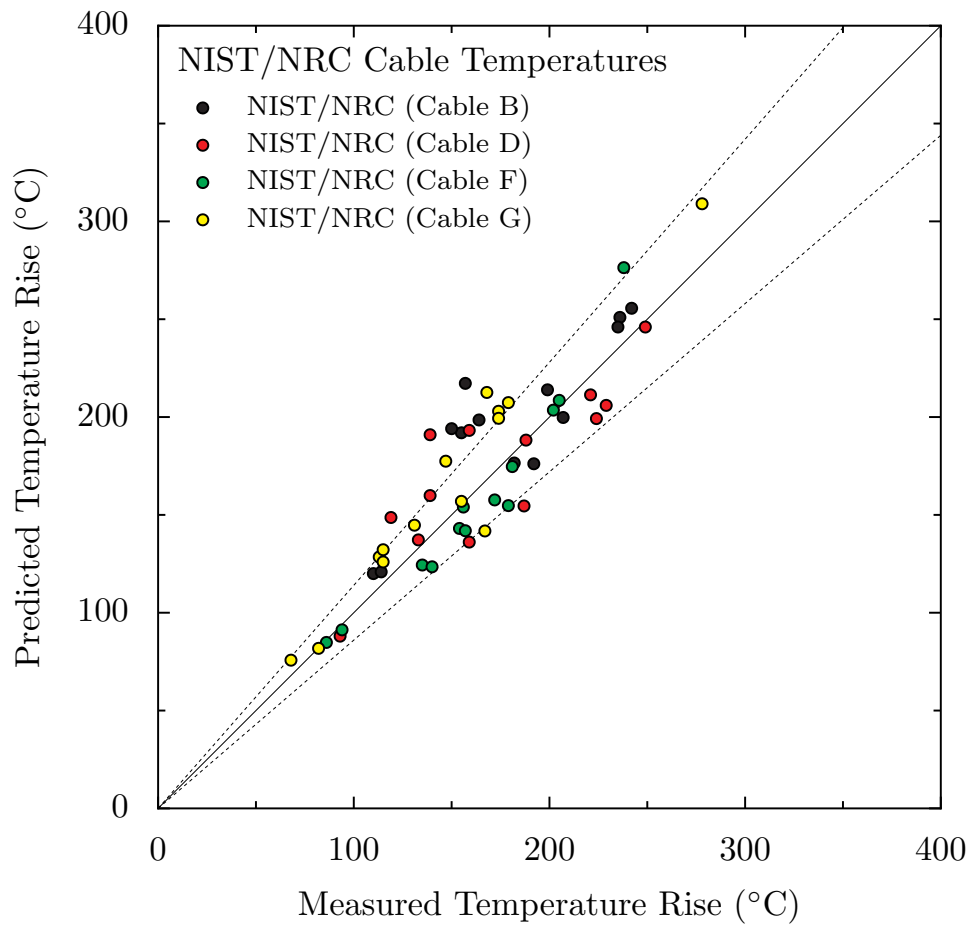


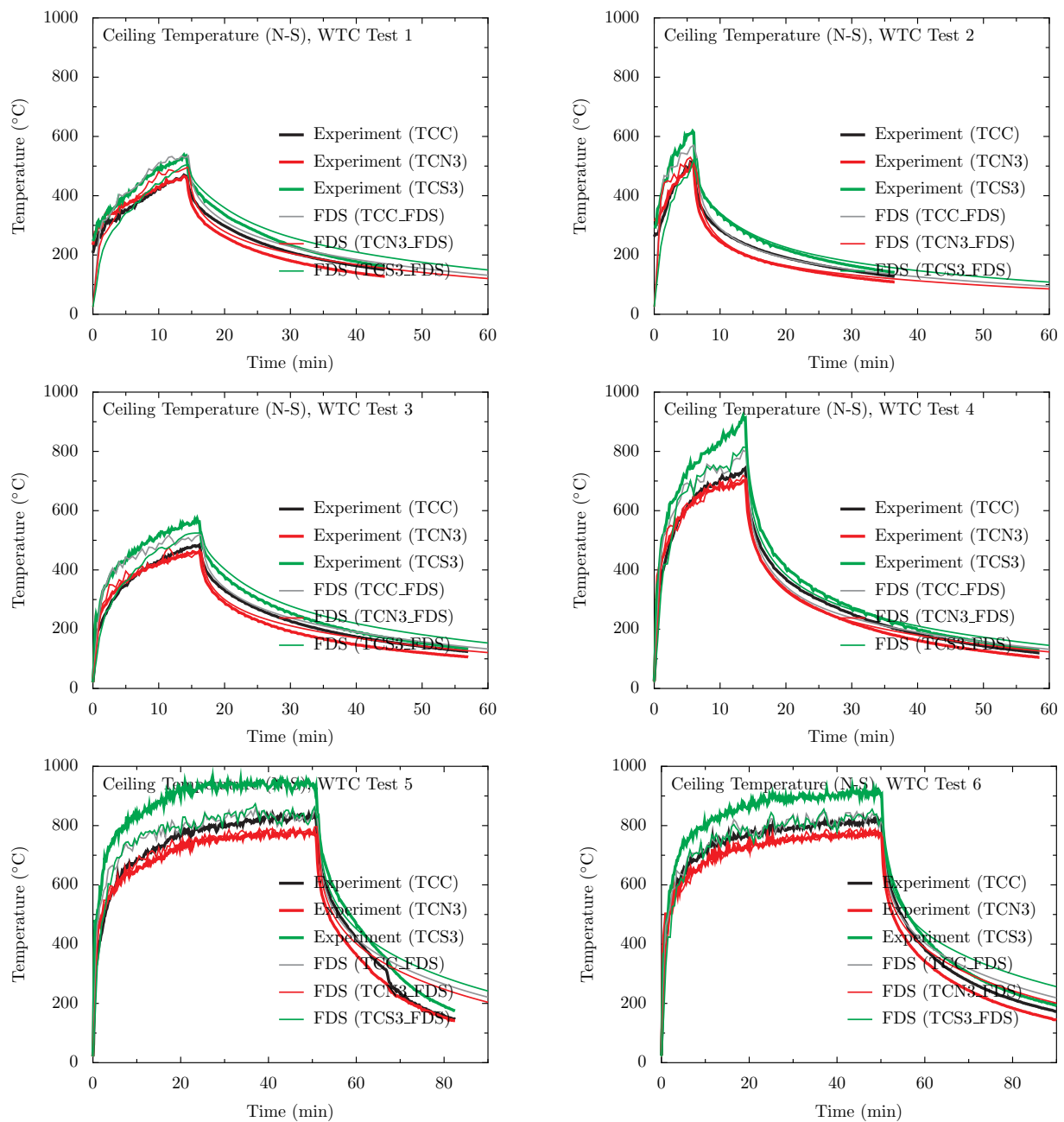
Figure 10.2: Summary of cable surface temperature predictions for the NIST/NRC test series.

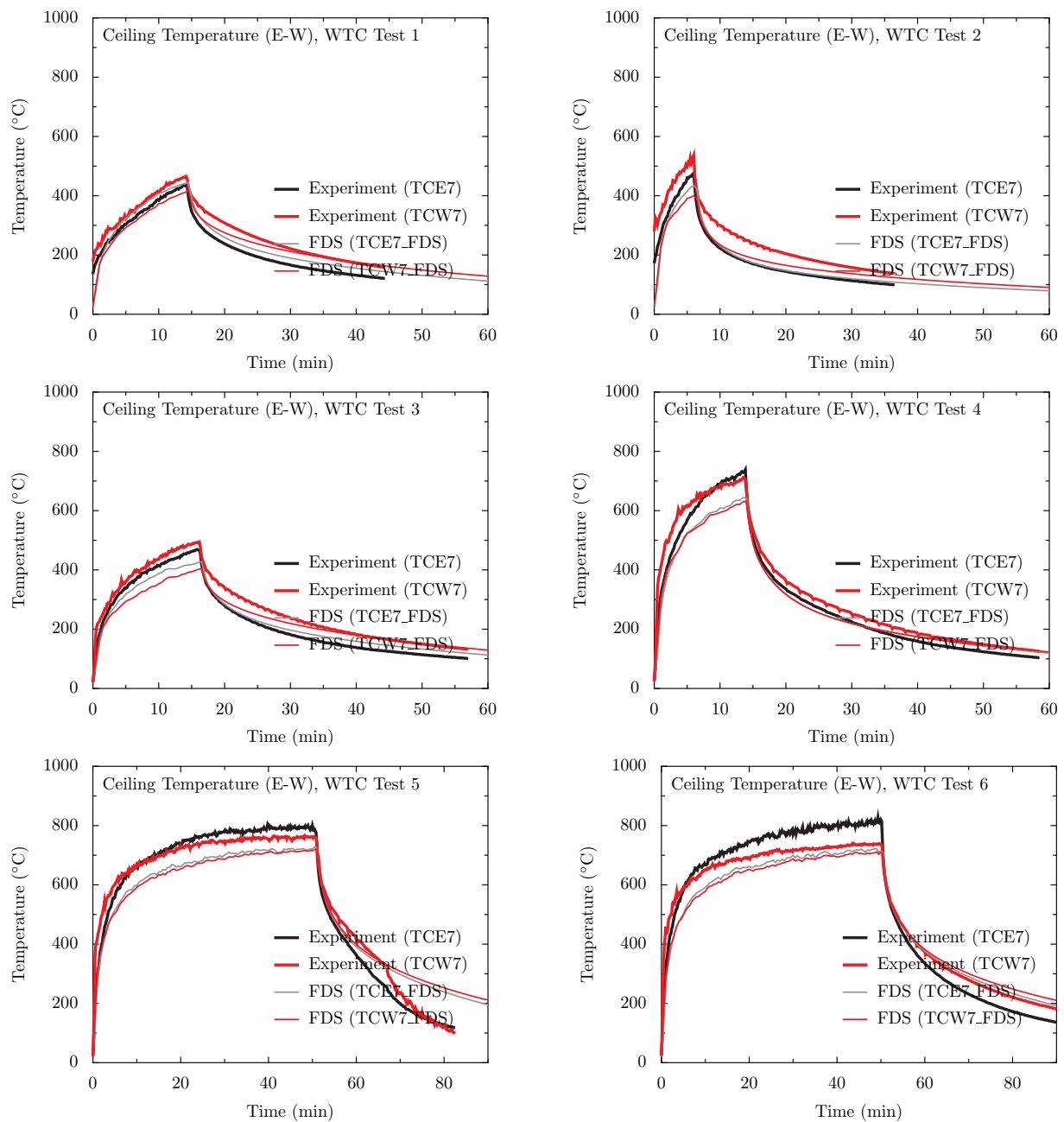
10.3 WTC Ceiling and Wall Temperatures

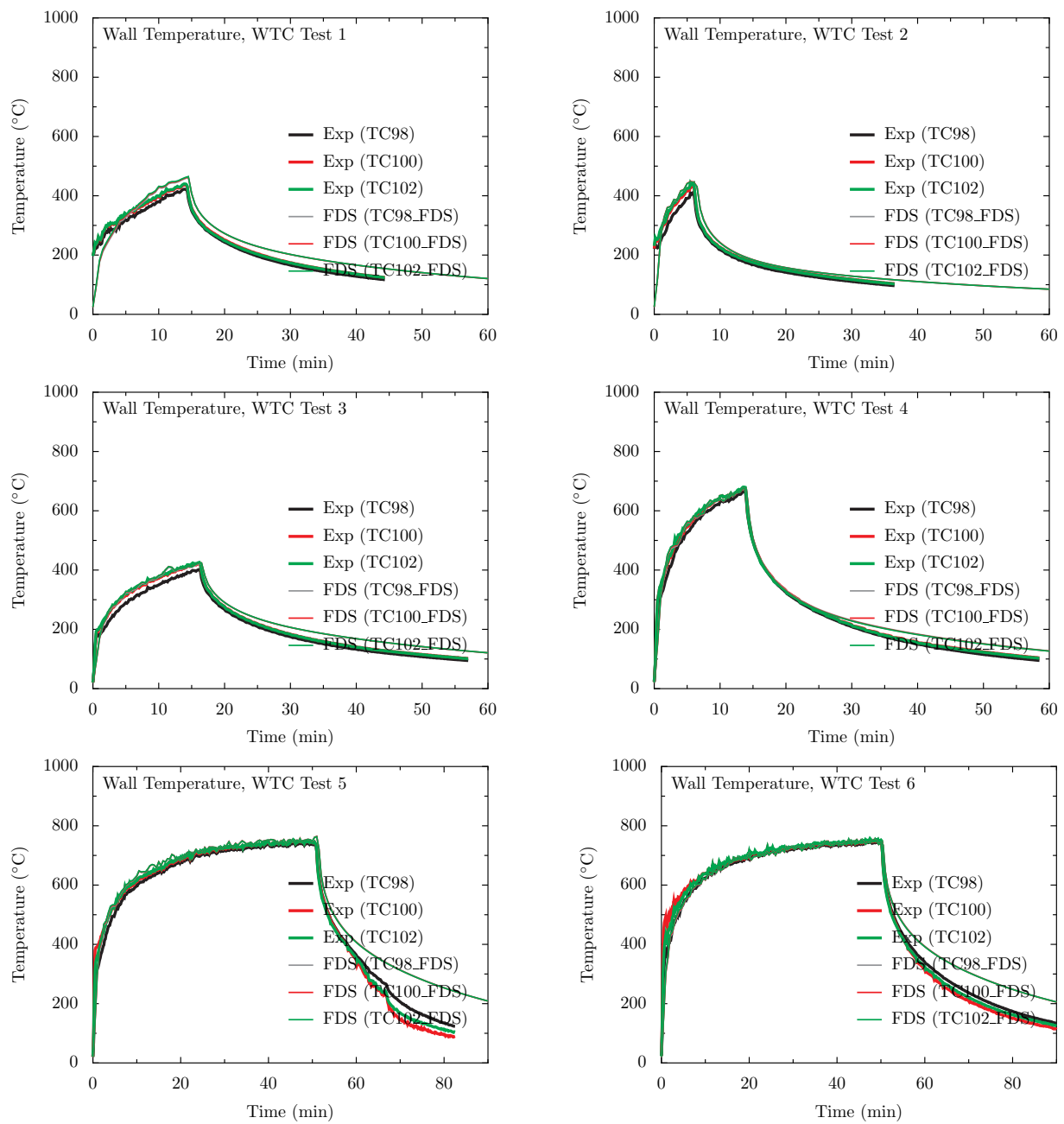
The following pages contain comparisons of predicted and measured ceiling temperatures, both at the surface and beneath a layer of marinite board. Table 10.1 below lists the coordinates of the measurement locations relative to the center of the fire pan. Names with “IN” appended are measurements made under the marinite board.

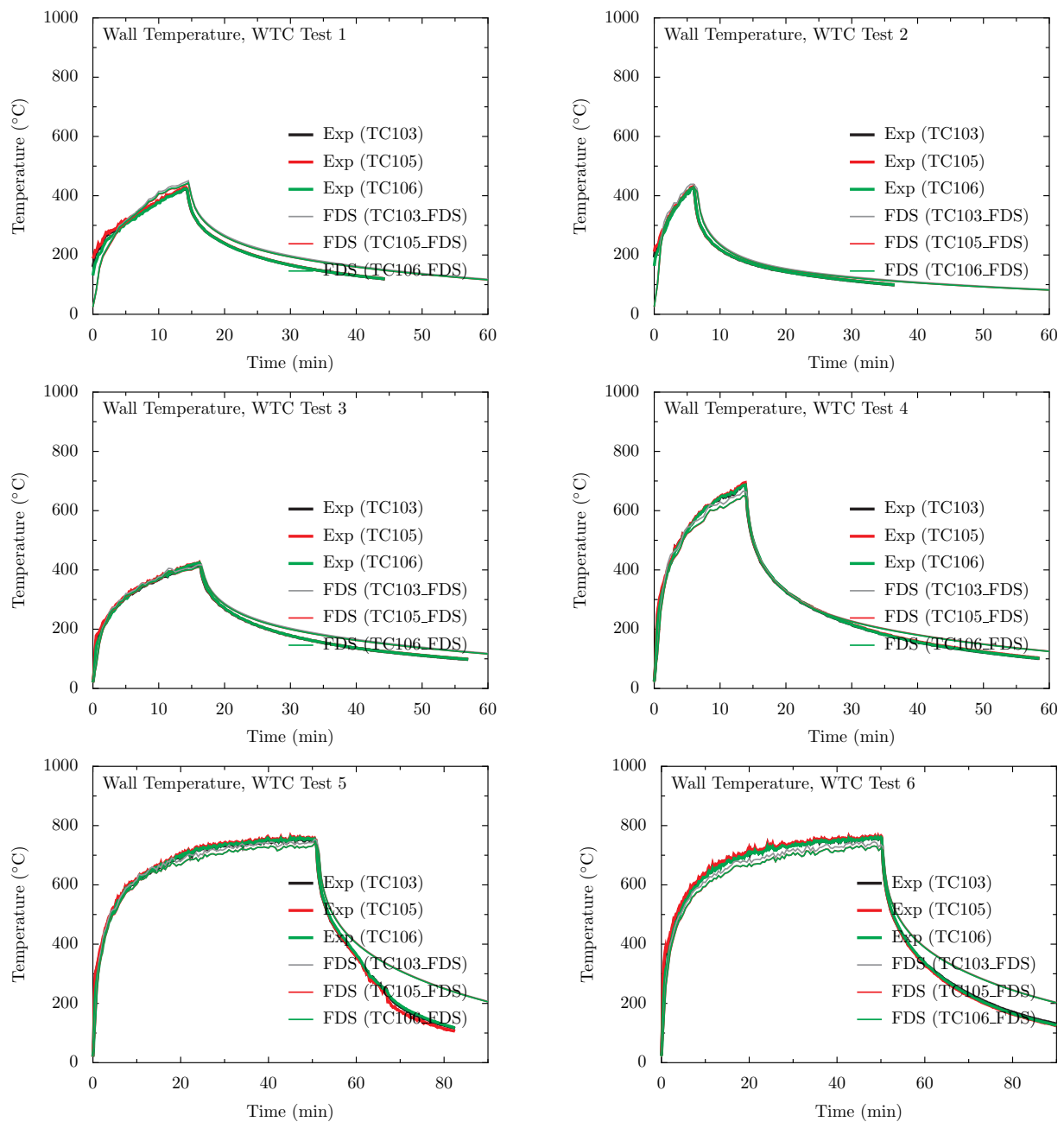
Table 10.1: Locations of ceiling surface temperature measurements relative to the fire pan in the WTC series.

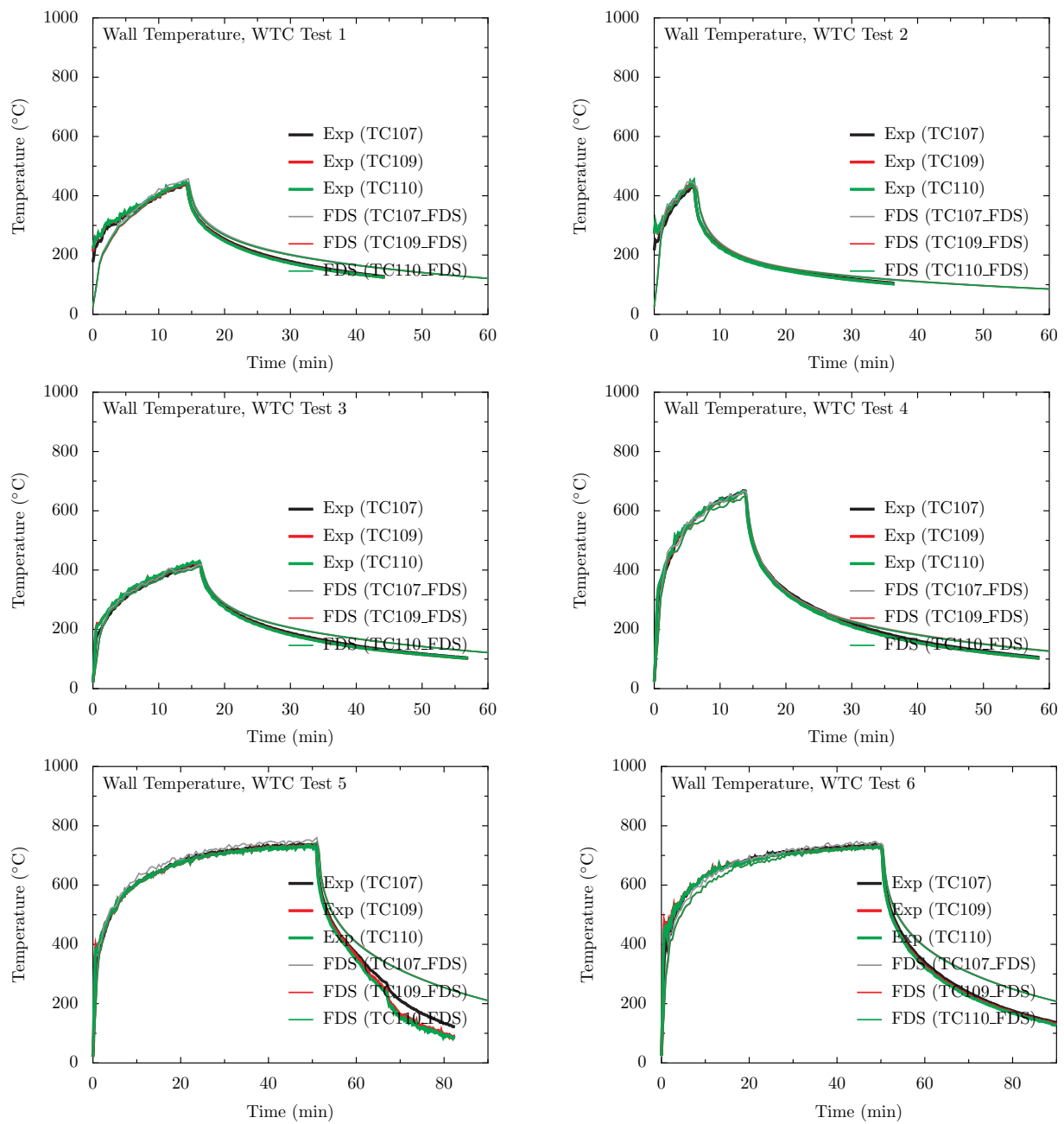
Name	x (m)	y (m)	z (m)
TCC	0.62	0.07	3.82
TCN3	0.62	0.67	3.82
TCS3	0.62	-0.53	3.82
TCE7	2.18	0.07	3.82
TCW7	-1.15	0.07	3.82
TCCIN	0.62	0.07	3.83
TCN3IN	0.62	0.67	3.83
TCS3IN	0.62	-0.53	3.83
TCE4IN	1.28	0.07	3.83
TCW4IN	0.05	0.07	3.83

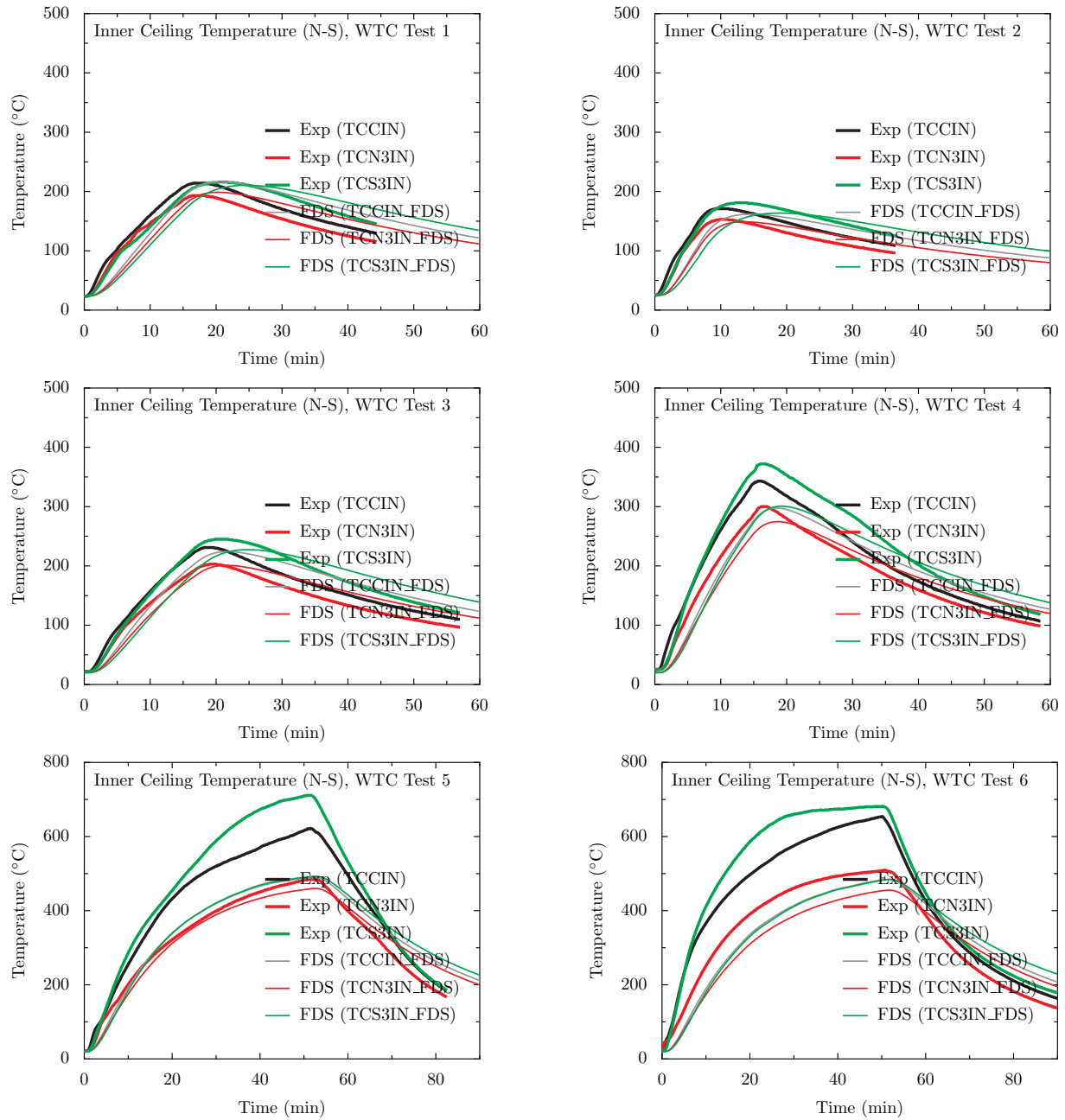


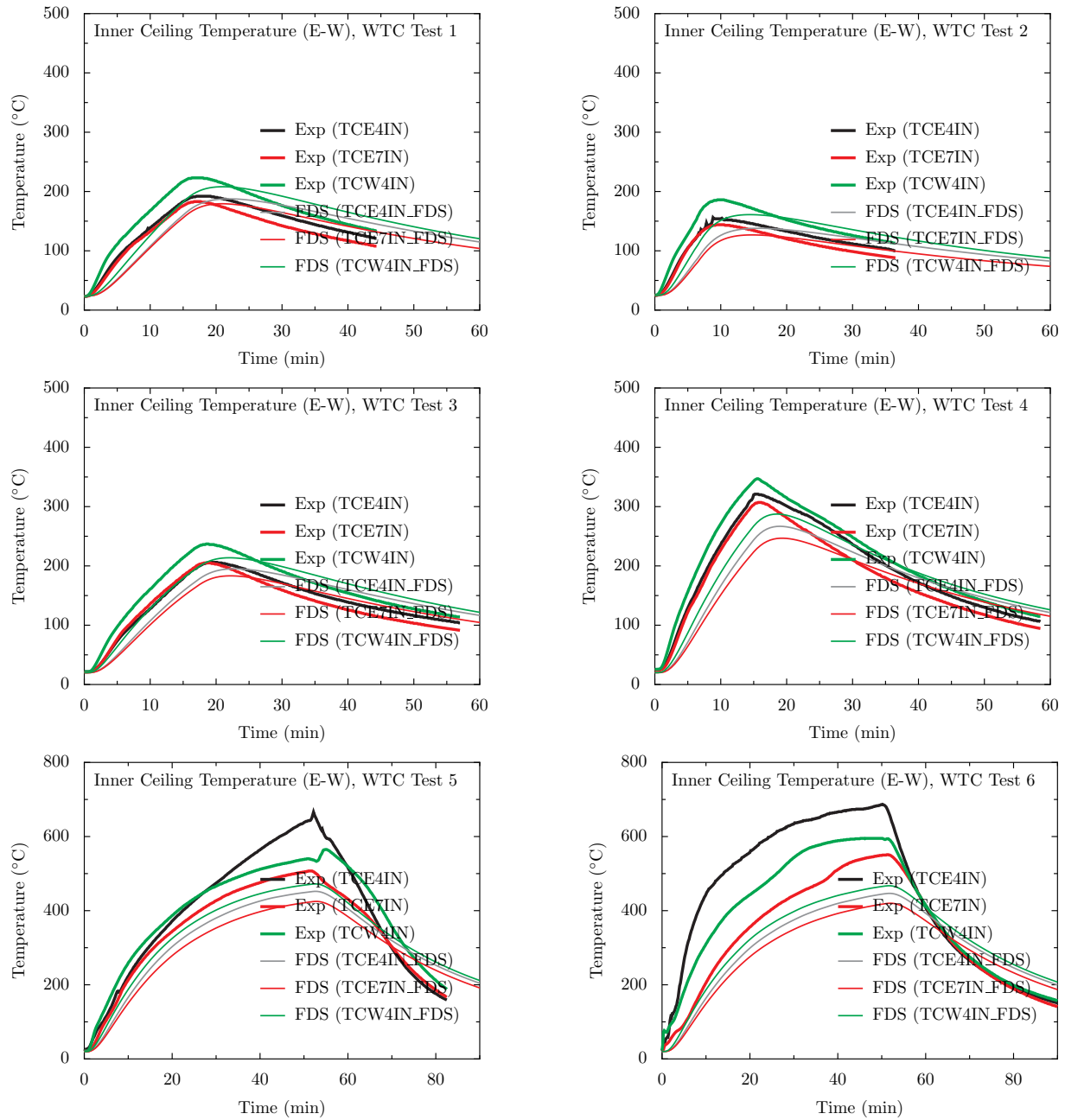


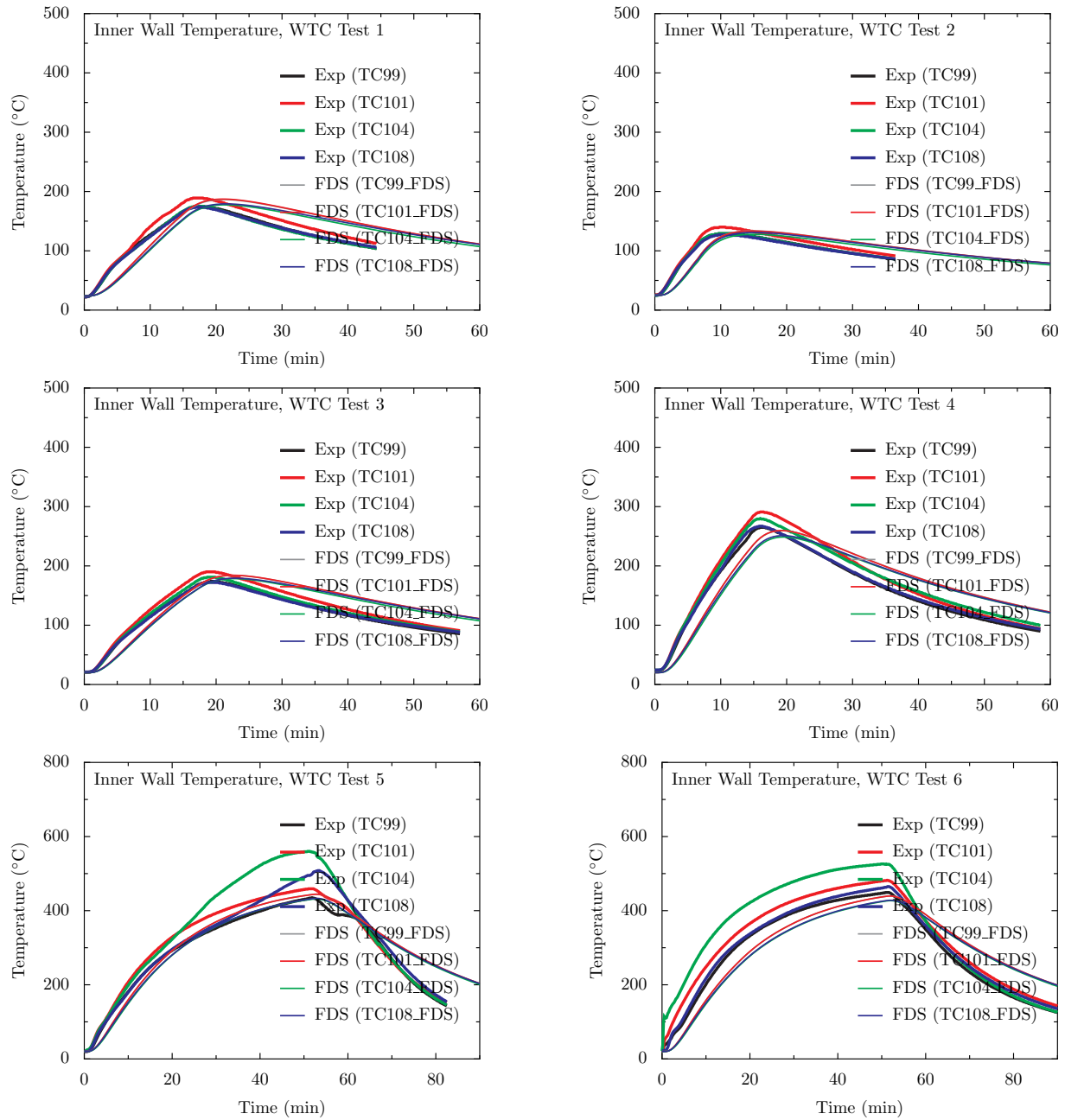












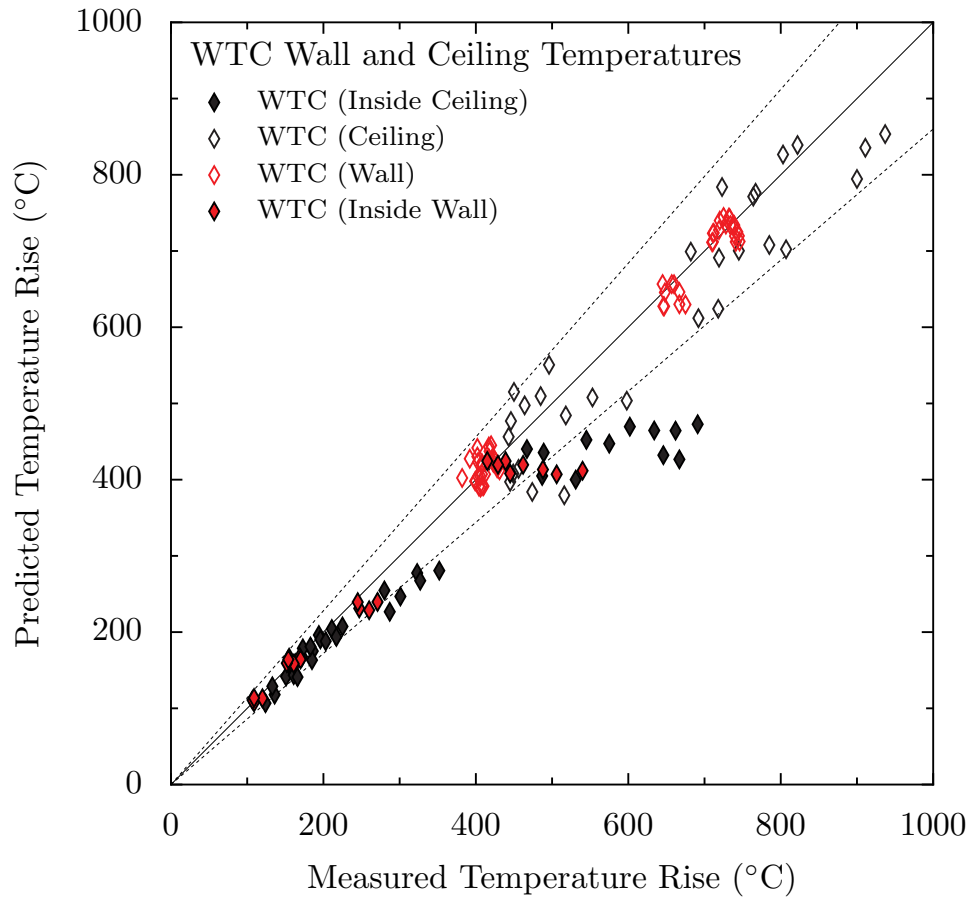


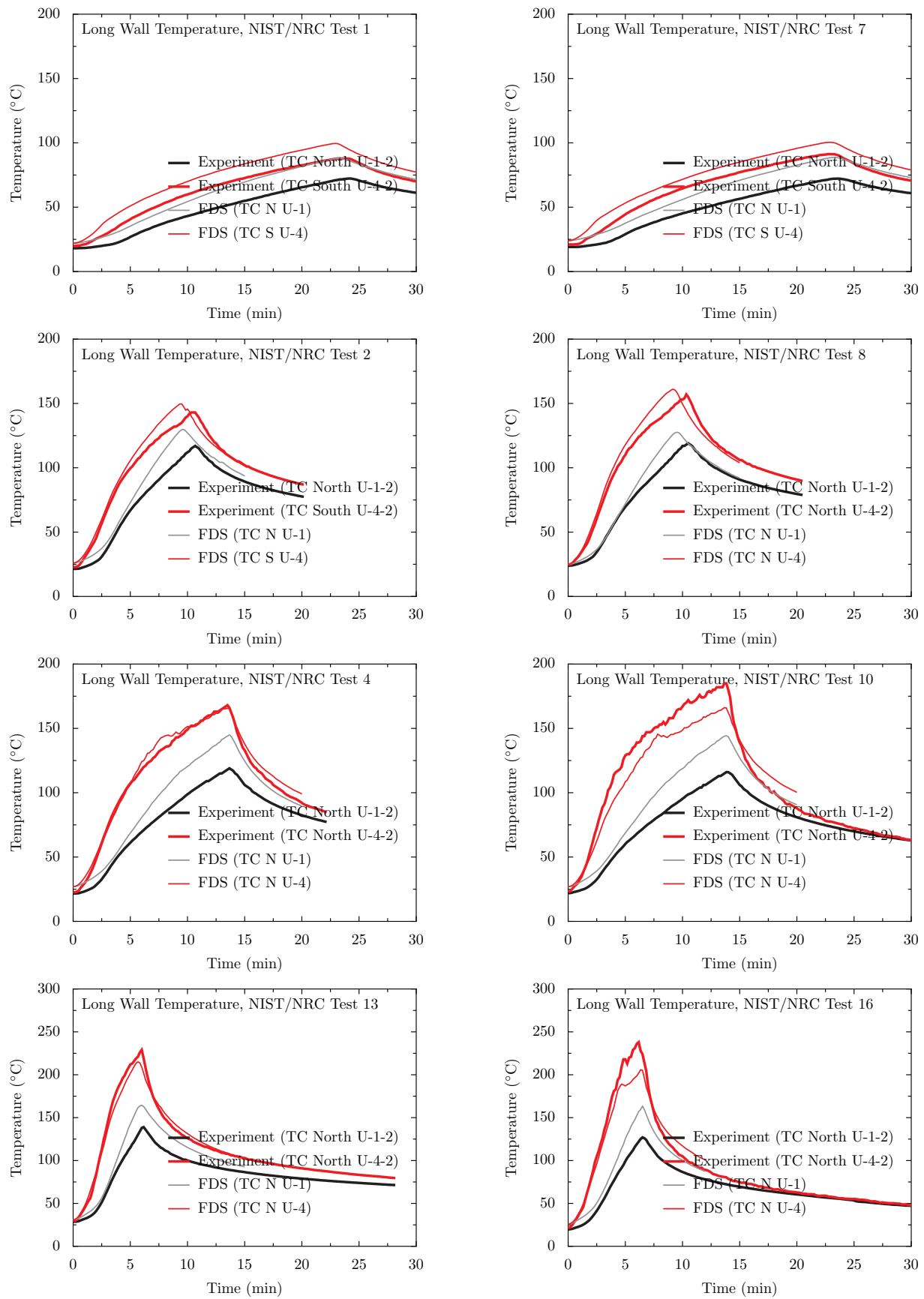
Figure 10.3: Summary of wall and ceiling temperature predictions for the WTC test series.

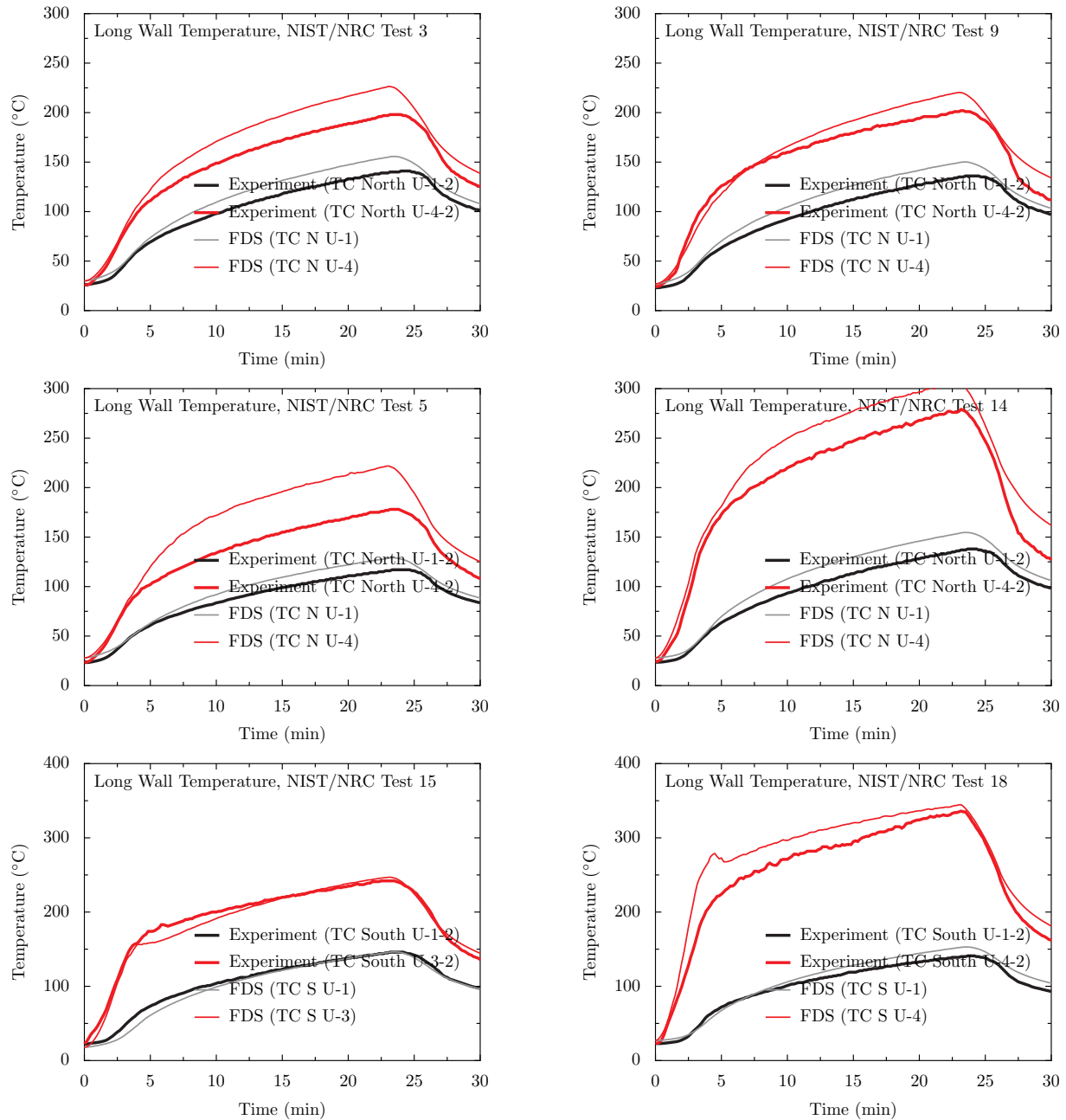
10.4 NIST/NRC Test Series, Compartment Walls, Floor and Ceiling

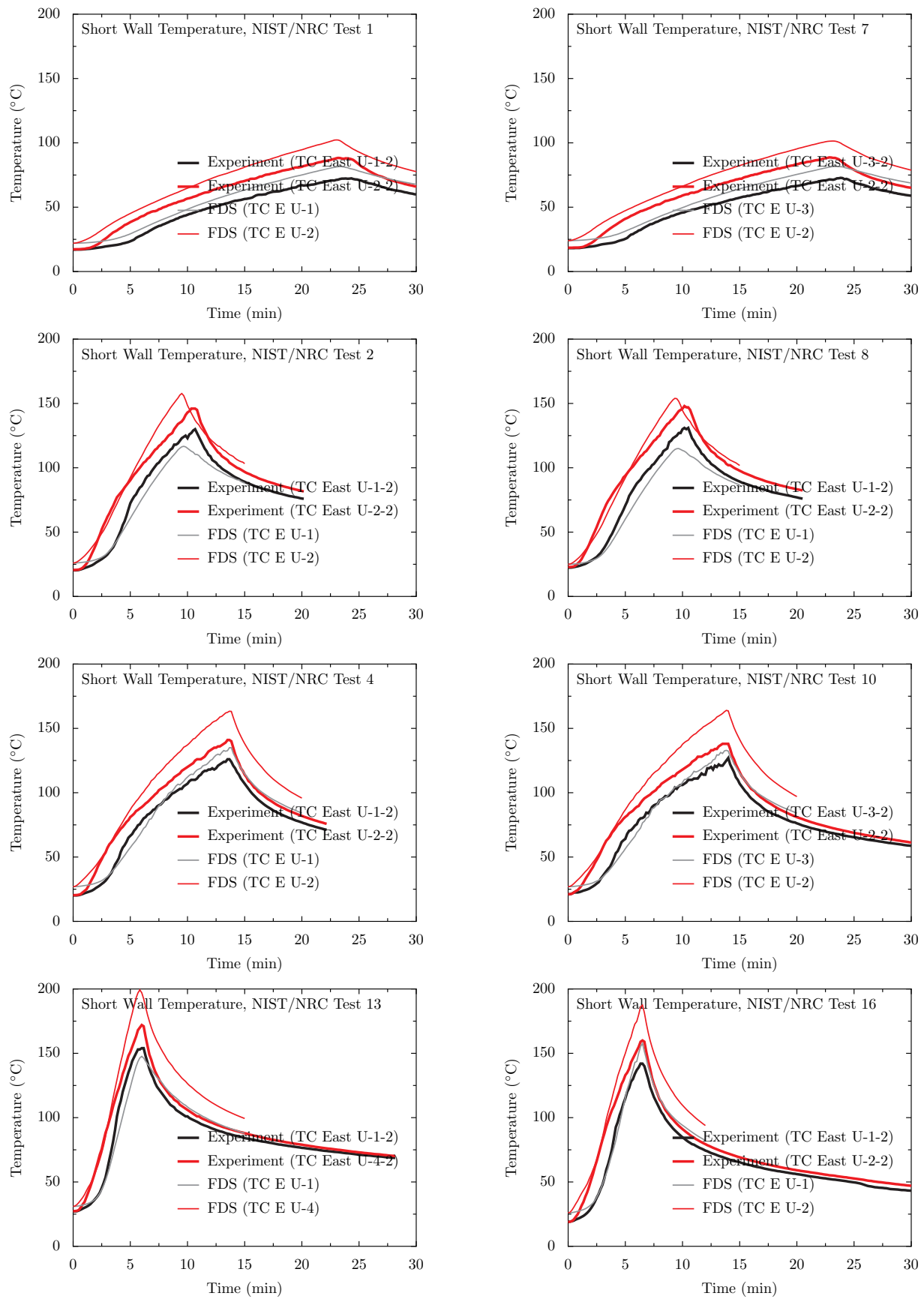
Thirty-six heat flux gauges were positioned at various locations on all four walls of the compartment, plus the ceiling and floor. Comparisons between measured and predicted heat fluxes and surface temperatures are shown on the following pages for a selected number of locations. Over half of the measurement points are in roughly the same relative location to the fire and hence the measurements and predictions are similar. For this reason, data for the east and north walls are shown because the data from the south and west walls are comparable. Data from the south wall is used in cases where the corresponding instrument on the north wall failed, or in cases where the fire is positioned close to the south wall. For each test, eight locations are used for comparison, two on the long (mainly north) wall, two on the short (east) wall, two on the floor, and two on the ceiling. Of the two locations for each panel, one is considered in the far-field, relatively remote from the fire; one is in the near-field, relatively close to the fire. How close or far varies from test to test. The two short wall locations are equally remote from the fire; thus, one location is in the lower layer, one in the upper. Table 10.2 lists the locations for each test.

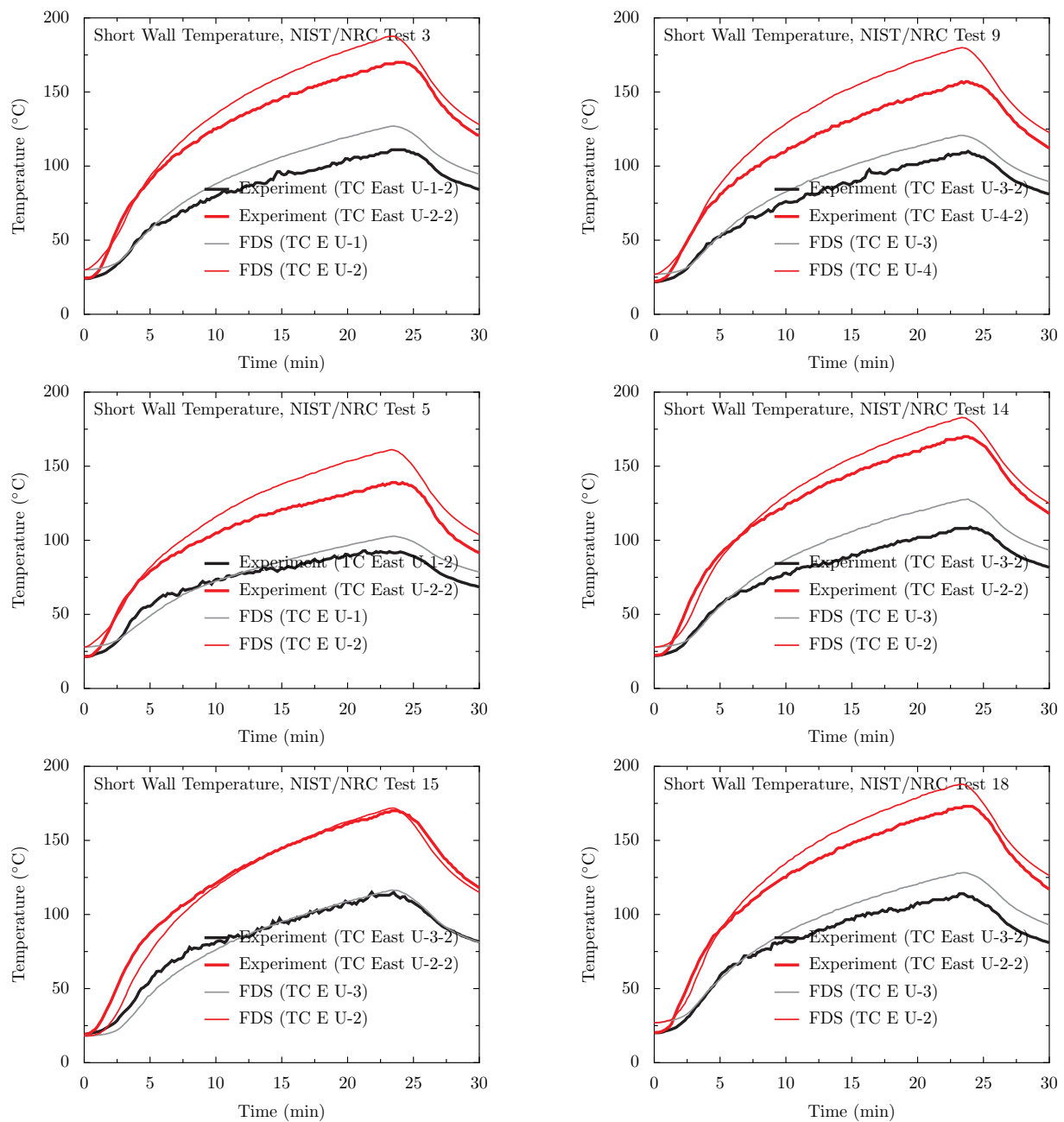
Table 10.2: Wall thermocouple positions for the NIST/NRC series. The origin of the coordinate system at the floor in the southwest corner of the compartment.

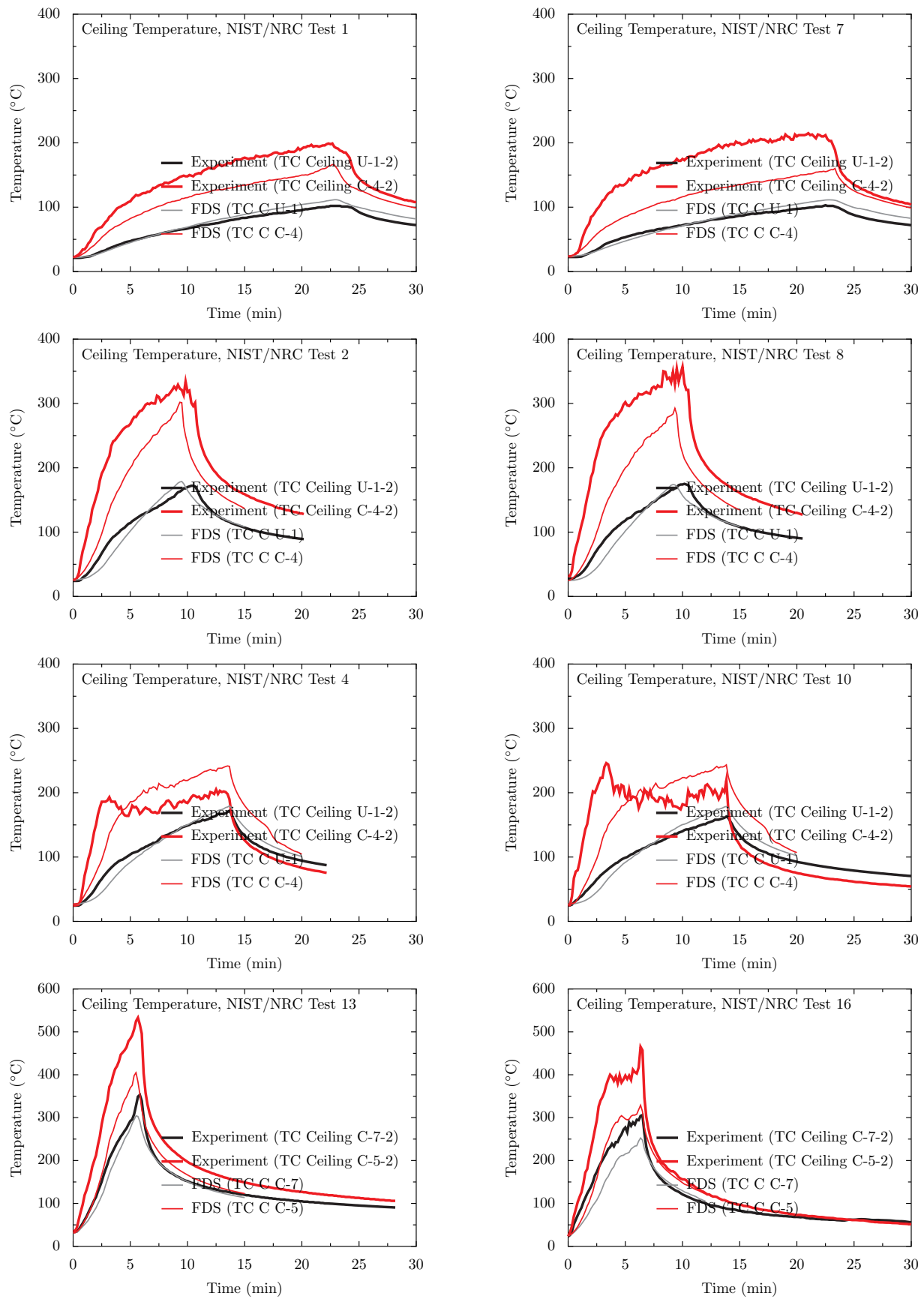
Name	<i>x</i>	<i>y</i>	<i>z</i>	Name	<i>x</i>	<i>y</i>	<i>z</i>
TC North U-1-2	3.85	7.04	1.49	TC Floor U-1-2	3.08	3.51	0
TC North U-2-2	3.86	7.04	3.71	TC Floor U-2-2	9.08	1.94	0
TC North U-3-2	9.48	7.04	1.86	TC Floor U-3-2	9.06	5.97	0
TC North U-4-2	12.07	7.04	1.88	TC Floor U-4-2	10.86	2.38	0
TC North U-5-2	17.69	7.04	1.49	TC Floor C-5-2	10.93	5.20	0.01
TC North U-6-2	17.69	7.04	3.69	TC Floor U-6-2	13.13	1.99	0
TC South U-1-2	3.86	0	1.49	TC Floor U-7-2	13.00	5.92	0
TC South U-2-2	3.86	0	3.82	TC Floor U-8-2	18.63	3.54	0
TC South U-3-2	9.54	0	1.86	TC Ceiling U-1-2	3.04	3.60	3.82
TC South U-4-2	12.08	0	1.86	TC Ceiling C-2-2	8.99	2.00	3.82
TC South U-5-2	17.69	0	1.50	TC Ceiling C-3-2	9.03	5.97	3.82
TC South U-6-2	17.74	0	3.70	TC Ceiling C-4-2	10.79	2.38	3.82
TC East U-1-2	21.66	1.52	1.12	TC Ceiling C-5-2	10.79	5.20	3.82
TC East U-2-2	21.66	1.52	2.40	TC Ceiling C-6-2	13.00	2.07	3.82
TC East U-3-2	21.66	5.68	1.13	TC Ceiling C-7-2	12.84	5.98	3.82
TC East U-4-2	21.66	5.70	2.42	TC Ceiling U-8-2	18.71	3.54	3.82

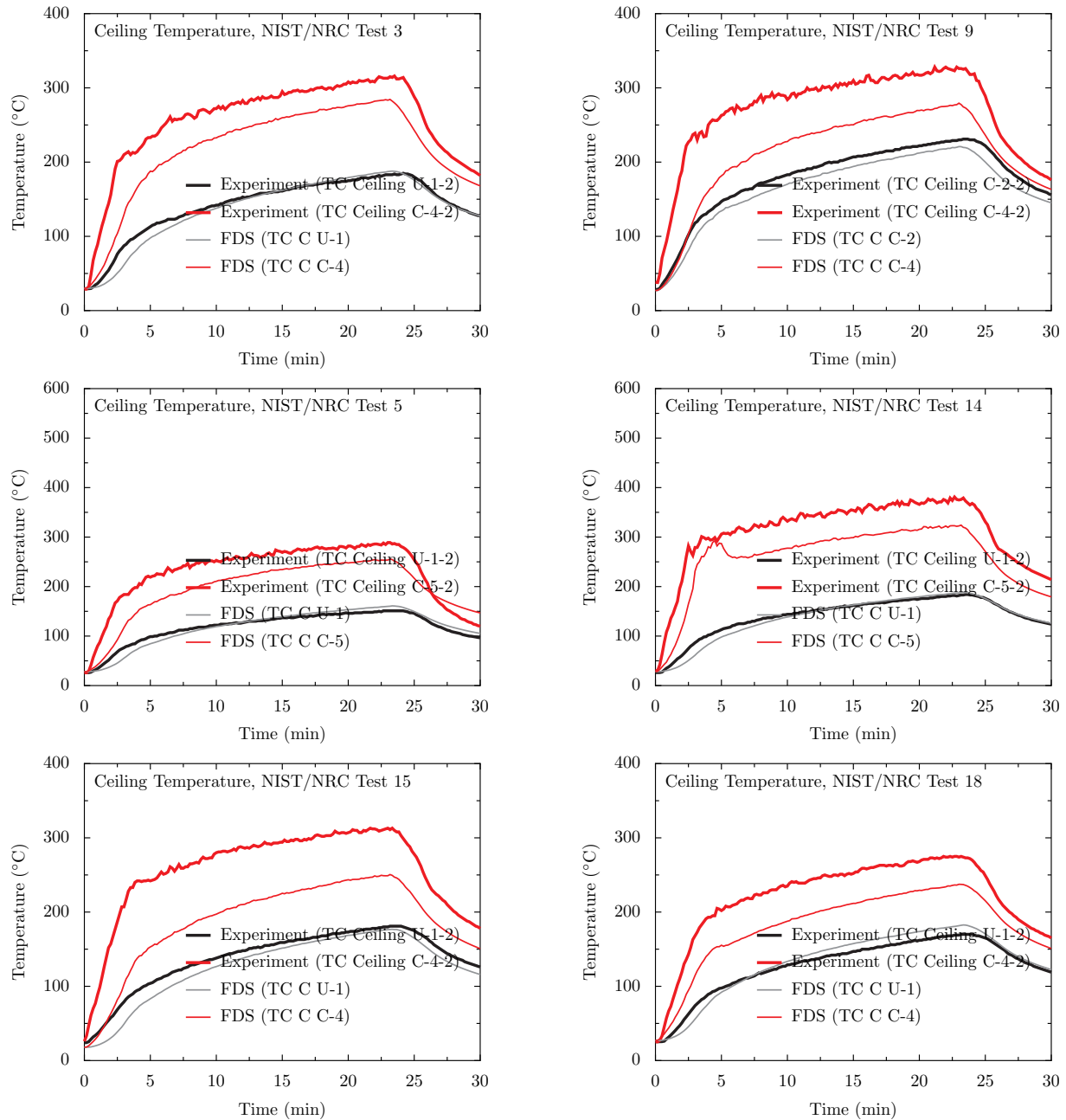


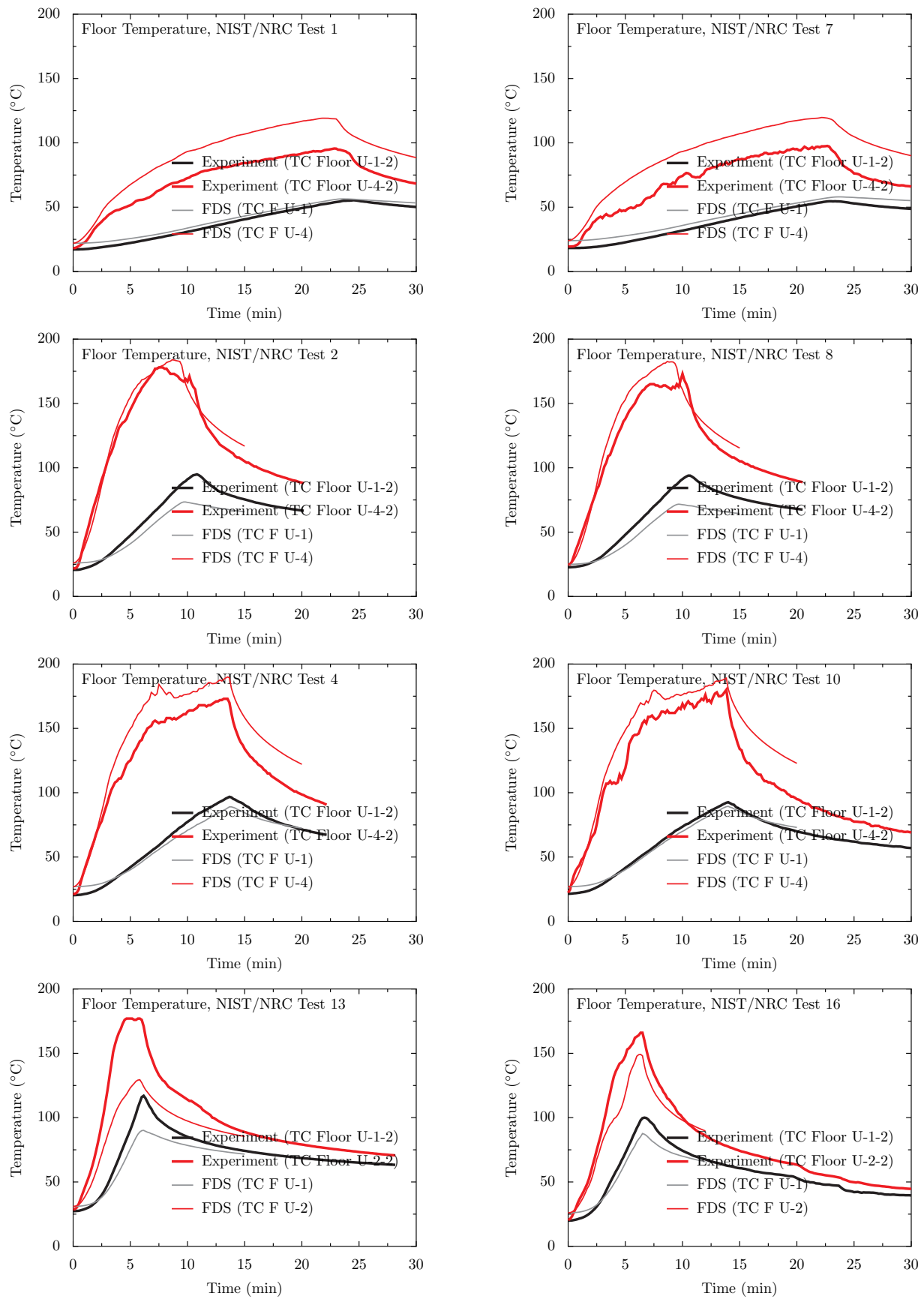


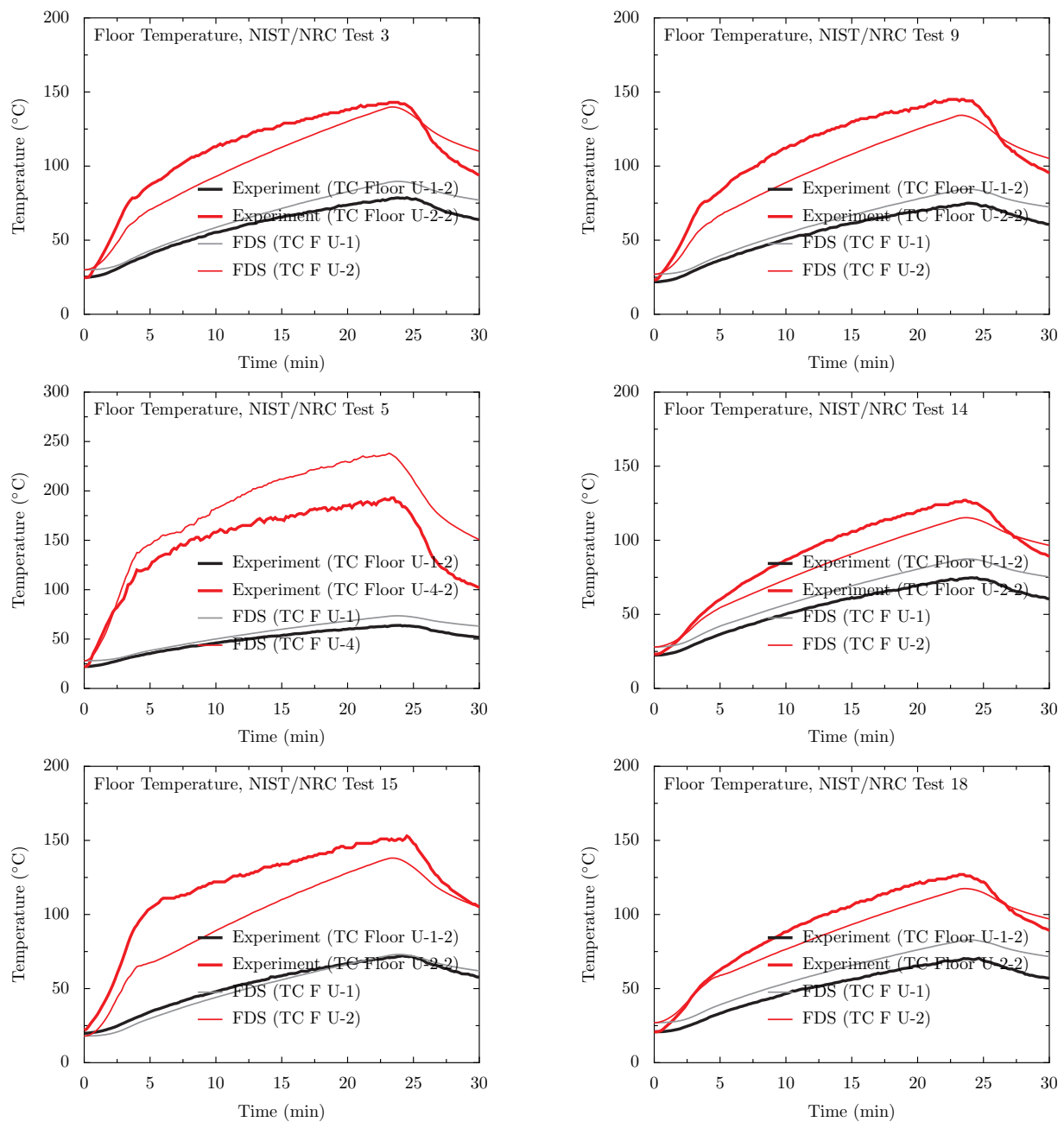












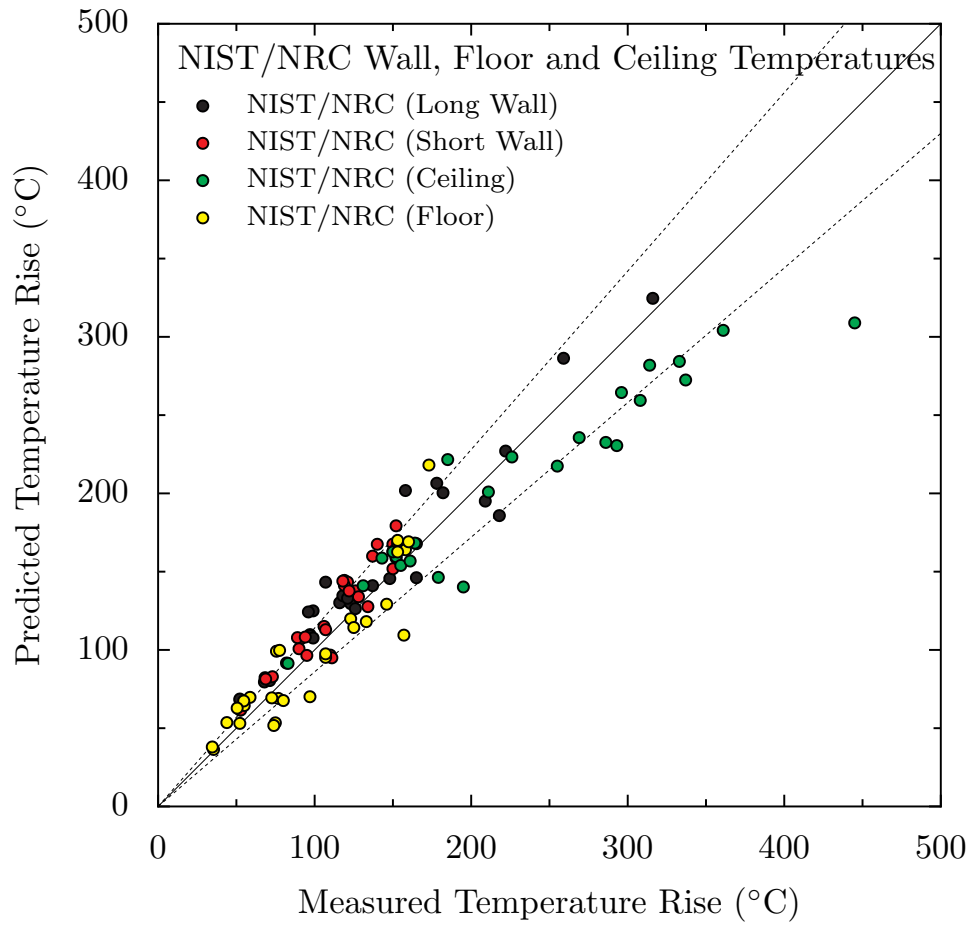


Figure 10.4: Summary of wall, floor and ceiling temperature predictions for the NIST/NRC test series.

Chapter 11

Heat Flux

Radiative heat transfer is included in FDS via the solution of the radiation transport equation for a gray gas, and in some limited cases using a wide band model. The equation is solved using a technique similar to finite volume methods for convective transport, thus the name given to it is the Finite Volume Method (FVM). Using approximately 100 discrete angles, the finite volume solver requires about 20 % of the total CPU time of a calculation, a modest cost given the complexity of radiation heat transfer. The absorption coefficients of the gas-soot mixtures are computed using RADCAL narrow-band model. Liquid droplets can absorb and scatter thermal radiation. This is important in cases involving mist sprinklers, but also plays a role in all sprinkler cases. The absorption and scattering coefficients are based on Mie theory.

This chapter contains a wide variety of heat flux measurements, ranging from less than a kW/m² from very small methane gas burners up to about 150 kW/m² in full-scale compartment fires.

11.1 Hamins Methane Burner Heat Flux Measurements

Predicted and measured radial and vertical heat flux profiles from six experiments conducted by Anthony Hamins at NIST are shown on the following pages. The relevant information about the fires is included in Table 11.1. These are challenging simulations because the neither the gray gas assumption nor the radiative fraction is assumed. Rather, the model is calculating the temperature and species concentrations necessary to predict the radiant energy from the fire.

Table 11.1: Summary of Hamins methane burner experiments.

Case	Test Number	D (m)	\dot{Q} (kW)	\dot{Q}'' (kW/m ²)	Q^*
A	1	0.10	0.42	53.8	0.12
B	5	0.10	1.88	240	0.53
C	23	0.38	33.5	295	0.34
D	21	0.38	175	1550	1.8
E	7	1.0	49.0	62.4	0.044
F	19	1.0	162	206	0.14

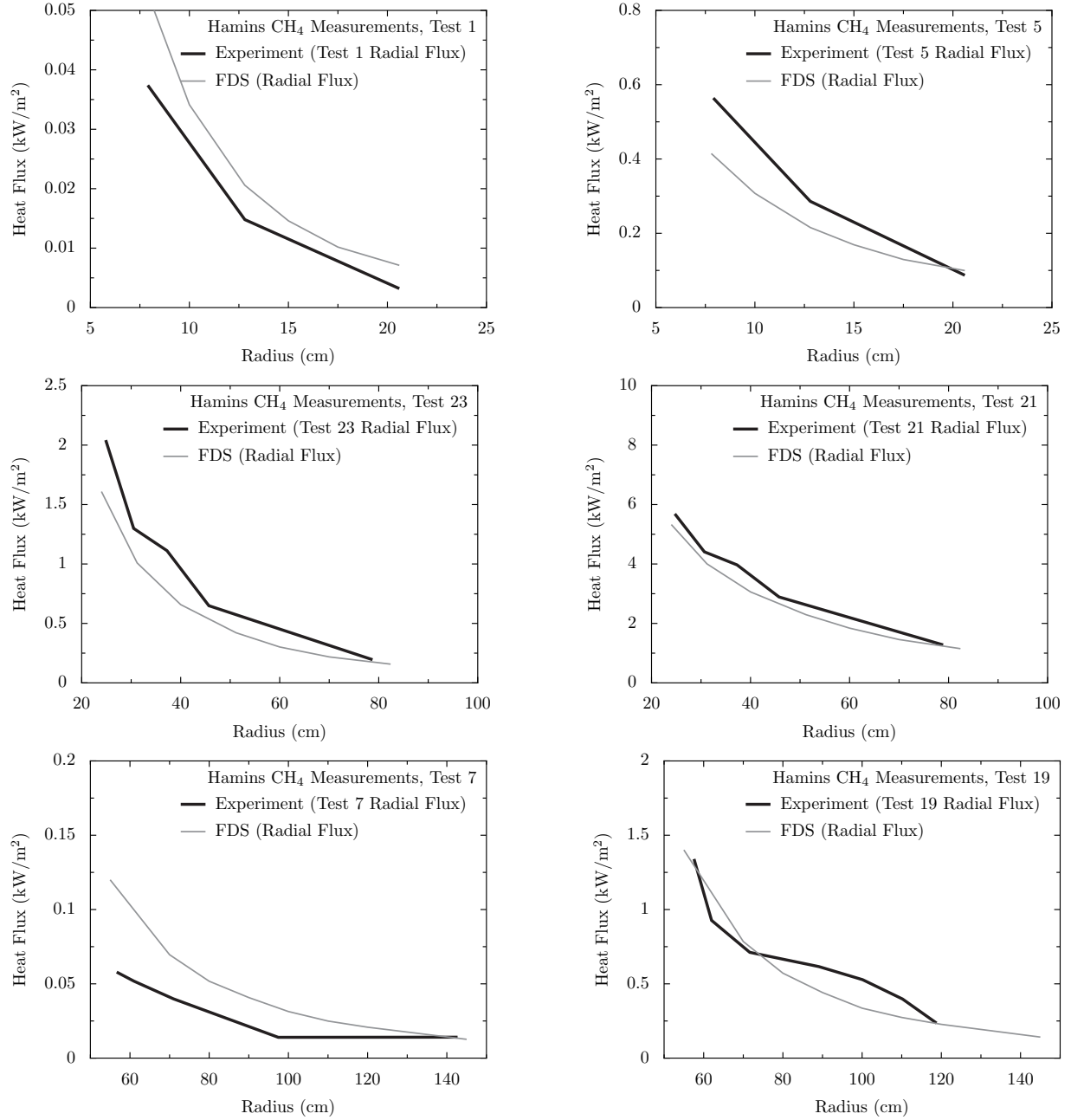


Figure 11.1: Comparison of predicted and measured heat fluxes to the “floor” as a function of radial distance from a methane burner, Hamins experiments.

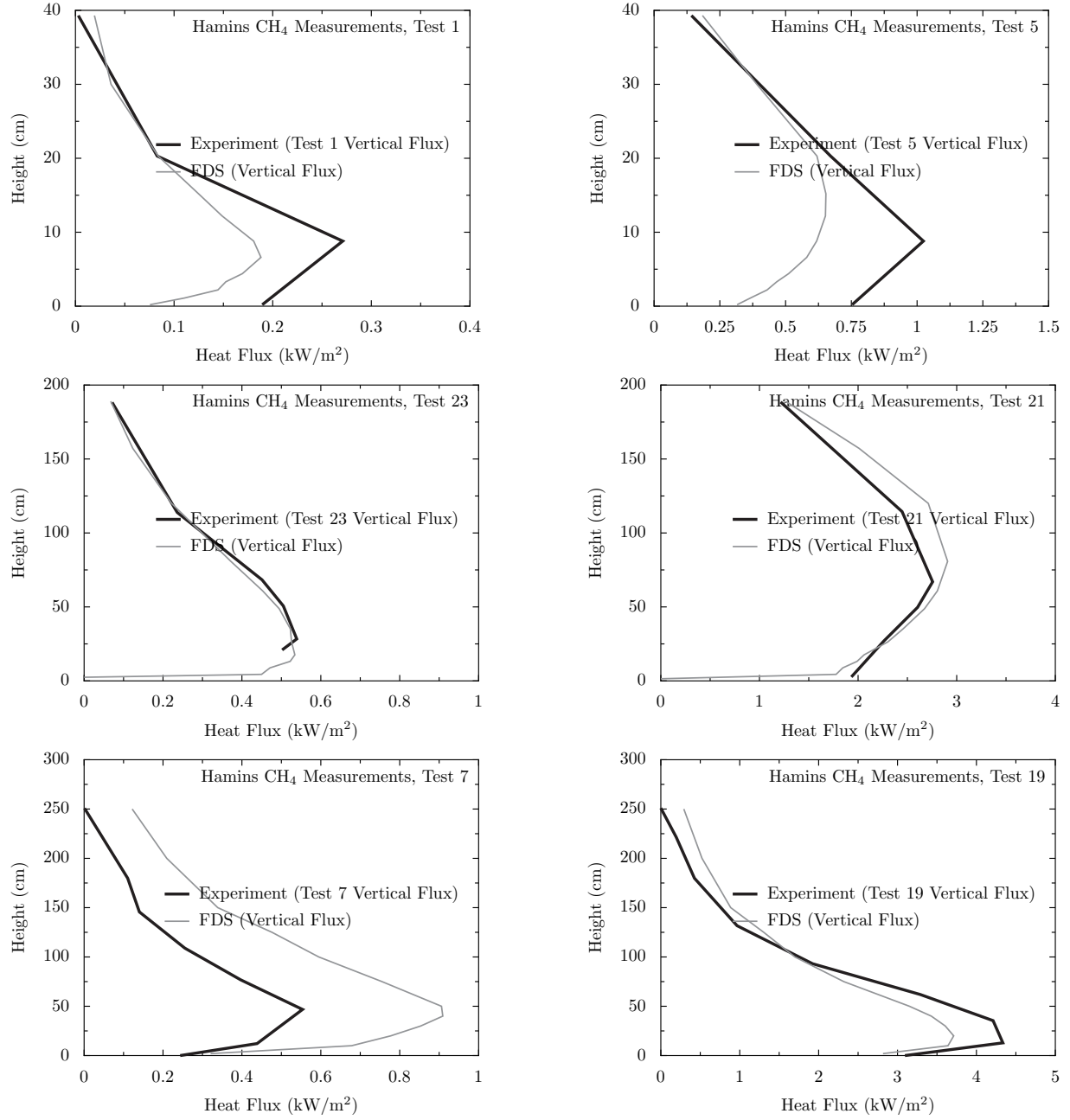


Figure 11.2: Comparison of predicted and measured heat fluxes from a methane burner to a “wall” as a function of the height from the burner surface, Hamins experiments.

11.2 NRL/HAI Wall Heat Flux Measurements

Predicted and measured vertical heat flux profiles from 9 propane sand burner fires are shown on the following pages. The parameters for each experiment are listed in Table 11.2 below. Note that all the FDS simulations were performed with a grid resolution such that $D^*/\delta x = 10$.

Table 11.2: Summary of the NRL/HAI Wall Heat Flux Measurements.

Test Number	D (m)	D^* (m)	\dot{Q} (kW)	Q^*	Observed Flame Height (m)
1	0.28	0.30	53	0.85	0.79
2	0.70	0.30	56	0.09	0.36
3	0.48	0.33	68	0.28	0.60
4	0.37	0.39	106	0.84	1.00
5	0.48	0.43	136	0.57	0.87
6	0.48	0.51	204	0.85	1.45
7	0.70	0.52	220	0.36	1.20
8	0.57	0.60	313	0.85	2.20
9	0.70	0.74	523	0.85	2.9 (based on 500 °C)

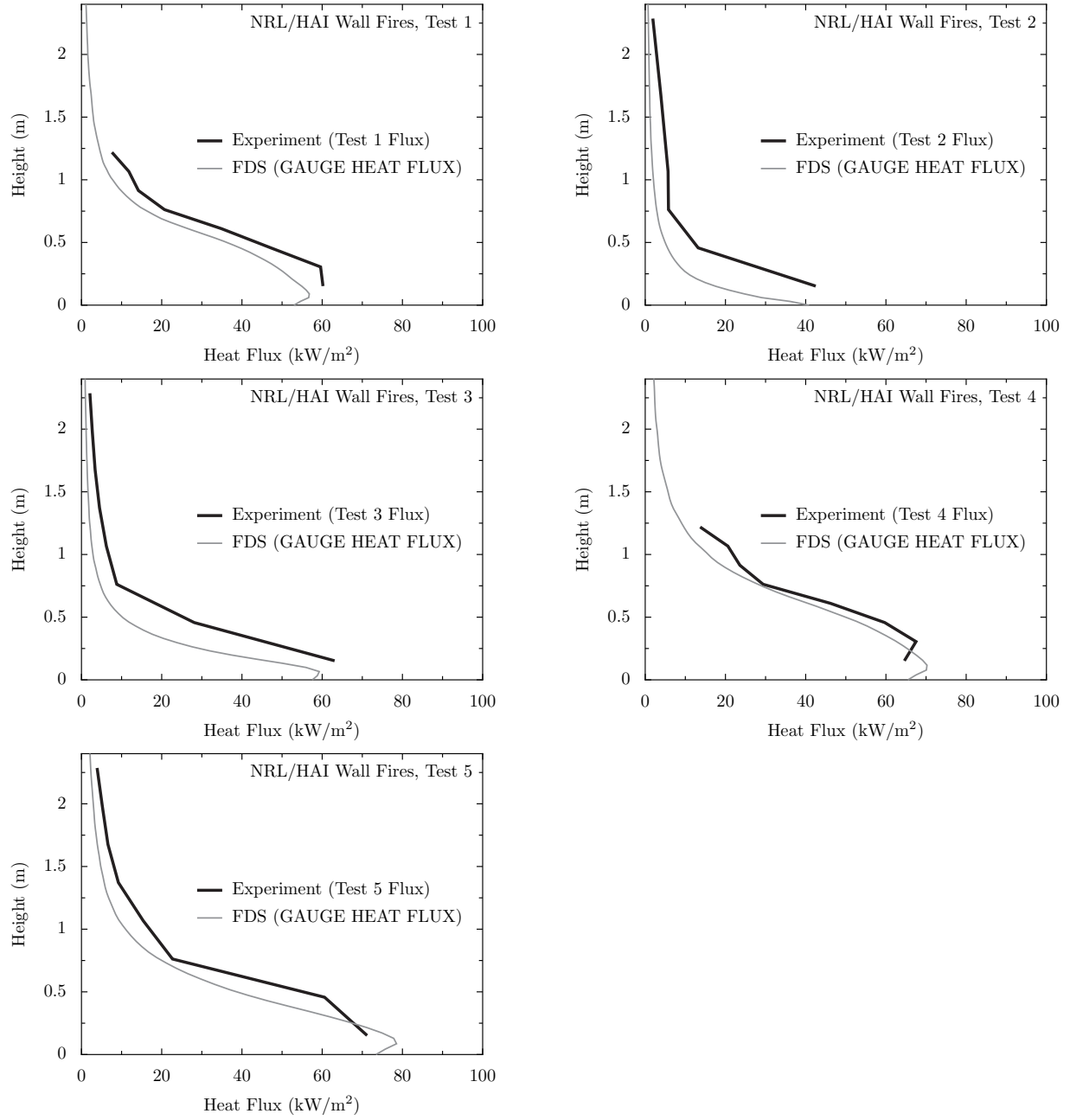


Figure 11.3: Comparison of predicted and measured heat fluxes to the wall from an adjacent propane sand burner, NRL/HAI experiments.

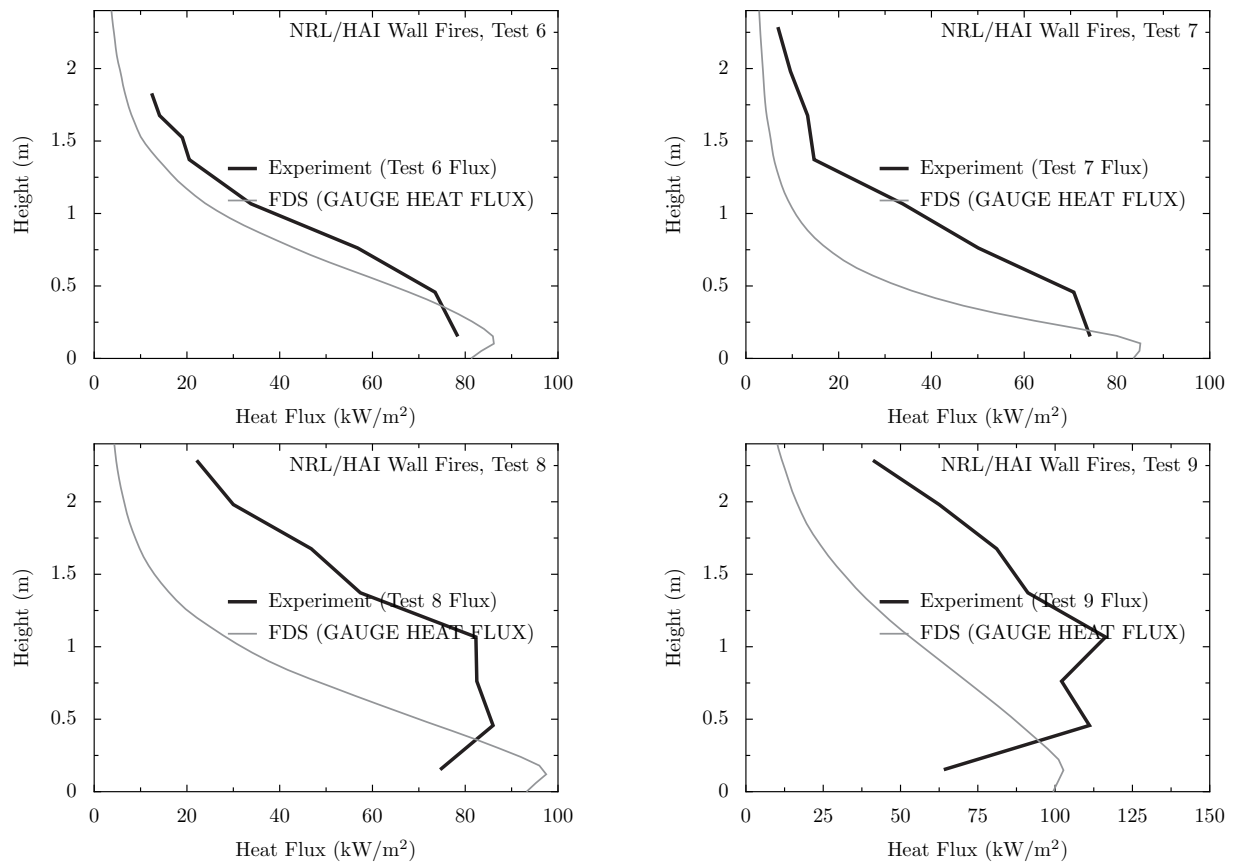


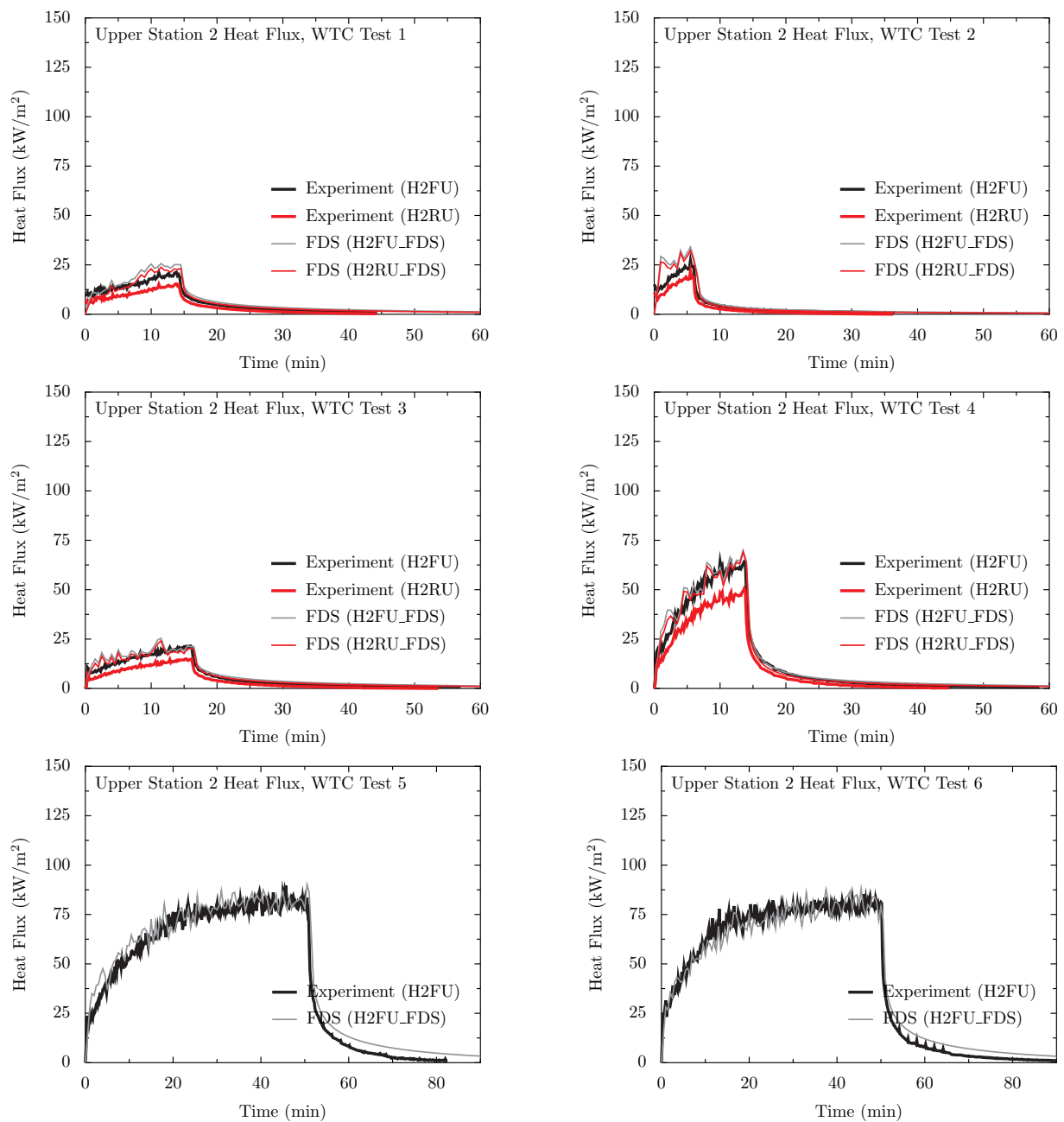
Figure 11.4: Comparison of predicted and measured heat fluxes to the wall from an adjacent propane sand burner, NRL/HAI experiments.

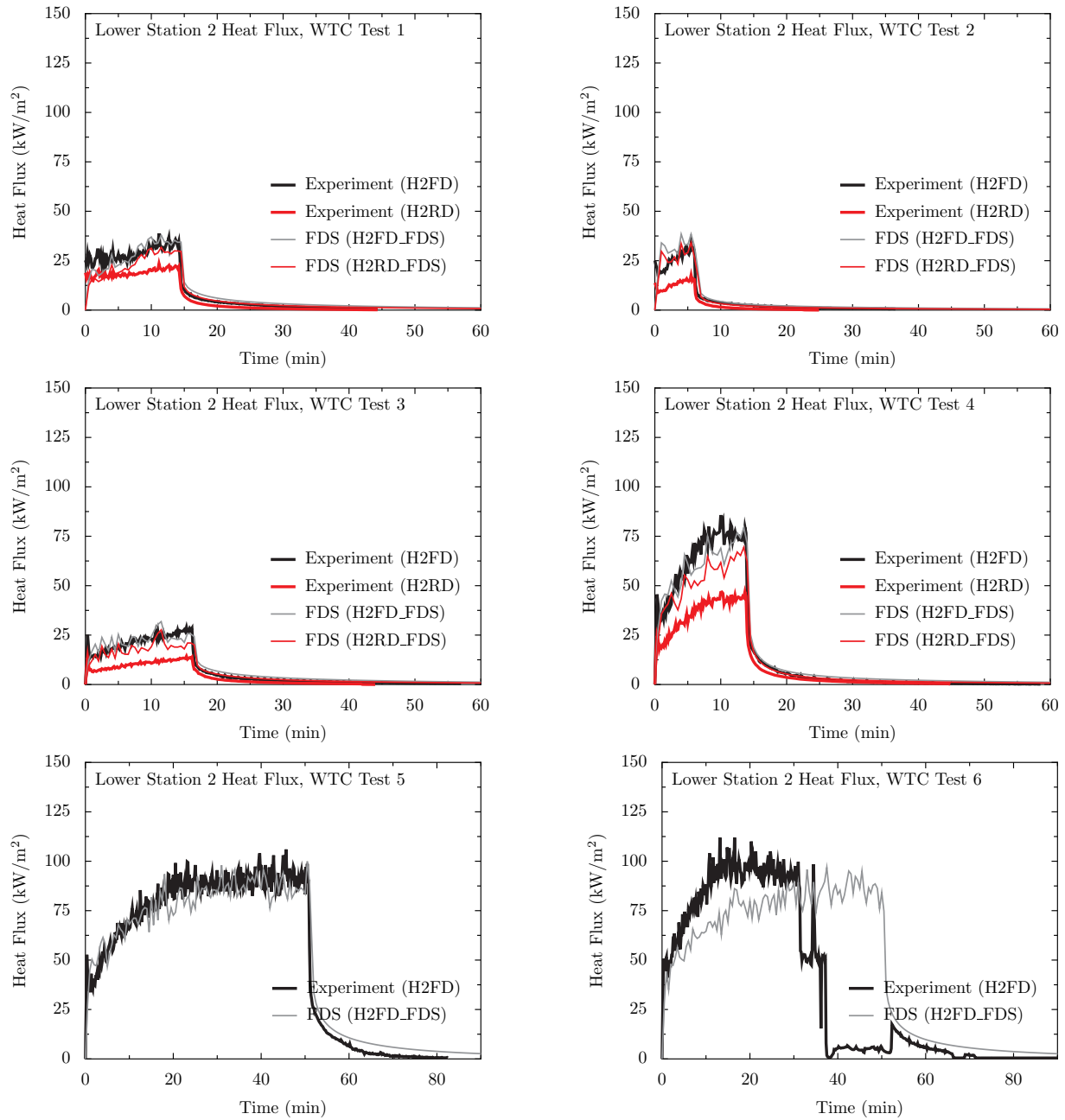
11.3 WTC Heat Flux Measurements

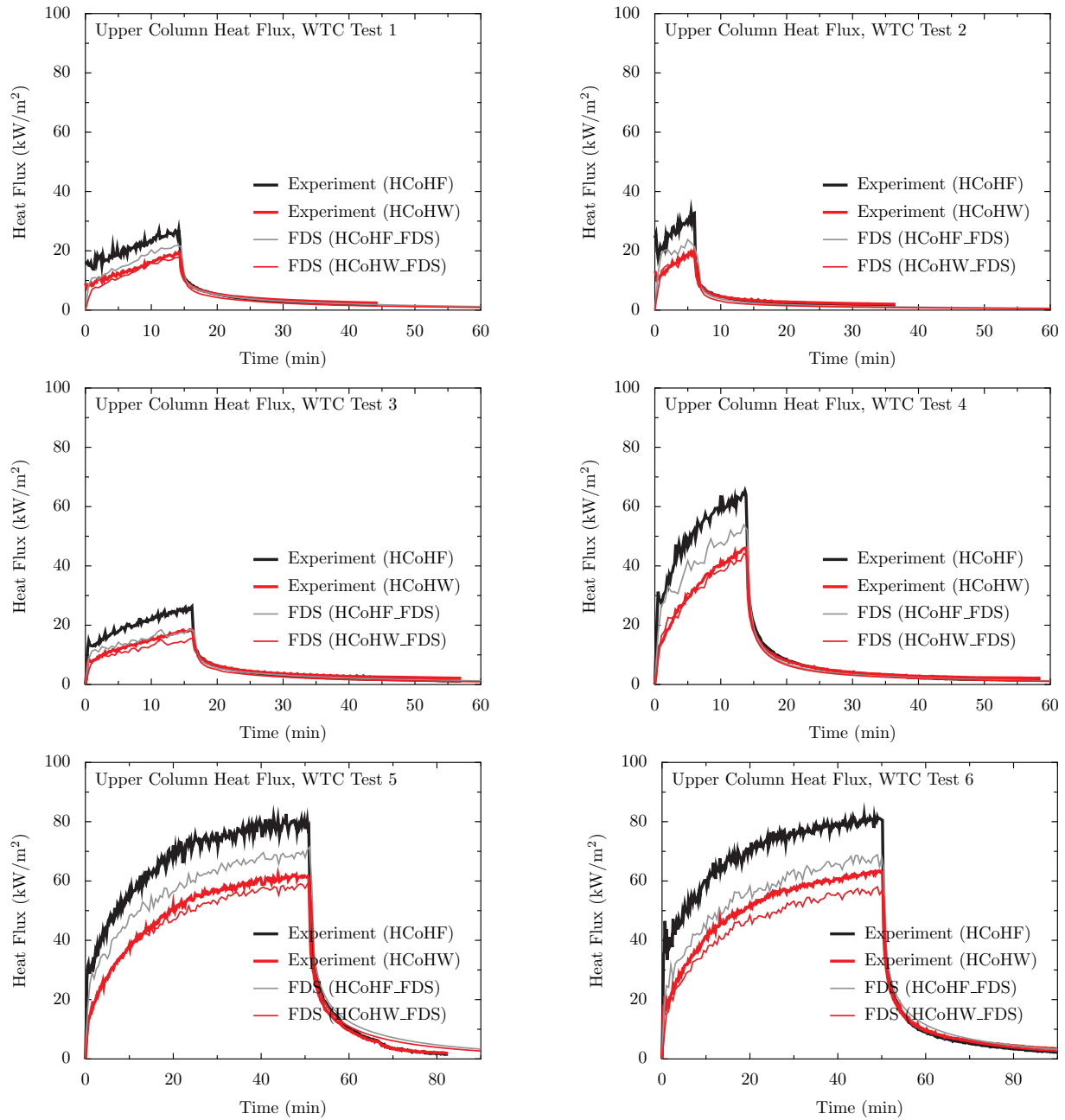
There were a variety of heat flux gauges installed in the test compartment. Most were within 2 m of the fire. Their locations and orientations are listed in Table 11.3.

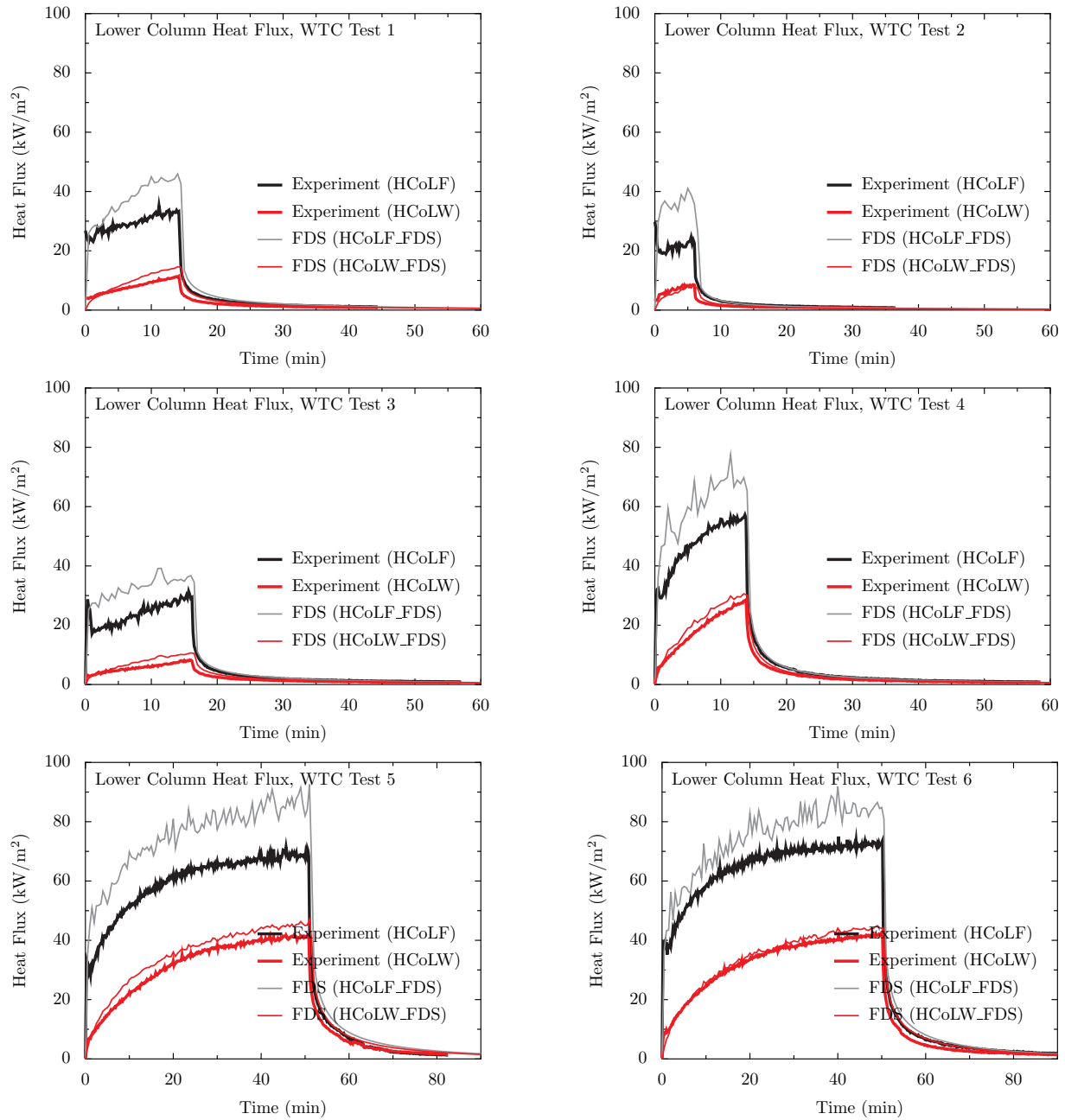
Table 11.3: Heat flux gauge positions relative to the center of the fire pan in the WTC series.

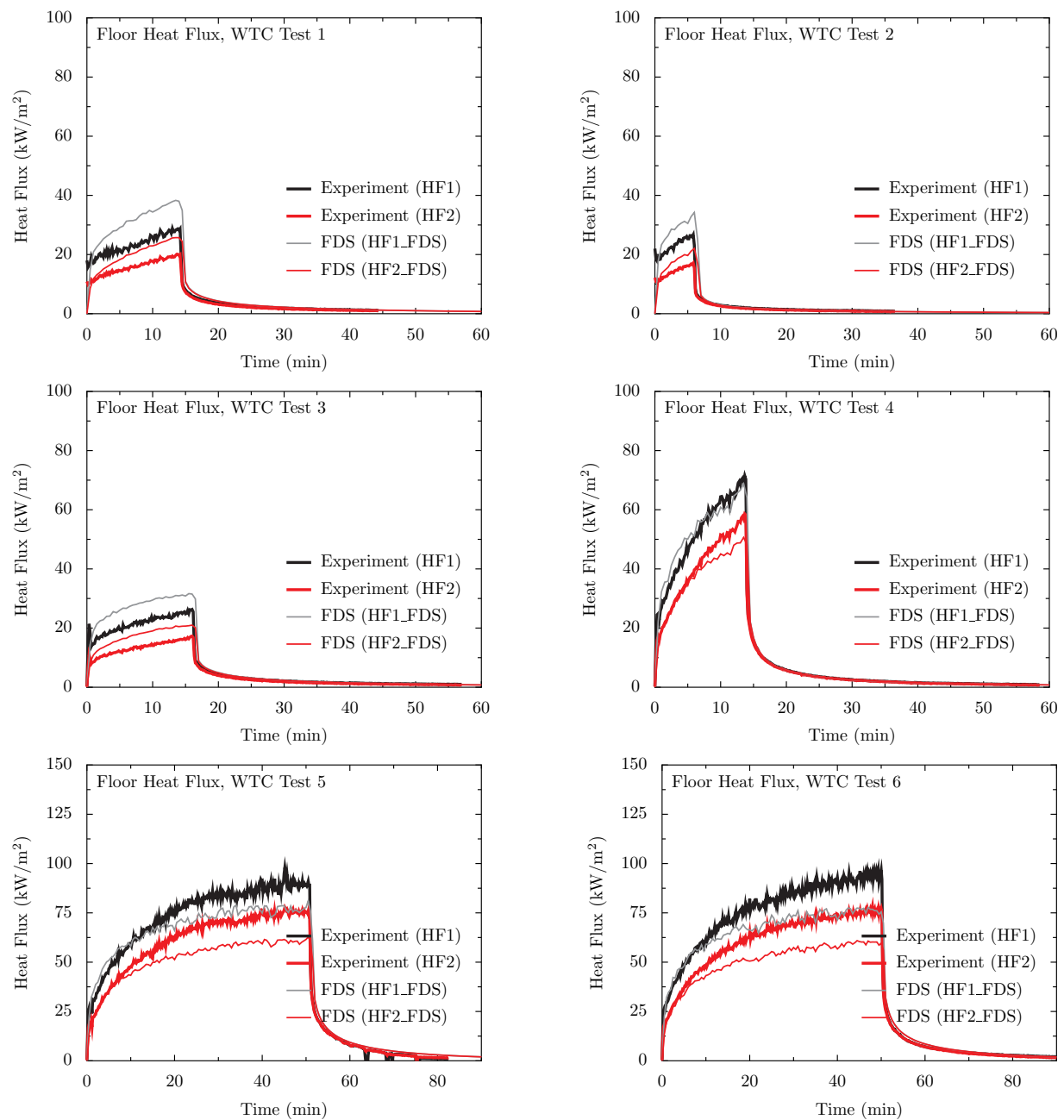
Name	x (m)	y (m)	z (m)	Orientation	Location
H2FU	0.64	0.63	3.30	+z	Truss Support
H2RU	0.64	0.51	3.30	+z	Truss Support
H2FD	0.64	0.30	3.15	-z	Truss Support
H2RD	0.64	0.42	3.15	-z	Truss Support
HCoHF	-0.90	0.84	3.46	+x	Column, facing fire
HCoHW	-0.97	0.92	3.27	+y	Column, facing north
HCoLF	-0.90	0.84	0.92	+x	Column, facing fire
HCoLW	-0.97	0.92	1.02	+y	Column, facing north
HF1	1.06	0.13	0.13	+z	Floor
HF2	1.56	0.10	0.13	+z	Floor
HCe1	-0.45	0.35	3.82	-z	Ceiling
HCe2	0.05	0.35	3.82	-z	Ceiling
HCe3	0.80	0.35	3.82	-z	Ceiling
HCe4	2.56	0.35	3.82	-z	Ceiling

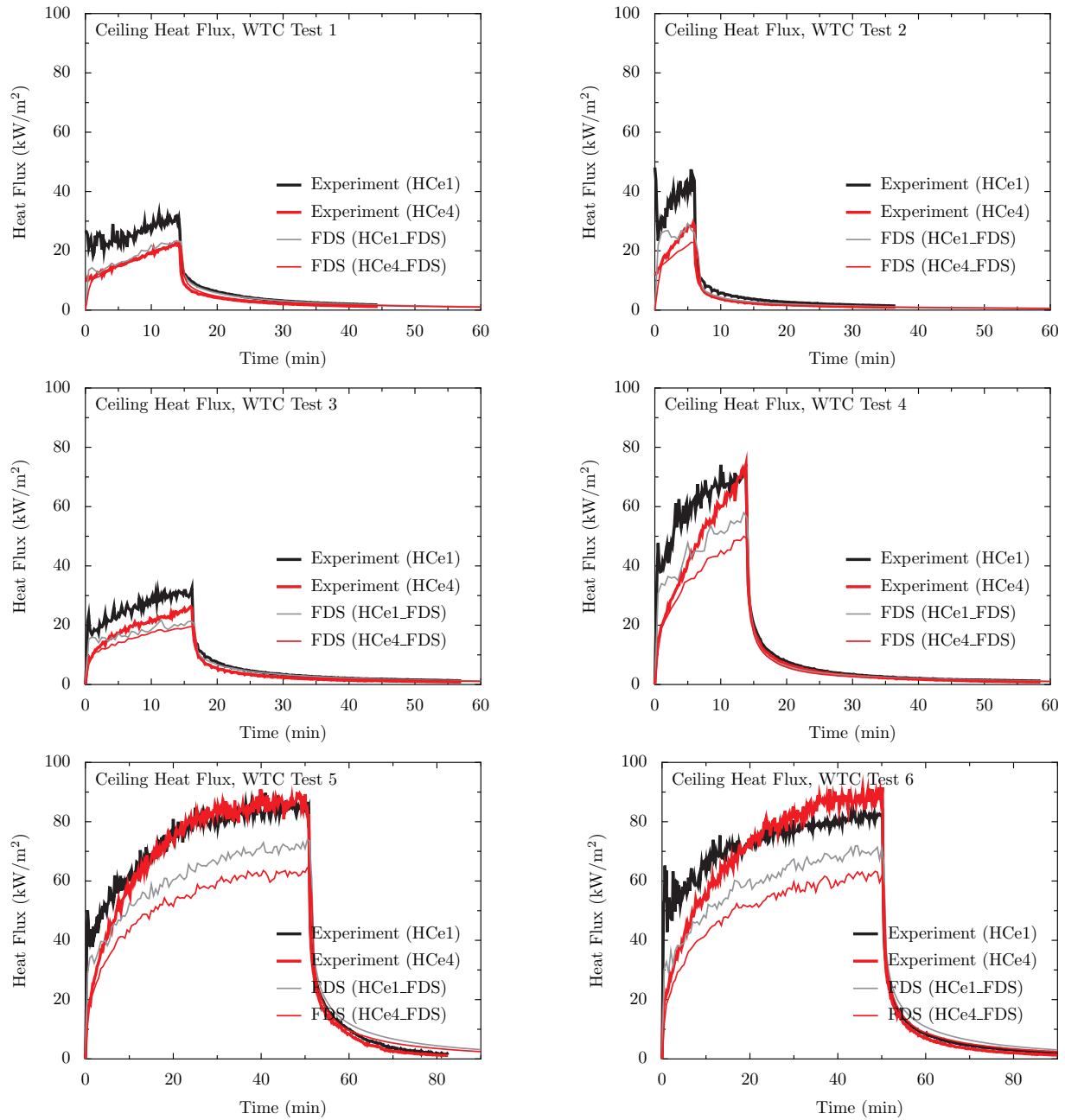


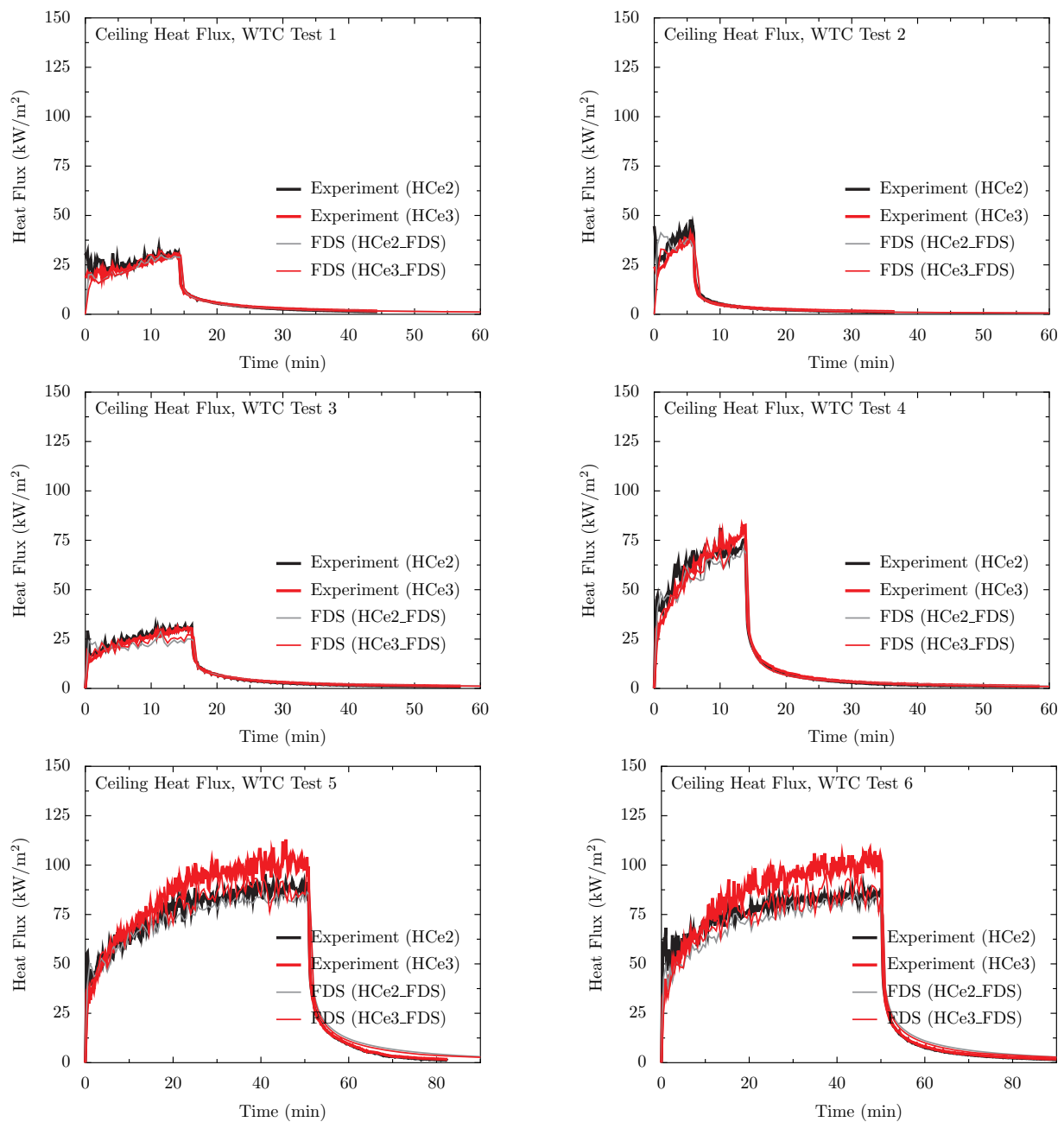












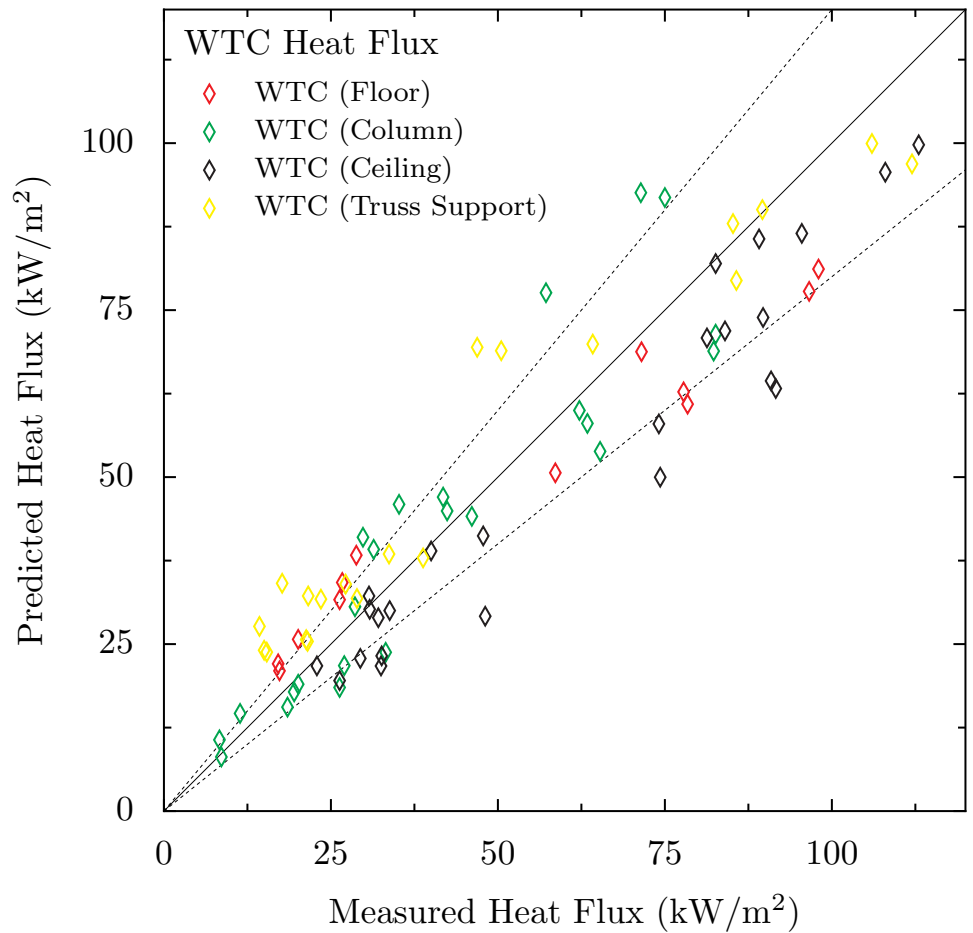
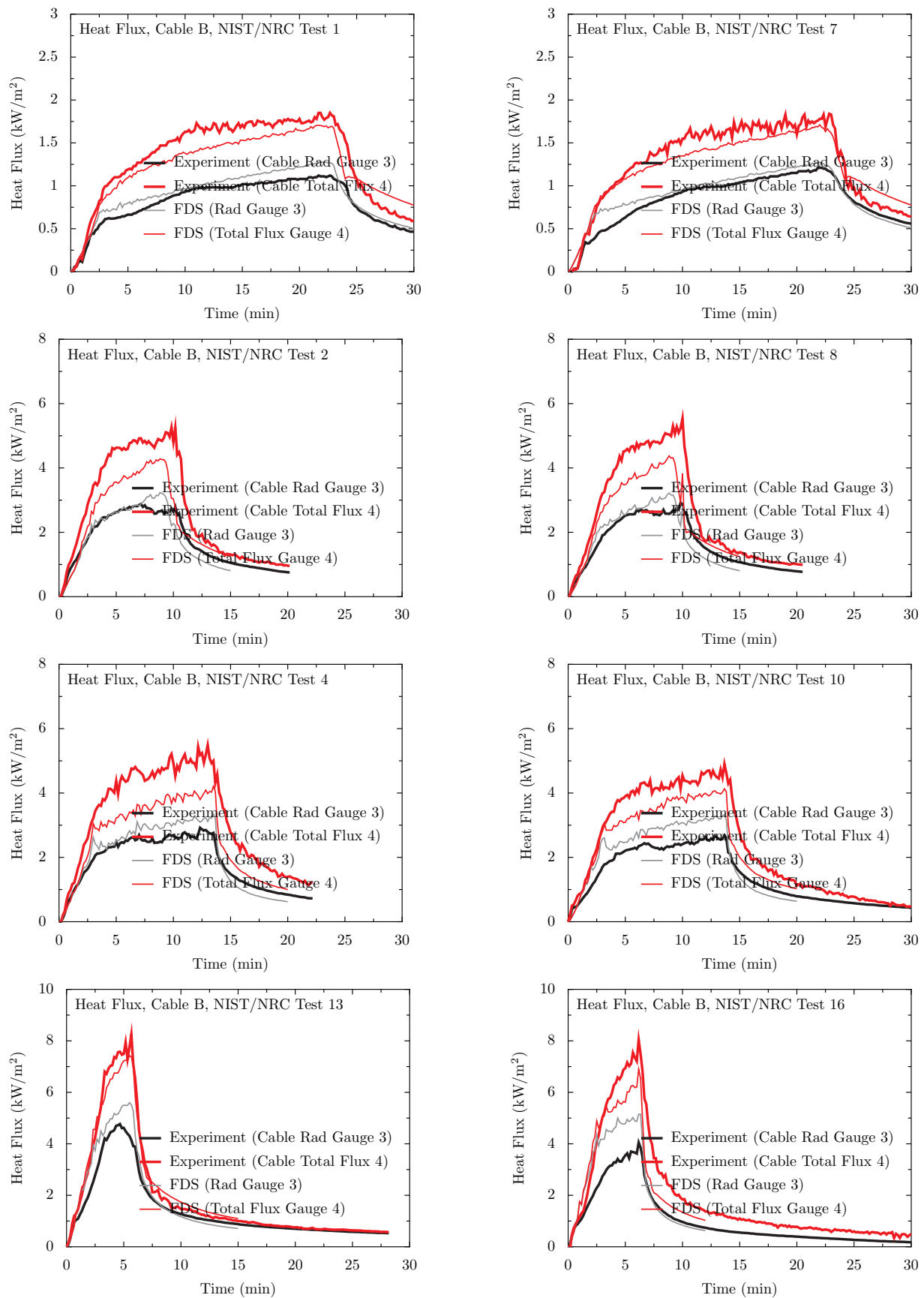
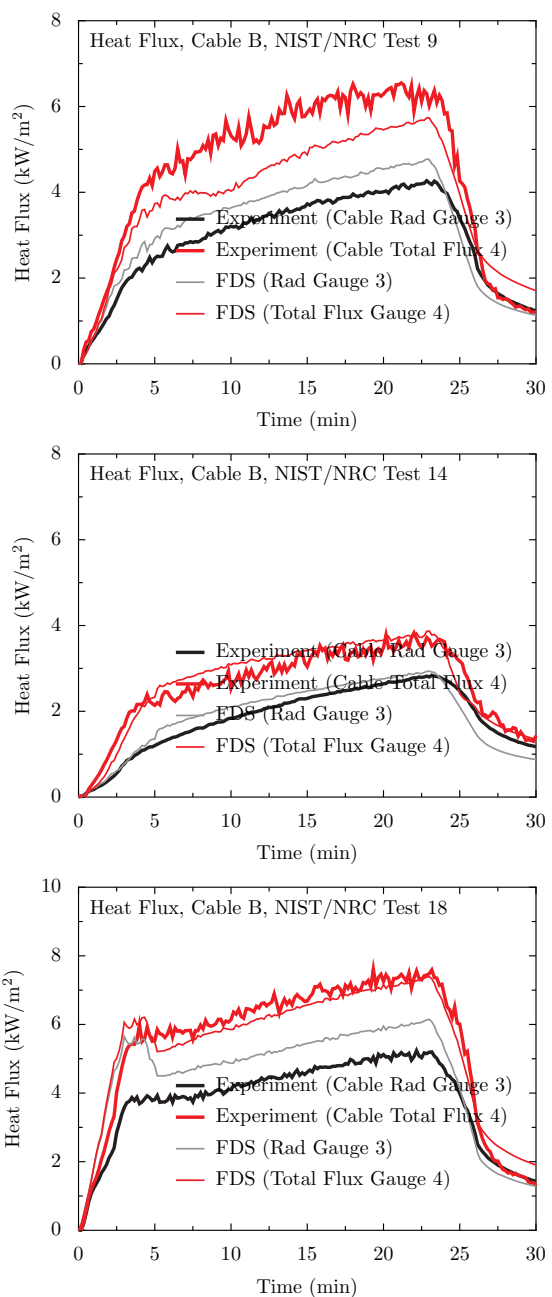
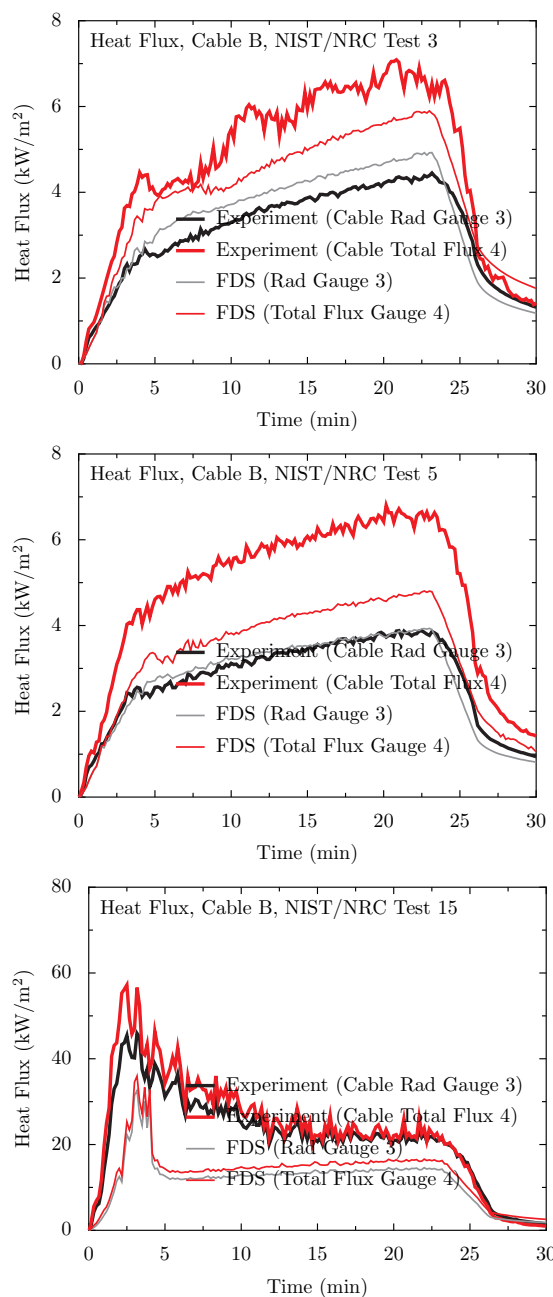


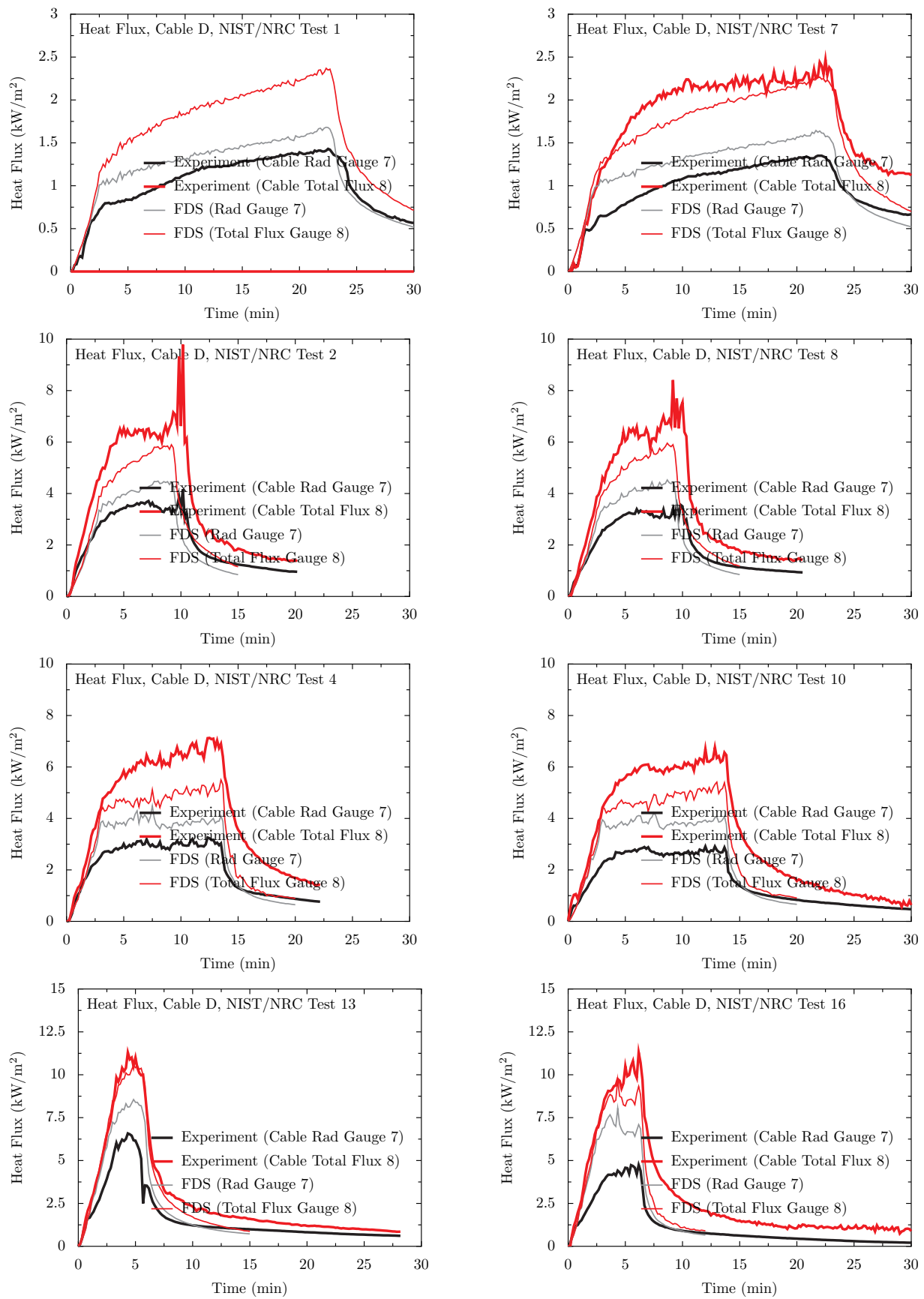
Figure 11.5: Summary of heat flux predictions for the WTC test series.

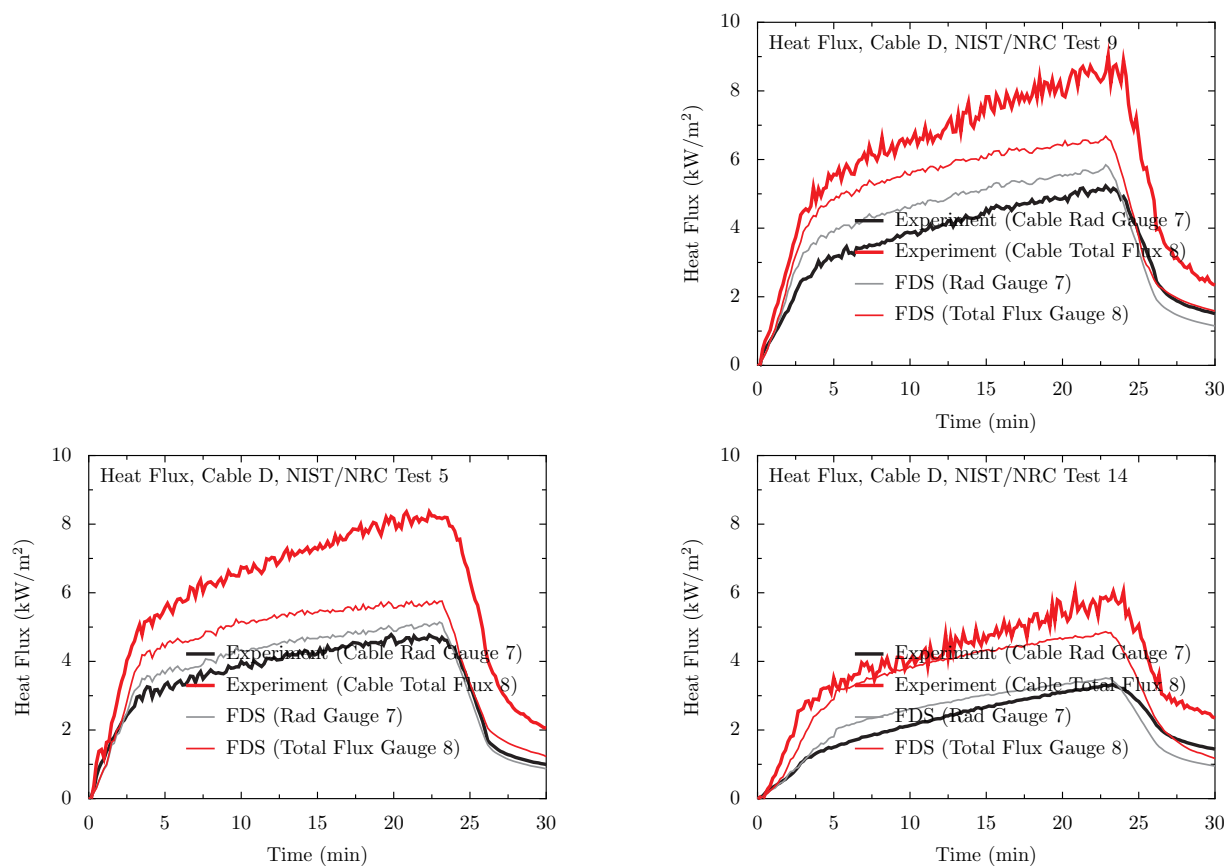
11.4 NIST/NRC Test Series, Heat Flux to Cables

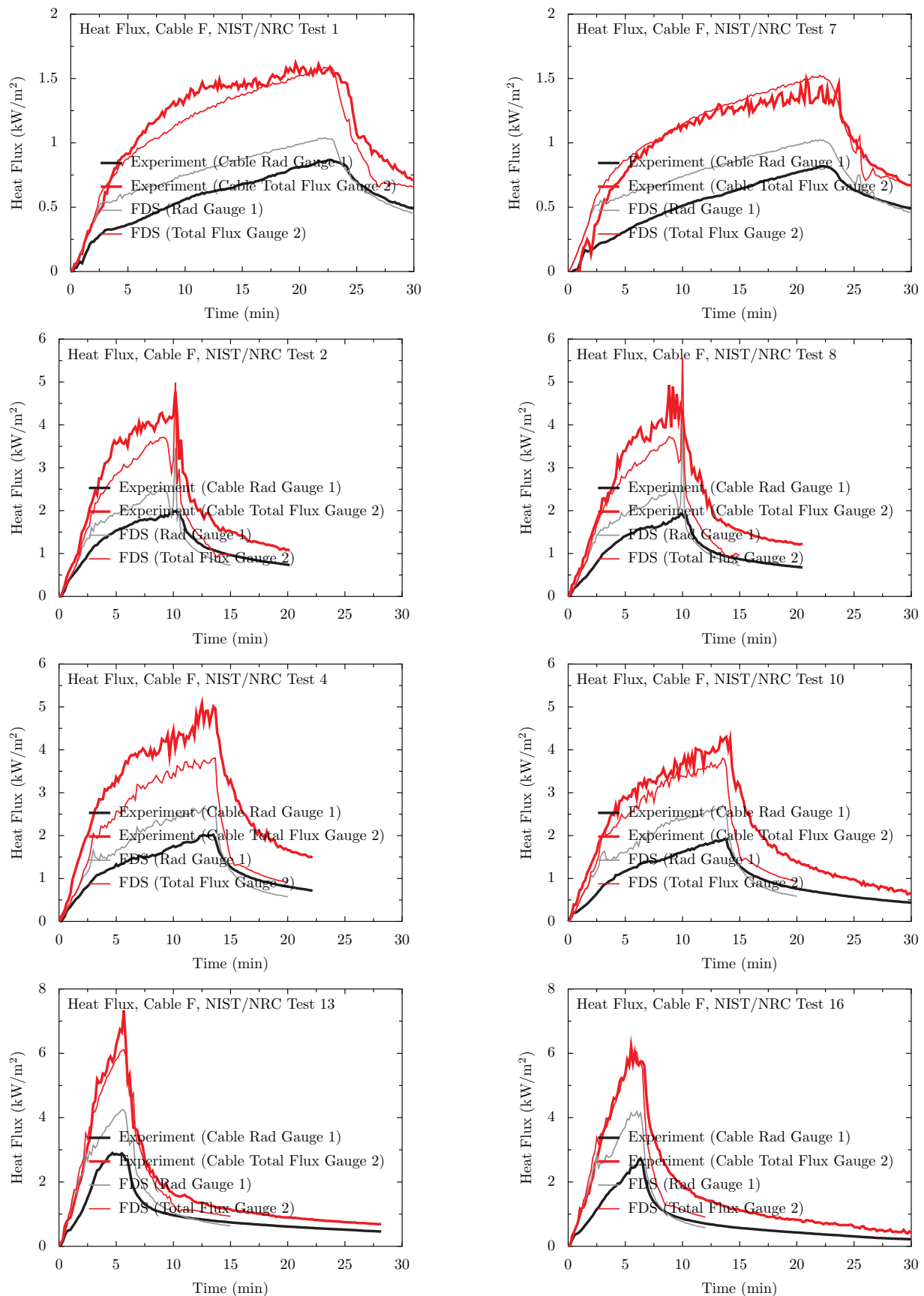
Cables in various types (power and control), and configurations (horizontal, vertical, in trays or free-hanging), were installed in the test compartment. For each of the four cable targets considered, measurements of the radiative and total heat flux were made with gauges positioned near the cables themselves. The following pages display comparisons of these heat flux predictions and measurements for Control Cable B, Horizontal Cable Tray D, Power Cable F and Vertical Cable Tray G.

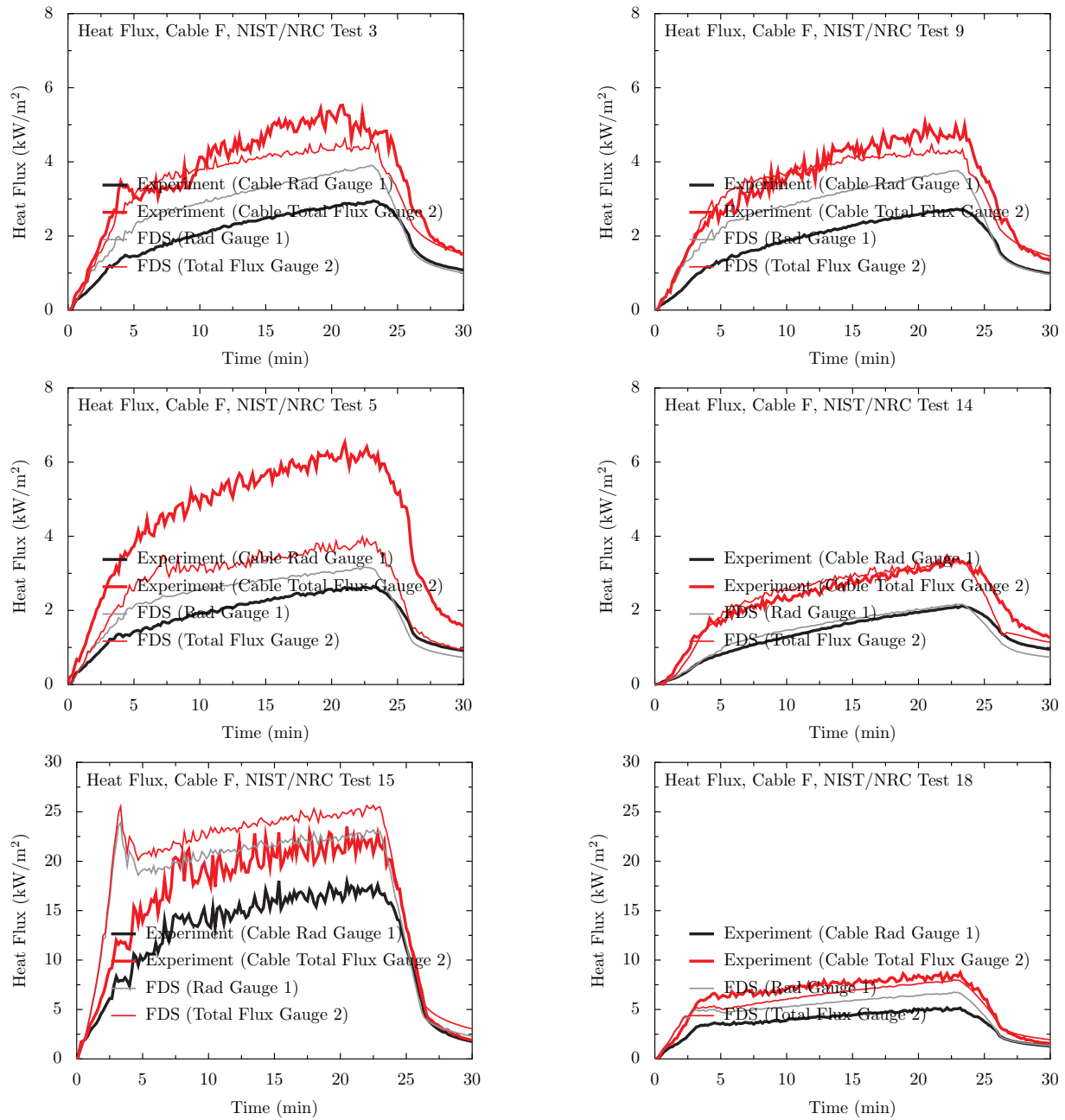


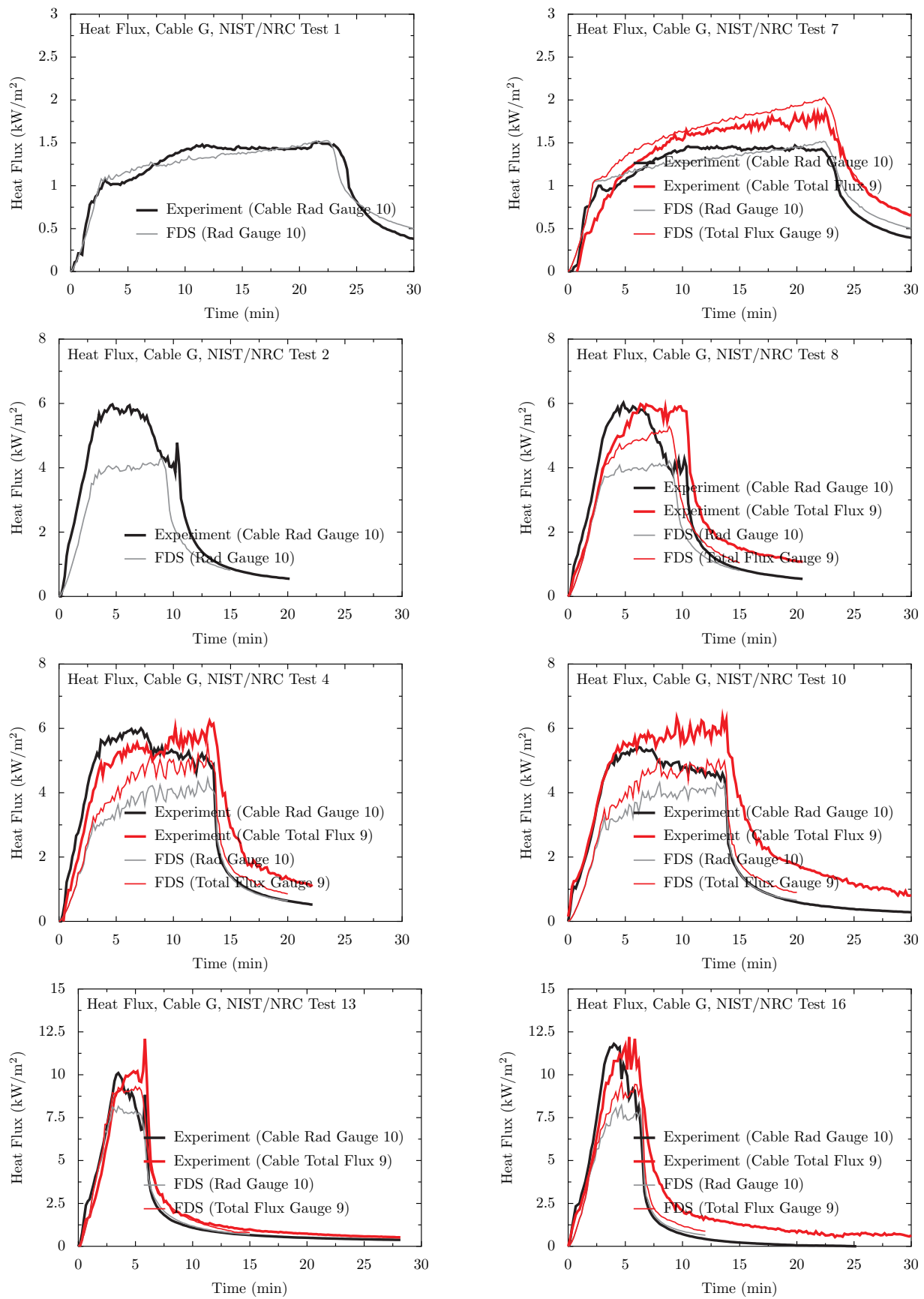


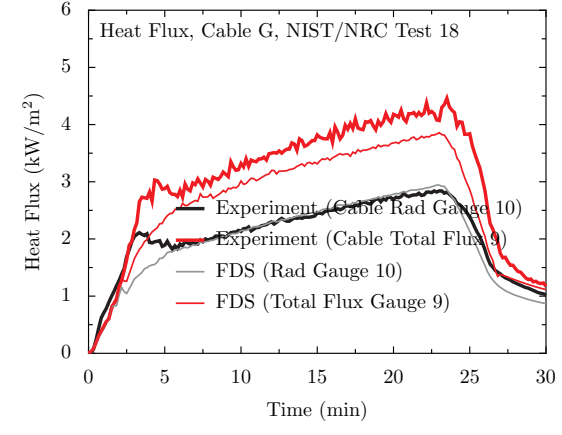
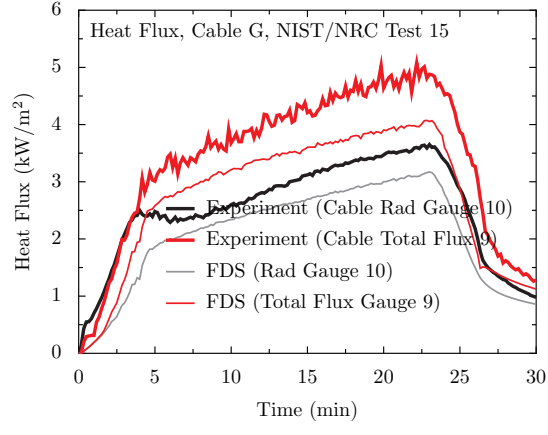
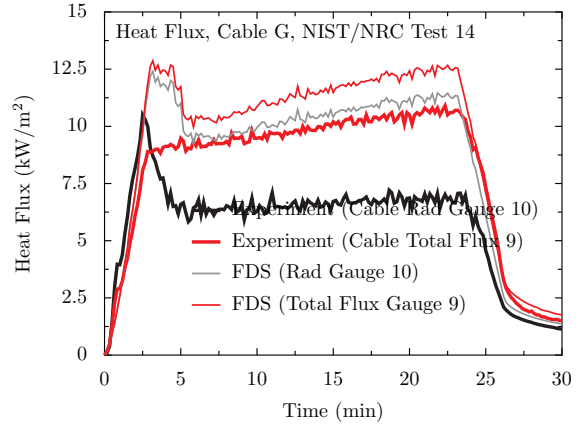
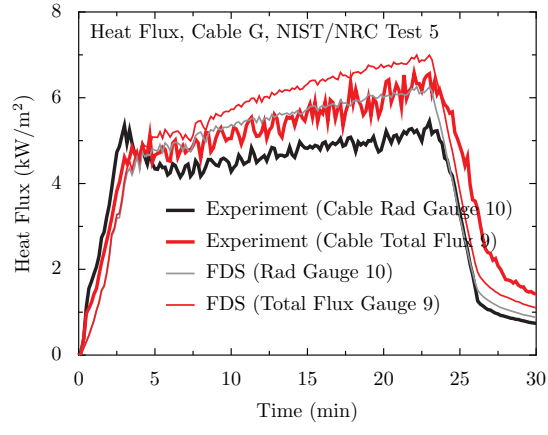
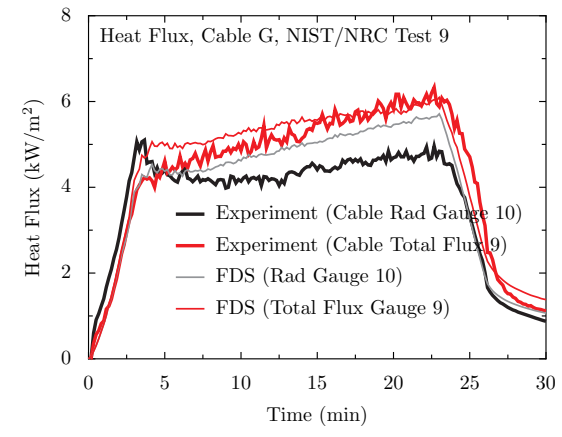
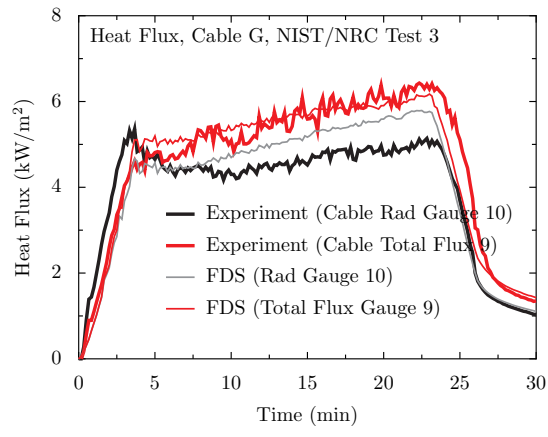












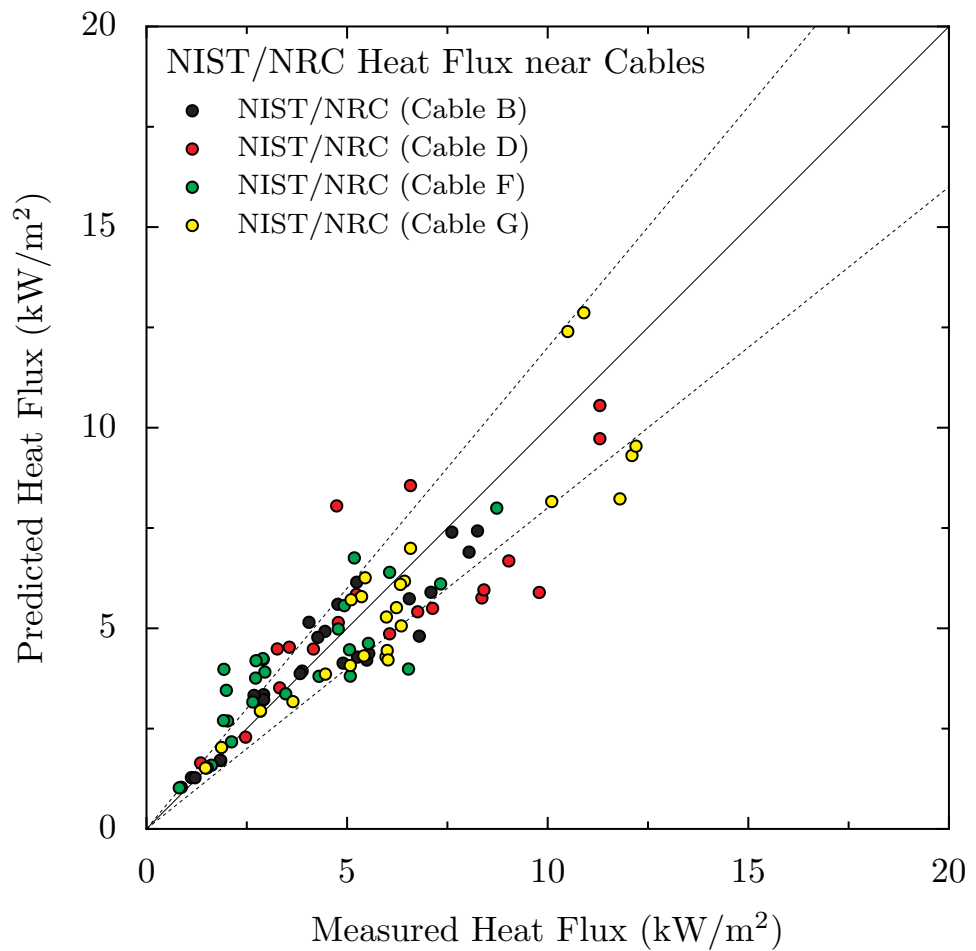


Figure 11.6: Summary of heat flux predictions to the cables in the NIST/NRC test series.

Bibliography

- [1] K.B. McGrattan, B.W. Klein, S. Hostikka, and J.E. Floyd. Fire Dynamics Simulator (Version 5), User's Guide. NIST Special Publication 1019-5, National Institute of Standards and Technology, Gaithersburg, Maryland, October 2007. [i](#)
- [2] American Society for Testing and Materials, West Conshohocken, Pennsylvania. *ASTM E 1355-04, Standard Guide for Evaluating the Predictive Capabilities of Deterministic Fire Models*, 2004. [i](#), [1](#)
- [3] R.G. Rehm and H.R. Baum. The Equations of Motion for Thermally Driven, Buoyant Flows. *Journal of Research of the NBS*, 83:297–308, 1978. [5](#)
- [4] H.R. Baum, R.G. Rehm, P.D. Barnett, and D.M. Corley. Finite Difference Calculations of Buoyant Convection in an Enclosure, Part I: The Basic Algorithm. *SIAM Journal of Scientific and Statistical Computing*, 4(1):117–135, March 1983. [5](#)
- [5] R.G. Rehm, P.D. Barnett, H.R. Baum, and D.M. Corley. Finite Difference Calculations of Buoyant Convection in an Enclosure: Verification of the Nonlinear Algorithm. *Applied Numerical Mathematics*, 1:515–529, 1985. [5](#)
- [6] R.G. Rehm, H.R. Baum, D.W. Lozier, H. Tang, and J. Sims. Buoyant Convection in an Inclined Enclosure. In *Fire Safety Science – Proceedings of the Third International Symposium*, pages 313–323. International Association for Fire Safety Science, 1991. [5](#)
- [7] H.R. Baum, O.A. Ezekoye, K.B. McGrattan, and R.G. Rehm. Mathematical Modeling and Computer Simulation of Fire Phenomenon. *Theoretical and Computational Fluid Dynamics*, 6:125–139, 1994. [5](#)
- [8] K.B. McGrattan, R.G. Rehm, and H.R. Baum. Fire-Driven Flows in Enclosures. *Journal of Computational Physics*, 110(2):285–291, 1994. [5](#)
- [9] R.G. Rehm, K.B. McGrattan, H.R. Baum, and K.W. Cassel. Transport by Gravity Currents in Building Fires. In *Fire Safety Science – Proceedings of the Fifth International Symposium*, pages 391–402. International Association for Fire Safety Science, 1997. [5](#)
- [10] H.R. Baum, K.B. McGrattan, and R.G. Rehm. Three Dimensional Simulations of Fire Plume Dynamics. In *Fire Safety Science – Proceedings of the Fifth International Symposium*, pages 511–522. International Association for Fire Safety Science, 1997. [5](#)
- [11] H.R. Baum, K.B. McGrattan, and R.G. Rehm. Large Eddy Simulations of Smoke Movement in Three Dimensions. In *Proceedings of the Seventh International Interflam Conference*, pages 189–198. Interscience Communications, London, 1996. [5](#)

- [12] H.R. Baum and B.J. McCaffrey. Fire Induced Flow Field – Theory and Experiment. In *Fire Safety Science – Proceedings of the Second International Symposium*, pages 129–148. International Association for Fire Safety Science, 1989. [5](#)
- [13] H.R. Baum, K.B. McGrattan, and R.G. Rehm. Three Dimensional Simulations of Fire Plume Dynamics. *Journal of the Heat Transfer Society of Japan*, 35(139):45–52, 1997. [5](#)
- [14] J.M. Clement and C.M. Fleischmann. Experimental Verification of the Fire Dynamics Simulator Hydrodynamic Model. In *Fire Safety Science – Proceedings of the Seventh International Symposium*, pages 839–862. International Association for Fire Safety Science, 2002. [5](#)
- [15] K.B. McGrattan, H.R. Baum, and R.G. Rehm. Large Eddy Simulations of Smoke Movement. *Fire Safety Journal*, 30:161–178, 1998. [5](#)
- [16] W. Mell, K.B. McGrattan, and H. Baum. Numerical Simulation of Combustion in Fire Plumes. In *Twenty-Sixth Symposium (International) on Combustion*, pages 1523–1530. Combustion Institute, Pittsburgh, Pennsylvania, 1996. [5](#)
- [17] T. Cleary, M. Anderson, J. Averill, and W. Grosshandler. Evaluating Multi-Sensor Fire Detectors in the Fire Emulator/Detector Evaluator. In *Proceedings of the Eighth International Interflam Conference*, pages 453–464. Interscience Communications, June 1999. [5](#)
- [18] W. Davis, K Notarianni, and K. McGrattan. Comparison of Fire Model Predictions with Experiments Conducted in a Hangar with a 15 Meter Ceiling. NISTIR 5927, National Institute of Standards and Technology, Gaithersburg, Maryland, December 1996. [6](#)
- [19] S.J. Emmerich and K.B. McGrattan. Application of a Large Eddy Simulation Model to Study Room Airflow. *ASHRAE Transactions*, 104(1):1–9, 1998. [6](#)
- [20] S.J. Emmerich. Use of Computational Fluid Dynamics to Analyze Indoor Air Quality Issues. NISTIR 5997, National Institute of Standards and Technology, Gaithersburg, Maryland, April 1997. [6](#)
- [21] K.B. McGrattan, H.R. Baum, and R.G. Rehm. Numerical Simulation of Smoke Plumes from Large Oil Fires. *Atmospheric Environment*, 30(24):4125–4136, 1996. [6](#)
- [22] T. Yamada. Smoke Plume Trajectory from In-Situ Burning of Crude Oil in Tomakomai. Technical report, National Research Institute of Fire and Disaster, Japan, November 1998. [6](#)
- [23] A. Hamins, A. Maranghides, K.B. McGrattan, E. Johnsson, T. Ohlemiller, M. Donnelly, J. Yang, G. Mulholland, K. Prasad, S. Kukuck, R. Anleitner, and T. McAllister. Federal Building and Fire Safety Investigation of the World Trade Center Disaster: Experiments and Modeling of Structural Steel Elements Exposed to Fire. NIST NCSTAR 1-5B, National Institute of Standards and Technology, Gaithersburg, Maryland, September 2005. [6, 22](#)
- [24] A. Hamins, A. Maranghides, K.B. McGrattan, Ohlemiller, and R. Anletiner. Federal Building and Fire Safety Investigation of the World Trade Center Disaster: Experiments and Modeling of Multiple Workstations Burning in a Compartment. NIST NCSTAR 1-5E, National Institute of Standards and Technology, Gaithersburg, Maryland, September 2005. [6](#)
- [25] K. McGrattan, C. Bouldin, and G. Forney. Federal Building and Fire Safety Investigation of the World Trade Center Disaster: Computer Simulation of the Fires in the WTC Towers. NIST NCSTAR 1-5F, National Institute of Standards and Technology, Gaithersburg, Maryland, September 2005. [7](#)

- [26] W.K. Chow and R. Yin. Discussion on Two Plume Formulae with Computational Fluid Dynamics. *Journal of Fire Sciences*, 20:179–201, May 2002. [7](#)
- [27] F. Battaglia, K. McGrattan, R. Rehm, and H. Baum. Simulating Fire Whirls. *Combustion Theory and Modeling*, 4:123–138, 2000. [7](#)
- [28] K.M. Liang, T. Ma, J.G. Quintiere, and D. Rouson. Application of CFD Modeling to Room Fire Growth on Walls. NIST GCR 03-849, National Institute of Standards and Technology, Gaithersburg, Maryland, April 2003. [7](#), [10](#)
- [29] T. Ma and J. Quintiere. Numerical Simulation of Axi-Symmetric Fire Plumes: Accuracy and Limitations. *Fire Safety Journal*, 38:467–492, 2003. [7](#), [10](#)
- [30] G. Heskestad. *SFPE Handbook of Fire Protection Engineering*, chapter Fire Plumes, Flame Height and Air Entrainment. National Fire Protection Association, Quincy, Massachusetts, 3rd edition, 2002. [7](#), [62](#)
- [31] Y. Xin. Baroclinic Effects on Fire Flow Field. In *Proceedings of the Fourth Joint Meeting of the U.S. Sections of the Combustion Institute*. Combustion Institute, Pittsburgh, Pennsylvania, March 2005. [7](#)
- [32] Y. Xin, J.P. Gore, K.B. McGrattan, R.G. Rehm, and H.R. Baum. Fire dynamics simulation of a turbulent buoyant flame using a mixture-fraction-based combustion model. *Combustion and Flame*, 141:329–335, 2005. [7](#)
- [33] Y. Xin, J.P. Gore, K.B. McGrattan, R.G. Rehm, and H.R. Baum. Large Eddy Simulation of Buoyant Turbulent Pool Fires. In *Twenty-Ninth Symposium (International) on Combustion*, pages 259–266. Combustion Institute, Pittsburgh, Pennsylvania, 2002. [7](#)
- [34] S. Hostikka, K.B. McGrattan, and A. Hamins. Numerical Modeling of Pool Fires using Large Eddy Simulation and Finite Volume Method for Radiation. In *Fire Safety Science – Proceedings of the Seventh International Symposium*, pages 383–394. International Association for Fire Safety Science, 2002. [8](#), [28](#)
- [35] J. Hietaniemi, S. Hostikka, and J. Vaari. FDS Simulation of Fire Spread – Comparison of Model Results with Experimental Data. VTT Working Papers 4, VTT Building and Transport, Espoo, Finland, 2004. [8](#), [13](#)
- [36] A. Musser, K. B. McGrattan, and J. Palmer. Evaluation of a Fast, Simplified Computational Fluid Dynamics Model for Solving Room Airflow Problems. NISTIR 6760, National Institute of Standards and Technology, Gaithersburg, Maryland, June 2001. [8](#)
- [37] X. Yuan, Q. Chen, L.R. Glicksman, Y. Hu, and X. Yang. Measurements and Computations of Room Airflow with Displacement Ventilation. Technical Report RP-949, American Society of Heating, Refrigerating, Air-Conditioning Engineers, 1999. [8](#)
- [38] A. Musser and L. Tan. Control of Diesel Exhaust Fumes in Enclosed Locomotive Facilities. Technical Report RP-1191, American Society of Heating, Refrigerating, Air-Conditioning Engineers, 2003. [8](#)
- [39] K. Mniszewski. The Use of FDS for Estimation of Flammable Gas/Vapor Concentrations. In *Proceedings of the 3rd Technical Symposium on Computer Applications in Fire Protection Engineering*, pages 143–155. Society for Fire Protection Engineers, Bethesda, Maryland, September 2001. [8](#)

- [40] S. Kerber and W. Walton. Characterizing Positive Pressure Ventilation using Computational Fluid Dynamics. NISTIR 7065, National Institute of Standards and Technology, Gaithersburg, Maryland, February 2003. 8
- [41] R. Rehm, K. McGrattan, H. Baum, and E. Simiu. An Efficient Large Eddy Simulation Algorithm for Computational Wind Engineering: Application to Surface Pressure Computations on a Single Building. NISTIR 6371, National Institute of Standards and Technology, August 1999. 8
- [42] R.G. Rehm, K.B. McGrattan, and H.R. Baum. Large Eddy Simulation of Flow over a Wooded Building Complex. *Wind & Structures*, 5(2):291–300, 2002. 8
- [43] H.Y. Wang and P. Joulain. Numerical Simulation of Wind-Aided Turbulent Fires in a Ventilated Model Tunnel. In *Fire Safety Science – Proceedings of the Seventh International Symposium*, pages 161–172. International Association for Fire Safety Science, 2002. 8
- [44] F. Magnussen and B.H. Hjertager. On Mathematical Modeling of Turbulent Combustion with Special Emphasis on Soot Formation and Combustion. In *Proceedings of the Sixteenth Symposium (International) on Combustion*, pages 719–729. Combustion Institute, Pittsburgh, Pennsylvania, 1977. 9
- [45] C.H. Chang and R.N. Meroney. Concentration and flow distributions in urban street canyons: wind tunnel and computational data. *Journal of Wind Engineering and Industrial Aerodynamics*, 91:1141–1154, 2003. 9
- [46] R. Vettori. Effect of an Obstructed Ceiling on the Activation Time of a Residential Sprinkler. NISTIR 6253, National Institute of Standards and Technology, Gaithersburg, Maryland, November 1998. 9
- [47] R. Vettori. Effect of a Beamed, Sloped, and Sloped Beamed Ceilings on the Activation Time of a Residential Sprinkler. NISTIR 7079, National Institute of Standards and Technology, Gaithersburg, Maryland, December 2003. 9
- [48] J. Floyd. Comparison of CFAST and FDS for Fire Simulation with the HDR T51 and T52 Tests. NISTIR 6866, National Institute of Standards and Technology, Gaithersburg, Maryland, March 2002. 9
- [49] J.E. Floyd, K.B. McGrattan, S. Hostikka, and H.R. Baum. CFD Fire Simulation Using Mixture Fraction Combustion and Finite Volume Radiative Heat Transfer. *Journal of Fire Protection Engineering*, 13:11–26, February 2003. 9, 12
- [50] A. Kashef, N. Benichou, G.D. Lougheed, and C. McCartney. A Computational and Experimental Study of Fire Growth and Smoke Movement in Large Spaces. Technical Report NRCC-45201, National Research Council Canada, 2002. 9
- [51] K.B. McGrattan, T. Kashiwagi, H.R. Baum, and S.L. Olson. Effects of Ignition and Wind on the Transition to Flame Spread in a Microgravity Environment. *Combustion and Flame*, 106:377–391, 1996. 10
- [52] T. Kashiwagi, K.B. McGrattan, S.L. Olson, O. Fujita, M. Kikuchi, and K. Ito. Effects of Slow Wind on Localized Radiative Ignition and Transition to Flame Spread in Microgravity. In *Twenty-Sixth Symposium (International) on Combustion*, pages 1345–1352. Combustion Institute, Pittsburgh, Pennsylvania, 1996. 10

- [53] W. Mell and T. Kashiwagi. Dimensional Effects on the Transition from Ignition to Flame Spread in Microgravity. In *Twenty-Seventh Symposium (International) on Combustion*, pages 2635–2641. Combustion Institute, Pittsburgh, Pennsylvania, 1998. 10
- [54] W. Mell, S.L. Olson, and T. Kashiwagi. Flame Spread Along Free Edges of Thermally-Thin Samples in Microgravity. In *Twenty-Eighth Symposium (International) on Combustion*, pages 2843–2849. Combustion Institute, Pittsburgh, Pennsylvania, 2000. 10
- [55] K. Prasad, Y. Nakamura, S.L. Olson, O. Fujita, K. Nishizawa, K. Ito, and T. Kashiwagi. Effect of Wind Velocity on Flame Spread in Microgravity. In *Twenty-Ninth Symposium (International) on Combustion*, pages 2553–2560. Combustion Institute, Pittsburgh, Pennsylvania, 2002. 10
- [56] Y. Nakamura, T. Kashiwagi, K.B. McGrattan, and H.R. Baum. Enclosure Effects on Flame Spread over Solid Fuels in Microgravity. *Combustion and Flame*, 130:307–321, 2002. 10
- [57] W.E. Mell, K.B. McGrattan, and H.R. Baum. g-Jitter Effects on Spherical Diffusion Flames. *Microgravity Science and Technology*, 15(4):12–30, 2004. 10
- [58] S. Hostikka and K.B. McGrattan. Large Eddy Simulations of Wood Combustion. In *Proceedings of the Ninth International Interflam Conference*, pages 755–762. Interscience Communications, London, 2001. 10
- [59] S.J. Ritchie, K.D. Steckler, A. Hamins, T.G. Cleary, J.C. Yang, and T. Kashiwagi. The Effect of Sample Size on the Heat Release Rate of Charring Materials. In *Fire Safety Science - Proceedings of the 5th International Symposium*, pages 177–188. International Association For Fire Safety Science, 1997. 10
- [60] K.B. McGrattan, A. Hamins, and D. Stroup. Sprinkler, Smoke & Heat Vent, Draft Curtain Interaction — Large Scale Experiments and Model Development. NISTIR 6196-1, National Institute of Standards and Technology, Gaithersburg, Maryland, September 1998. 10
- [61] A. Hamins and K.B. McGrattan. Reduced-Scale Experiments to Characterize the Suppression of Rack Storage Commodity Fires. NISTIR 6439, National Institute of Standards and Technology, Gaithersburg, Maryland, 1999. 10
- [62] A. Hamins and K.B. McGrattan. Reduced-Scale Experiments on the Water Suppression of a Rack-Storage Commodity Fire for Calibration of a CFD Fire Model. In *Fire Safety Science – Proceedings of the Seventh International Symposium*, pages 457–468. International Association for Fire Safety Science, 2002. 10
- [63] S. Olenick, M. Klassen, and R.J. Roby. Validation Study for FDS for a High Rack Storage Fire Involving Pool Chemicals. In *Proceedings of the 3rd Technical Symposium on Computer Applications in Fire Protection Engineering*. Society of Fire Protection Engineers, Bethesda, Maryland, September 2001. 11
- [64] S.C. Kim and H.S. Ryou. An Experimental and Numerical Study on Fire Suppression using a Water Mist in an Enclosure. *Building and Environment*, 38:1309–1316, 2003. 11
- [65] S.C. Kim and H.S. Ryou. The Effects of Water Mist on the Compartment Fire. *International Journal of Air-Conditioning and Refrigeration*, 12(1):30–36, 2004. 11

- [66] B.P. Hume. Water Mist Suppression in Conjunction with Displacement Ventilation. Master's thesis, University of Canterbury, Christchurch, New Zealand, February 2003. Fire Engineering Research Report 03/4. [11](#)
- [67] S. Hostikka and K.B. McGrattan. Numerical modeling of radiative heat transfer in water sprays. *Fire Safety Journal*, 41:76–86, 2006. [11](#)
- [68] P. Friday and F. W. Mowrer. Comparison of FDS Model Predictions with FM/SNL Fire Test Data. NIST GCR 01-810, National Institute of Standards and Technology, Gaithersburg, Maryland, April 2001. [11](#)
- [69] W. Zhang, A. Hamer, M. Klassen, D. Carpenter, and R. Roby. Turbulence Statistics in a Fire Room Model by Large Eddy Simulation. *Fire Safety Journal*, 37:721–752, 2002. [11](#)
- [70] S. Cochard. Validation of Fire Dynamics Simulator (Version 2.0) Freeware. *Tunnel Management International Journal*, 6(4), December 2003. [11](#)
- [71] K. B. McGrattan and A. Hamins. Numerical Simulation of the Howard Street Tunnel Fire, Baltimore, Maryland, July 2001. NISTIR 6902, National Institute of Standards and Technology, Gaithersburg, Maryland, January 2003. Joint Publication of NIST and the US Nuclear Regulatory Commission (NUREG/CR-6793). [11](#)
- [72] A. Piergiorgio, D. Giuseppe, F. Dino, G. Zappellini, and A. Ferrari. CFD Simulations of a Truck Fire in the Underground Gran Sasso National Laboratory. In *Proceedings of the 5th Italian Conference on Chemical and Process Engineering*, volume 5 of *AIDIC Conference Series*. Associazione Italiana Di Ingegneria Chimica (AIDIC), Elsevier, May 2002. Papers presented at ICeAP-5, Florence, Italy, May 20-23, 2001. [12](#)
- [73] J.C. Edwards, R.A. Franks, G.F. Friel, and L. Yuan. Experimental and Modeling Investigation of the Effect of Ventilation on Smoke Rollback in a Mine Entry. In *Proceedings of the SME Annual Meeting*, pages 1–6. Society for Mining, Metallurgy and Exploration, 2005. [12](#)
- [74] C.C. Hwang and J.C. Edwards. The critical ventilation velocity in tunnel fires – a computer simulation. *Fire Safety Journal*, 40:213–244, 2005. [12](#)
- [75] J.C. Edwards and C.C. Hwang. CFD Modeling of Fire Spread Along Combustibles in a Mine Entry. In *Proceedings of the SME Annual Meeting*, pages 1–5. Society for Mining, Metallurgy and Exploration, 2006. [12](#)
- [76] V. D'Souza, J.A. Sutula, S.M. Olenick, W. Zhang, and R.J. Roby. Use of Fire Dynamics Simulator to Predict Smoke Detector Activation. In *Proceedings of the 2001 Fall Technical Meeting, Eastern States Section*, pages 175–178. Combustion Institute, Pittsburgh, Pennsylvania, December 2001. [12](#)
- [77] W. Zhang, S.M. Olenick, M.S. Klassen, D.J. Carpenter, R.J. Roby, and J.L. Torero. A smoke detector activation algorithm for large eddy simulation fire modeling. *Fire Safety Journal*, 43:96–107, 2008. [12](#)
- [78] D.R. Brammer. A Comparison between Predicted and Actual Behaviour of Domestic Smoke Detectors in a Realistic House Fire. Master's thesis, University of Canterbury, Christchurch, New Zealand, 2002. [12](#)

- [79] T. Cleary, M. Donnelly, G. Mulholland, and B. Farouk. Fire Detector Performance Predictions in a Simulated Multi-Room Configuration. In *Proceedings of the 12th International Conference on Automatic Fire Detection (AUBE '01)*. National Institute of Standards and Technology, Gaithersburg, Maryland, March 2001. NIST SP 965. 12
- [80] A. Mukhopadhyay and I.K. Puri. An Assessment of Stretch Effects on Flame Tip Using the Thin Flame and Thick Formulations. *Combustion and Flame*, 133:499–502, 2003. 12
- [81] A. Hamins, M. Bundy, I.K. Puri, K.B. McGrattan, and W.C. Park. Suppression of Low Strain Rate Non-Premixed Flames by an Agent. In *Proceedings of the 6th International Microgravity Combustion Workshop, NASA/CP-2001-210826*, pages 101–104. National Aeronautics and Space Administration, Lewis Research Center, Cleveland, Ohio, May 2001. 12
- [82] S. Dillon and A. Hamins. Ignition Propensity and Heat Flux Profiles of Candle Flames for Fire Investigation. In Vytenis Babrauskas, editor, *Fire Science Applications to Fire Investigations*, pages 363–376. Interscience Communications, London, 2003. 12
- [83] A. Hamins, M. Bundy, and S.E. Dillon. Characterization of Candle Flames. *Journal of Fire Protection Engineering*, 15(4):265–285, 2005. 12
- [84] J.E. Floyd, C. Wieczorek, and U. Vandsburger. Simulations of the Virginia Tech Fire Research Laboratory Using Large Eddy Simulation with Mixture Fraction Chemistry and Finite Volume Radiative Heat Transfer. In *Proceedings of the Ninth International Interflam Conference*. Interscience Communications, London, 2001. 12
- [85] Y. Xin and J.P. Gore. Measurements and Calculations of Spectral Radiation Intensities in Buoyant Turbulent Flames. In *Proceedings of the Third Joint Meeting of the U.S. Sections of the Combustion Institute*. Combustion Institute, Pittsburgh, Pennsylvania, 2003. 13
- [86] W. Zhang, N. Ryder, R.J. Roby, and D. Carpenter. Modeling of the Combustion in Compartment Fires Using Large Eddy Simulation Approach. In *Proceedings of the 2001 Fall Technical Meeting, Eastern States Section*. Combustion Institute, Pittsburgh, Pennsylvania, December 2001. 13
- [87] D. Madrzykowski and R.L. Vettori. Simulation of the Dynamics of the Fire at 3146 Cherry Road NE Washington D.C., May 30, 1999. NISTIR 6510, National Institute of Standards and Technology, Gaithersburg, Maryland, April 2000. 13
- [88] R.L. Vettori, D. Madrzykowski, and W.D. Walton. Simulation of the Dynamics of a Fire in a One-Story Restaurant – Texas, February 14, 2000. NISTIR 6923, National Institute of Standards and Technology, Gaithersburg, Maryland, October 2002. 14
- [89] D. Madrzykowski, G.P. Forney, and W.D. Walton. Simulation of the Dynamics of a Fire in a Two-Story Duplex – Iowa, December 22, 1999. NISTIR 6854, National Institute of Standards and Technology, Gaithersburg, Maryland, January 2002. 14
- [90] G. Rein, A. Bar-Ilan, N. Alvares, and A.C. Fernandez-Pello. Estimating the Performance of Enclosure Fire Models by Correlating Forensic Evidence of Accidental Fires. In *Proceedings of the Tenth International Interflam Conference*, pages 1183–1194. Interscience Communications, London, 2004. 14
- [91] M. Spearpoint, F.W. Mowrer, and K. McGrattan. Simulation of a Compartment Flashover Fire Using Hand Calculations, Zone Models and a Field Model. In *Proceedings of the Third International*

Conference on Fire Research and Engineering (ICFRE3), pages 3–14. Society of Fire Protection Engineers, Bethesda, Maryland, 1999. [14](#)

- [92] D.J. Carpenter and C.B. Wood, editors. *Proceedings of the 3rd Technical Symposium on Computer Applications in Fire Protection Engineering*. Society for Fire Protection Engineers, Bethesda, Maryland, September 2001. [14](#)
- [93] A.M. Christensen and D.J. Icove. The Application of NIST's Fire Dynamics Simulator to the Investigation of Carbon Monoxide Exposure in the Deaths of Three Pittsburgh Fire Fighters. *Journal of Forensic Sciences*, 49(1):1–4, 2004. [14](#)
- [94] S. Hostikka, Kokkala, and J. Vaari. Experimental Study of the Localized Room Fires. VTT Research Notes 2104, VTT Technical Research Centre of Finland, Espoo, Finland, 2001. [15](#)
- [95] A. Tewarson. *SFPE Handbook of Fire Protection Engineering*, chapter Generation of Heat and Chemical Compounds in Fires. National Fire Protection Association, Quincy, Massachusetts, 3rd edition, 2002. [16](#)
- [96] D.T. Sheppard and D.R. Steppan. Sprinkler, Heat & Smoke Vent, Draft Curtain Project – Phase 1 Scoping Tests. Technical report, Underwriters Laboratories, Northbrook, Illinois, May 1997. [18](#)
- [97] A. Hamins, A. Maranghides, R. Johnsson, M. Donnelly, G. Yang, G. Mulholland, and R.L. Anleitner. Report of Experimental Results for the International Fire Model Benchmarking and Validation Exercise 3. NIST Special Publication 1013-1, National Institute of Standards and Technology, Gaithersburg, Maryland, May 2006. Joint Publication of NIST and the US Nuclear Regulatory Commission (NUREG/CR-6905). [20](#)
- [98] S.P. Nowlen. Enclosure Environment Characterization Testing for the Baseline Validation of Computer Fire Simulation Codes. NUREG/CR-4681 (SAND86-1296), Sandia National Laboratory, Albuquerque, New Mexico, March 1987. Work performed under contract to the US Nuclear Regulatory Agency, Washington DC. [22](#)
- [99] J.M. Chavez and S.P. Nowlen. An Experimental Investigation of Internally Ignited Fires in Nuclear Power Plant Control Cabinets, Part II: Room Effects Tests. NUREG/CR-4527 (SAND86-0336), Sandia National Laboratory, Albuquerque, New Mexico, November 1988. Work performed under contract to the US Nuclear Regulatory Agency, Washington DC. [22](#)
- [100] R.D. Peacock, S. Davis, and W.T. Lee. An Experimental Data Set for the Accuracy Assessment of Room Fire Models. NBSIR 88-3752, National Bureau of Standards (now NIST), Gaithersburg, Maryland, April 1988. [25](#)
- [101] B.J. McCaffrey. Purely Buoyant Diffusion Flames: Some Experimental Results. NBSIR 79-1910, National Bureau of Standards (now NIST), Gaithersburg, Maryland, October 1979. [28](#)
- [102] K.D. Steckler, J.G. Quintiere, and W.J. Rinkinen. Flow Induced By Fire in A Compartment. NBSIR 82-2520, National Bureau of Standards (now NIST), Gaithersburg, Maryland, September 1982. [27](#), [50](#), [75](#)
- [103] T.S. Norton, K.C. Smyth, J.H. Miller, and M.D. Smooke. Comparison of Experimental and Computed Species Concentration and Temperature Profiles in Laminar, Two-Dimensional Methane/Air Diffusion Flames. *Combustion Science and Technology*, 90:1–34, 1993. [28](#)

- [104] K.C. Smyth. NO Production and Destruction in a Methane/Air Diffusion Flame. *Combustion Science and Technology*, 115:151–176, 1996. 28
- [105] C. Belyer. Major Species Production by Diffusion Flames in a Two-Layer Compartment Fire Environment. *Fire Safety Journal*, 10:47–56, 1986. 28
- [106] N. Bryner, E. Johnsson, and W. Pitts. Carbon Monoxide Production in Compartment Fires - Reduced-Scale Test Facility. NISTIR 5568, National Institute of Standards and Technology, Gaithersburg, MD, 1994. 28, 103
- [107] G. Back, C. Beyler, P. DiNenno, and P. Tatem. Wall Incident Heat Flux Distributions Resulting from an Adjacent Fire. In *Fire Safety Science – Proceedings of the Fourth International Symposium*, pages 241–252. International Association of Fire Safety Science, 1994. 28
- [108] Verification and Validation of Selected Fire Models for Nuclear Power Plant Applications. NUREG 1824, United States Nuclear Regulatory Commission, Washington, DC, 2007. 29
- [109] M.L. Janssens and H.C. Tran. Data Reduction of Room Tests for Zone Model Validation. *Journal of Fire Science*, 10:528–555, 1992. 31
- [110] Y.P. He, A. Fernando, and M.C. Luo. Determination of interface height from measured parameter profile in enclosure fire experiment. *Fire Safety Journal*, 31:19–38, 1998. 32